EFFECTS OF PAR AND HIGH UVR ON ENZYMES AND OTHER PROTEINS INVOLVED IN THE FUNCTION AND PROTECTION OF PHOTOSYNTHETIC APPARATUS OF MARINE MACROALGAE

A dissertation submitted for the degree of Dr. rer. nat. (*rerum naturalium*) to the Department of Biology, Faculty of Mathematics, Informatics and Natural Sciences, University of Hamburg

prepared by

HAZLINA AHAMAD ZAKERI
Malaysia

April 2010

Genehmigt vom Department Biologie
der Fakultät für Mathematik, Informatik und Naturwissenschaften
an der Universität Hamburg
auf Antrag von Herr Professor Dr. D. HANELT
Weiterer Gutachter der Dissertation:
Professor Dr. K. BISCHOF
Tag der Disputation: 26. März 2010

Hamburg, den 11. März 2010

Universität Hamburg
64
Fakultät
Mathematik, Informatik und Naturwissenschaften

Professor Dr. Axel Temming
Leiter des Departments Biologie

TABLE OF CONTENTS

LIST OF ABBREVIATIONS

λ	wavelength
^{1}Chl, ^{3}Chl	singlet chlorophyll, triplet chlorophyll
$^1O_2$, O_2^-	singlet oxygen, superoxide radical
A, V, X, Z	anteraxanthin, violaxanthin, xanthophyll, zeaxanthin
AL	actinic light
AP	alkaline phosphatase
APX	ascorbate peroxidase
AsA	ascorbic acid
CAT	catalase
Chl	chlorophyll
$CuSO_4$	copper sulphate
Ddx, Dtx	diadinoxanthin, diatoxanthin
dH_2O	distilled water
DHA	dehydroascorbate
DMF	dimethylformamide
DMSO	dimethylsulphoxide
ETC	electron transport chain
FI	fluorescence induction
FR	far-red light
FW	fresh weight
GAP	glyceraldehyde-3-phosphate
GAPDH	glyceraldehyde-3-phosphate dehydrogenase
GR	glutathione reductase
GSH, GSSG	glutathione, oxidized glutathione
H&L	heavy and light chains of antibodies
H_2O_2	hydrogen peroxide
HRP	horse radish peroxidase
HSP	heat shock protein
IC	induction curve
K_2CrO_4	potassium chromate
KNO_3	potassium nitrate
LHC	light harvesting complex
LSD	least significance difference

LSU, SSU	large subunit and small subunit of RuBisCO
Lut, Lx	lutein, lutein epoxide
ML	measuring light
MAA	mycosporine-like amino acid
PAM	pulse amplitude modulation
PAR	photosynthetically active radiation (400-700 nm)
PAR+UVR	PAR+UVA and PAR+UVA+UVB
PFR	photon fluence rate
PGA	phosphoglycerate
P-I	photosynthesis-irradiance curve
PPFD	photosynthesis photon flux density
PSI, PSII	photosystem I, photosystem II
PSU	photosynthetic unit
PVPP	polyvinylpolypyrrolidone
RC	recovery curve
rETR	relative electron transport rate
RLC	rapid light curve
ROS	reactive oxygen species
R-PC	R-phycoerythrin
R-PE	R-phycocyanin
RuBisCO	ribulose-1,5-bisphosphate carboxylase/oxygenase
RuBP	ribulose bisphosphate
SNK	Student-Neumann-Keuls test
SOD	superoxide dismutase
SP	saturation pulse
Trp	tryptophan
TSP	total soluble proteins
U	enzyme unit
UVA	ultraviolet A (320-400 nm)
UVB	ultraviolet B (290-320 nm)
UVC	ultraviolet C (200-290 nm)
UVR	ultraviolet radiation, UVA and/or UVB
VIS	visible light

LIST OF TERMINOLOGIES

(1-qP)/NPQ	susceptibility of PSII to light stress index
$\Delta F/F_m'$ or ΦPSII or Y	effective quantum yield of PSII $[(F_m'-F)/F_m']$
1-qP	excitation pressure of PSII
F or F_t	steady-state fluorescence yield
F_m, F_m'	dark-adapted maximal fluorescence yield; pre-illuminated maximal fluorescence yield
F_o, F_o'	dark-adapted minimal fluorescence yield; pre-illuminated minimal fluorescence yield
F_v	variable fluorescence yield, steady-state fluorescence yield
F_v/F_m	maximal quantum yield $[(F_m-F_o)/F_m]$
I_k	light saturation parameter
NPQ	Stern-Volmer's non-photochemical quenching parameter $[(F_m - F_m')/F_m']$
qE	non-photochemical energy-dependent quenching parameter
qI	non-photochemical inhibitory quenching parameter
qN	non-photochemical quenching parameter $[1- ((F_m' - F_o')/(F_m - F_o))]$
qP	photochemical quenching parameter $[(F_m' - F)/(F_m' - F_o')]$
qT	non-photochemical state transitions quenching parameter
$rETR_{max}$	maximal relative electron transport rate
vide infra, vide supra	refer text below, refer text above
α	photosynthetic efficiency parameter $[rETR_{max}/I_k]$

SUMMARY

The changes in the quality and quantity of the solar radiation may affect photosynthetic organisms. An increase in irradiation of UVB (290-320 nm) of the solar radiation that reaches the earth's surface due to thinning of the ozone layer, for instance, can cause destructive consequences to these photoautotrophs. Thus, like any other photoautotrophs, macroalgae are deemed to be affected and loss of these important biomass producers of the aquatic ecosystem may disrupt the primary productivity and the whole ecosystem integrity. However, the macroalgae have somehow developed protective mechanisms to ensure their survivality in the extreme environment.

In this study, short-term responses of five marine macroalgae, *Solieria chordalis*, an intertidal red alga; *Palmaria palmata*, an intertidal or upper sublittoral red alga; *Laminaria digitata*, an upper to middle sublittoral brown alga; *Dictyota dichotoma*, an upper sublittoral brown alga; and, *Ulva lactuca*, an intertidal or upper sublittoral green alga, to ultraviolet radiation (UVR) were investigated. The algae were originally collected from the North Sea islands of Sylt and Helgoland and were further cultivated in a temperature-controlled laboratory under ~32 µmol m^{-2} s^{-1} of white light at 12.5±0.5˚C. The algae were irradiated for 5 h to a high UVR in combination with either low or high background photosynthetically active radiation (PAR, 400-700 nm) emitted by fluorescent lamps or a sun simulator, respectively. Four light regimes were created using cut-off filters: PAR, PAR+UVA (UVA, 320-400 nm), PAR+UVA+UVB or UVA+UVB. Recovery kinetics were also determined by incubating the irradiated algae in dim light for 18 h. Responses were evaluated on the basis of photosynthetic performance (i.e. F_v/F_m, $rETR_{max}$, α and I_k), photodamage or photoinactivation (i.e. *via* pigments analysis, total soluble proteins content, RuBisCo activity and its large subunit (LSU) composition, GAPDH activity and D1 protein content), and photoprotective mechanisms (i.e. *via* antioxidative enzymes activity, presence of stress proteins and non-photochemical quenching).

Higher reductions in F_v/F_m were observed with high UV and high background PAR than under low PAR and additional UVB caused the highest reduction. Most of the algae showed high F_v/F_m with UV alone. Low PAR alone had weak or no effect on the algae. Recovery was the fastest with PAR alone but was slow with additional UVB, indicating permanent damage may have occurred in the PSII reaction centres. Some algae showed a delay in recovery with UV alone. All affected algae showed signs of recovery from the stress with one exception. UV strongly reduced the convexity of the rETR vs. irradiance plot resulting in a lower $rETR_{max}$, a lower α and a higher I_k compared to the controls indicating damage or inactivation to the reaction centres. It is probable that UV- or high PAR-induced inhibition in all species caused accumulation of reactive oxygen species (ROS) especially H_2O_2 as indicated by increase in the antioxidative enzymes. The production of ROS may be triggered by the photosynthetic pigments (i.e. chlorophylls and phycobiliproteins) which were subsequently damaged through absorption with UV and high PAR, hence, a reduction in the pigments content was also observed. In addition, accumulation of ROS may also result from the photorespiratory pathway indicated by high induction of catalase. As a consequence, low content of D1 protein, loss of total soluble proteins, low activity of RuBisCO and its LSU composition, and low activity of GAPDH were observed during the inhibitory phase. High content of antioxidative enzymes and stress proteins, HSP60 and HSP70, detected in the irradiated algae indicated the trigger of photoprotective mechanisms functioning in the repair and recovery processes; hence, all species were able to recover from stress. However, rate of inhibition and recovery differed between the light treatments indicating different mechanisms of inactivation and protection which were induced by each of the different spectral wavelength ranges.

UV and high PAR significantly reduced the fluorescence yield signal (i.e. ΔF, F_m'-F_o'), the effective quantum yield (Y) and photochemical quenching parameter (qP) of the irradiated algae. In addition, non-photochemical quenching parameters, qN and NPQ of the irradiated algae were induced indicating high ability to dissipate excess energy as heat. Dark relaxation kinetics revealed that in the irradiated algae, most of the NPQ were made up of photoinhibitory quenching (qI). Furthermore, Y showed a steady but slow recovery during the dark phase as well indicating that damage may have occurred in the reaction

centres. Higher 1-qP and lower (1-qP)/NPQ indices were measured in irradiated algae compared to the controls. Reduced Q_A accumulated in the irradiated algae as indicated by the complete quenching of the second rise of the fluorescence signal of the rapid induction curve. Within the ratio of PAR:UVA:UVB close to the natural conditions, the algae were more tolerant to high UVB and low UVA than low UVB and high UVA with high background PAR. In contrast, most of the algae showed low inhibition at low UVB flux in combination with low background PAR.

In addition to the above observations, it was interesting to note that in some species, UVB showed an ameliorating effect on the recovery of the algae as indicated by faster recovery with PAR+UVA+UVB than PAR+UVA. This effect was observed in *D. dichotoma* irradiated at high UV/high PAR and *P. palmata* irradiated at high UV/low PAR. This supporting role of UVB was reflected in most of the parameters analyzed. It is probable that UVB might induce the transcription of *PsbA* genes of D1 protein leading to a faster recovery in PAR+UVA+UVB than PAR+UVA. Significant delay in recovery of PAR+UVA compared to PAR+UVA+UVB was also observed in *U. lactuca* while similar trend was detected in *S. chordalis* and *L. digitata* irradiated at low UV/high PAR. Comparatively, some of the species were shown to respond more to UVA than UVB and this could be an ecological importance as well.

The results obtained showed that the algae responded according to the zonation pattern of their natural habitats. For instance, the sublittoral *L. digitata* was the most inhibited by the high UV/high PAR stresses. Several dissimilarities in the behaviour between the two brown algae, *L. digitata* and *D. dichotoma*, in counteracting the damaging effect of UVR could be observed. *L. digitata* was strongly affected by UVB but in *D. dichotoma*, UVB showed an ameliorating effect. UV alone caused chronic photoinhibition in *L. digitata* but dynamic photoinhibition in *D. dichotoma*. At high UV/low PAR irradiance, *L. digitata* was less affected than *D. dichotoma*. An increase in $rETR_{max}$ was apparent in *L. digitata* parallel to a decrease in α and an increase in I_k at high UV/low PAR irradiance. This characteristic of *L. digitata* was not displayed by any other species which was also observable at low UV/low PAR. *D. dichotoma* exhibited

high fucoxanthin content in response to high PAR and high UVA but not when supplemented with UVB. Catalase activity at high UV/low PAR increased two-fold in *L. digitata* in comparison to *D. dichotoma.* Responses of both brown algae which were different from other algal classes include a decrease in 1-qP and an increase in NPQ after irradiation but with a slower onset of qN.

The intertidal *S. chordalis* and the upper sublittoral *P. palmata* were more sensitive to the high light stress than the green alga. Upon irradiation, higher antioxidative enzymes were observed in these algae than the other two classes indicating higher oxidative stress conditions. Furthermore, maximal 1-qP was measured in the irradiated algae and the ability to induce qN and NPQ was much lower than the other classes. Thus, the red algae generally showed a slower recovery and adaptation than the other species. In addition, *S. chordalis* was more affected by the low PAR alone in comparison to the other species. Comparatively, the intertidal or upper sublittoral *U. lactuca* was the least affected among the species. Most obvious response shown by *U. lactuca* was the rapid recovery of most of the parameters with all light treatments excluding UV alone. Therefore, *U. lactuca* was said to be well-prepared and well-adapted with the high light stress in comparison to the other species. Indeed, this alga was more inhibited under a low UVB flux and showed an ameliorating UVB effect at this ratio. The highest induction of stress proteins was observed in *U. lactuca* as well. The activity of the antioxidative enzymes was generally low in *U. lactuca*, indicating low oxidative stress in the cells.

In conclusion, all of the algae examined were strongly inhibited by the high UV and high PAR. High tolerance to UVB was displayed by the algae at much lower UVB fluxes. Even though UVB generally caused damaging effects, some of the algae responded positively to UVB. Whilst the brown algae *L. digitata* and *D. dichotoma* collectively showed the highest inhibition, the green alga *U. lactuca* was the least affected and was well-prepared and well-adapted to the high light effect. The red algae *S chordalis* and *P. palmata* were also strongly inhibited but recovered more slowly than the rest of the algal classes.

ZUSAMMENFASSUNG

Veränderungen in der Qualität und Quantität der Sonneneinstrahlung können photosynthetische Organismen beeinflussen. Eine Zunahme im kurzwelligen Anteil des UVB (290-320 nm), der die Erdoberfläche wegen der Ausdünnung der Ozon-Schicht erreicht, kann zerstörende Folgen für photoautotrophe Organismen haben. So wie bei allen anderen photoautotrophen Organismen ist davon auszugehen, dass auch Makroalgen betroffen sein werden und der Verlust dieser wichtigen aquatischen Primärproduzenten die ganze Ökosystem-Integrität stören wird. Jedoch haben Makroalgen bestimmte Schutzmechanismen entwickelt, um ihr Überleben unter widrigen Bedingungen zu sichern.

In dieser Studie wurde die Kurzzeitwirkung von ultravioletter Strahlung (UVR) auf fünf marinen Makroalgen untersucht: *Solieria chordalis* eine Rotalge der Gezeitenzone, *Palmaria palmata* eine Rotalge die im unteren Eu- und oberen Sublittoral lebt, *Laminaria digitata* eine Braunalge des oberen bis mittleren Sublittorals, *Dictyota dichotoma* eine Braunalge des oberen Sublittorals und *Ulva lactuca* eine Grünalge der Gezeitenzone. Die Algen entstammen aus Kulturen von Sylt und Helgoland und sie wurden in einer temperaturkontrollierten Kammer unter ~32 µmol m^{-2} s^{-1} weißem Lichtes kultiviert, bei einer Temperatur von 12.5±0.5˚C. Die Algen wurden für 5 Stunden einer hohen UV-Strahlung in Kombination entweder mit einer niedrigen oder hohen photosynthetisch aktiven Hintergrundstrahlung (PAR, Leuchtstofflampen) ausgesetzt oder unter einem Sonnensimulator bestrahlt. Vier Bestrahlungsvarianten wurden unter Verwendung von sogenannten Cut-off Filtern erstellt: PAR (400-700 nm), PAR+UVA (UVA, 320-400 nm), PAR+UVA+UVB oder UVA+UVB. Erholungskinetiken wurden gemessen, indem die vorher bestrahlten Algen für 18 Stunden unter Schwachlichtbedingungen inkubiert wurden. Als Photosyntheseparameter dienten hierbei: F_v/F_m, $rETR_{max}$, α und I_k, Pigmentgehalte, Gesamtgehalt löslicher Proteine, RuBisCO-Aktivität und Menge der großen Untereinheit (LSU), GAPDH-Aktivität und D1-Proteinanteil. Zusätzlich wurden photoprotektive Vorgänge über die Bestimmung antioxidativer Enzymaktivitäten, Vorhandensein von Stressproteinen und nicht-photochemisches Quenching charakterisiert.

Die stärkste Abnahme von F_v/F_m wurde bei Bestrahlung mit hohem UV Anteil bei hoher photosynthetisch aktiver Hintergrundstahlung (PAR) beobachtet, als bei Bestrahlung mit schwachem Hintergrundlicht (PAR), wobei die starke Abnahme durch die UVB Strahlung induziert wurde. Die meisten Algen zeigten die höchsten F_v/F_m Werte unter UV allein. Niedriges PAR hatte nur schwache oder keine Wirkung auf die Algen. Die Erholung war am schnellsten unter PAR alleine. Zusätzliches UVB verlangsamte den Erholungsprozess, so dass ein dauerhafter Schaden in den PSII Reaktionszentren vermutet werden kann. Einige Algen zeigten eine deutlich langsamere Erholung, wenn mit sie nur mit UV bestrahlt wurden. Hierbei reduzierte UV stark die Konvexität der rETR-Kurven, wenn diese gegen die Bestrahlungsintensität aufgetragen wurde. Dies äußerte sich in niedrigerem $rETR_{max}$, α und einem höheren I_k-Wert im Vergleich zu den Kontrollen, so dass Schäden an oder eine Inaktivierung der Reaktionszentren angenommen werden kann. Es ist wahrscheinlich, dass eine durch UV- oder hohe PAR induzierte Hemmung in den untersuchten Arten die Bildung reaktiver Sauerstoffarten (ROS), besonders H_2O_2, auslöste, was durch die Zunahme von antioxidativer Enzymen gezeigt wurde. Die Produktion von ROS könnte durch die photosynthetischen Pigmente gesteuert worden sein (d. h. Chlorophylle und Phycobiliproteine), die durch Absorption von UV und hohe Bestrahlungsflüssen mit PAR geschädigt wurden. Hierauf würde die beobachtete Verminderung der Pigmentkonzentrationen hinweisen. Auch könnte die vermehrte Bildung von ROS aus der photorespiratorischen Reaktion resultieren, hierauf weist eine gesteigerte Katalasebildung hin. Hieraus resultieren die verringerte Mengen des D1-Proteine, Abnahme des Gehaltes an löslichen Gesamtproteinen, verminderte RuBisCO Aktivität und der Veränderung des LSU Gehalts sowie verminderte GAPDH-Aktivität während der inhibitorischen Starklicht-Phase.

Hohe Gehalte an antioxidativen Enzymen, Stress Proteinen (HSP60 und HSP70) in den bestrahlten Algen deuten auf das Wirken von Reparatur- und Photoprotektionsmechanismen während des Erholungsprozesses hin. Alle untersuchten Arten waren im Stande, sich von der Starklicht-Bestrahlung zu erholen. Sie unterschieden sich jedoch je nach Bestrahlungsprogramm hinsichtlich des Umfangs der Inhibition und der Erholung, so dass verschiedene Inaktivierungs- und Schutzmechanismen für die

unterschiedlichen Wellenlängenbereiche vermutet werden müssen. Bestrahlung durch UV und hohe PAR Intensitäten reduzierten die Fluoreszenzausbeuten im Licht (d. h. ΔF, F_m'-F_o'), den effektiven Quantenertrag (Y) und die photochemische Fluoreszenzlöschung (qP) der bestrahlten Algen. Außerdem wurden die nichtphotochemische Fluoreszenzlöschung (qN oder NPQ) der bestrahlten Algen induziert, was die Fähigkeit anzeigt übermäßig absorbierte Energie als Wärme abzustrahlen. Erholungskinetiken in der Dunkelheit offenbarten, dass in den bestrahlten Algen der größten Anteil an NPQ aus dem photoinhibitorischen Quench (qI) besteht. Zudem zeigte Y eine konstante aber langsame Erholung während der Dunkelphase, was anzeigt, dass Schäden in den Reaktionszentren aufgetreten sein können. Höherer 1-qP und niedrigere (1-qP)/NPQ Indizes wurden in bestrahlten als in den Kontrollalgen gemessen. Reduziertes Q_A stieg in den bestrahlten Algen an, was durch die vollständige Löschung des sekundären Anstiegs des Fluoreszenz-Signals in den schnellen Induktionskurven angezeigt wird. Wenn das PAR:UVA:UVB Verhältnis mehr den natürlichen Bedingungen entsprach, waren die Algen toleranter für höhere UVB plus geringerer UVA-Strahlung als für niedrige UVB plus höherer UVA Strahlung bei hoher PAR-Hintergrundstrahlung. Im Gegensatz zeigten die meisten Algen geringe Hemmung bei niedrigem UVB in Kombination mit niedrigen Hintergrund-PAR.

Zusätzlich zu den obengenannten Beobachtungen zeigte sich, dass in einigen Arten UVB eine positive Wirkung auf den Erholungsprozess der Algen ausübte. Dies trat in den Versuchen PAR+UVA+UVB im Vergleich zu PAR+UVA auf. Dieser Effekt wurde bei *D. dichotoma*, welche mit hohen UV und hohen PAR Intensitäten, sowie bei *P. palmata* mit UV und niedrigen PAR bestrahlt wurde, beobachtet. Diese schützende Wirkung von UVB spiegelte sich in den meisten untersuchten Parametern wider. Wahrscheinlich induziert UVB die Transkription der *PsbA* Gene des D1 Proteins, mit der Folge einer rascheren Erholung unter Einfluss von PAR+UVA+UVB. Die deutliche Verzögerung in der Erholung bei Bestrahlung mit PAR+UVA verglichen mit PAR+UVA+UVB wurde auch bei *U. lactuca* beobachtet. Ähnliche Tendenzen konnten auch bei *S. chordalis* und *L. digitata* nach Bestrahlung mit niedrigem UV und hoher PAR Intensität beobachtet werden. Andererseits konnte auch gezeigt werden, dass einige der

Arten stärker auf Bestrahlung mit UVA reagierten als auf UVB. Dies könnte ebenfalls ökologisch bedeutsam sein.

Die Ergebnisse zeigen, dass die untersuchten Algen entsprechend ihrer natürlichen Zonierung reagierten. So wurde z.B. die sublittorale *L. digitata* durch hohe UV und hohe PAR Intensitäten am stärksten inhibiert. Mehrere Unterschiede charakterisierten die Reaktion der beiden Braunalgen *L. digitata* und *D. dichotoma* unter der Abschwächung der inhibitorischen Wirkung von UVR. *L. digitata* wurde durch UVB stark inhibiert, wohingegen bei *D. dichotoma* die Schädigung verringert wurde. UV Bestrahlung verursacht bei *L. digitata* eine chronische, bei *D. dichotoma* hingegen eine dynamische Photoinhibition. *L. digitata* wurde dagegen durch hohes UV und niedrige PAR Intensitäten weniger beeinflusst. Unter diesen Bestrahlungsbedingungen konnten bei *L. digitata* eine Zunahme von $rETR_{max}$ und I_k, und parallel dazu eine Abnahme von α beobachtet werden. Keine der anderen untersuchten Arten zeigte dieses Verhalten unter diesen speziellen Bestrahlungsbedingungen. *D. dichotoma* wies erhöhte Fucoxanthin-gehalte als Antwort auf die Bestrahlung mit hohen UVA und hohen PAR Intensitäten auf, jedoch nicht wenn gleichzeitig UVB eingestrahlt wurde. Bei Bestrahlung mit hohem UV und niedrigen PAR Intensitäten war die Katalase-Aktivität bei *L. digitata* im Vergleich zu *D. dichotoma* doppelt so hoch. Des Weiteren unterschieden sich diese beiden Braunalgen von den anderen untersuchten Arten dadurch, dass nach der Bestrahlung 1-qP abnahm, NPQ hingegen anstieg, wobei qN sich verzögert einsetzte.

S. chordalis aus der Gezeitenzone sowie *P. palmata* aus dem Sublittoral reagierten auf Lichtstress empfindlicher als die Grünalge *U. lactuca*. Nach Bestrahlung wiesen diese Algen höhere Gehalte an antioxidativen Enzymen auf als die anderen Algengruppen. Dies deutet auf erhöhte Empfindlichkeit gegenüber oxidativem Stress hin. Außerdem wurde ein maximaler 1-qP in den bestrahlten Algen festgestellt und eine verminderte Fähigkeit qN und NPQ zu induzieren, als bei den anderen untersuchten Algengruppen. Es ist daher davon auszugehen, dass die untersuchten Rotalgen im Allgemeinen eine verlangsamte Starklicht-Anpassung und Erholung aufweisen. Zusätzlich reagierte *S. chordalis* empfindlich auf die Bestrahlung mit niedrigen PAR Intensitäten. Im Gegensatz hierzu war die aus der

Gezeitenzone bzw. dem oberen Sublittoral stammende *U. lactuca* am wenigsten beeinträchtigt. Am auffälligsten war bei dieser Art die schnelle Erholung bei allen Bestrahlungsvarianten mit Ausnahme der alleinigen Bestrahlung mit UV. Es ist daher festzustellen, dass *U. lactuca* unter den untersuchten Arten am besten angepasst ist, um starken Lichtstress zu tolerieren. Inhibition der Photosynthese trat stärker unter der niedrigen UV-B Bestrahlungsstärke auf, zeigte aber wiederum eine schützende Wirkung unter diesen Bedingungen. Die stärkste Induktion von Stressproteinen wurde ebenfalls in *U. lactuca* beobachtet. Eine geringe Aktivität der antioxidativer Enzyme in *U. lactuca* weist zudem auf einen geringen oxidativen Stress der Zellen hin.

Zusammenfassend lässt sich feststellen, dass alle untersuchten Algen durch hohe UV und PAR Intensitäten stark inhibiert wurden. Eine hohe Toleranz gegenüber UVB zeigt sich bei niedrigen UVB-Bestrahlungsstärken. Obwohl UVB stets zu Schäden führte, reagierten dennoch einige Algen auch positiv auf die UVB Bestrahlung, da sie Schutz- und Erholungsmechanismen induziert. Während die Braunalgen *L. digitata* und *D. dichotoma* insgesamt die höchste Inhibitionsraten aufwiesen, war die Grünalge *U. lactuca* am wenigsten betroffen und gut an Starklicht adaptiert. Die Rotalgen *S. chordalis* und *P. palmata* waren ebenfalls stark inhibiert und wiesen von den untersuchten Arten die langsamste Erholung auf.

1.0 INTRODUCTION

1.1 A short note on the photosynthetic algae

Algae are a large and diverse group of simple, autotrophs eukaryotic organisms (with the exception of cyanobacteria). They lack roots, leaves and other structures typical of true plants. Algae, especially that inhabit marine ecosystems, are abundant and occupy the base of the food chain. Therefore, they are ecologically and economically important organisms. In addition to as food and oxygen provider, they produce extracts such as agar, carrageenan and alginates (for e.g. Falshaw et al., 1998; Torres et al., 2007; Villaneuva et al., 2009). These extracts are used in numerous foods, nutraceutical, pharmaceutical and industrial applications. Moreover, algae can also be used as biological bioindicators of environmental pollution (Torres et al., 2008). Classically, the algae were divided into three main classes, the red algae (Rhodophyta), the brown algae (Phaeophyta) and the green algae (Chlorophyta) (Douglas et al., 2003; Sheath, 2003; Wehr, 2003; see van den Hoek et al., 1995 for complete hierarchy). Morphologically, these algae range in size from microscopic unicells, as in phytoplankton, to macroscopic organisms as in the macroalgae or seaweeds (Douglas et al., 2003).

Algae can thrive in many diverse habitats (van den Hoek et al., 1995). The phytoplankton floats and swims in lakes and oceans. The seaweeds can stretch about 100 m from the bottom of the ocean to the water's surface. Most other algae grow in freshwater or seawater, on soil, trees and animals, under porous rocks and can even tolerate a wide range of temperatures by growing in hot springs, on snow banks or deep within the ice. Of importance in this study are the algae that inhabit the marine ecosystem, particularly the seaweeds. The ecology of seaweeds is dominated by two specific environmental requirements. These are the presence of seawater (or at least brackish water) and the presence of light sufficient to drive photosynthesis. A very common requirement is also to have a firm point of attachment. As a result, seaweeds are most commonly found in the littoral zone and within that zone more frequently on rocky shores than on sand or shingle. The littoral (or euphotic) zone is the part of the ocean that is the

closest to the shore, the 'sunlit' zone that receives sufficient light to satisfy the photosynthetic requirements with lower limit around 200 m to a maximum of 270 m in clear waters (Lüning, 1990). It is subdivided into supralittoral zone, reachable by spray water; eulittoral or intertidal zone, which is submersed and emersed, either periodically due to tides or aperiodically due to irregularly occurring factors; and, sublittoral zone, submersed with the upper part at extreme low water levels occasionally emersing (Lüning, 1990). Furthermore, algae which grow in the eulittoral are exposed to solar radiation including ultraviolet (UV), while algae growing in the sublittoral are exposed mainly to photosynthetically active radiation (PAR) (Sinha et al., 2001). In my study, five marine macroalgae (or seaweeds) are chosen, namely (Appendix 1), *Solieria chordalis* (C. Agardh) J. Agardh, an intertidal red alga; *Palmaria palmata* (L), an intertidal or upper sublittoral red alga; *Laminaria digitata* (Hudson) J.V. Lamouroux, an upper-middle sublittoral brown alga; *Dictyota dichotoma* (Hudson) J.V. Lamouroux, an upper sublittoral brown alga; and, *Ulva lactuca* (L), an intertidal or upper sublittoral green alga (Lüning, 1990; Aguilera et al., 2002b; Häder et al., 2002).

Algae like any other photoautotrophs exploit photosynthesis to make food. Photosynthesis-wise, the light reactions of many algae differ from those of land plants because some of them use different secondary pigments to harvest light. Rhodophytes, for example, are red because of the pigment phycoerythrin (a type of phycobiliproteins and a bluish phycobiliproteins, phycocyanin is also present in the red algae) (Grossman et al., 1993; Talarico and Maranzana, 2000) and the Phaeophytes are brownish or yellowish in colour due to the carotenoids (in particular, fucoxanthin) (Douady et al., 1993; Haugan and Liaaen-Jensen, 1994), while the chlorophylls (Chls) (i.e. Chl b) are dominant in the Chlorophytes. Additionally, all algae use Chl a to collect photosynthetically active light. Generally, Chls absorb primarily of the blue and red light, whereas carotenoids absorb primarily blue and green light, and phycobiliproteins absorb primarily green or red light (Nobel, 2005). Since the amount of light absorbed depends upon the pigment composition and concentration found in the alga, some algae absorb more light at a given wavelength, and therefore, potentially, those algae can convert more light energy of that wavelength to chemical energy *via* photosynthesis. Because blue light penetrates water to a greater depth than light of longer

wavelengths, phycoeryhtrins allow red algae to photosynthesize and live at somewhat greater depths than most other algae (Talarico and Maranzana, 2000). Moreover, the red algae have plastids with two envelopes where the thylakoids are not stacked since the phycobilisomes attached to them act as spacers. Thus, all thylakoid membranes are biochemically and functionally equal (no lateral heterogeneity as in green algae). Despite the structure, red algae can regulate the allocation of excitation energy between the two photosystems very efficiently (Häder et al., 1998c).

1.2 Ultraviolet radiation (UVR) and the ozone layer

Sun radiation, in a broad sense is the total spectrum of the electromagnetic radiation given off by the sun. On earth, sunlight is filtered by the atmosphere of what we perceive as daylight. The electromagnetic spectrum covers a wide range of wavelengths and photon energies. The photons with the highest energy correspond to the shortest wavelength (λ). Regions in the electromagnetic spectrum include (in order of decreasing wavelength): radio waves, microwaves, infrared, visible (VIS) light, UV radiation (UVR), X-rays and gamma-rays. Human eyes, cannot detect all types of electromagnetic radiation except for VIS as the colour of the rainbow. VIS corresponding to PAR (λ= 400-700 nm) is primarily utilized in photosynthesis by the photoautotrophs including the algae. UVR is divided into three types depending on the λ. According to the definition put forward at the Copenhagen meeting of the Second International Congress on Light held during August 1932, UVA is emitted at λ between 315 and 400 nm, UVB at 280-315 nm and UVC at 100-280 nm (Diffey, 2002). Environmental and dermatological photobiologists, on the other hand, normally define the λ regions as UVA 320-400 nm, UVB 290-320 nm and UVC 200-290 nm (Diffey, 2002). Due to its short λ, UVR often carry the unfortunate circumstances in having too much energy. This ‘extra’ energy can cause changes in the chemical structure of molecules which can be detrimental to living organisms. In fact, many authors have reported that UVR brought more damage than benefits. Luckily we have the ozone layer which can filter out these harmful UVRs. In addition, apart

from a small portion near the UVA waveband, UVR is not photosynthetically active (Holzinger and Lütz, 2006).

The ozone layer protects the organisms from harmful UVR. Ozone (i.e. molecular formula of O_3) is generated when UVR from the sun reacts with the stratospheric atmosphere and oxygen molecule (O_2) and forms a layer of about 15-45 km above the earth's surface, thus, reducing the penetration of UVR and preventing it from reaching the earth (Peter, 1994). The ozone layer absorbs 93-99% of the sun's UVR. It efficiently filters out most of the detrimental, shortwave UVR, shorter than 280 nm. The absorption coefficient of ozone decreases rapidly at wavelengths longer than 280 nm and approaches zero at about 330 nm (Robberecht, 1989, cited in Hollósy, 2002), Therefore, UVC is completely absorbed by the layer while permitting small amount of UVB to pass through and allows UVA to go through almost unfiltered. Hence, the thinning of the ozone layer can create problems concerning the amount of UVB reaching the earth's surface since UVB is known to have significant biological effects. Generally, each 1% reduction in ozone causes an increase of 1.3–1.8% in UVB radiation reaching the biosphere (Hollósy, 2002). The ozone layer can be depleted by man-made organohalogen compounds, especially chlorofluorocarbons (Ricaud and Lefévre, 2006) and bromofluorocarbons (Schauffler et al., 1993). These highly stable compounds are capable of surviving the rise to the stratosphere, where chlorine (Cl), bromine (Br) and fluorine (Fl) radicals are liberated by the action of UVR. Each radical is then free to initiate and catalyze a chain reaction capable of breaking down the ozone molecules (Turco and Whitten, 1975). The breakdown of ozone in the stratosphere results in the increase in the ground level of UVB radiation.

The first ozone hole in Antarctica was discovered unexpectedly in the late 1970s (Farman et al., 1985, cited in Peter, 1994). In an article by Kane (2008), since it began, the ozone layer in the Antarctic seems to have reached a maximum level in about 1996 and a recovery seems to have occurred thereafter up to 2003 and a relapse occurred in the succeeding years 2004–2006. In addition, ozone depletion in this region had caused irradiances at UVB wavelengths to increase 14-fold (Booth and Madronich, 1994) while the ratio of UVB:PAR and UVB:UVA has increased more than two-fold (Smith et al., 1992). There

is also a steadily increasing evidence that climate change is worsened in the polar regions (Helmig et al., 2007). Severe depletion of stratospheric ozone has also been reported in the Arctic since 1995-1996 (Dahlback, 2002). In the tropics, UVR flux is extremely high due to the low zenith angle of the sun and naturally low concentrations of stratospheric ozone (Holm-Hansen et al., 1993).

The penetration of the sun's energy into natural waters (oceans, lakes, rivers, etc.) is dependent upon the incident solar radiation, the state of the wind-blown surface, bottom reflectance in shallower waters, and the inherent optical properties of the water body (Smith and Mobley, 2007). In turn, the optical properties are dependent upon the absorption coefficient and the volume scattering function of the dissolved and suspended material within the water (Smith and Mobley, 2007). Higher concentration of these materials can be found in coastal waters compared to the open ocean (Hanelt et al., 2003). Therefore, large temporal changes and regional differences in the concentration of dissolved and particulate matter are expected in coastal waters which will influence the penetration of the solar radiation (Hanelt et al., 2003). UVB does not generally penetrate very deeply into the coastal water body due to the dissolved organic matters and the wavelength dependent absorption in the water column (Hanelt et al., 2000). This also includes water bodies that are turbid. In clear water like the open ocean, UVB might penetrate to tens of meters (Smith et al., 1992). Moreover, any activity that increases water clarity could increase exposure of vast majority of aquatic organisms to UVB (Little and Fabacher, 2003). In general, species that are naturally adapted to high levels of solar radiation exposure would be more tolerant to high levels of UVB than species not naturally adapted (i.e. in deep waters). For instance, macroalgae living in the intertidal zone are, in general, a group especially vulnerable to solar radiation because they are exposed to fluctuating radiation regimes during the day as a consequence of their growth site which in turn are associated to tide levels (Hanelt et al, 2003). The algae are completely exposed to solar radiation during low tide while during high tides, they are partial or completely submerged. In addition, these macroalgae may be exposed to relatively high radiation levels, especially when low tides coincide with the local noon.

1.3 Mechanisms of photosynthetically active radiation- (PAR-) and UVR-induced photoinhibition

PAR and UV are basically considered as non-ionizing (Kovács and Keresztes, 2002). Being non-ionizing radiations, PAR and UV photons only have sufficient energy to cause excitation and induce photochemical reactions or accelerate radical reactions. Subsequently, these processes will elicit the biological effects observed in affected organisms. However, UV differs from PAR in a way that it can also ionize certain types of molecules under specific conditions (Kovács and Keresztes, 2002). Thus, both PAR and UVR can induce different types of biological effects. UVB, for instance, is known to cause damage to nucleic acid, DNA, RNA, proteins, lipids and other important biological materials which are in turn will affect the ultrastructure, biomass, growth, photosynthesis, productivity, mobility and survival of the aquatic organisms (see Häder et al., 1998a; Häder, 2000; Sinha et al., 2001; Xue et al., 2005; Holzinger and Lütz, 2006; Roleda et al., 2007 for reviews). Unlike the wealth of informations gain from UVB, there is not much information on the impact of UVA. Even though it has less energy than UVB, UVA is also able to induce comparable damaging effects on living organisms. In fact, it has been proven that UVA can induced similar effects as UVB (Turcsányi and Vass, 2000; Vass et al., 2002). This is of ecologically important since not only the sunlight contains more UVA than UVB, UVA can penetrate at greater depths into the leaves than UVB as well where more significant damages may occur (Day et al., 1994). In some environments, UVA has been reported to be responsible for a major fraction of photoinhibition but UVA may also be beneficial for attenuating UVB effects (Quesada et al, 1995; Han et al., 2001; Joshi et al, 2007).

Among the various physiological processes affected by PAR and UVR, photosynthesis is potentially the main target, not only in the aquatic but also in the terrestrial ecosystems (see Sullivan and Rozema, 1999 and Kakani et al, 2003 for reviews). An excess of energy brings about the inactivation of photosynthesis, a phenomenon known as photoinhibition (see Powles, 1984; Long et al, 1994; Hanelt, 1996; Alves et al., 2002; Adir et al., 2003; Murata et al., 2007 and Takahashi and Murata, 2008 for reviews). Excess energy, in this context, has been defined as energy that is absorbed by photosystem II (PSII) but is neither used in

photochemistry nor safely dissipated by light-inducible non-photochemical quenching (Demmig-Adams et al., 1996). Thus, photoinhibition is defined as the light-dependent reduction in photosynthetic efficiency (light-limited photosynthesis) occurring when photons are absorbed in excess of those which can be used for photosynthesis (Powles, 1984; Long et al, 1994; Osmond, 1994). The extent to which the photosynthetic apparatus is affected by light stress is explained by two types of photoinhibition, dynamic and chronic photoinhibition. Dynamic photoinhibition is a down-regulation process of photosynthetic apparatus associated with dissipation of excess energy as heat (Osmond, 1994; Osmond and Grace, 1995; Hanelt, 1996). In addition, down-regulation process maintains the balance between energy source and sink required for controlled metabolic activity, preventing irreversible damage to cellular components (Franklin and Forster, 1997). This type of photoinhibition is considered as a photoprotective mechanism allowing the recovery of photosynthetic activity as soon as excess radiant is removed (Osmond, 1994; Hanelt, 1996). Chronic photoinhibition, on the other hand, is characterized by a slowly reversible loss of PSII reaction centres in which repair and recovery takes many hours or days (Osmond, 1994; Osmond and Gracie, 1995).

In natural conditions, quantity of PAR impinging on photosynthetic organisms is usually far in excess of that needed to saturate photosynthesis and high PAR and UVB are inextricably linked with each other. According to Roy (2000), cells can sense an increase in light intensity in the UVA and PAR ranges, and respond to it but they cannot sense an increase in UVB range unaccompanied by concurrent increases in other wavelengths ranges as is the case with ozone depletion. Thus, photoinhibition can be caused either by PAR or by UV or by interaction between PAR and UV (Powles, 1984). However, Hanelt and co-workers (2003) had pointed out that UVR, cannot be regarded as being an ‘excessive energy input’ in a proper sense since the maximal irradiance of UVR is much smaller than PAR and the UV wavebands do not contribute considerably to the photosynthetic energy supply. An increasing body of evidence indicates that photoinactivation due to PAR and that due to UV are only partially related phenomena, as inactivation occurs at different sites of the photosynthetic electron transport chain (ETC). Hence, it is

important to be able to distinguish between the two effects and to be able to determine whether the response to one type of radiation stress affects the response to the other (Franklin and Forster, 1997).

The main molecular target site of photoinhibition is the PSII reaction centres (Long et al., 1994). The oxygen electron complex (OEC) of PSII, which is responsible for oxidation of water and donates electrons to P680 *via* a redox active tyrosine residue Tyr-Z of D1 protein, is particularly sensitive to PAR (Hakala et al., 2005; Ohnishi et al., 2005; Tyystjärvi, 2008) and UV (Vass et al., 1996; Turcsányi and Vass, 2000; Zsiros et al., 2006; Szilárd et al., 2007). It has been demonstrated that photoinhibition, either by PAR or UVR, begins with the inactivation of OEC and when this reaction is completed, only than that subsequent inactivation event occurs at the other parts of PSII ETC by light that is absorbed by chlorophylls (Chls) (Hakala et al., 2005; Ohnishi et al., 2005). In the latter case, photoinactivation of PSII is mainly due to D1 protein, which forms a dimer with D2 protein at the reaction centre, and subsequent rapid degradation of the protein (Barber and Andersson, 1992; Aro et al., 1993; Long et al., 1994).

In photosynthesis, light is absorbed by photosynthetic pigments acting as photoreceptors. The absorbed light can induce adverse effect on a biomolecule which usually happens through the formation of a triplet state of a sensitizing chromophore or photoreceptor (Lesser, 2006). The photosensitize chromophore may become damaged itself or may damage other neighbouring molecules. The excited photosensitizers can induce cellular damage by two mechanisms: (a) electron transfer and hydrogen abstraction processes to yield free radicals (Type I); or (b) energy transfer with O_2 to yield the reactive excited state, singlet oxygen ($^1O_2$) (Type II) (Pattison and Davies, 2006). Chl, for instance, is a potent photosensitizer in which triplet Chl (^{3}Chl) is formed when light is absorbed which will subsequently activate O_2 to form $^1O_2$ while returning to its ground state. This will occur when the energy from ^{3}Chl is not immediately quenched by other Chl or carotenoids in its vicinity to be utilized in photosynthesis. Accumulation of $^1O_2$ and other reactive oxygen species (ROS) such as superoxide radical (O_2^-), hydrogen peroxide (H_2O_2) and hydroxyl radical ($OH^\bullet$) create an 'oxidative burst' which often occurs when photosynthetic organisms are under stress. During photoinhibition by PAR and UV, both $^1O_2$ and O_2^- are produced, PAR inducing mainly

production of $^1O_2$ while UV-photoinhibition preferentially induces production of O_2^- (Hideg et al., 2000; Tyystsjärvi, 2008). In addition to Chl, a wide range of molecules in the PSII centres can act as photosensitizers to UV. These include the plastosemiquinones (Rodrigues et al., 2006) and manganese complex (Barbato et al., 1995).

A common characteristic of the different types of ROS is the ability to cause oxidative damage to proteins, DNA and lipids (Nishiyama et al., 2001; He and Häder, 2002; Apel and Hirt, 2004; Lesser, 2006), thereby affecting the photosynthetic apparatus as a whole. Thus, the damage to photosynthetic apparatus induces the inhibition of photosynthesis that is mediated partially by ROS. However, it has been reported that ROS increase the extent of photoinhibition by inhibiting the synthesis of PSII proteins needed for repair and not by accelerating the photodamage to PSII (Nishiyama et al. 2001; Nishiyama et al, 2006; Murata et al., 2007 for review). For instance, ROS has been linked to the inhibition of translation of *PsbA* gene which encodes the precursor to D1 protein as well as other proteins needed for PSII repair (Nishiyama et al., 2001; Nishiyama et al., 2006).

There are two well-characterized mechanisms that explain the photoinhibition by PAR. In the acceptor-side photoinhibition, impairment of Q_A and Q_B electron acceptors promotes the formation of P680 triplet from which $^1O_2$ is formed, with the subsequent induction of oxidative damage to the D1 protein (Vass et al., 1992). Triplet P680 may also forms through the recombination reactions between the quinone acceptors and the S_2 and S_3 states of OEC leading to $^1O_2$-induced damage which can be observed under low light intensities and during flash illumination (Keren et al., 1997). Donor-side photoinhibition, on the other hand, results from the impairment of electron transfer between the manganese cluster of OEC with $P680^+$ leading to accumulation of highly oxidizing cations such as $P680^+$ and/or $TyrZ^+$ which can provide driving force for direct photochemical cleavage of the protein (Aro et al., 1993). However, so far there is no direct evidence that PAR itself could damage the donor-side of PSII in initially intact samples and could lead to donor-side induced photoinhibition without pre-inactivation of the manganese cluster (Sicora et al., 2003). Anderson (2001) on the other hand, has proposed that PAR could inactivate the PSII

donor-side, which then would convert the reaction centre into a conformation that facilitates $^1O_2$ formation. Furthermore, in a review by Tyystjärvi (2008), it has been suggested that the manganese cluster could be impaired by PAR in a low efficiency process *via* the same mechanism as induced by UV. Whilst acceptor-side photoinhibition requires high light conditions to occur, donor-side photoinhbition can occur under both low and high light (Aro et al., 1993).

Comparatively, the primary target of UVA and UVB is at the donor-side of PSII, at the level of the manganese cluster of water oxidation (Vass et al. 1996; Turcsányi and Vass, 2000). In addition, UVR affects the Tyr-Z and Tyr-D electron donors, thus both D1 and D2 proteins of PSII can become inactivated (Melis et al., 1992; Friso et al., 1994a,b; Vass et al., 1996; Vass et al., 2002), as well as the quinone electron acceptors Q_A and Q_B (Vass et al., 1999). Like PAR photoinhibition, increased degradation of D1 protein is a major effect of UV photodamage, but UVB has multiple effects on the photosynthetic apparatus, including loss of plastoquinones (Melis et al. 1992; Barbato et al., 1995), photosynthetic pigments (Strid et al., 1990; Lao and Glazer, 1996; Rinalducci et al., 2006; Zvezdanović et al., 2009), the Calvin cycle enzymes ribulose-1,5-bisphosphate carboxylase/oxygenase (RuBisCO) (Wilson et al., 1995; Ferreira et al., 1996; Bischof et al., 2000a; Bischof et al., 2002a) and glyceraldehyde-3-phosphate dehydrogenase (GAPDH) (Bischof et al., 2000a) and membrane components (He and Häder, 2002).

A wider range of biological effects are observed with UV-induced photoinhibition since UV can mediate damage *via* two different mechanisms: (a) direct absorption of the incident radiation by the cellular components (i.e. acting as chromophores), resulting in excited state formation and subsequent chemical reaction, and, (b) similar to PAR-induced photoinhibition, by photosensitization mechanisms, where the radiation is absorbed by endogenous (or exogenous) sensitizers that are excited to their triplet states. Nucleic acids and proteins are very effective UV absorbers. For instance, DNA bases can directly absorb incident quanta in the λ range of 290-320 nm (Ravanat et al., 2001) resulting in two major classes of UVB-induced DNA lesions: the most abundant and cytotoxic cyclobutane–pyrimidine dimers (CPDs) and

the potentially lethal mutagenic 6–4 photoproducts (6–4PPs, which are pyrimidine adducts) (Sinha and Häder, 2002; Britt, 2004). These DNA lesions, if unrepaired, may interfere with DNA transcription and replication and can lead to misreading of the genetic code and cause mutations and death. Different from UVB, UVA is less efficient in inducing DNA damage because it is not absorbed by native DNA (except at around λ of 360 nm) but can still produce secondary photoreactions of existing DNA photoproducts or damage DNA *via* indirect photosensitizing reactions (Ravanat et al., 2001; Sinha and Häder, 2002).

Most proteins only absorb UV relatively weak in the region of the spectrum to which they are often subjected (i.e. $\lambda > 290$ nm). Furthermore, they do not typically contain any functional groups which absorb at $\lambda \geq$ ca. 320 nm (Davies, 2003). However, aromatic amino acids tryptophan (Trp), tyrosine (Tyr), phenylalanine (Phe), histidine (His), cysteine (Cys) and cystine have strong absorption at about 280 nm, and also at higher λ of the UVB region and thus can be direct targets of UVBR (Vass et al, 2005). All other major amino acids do not absorb significantly at $\lambda > 230$ nm and peptide bonds only exhibit a weak absorption band at 210-220 nm resulting in an insignificant absorption of UV by the protein backbone (Davies, 2003). However, some oxidation products (e.g. of Trp) or derivatives of the chromophoric amino acids are more efficient sensitizers (Davies, 2003).

Similar to DNA, photo-oxidation of proteins can occur *via* two major routes. The first is direct photo-oxidation whereby the protein structure or bound chromophores absorb UVR generating excited state species or radicals as a result of photo-ionisation, which is only a significant process if the incident radiation is absorbed by the protein. The second involves indirect oxidation of the protein *via* the formation and subsequent reactions of $^1O_2$ generated by the transfer of energy to ground state (triplet) O_2 by either protein-bound, or other chromophores (Davies and Truscott, 2001; Davies, 2003). Photo-oxidized proteins may undergo: an increase in susceptibility of the oxidized protein to proteolytic enzymes; alterations in mechanical properties; an increased extent or susceptibility to unfolding; changes in conformation; an increase in hydrophobicity; altered light scattering properties and optical rotation; and changes in binding of co-factors and metal ions (Davies and Truscott 2001; Davies 2003).

Irrespective of the underlying mechanism of damage, the structure and functions of photodamaged PSII centres can be repaired. The critical step in the repair process involves the *de novo* synthesis of damaged D1 protein subunit. When the rate of damaged D1 protein exceeds that of its repair process, photodamage or chronic photoinhibition will occur (Aro et al., 1993; Hanelt, 1996). Thus, the extent of recovery from chronic photoinhibition depends on the synthesis of new protein D1 and on the reassembly of repaired PSII centres (Aro et al., 1993). The D1 'damage-repair cycle' constitutes of photodamage to D1 followed by, a prompt and partial disassembly of the PSII holocomplex; exposure of the photodamaged PSII core to the stroma of the chloroplast; degradation of photodamaged D1; *de novo* D1 biosynthesis and insertion in the thylakoid membrane and finally, re-assembly of the PSII holocomplex, followed by activation of the electron-transport process through the reconstituted D1/D2 heterodimer (Aro et al., 1993; Melis, 1999). The activity of UV-photoinhibited PSII is restored *in vivo via* a similar repair process that restores the activity of PSII after PAR photoinhibition. In addition, protein repair of PSII is induced and regulated by both UVB and PAR, and can potentially influence each other's effects in PSII repair (Sicora et al., 2003).

On a last note, ameliorating effects of UVB had recently been reported in several aquatic plants of New Zealand (Hanelt et al., 2006), in marine macrophytes growing on the coastal barrier reef of Belize (Hanelt and Roleda, 2009) and in a Mediterranean brown alga (Flores-Moya et al., 1999), which is of ecologically important phenomena.

1.4 Defence and protection mechanisms against UVR

Sessile organisms such as seaweeds are not able to avoid harmful irradiation by moving to deeper regions or shaded locations. Therefore, they have developed a panoply of protective mechanisms to avoid the harmful UVR. Four mechanisms have been identified that protect organisms against UV damage namely, avoidance, screening, quenching and repair and these protective mechanisms may operate in concert

(Roy, 2000). In avoidance mechanism, a plant suddenly exposed to high light, for instance, may reduce the amount of absorbed light by changing the orientation of its chloroplast (Hanelt and Nultsch, 1990; Hanelt and Nultsch, 1991; Takagi, 2003). In red algae, changes in the morphology, for example in the branching of the thalli and thickness of the cell wall, were observed in response to various light regimes. These changes may be interpreted as a way for the algae to increase surface area of its cell wall that it presents to the incident light and also as a defence mechanism against excess light (Talarico and Maranzana, 2000). Some algae can even secrete excess H_2O_2 into its surrounding thus minimising the occurrence of oxidative damage (Choo et al., 2004; Shiu and Lee, 2005).

UVB screening pigments are considered as the first line of defence against UVB-induced damage. These screening pigments must absorb in the UVB range and also allows other wavelengths to pass through (Jordan, 2002). Mycosporine-like amino acids (MAAs), for instance, are water-soluble substances characterized by a cyclohexenone or cyclohexenimine chromophore conjugated with the nitrogen substituent of an amino acid or its imino alcohol, having absorption maxima in the UVB and UVA regions between 310 and 360 nm (Sinha et al., 1998). They are synthesized in a wide variety of marine organisms including the macroalgae (Gómez et al., 1998; Karsten et al., 1998; Bischof et al., 2000b; Kräbs et al., 2002; Helbling et al., 2004), cyanobacteria (Sinha and Häder, 2008) and the dinoflagellate (Montero and Lubián, 2003). It has also been demonstrated that MAAs can serve as antioxidants for protection against photo-oxidative stress induced by free radicals and other active oxygen species (Dunlap and Yamamoto, 1995). Scytonemin, a yellow-brown lipid-soluble dimeric pigment, also functions as UV-photoprotectant in cyanobacteria. It has an *in vivo* absorption maximum at 370 nm while purified scytonemin has a maximum absorption at 386 nm but also absorbs significantly at 252, 278 and 300 nm (Sinha and Häder, 2008). Additionally, UVB induce the production of phlorotannins in brown algae suggesting that they might also play a role in chemical UV defence (Pavia et al., 1997).

An essential part of the protective mechanisms relies on the presence of carotenoids. In most of the photosynthetic organisms, for example, a process known as non-photochemical mechanism is activated to

quench singlet-excited Chl and harmlessly dissipate excess excitation energy as heat. These processes help to regulate and protect photosynthesis in environments in which light energy absorption exceeds the capacity for light utilization (Müller et al., 2001). It is believed that these processes are activated *via* several reversible pathways that utilize conversion of epoxidized xanthophyll (X), an oxygenated carotene, to its deepoxidized states. For instance, in the violaxanthin (V) cycle that is dominant in higher plants, green algae and brown algae, V is deepoxidized to anteraxanthin (A) then to zeaxanthin (Z) by V deepoxidase (Niyogi et al., 1997; Havaux and Niyogi, 1999; Jin et al., 2003; Masojídek et al., 2004). The other types of X cycle existed are: the diadinoxanthin (Ddx) cycle, converts Ddx to diatoxanthin (Dtx) by Ddx deepoxidase which can be found in the Chromophytes (Goss et al., 1999; Lohr and Wilhelm, 1999) and lutein epoxide (Lx) cycle, involving interconversion of Lx to lutein in some plant species (García-Plazaola et al., 2007). However, it should be noted that the presence of V cycle in the red algae is controversial and has not yet been conclusively demonstrated. Changes in the concentration of VAZ pigments under different light conditions have been determined in the red alga by Rmiki et al. (1996) but the X composition was unchanged in other experiments (Marquardt and Hanelt, 2004; see Schubert and Garcia-Mendoza, 2006 for red algae carotenoid composition). Simultaneously, plants can prevent the build up of electrons in the ETC by providing alternative electron acceptors when carbon dioxide is limiting. These alternative electron transport pathway may direct excess electrons either to water *via* a water-water cycle (Mehler reaction) (Miyake et al., 2002; Miyake et al., 2004; Miyake et al., 2005) or to oxygen *via* a chlororespiratory or photorespiratory pathway (Bennoun, 2001; Noguchi and Yoshida, 2008).

In addition to light harvesting and thermal quenching roles of carotenoids, they can also function as antioxidants (Murthy et al., 2005; Lee and Shiu, 2009). Antioxidants such as carotenoids, ascorbic acid (AsA), glutathione (GSH) and α-tocopherol constitute the non-enzymatic pathways for detoxification or scavenging of ROS while the enzymatic pathway consists of the antioxidative enzymes, among others, superoxide dismutase (SOD; EC 1.15.1.1), catalase (CAT; EC 1.11.1.6), ascorbate peroxidase (APX; EC 1.11.1.11) and glutathione reductase (GR; EC 1.6.4.2) (see Niyogi, 1999 for reviews). Thus, the steady-

state level of ROS in the different cellular compartments is determined by the interplay between multiple ROS-producing pathways, and ROS-scavenging mechanisms. SOD is considered as the first line of detoxifying enzymes that converts O_2^- to a less toxic H_2O_2. Then, APX degrades H_2O_2 *via* AsA oxidation and oxidized AsA, such as dehydroascorbate (DHA), is reduced to regenerate AsA by dehydroascorbate reductase (DHAR; EC 1.8.5.1) using GSH as the electron donor (Asada, 1999). Oxidized GSH, GSSG, is reduced to GSH by GR utilizing reducing equivalents from NAD(P)H. Catalase (CAT; EC 1.11.1.6) is also responsible for H_2O_2 removal (Willekens et al., 1997).

Existence of antioxidants as well as induction of antioxidative enzymes are evident in cells that are experiencing photo-oxidative stress (Aguilera et al., 2002b; Dummermuth et al., 2003; van de Poll et al., 2009). For instance, in green algae that are inhabiting the upper part of the shore at the Kongsfjord in Spitsbergen, Norway, the amount of AsA and the antioxidative enzymes, SOD, CAT, APX and GR were found to be high, suggesting that this species have developed an efficient biochemical defence system when exposed to drastic and rapid changes in environmental radiation conditions (Aguilera et al., 2002b). Activities of SOD, CAT, APX and GR were stimulated in thalli of the red alga *Polysiphonica arctica* exposed to various concentrations of H_2O_2 while the content of AsA was reduced under high H_2O_2 (Dummermuth et al., 2003).

By having a network of repair mechanisms, UVB-induced DNA damages are corrected, for example, by nucleotide excision repair and photoreactivation (see Britt, 2004; Häder and Sinha, 2005 and Weber, 2005 for reviews). Of importance is the process photoreactivation which utilizes the enzyme photolyase which reverses the damage with the help of UVA and blue light (Heelis et al., 1995; Sancar, 2000; Carell et al., 2001). Photolyase binds to UV-DNA in the dark and is released upon illumination with VIS from the repaired DNA (Sancar, 2000). Photoreactivation in terms of reversing the effect of UVB by UVA/blue light was demonstrated in *Anabaena* sp. (Han et al., 2001). After exposure to moderate levels of UVB irradiation, subsequent exposure to white light caused recovery of Chl fluorescence yield in this species. This photoreactivation of UV-induced inhibition of photosynthesis increased in proportion to the

irradiance of white light and is wavelength-dependent, showing significant recovery in blue light compared to no measurable recovery at other photosynthetically active wavebands.

Another key component that functions during the repair cycle is the heat shock proteins (HSPs) or currently known as stress proteins. Normally, HSPs serve as molecular chaperones which are responsible for protein folding, assembly, translocation and degradation in a broad array of normal cellular processes; they also function in the stabilization of proteins and membranes, and can assist in protein refolding under stress conditions (see Georgopoulos and Welch, 1993; Feder and Hofmann, 1999; Bierkens, 2000 and Wang et al., 2004 for reviews on HSPs). Some HSPs are constitutively expressed, they are present at lower concentrations in normal conditions, and some are inducible by the presence of proteotoxic stressors (Bierkens, 2000; Sharkey and Schrader, 2006). Families of HSPs include HSP100, HSP90, HSP70 (or DnaK), HSP60 (or GroEL) and small HSPs. Two widely studied HSPs are the HSP70/DnaK and HSP60/GroEL. Early studies on HSP60 relate this chaperones with that of RuBisCO (Bertsch et al., 1992; Schneider et al., 1992; Schmitz et al., 1996; Houtz and Portis, 2003; Yong et al., 2006; Salvucci, 2008) but other functions of HSP60 and its homologs are reported (Madueno et al., 1993; Tsugeki and Nishimura, 1993; Naletova et al., 2006). HSP70 also helps in the assembly of RuBisCO subunit (Portis, 2003) in addition to the repair of the photosynthetic machinery (Madueno et al., 1993; Kettunen et al., 1996; Schroda et al., 1999; Ivey III et al., 2000; Schroda et al., 2001; Yokthongwattana et al., 2001; Aarti et al., 2006). The role of small HSPs in photosynthesis had been reported as well (Heckathorn et al., 1999; Nakamoto et al., 2000; Heckathorn et al., 2004).

1.5 A short note on UVR studies of algae

1.5.1 UV lamps and the sun simulator

There have been hundreds of studies on the impacts of UVB on the algae. Some involved a single species or genus (for e.g., Gómez and Figueroa, 1998; Altamirano et al., 2000; Han et al., 2003; Gómez et al., 2005; Han and Han, 2005; Villafañe et al., 2005; Fredersdorf and Bischof, 2007; Aguilera et al., 2008), some dealt with multiple species (for e.g., Dring et al., 1996; Hanelt et al., 1997; Bischof et al., 1998a,b; Hanelt, 1998; Bischof et al., 2000b; Brouwer et al., 2000; Dring et al., 2001; Aguilera et al., 2002a,b; Hanelt and Roleda, 2009) and only a handful on algal communities and ecosystems (for e.g., Bischof et al., 2002a,b; Bischof et al., 2003; Gómez et al., 2004).

Most of these studies were short-term, over a few hours or a few days in growth chambers (for e.g. White and Jahnke, 2002; Roleda et al., 2004a; Roleda et al., 2005; Roleda et al., 2006b,c) or in outdoor culture tanks (for e.g. Aguirre-von-Wobeser et al. 2000, Cabello-Pasini et al. 2000) or even under field conditions (for e.g. Cordi et al., 1999; Dring et al. 2001; Häder et al., 2001a,b; Aguilera et al., 2002a;, Gómez et al., 2004). Even though experiments done in growth chambers have many advantages, such as we can manipulate the environmental variable conditions (i.e. temperature, CO_2 or light levels), these often underestimate UVB effects (Shen and Harte, 2000). Nevertheless, results obtained from several studies suggest that different plant species show large differences in sensitivity to UVB, thus it is difficult to extrapolate results, for instance, from chamber studies of single-species response to UVBR alteration to whole-ecosystem response (Shen and Harte, 2000). In addition, according to Brouwer and co-workers (2000), in field investigations, not only the UVR increased but also PAR and this is a disadvantage since ozone depletion results in increase only in UVB, changing the PAR:UVR ratio.

For many experimental studies in photobiology it is simply not practicable to use natural sunlight and so artificial sources of UVR are designed to simulate the UV component of sunlight (Diffey, 2002). Nonetheless, no such source will match exactly the spectral power distribution of sunlight and as the shorter UV wavelengths (less than around 340nm) are generally more photobiologically active than longer UV wavelengths, the usual goal is to match as closely as possible the UVB and UVAII (320-340 nm) regions (Diffey, 2002). The artificial UVR sources are based on either optically filtered xenon arc

lamp or fluorescent lamps (Diffey, 2000) with the latter are commonly utilized as convenient source of energy in photobiological experiments (Brown et al., 2000).

The development of fluorescent sunlamps greatly improved the ability to perform UV-related studies due to their low cost, facile set up, and ease of replacement (Brown et al., 2000). A drawback is that their output is a poor representation of the solar spectrum. In particular, the lamps emit a small but significant amount of UVC which is not found in sunlight at the surface of the earth since UVC is mainly absorbs by ozone (Gast et al., 1965, cited in Brown et al., 2000). Comparison between these sunlamps (e.g. Kodacel and FS-40 sunlamps) with an energy source designated as UVA-340, had made Brown and co-workers (2000) as well as Nakano and co-workers (2001) to conclude that the unfiltered sunlamps are inadequate source for mimicking the environmental relevant UVB and shorter UVA wavelengths while UVA-340 is significantly more relevant to natural sunlight. For reference, Q-panel UVA-340 lamps output closely matches the spectrum of natural sunlight over the range of 295-350 nm (Bischof et al., 1998b; Brown et al., 2000 and Tripp et al., 2003 for examples of spectral irradiance of UVA-340). Thus, UVA-340 lamps have been widely used nowadays in studies emanating from various aspects of UVR effects, among others, in acclimation study (Bischof et al., 1998a), on ultrastructure (Poppe et al., 2002; Poppe et al., 2003), on growth (Michler et al., 2002; Roleda et al., 2004a,b) on sediment loads on the photosynthetic performance (Roleda et al., 2008), on protective mechanisms (Aguilera et al., 2008) and on viability and DNA (Roleda et al., 2004b).

In addition to the fluorescent lamps, one other source of energy, as mentioned earlier, is the optically filtered xenon arc lamp. This type of lamp produces a smooth continuous spectrum in the UV range and has been utilized, for instance, in the solar simulator (Diffey, 2002). The solar simulator basically consists of a source of radiation in which its spectrum is shaped by optical filters or dichroic mirrors in order to obtain varying solar altitudes (Diffey, 2002). However, a drawback is that the arc lamp irradiation field is rather limited and even though it is possible to achieve uniform flux over a larger area, the irradiance will be reduced as well (Diffey, 2002). So, this will become a problem when large numbers of experimental

organisms are to be irradiated all at once. Furthermore, owing to their cost, the solar simulators were not widely used as routine research studies (Brown et al., 2000). Despite the drawbacks, solar simulator can provide an excellent representation of the sun spectrum. Thus, it can be used as an alternative to field investigations.

There are only several studies that employed the solar or sun simulator. Gao and co-workers (2007) for instance, used a solar simulator equipped with a 1000 W xenon arc lamp as a radiation source for the study on the effects of UVR on photosynthesis of the red tide alga *Heterosigma akashiwo.* In another study on a different red tide alga species, constant levels of PAR, UVA and UVB were provided by the solar simulator, also equipped with a 1000 W xenon arc lamp (Wu et al., 2009). Three experimental conditions were setup in the sun simulator for UV exclusion study in order to estimate photoinhibition caused by UVB and short wavelength of UVA in two unicellular flagellate algae (Herrmann et al., 1996). The sun simulator had also been used as a light source on the effects of UVR on photosynthesis of the red alga *Porphyra umbilicalis* grown in the laboratory (Häder et al., 1999). The resulting irradiances of the sun simulator were well below the measured under cloudless skies during the summer at the growth sites of the organism. Rae and co-workers (2001) employed the sun simulator to create PAR and UVR conditions that resemble the subsurface of Lake Coleridge, New Zealand where the freshwater macrophytes used in the experiments inhabit so that comparison can be made between the experimental setup of the sun simulator with natural conditions. Hanelt and co-workers (2006), on the other hand, adjusted the sun simulator to produce a spectrum comparable to the radiation occurring at about 3-7 m depth of three lakes in the South Island, New Zealand.

The last two studies used similar type and model of sun simulator as that applied in this study. In my study, a 400 W metallogen lamp is used as light source in which the spectrum can be adapted to the solar spectrum by adding some rare earth elements. In addition, the ratios of UVA,B:PAR in the sun simulator are comparable to that of the natural solar ratio (Hanelt et al., 2006). Furthermore, various filters can be used to simulate most natural irradiation situations. The sun simulator system used in this study has been

described in detail by Tüg (1996, cited in Hanelt et al., 2006) and Bracher and Wiencke (2000, cited in Rae et al., 2001). Examples of simulated spectrum of the sun simulator in comparison to that of sunlight are displayed in reports by Hanelt and co-workers (2006) and Herrmann and co-workers (1996).

1.5.2 Chlorophyll (Chl) a fluorescence study

Chl fluorescence has become one of the most powerful methods for assessing photosynthetic performance in algae or plant physiological experiments since the first discovery of the 'Kautsky effect' or the dark/light induction phenomena (Krause and Weis, 1991; Horton et al., 1994; Lazár, 1999; Schreiber, 2004). The measurement of Chl fluorescence is rapid, extremely sensitive and non-intrusive, and can be made on intact, attached leaves, as well as isolated chloroplast and subchloroplast particles (White and Critchley, 1999). At room temperature, fluorescence is emitted mainly from Chl a in the PSII reaction centres. The principle underlying the mechanism of Chl fluorescence is rather straightforward. Once the photon is absorbed by molecules of the antenna pigments, the excitation energy is transferred *via* excitons to reaction centres of PSII and PSI. The energy therein is used to drive photochemical reactions that initiate photosynthesis (i.e. photochemical quenching, qP) while excess energy that has not been used is either dissipated as heat (i.e. non-photochemical quenching, qN or NPQ) or emitted as fluorescence (Roháček and Barták, 1999). Thus, by measuring the yield of Chl fluorescence, the changes in the photochemical reaction as well as heat dissipation will be known (Maxwell and Johnson, 2000) as this is essential in estimating the PSII photochemistry of the photosynthesizing cells (Baker, 2008).

The introduction of a measuring system based on the pulse modulation principle by Schreiber and co-workers (1986) has made the measurement of Chl fluorescence possible. By repetitive application of short light pulses of saturating intensity, the fluorescence yield at complete suppression of photochemical quenching is repetitively recorded, allowing the determination of continuous plots of photochemical quenching and non-photochemical quenching (Schreiber et al., 1986). Pulse amplitude modulation (PAM) fluorometers developed based on this principle, use three different lights to manipulate the photosynthetic

apparatus, specifically the Chl a, which in turn emits different quantities of fluorescence (Schreiber, 2004; Ralph and Gademann, 2005). Firstly, a weak measuring light (ML) induces a fluorescence emission without inducing photosynthesis so as to determine the proportion of closed PSII reaction centres. Once a PSII reaction centre captures a photon, it must pass the energy to the ETC before it opens again and captures another photon. The fluorescence emitted (i.e. fluorescence yield) as a result of ML only, is called minimum fluorescence (F_o for dark-adapted and F for light-adapted samples as measured immediately before the saturating pulse). The second light source used to assess photosynthetic activity is a saturating pulse (SP) which is used to close all PSII reaction centres, resulting in a substantially greater fluorescence emission. This is called maximum fluorescence (F_m if dark-adapted or F_m' if light-adapted). Finally, the third light source is used to manipulate the photosynthetic apparatus and is known as actinic light (AL) which is to induce photosynthesis. In dark-adapted macroalgae or plants, PSII reaction centres are opened, ETC to be oxidized, photoprotective mechanisms (xanthophyll cycle) to be relaxed and the trans-thylakoid (ΔpH) gradient to be depleted (Ralph and Gademann, 2005).

The PAM-fluorescence technique allows both quantitative and qualitative informations on organization and functioning of a plant photosynthetic apparatus by analysis of slow and fast Chl fluorescence induction kinetics. The information gain from these kinetics can be decoded by using a set of Chl fluorescence parameters as defined among others, by van Kooten and Snel (1990), Roháček and Barták (1999) and Maxwell and Johnson (2000). For instance, dark-adapted ratio of F_v/F_m (where F_v is F_m minus F_o) has been used to measure the potential electron transfer quantum yield of PSII in the dark-adapted state, i.e. the probability that absorbed photons can drive electrons derived from water through oxidized (or `open') PSII reaction centres. This ratio is influenced by conditions such as the irradiance experienced by the macroalgae prior to the measurement showing the degrees of photoinhibition (Beer et al., 2000).

Data obtained from the fluorescence yield can be visualized by constructing a rapid light curve (RLC) resembling a traditional photosynthesis-irradiance (P-I) curve which provides detailed information on the saturation characteristics of electron transport as well as the overall photosynthetic performance of a plant

(White and Critchley, 1999; Schreiber, 2004; Ralph and Gademann, 2005). In addition, rapid induction and relaxation kinetics can reflect the quantum yield changes (quenching and dequenching) as well as changes in the number of PSII Chl a (Schansker et al., 2006; Zhu et al., 2005; Papageorgiou et al., 2007) showing convincingly how fast the photosynthetic apparatus can respond to the ambient light conditions (Häder et al., 2001b, 2003a and 2004).

1.6 Objectives

Therefore, the objectives of this study are:

1. to determine the degree of photoinhibition in macroalgae exposed to various conditions of PAR and UVR,
2. to evaluate the damaging effects of PAR and UVR stress on photosynthetic enzymes as well as D1 protein,
3. to assess the ability of macroalgae to induce protective mechanism in response to PAR and UVR stress,
4. to evaluate the capacity of stress proteins and antioxidative enzymes inductions in macroalgae in response to PAR and UVR stress,
5. to evaluate the capacity of macroalgae to adapt to the fast changing light conditions *via* analysis of Chl fluorescence kinetics,
6. to compare which macroalgal species examined in this study is photoinhibited the most in various conditions of PAR and UVR examined, and
7. to compare which macroalgal species examined in this study recovers the fastest in various conditions of PAR and UVR examined (i.e. has the most efficient protective mechanisms)

2.0 MATERIALS AND METHODS

2.1 Algal materials

The macroalgae examined were: the Rhodophytes (i.e. the red algae), *Solieria chordalis* (Agardh) J. Agardh and *Palmaria palmata* (L.) Kuntze; the Phaeophytes (i.e. the brown algae), *Laminaria digitata* (Hudson) J.V. Lamouroux and *Dictyota dichotoma* (Hudson) J.V. Lamouroux; and, the Chlorophyte (i.e. the green alga), *Ulva lactuca* (L.) (Fig. 44, Appendix 1). Samples of *S. chordalis* and *P. palmata* were collected from the island of Sylt while *L. digitata*, *D. dichotoma* and *U. lactuca* were collected from the island of Helgoland, both islands located within the North Sea. They were then cultivated at the Biocenter of Klein Flottbek, University of Hamburg. The algae were grown in a temperature-controlled laboratory under white light in a light-dark cycle (see Table 1 below for respective algal culture conditions) at 12.5±0.5˚C in aerated beakers filled with nutrient-enriched seawater after Provasoli (1968) with modifications. Prior to the experiments, the algae were cleaned to get rid of any parasites or unwanted particles which may interfere with the analyses.

Table 1: Cultivation conditions of the algal samples in the temperature-controlled laboratory.

Species	White light irradiance ($\mu mol\ m^{-2}\ s^{-1}$)	Light:dark cycle (h:h)
S. chordalis	1.1-3.3	10:14
P. palmata	16.2-31.8	16:8
L. digitata	14.9-31.2	16:8
D. dichotoma	14.5-31.0	16:8
U. lactuca	14.2-31.9	16:8

2.2 Irradiation treatments

Samples were irradiated either under the fluorescent lamps (Fig. 45, Appendix 2) or the sun simulator (Fig. 46, Appendix 2) to provide two different conditions of photosynthetically active radiation (PAR):

low and high, respectively. For both experiments, samples were irradiated with the corresponding irradiances for 5 h after which they were taken out from the chamber and incubated under dim white light (~0.46 µmol m^{-2} s^{-1} PAR) in the temperature-controlled laboratory for an 18 h recovery period. Measurements for photosynthetic activity and chlorophyll (Chl) a fluorescence kinetics were performed before the irradiation (i.e. pre-irradiation or control), after the 5 h irradiation (i.e. post-irradiation) and after the 18 h recovery (i.e. post-recovery). After the measurements, the samples were blotted dry, weighed and stored at -40˚C until further analyses.

2.2.1 The fluorescent lamps

Individual algal samples were exposed to artificial radiation produced by one natural daylight tube (TRUE-LIGHT 36T8, True-Light Int. GmbH) and one fluorescence tube (UVA-340, Q-Panel, USA) set inside a dark-curtained chamber in a temperature-controlled laboratory (at 12.5±0.5˚C). Both lamps were used to create almost identical conditions of the sun indoors where the daylight tube produced more or less identical full spectrum of the natural daylight while UVA-340 lamp produced a simulation of sunlight in the region from 365 nm down to the solar cut-off of 295 nm (Fig.1). The daylight tube was covered with black wire mesh to produce irradiance of ~25 µmol m^{-2} s^{-1} PAR. Prior to start of the experiment, the lamps were switched on for 30 min to create stable conditions of the radiation. For the experimental setup, the sample was immersed in fresh culture medium (i.e. Provasoli's nutrient-enriched seawater similar to that of culture medium) in a petri dish laid on a step-up ladder. To create maximum possible PAR and ultraviolet radiation (UVR) irradiances, the petri dish was placed at the centre of the lamps with the cut-off filters touching the lamps. Three different irradiation conditions were created by manipulating the horizontal and vertical positions of the petri dish along the lamps (Table 2). The respective irradiances are listed in RESULTS (sections 3.1, 3.3 and 3.4). For each experimental setups, the samples were covered with three different cut-off filters (Schott, Germany) in order to set three different light/UV conditions: GG400 ($\lambda \geq 400$ nm; i.e. PAR alone), WG320 ($\lambda \geq 320$ nm, i.e.

PAR+UVA) or WG295 (λ ≥ 295 nm, i.e. PAR+UVA+UVB) (see Fig. 2A for transmission spectrum of each filters).

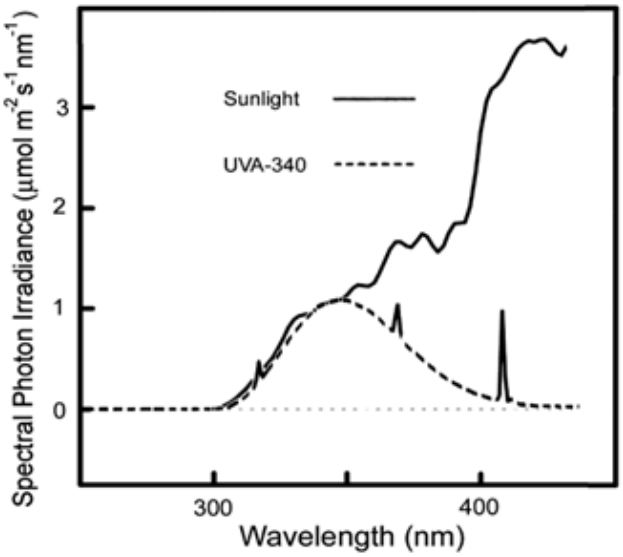

Fig. 1: Example of emission spectrum of UVA-340 lamp compared to the solar spectrum. (Adapted from: Tripp et al., 2003).

Table 2: Irradiation conditions for the fluorescent lamps experimental setup.

Setup	Irradiation conditions	Species studied
L_1 and L_{1B}	Low PAR, high UVA, high UVB	All species
L_2	Low PAR, low UVA, low UVB	*S. chordalis*, *L. digitata* and *U. lactuca*
L_3	Low PAR, medium UVA, medium UVB	*S. chordalis*, *L. digitata* and *U. lactuca*

The lamps radiation measurements were carried out using LI-1000 DataLogger (LI-COR Biosciences, USA) equipped with LI-190 (Q16231) quantum light sensor (400-700 nm) (LI-COR Biosciences, USA) for PAR measurement; and, UVA-Sensor Type 2.5 (310-400 nm) and UVB-Sensor Type 1.5 (265-315 nm) sensors (Indium Sensor, Germany) for UVA and UVB measurements, respectively. The UVA sensor measured the impinging unweighted energy (W m^{-2}) while the UVB sensor measured the erythermal-weighted energy (µW cm^{-2}). Data was converted to unweighted UVB irradiance according to McKenzie and co-workers (2004).

2.2.2 The sun simulator

The sun simulator (SonSi, iSiTEC GmbH, Germany) is as described by Hanelt and co-workers (2006). The samples were positioned in small plastic beakers filled with culture medium and were mounted on a rotating plate within a double-walled, water-filled glass jar. The temperature of the jar was kept at 12.5±0.5°C by a thermostated water jacket. To ensure that all samples received a constant fluence within the slightly inhomogeneous light field, the plate was rotated at 5 rph. The samples were irradiated with irradiance coming from a stabilized 400 W Metallogen lamp (Philips MSR 400 HR) consisting of a number of lanthanide rare earths which emanate a solar-like continuum. The irradiance from the lamp was focused to a parallel beam, and passed from above through a series of optical filters. A wire mesh screen acted as the first filter reducing the irradiance without changing the spectrum. Below the screen were three liquid filters with quartz windows and these were followed by a diffuser plate. The different liquids in the filters were aqueous solution of potassium chromate (K_2CrO_4), copper sulphate ($CuSO_4$) and potassium nitrate (KNO_3). The transmission spectrum of each solution is shown in Fig. 2B. The thickness and the concentration of these solutions can be manipulated so as to create almost natural radiation conditions within the simulator. In this study, three different radiation conditions were set up by manipulating the liquid filters (Table 3). Respective irradiances are listed in RESULTS (sections 3.2, 3.3 and 3.4).

Table 3: Sun simulator experimental setups listing conditions and liquid filters used to create the conditions. Each experiments were carried out using all species.

Setup	Irradiation conditions	Liquid filters used to create conditions
H_1 and H_{1B}	High PAR, high UVA, high UVB	200 mL of 4.6 g/L $CuSO_4$ solution
H_2	High PAR, low UVA, medium UVB	200 mL of 4.6 g/L $CuSO_4$ and 200 mL of 12 mg/L K_2CrO_4 solutions
H_3	High PAR, medium UVA, low UVB	200 mL of 4.6 g/L $CuSO_4$ and 150 mL of 1.5 g/L KNO_3 solutions

In addition, for each experimental setup, four light/UV regimes were created using a number of radiation cut-off glass filters. These filters were similar to that used for the fluorescent lamps experiments but of

different thickness and size (i.e. WG295, WG320 and GG400 of a 2 mm thickness) with additional UG5 filter which filters out the PAR from the irradiance transmittance (λ < 400 nm, i.e. UVA+UVB). The transmission spectrum of each radiation cut-off filters is shown in Fig. 2A.

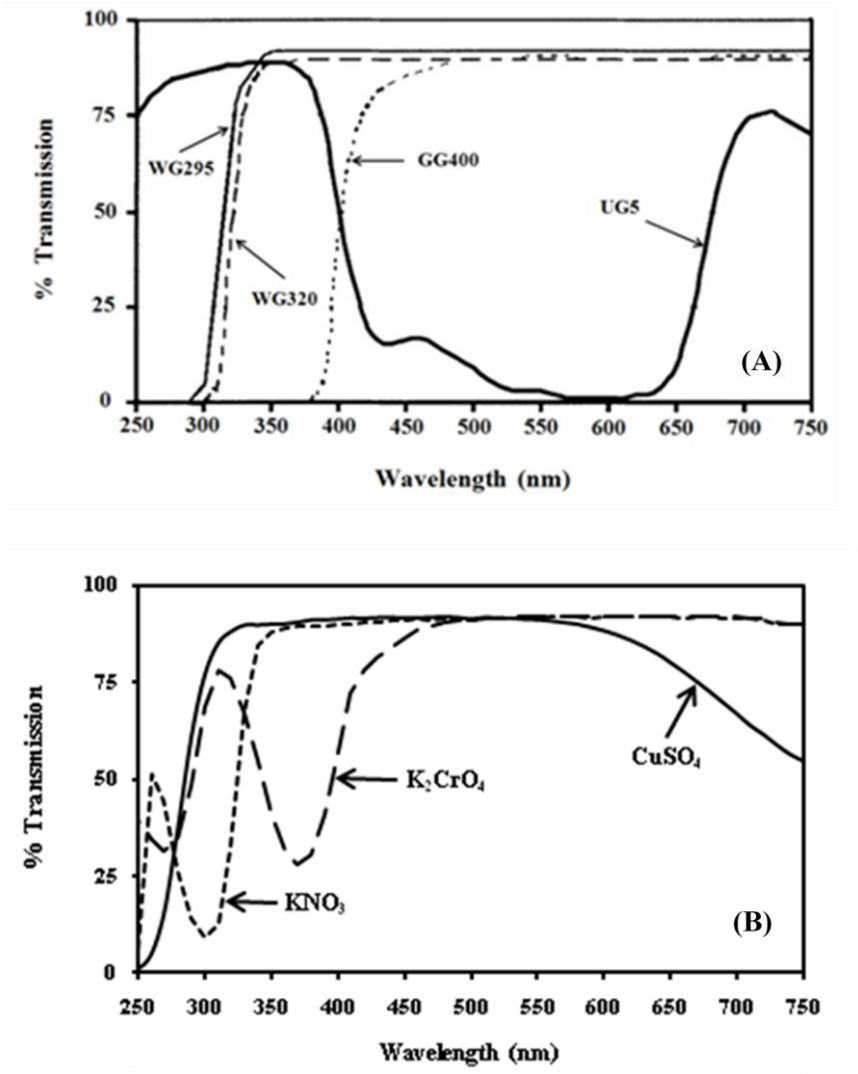

Fig. 2: Transmission spectra of (*A*) Schott cut-off filters: WG295, WG320, GG400 and UG5, used in the experiments, and, (*B*) liquid filters: $CuSO_4$ (4.6 g/L), K_2CrO_4 (12 mg/L) and KNO_3 (1.5 g/L) (see texts for explanation).

The spectrum within the sun simulator was measured using a special SonSi-spectrometer (Isitec, FRG). This spectrometer is equipped with a Zeiss monolithic miniature spectrometer module (MMS) including a diode array with sensitivity from 198 to 738 at about 2.2 nm intervals. The data was analysed by a Sonsi associated program. The data from the Sonsi-spectrometer was calibrated against the above sensors measured with the LI-COR datalogger. Examples of simulated spectra within the sun simulator are shown

in Fig. 3 represented by the four cut-off filters. In addition, Table 4 lists the irradiation conditions within the sun simulator transmitted by the cut-off filters as displayed by the spectra in Fig. 3.

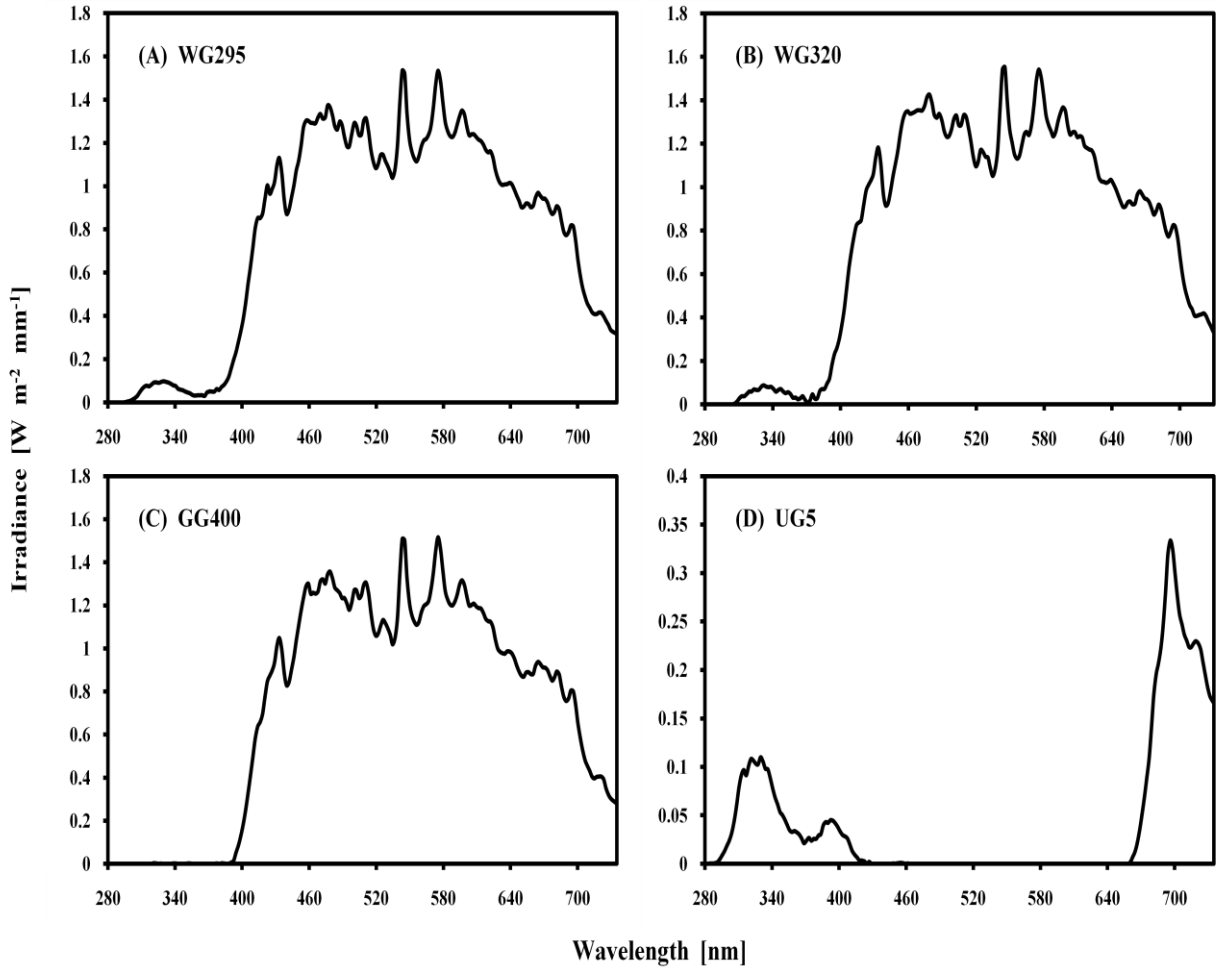

Fig. 3: Example of simulator spectrum representing the full spectrum at about 737 µmol m^{-2} s^{-1} (i.e. 155 Wm^{-2}) PAR, 3.4 Wm^{-2} UVA and 0.49 Wm^{-2} UVB (WG295, *A*), simulated spectrum without UVB (WG320, *B*), without UVR (GG400, *C*) and without PAR (UG5, *D*). See Table 4 for irradiation conditions for each optical filters.

Table 4: Irradiation conditions of the different spectral ranges of the sun simulator with the optical filters WG295, WG320, GG400 and UG5 as shown by the spectrum in Fig. 3.

	PAR (µmol m^{-2} s^{-1})	PAR (W m^{-2})	UVA (W m^{-2})	UVB (W m^{-2})
With filter WG295	737	155	3.4	0.49
With filter WG320	750	158	2.9	0.23
With filter GG400	710	149	0.3	0.00
With filter UG5	15	3	2.1	0.67

2.3 Measurement of photosynthetic performance and chlorophyll (Chl) a fluorescence kinetics

Chlorophyll (Chl) fluorescence was measured with a portable pulse amplitude modulation (PAM) Chl fluorometer, PAM-2000, and analyzed using the saturating-pulse mode and Data Acquisition Software DA-2000 (Walz, Effeltrich, Germany). The sample was mounted on the fiberoptics and immersed in a beaker of culture medium (i.e. Provasoli's nutrient-enriched sterilized seawater). The maximal quantum yield (i.e. F_v/F_m) of the samples was determined according to Hanelt (1998) and Bischof and co-workers (2000a). At the start of the measurement, the red algae were subjected to a 5 s far-red pulse (FR, ~30 µmol m^{-2} s^{-1} at 735 nm) to fully oxidise the electron transport chain and the samples were then kept in darkness for about 5 min so that the energy-dependent fluorescence quenching (qE) and quenching by state transitions (qT) can decline. After the 5 min darkness, a short, red, actinic pulse (AL, ~7 µmol m^{-2} s^{-1} at 655 nm) was prompted for 5 s to ensure a stabilized fluorescence emission during the following F_m measurement. For the red algae, this pulse will excite mainly the photosystem (PS) I, and the onset of the F_m decline during a saturation pulse is delayed (Hanelt, 1998). Following that, a 5-s far-red pulse application was repeated. Then F_o was measured with a pulsed, red measuring light (ML, ~0.3 µmol m^{-2} s^{-1} at 650 nm), and F_m was determined with a 0.6 s, saturating white light pulse (SP, ~9200 µmol m^{-2} s^{-1}). For the brown and green algae, the method was changed slightly. Samples were subjected to a 5-s FR (~30 µmol m^{-2} s^{-1}) and subsequently darkened for 5 min. Then, F_o was measured with a ML (~0.3 µmol m^{-2} s^{-1}) and F_m was determined with a 0.6-0.8 s SP (~9200 µmol m^{-2} s^{-1}). The maximal quantum yield was then calculated as:

$$F_v/F_m = (F_m - F_o)/F_m$$

Immediately after the F_v/F_m determination, rapid photosynthesis vs. irradiance curve (i.e. rapid light curve, RLC) was recorded with the fluorometer. Samples were irradiated with increasing irradiances of actinic red light (PPFD = 7.3-334 µmol m^{-2} s^{-1}) at which for every 30 s, a saturating pulse was applied to measure effective quantum yield of photosystem II (PSII) ($\Delta F/F_m'$) before actinic irradiation was further

increased. Relative electron transport rate (rETR) was calculated by multiplying $\Delta F/F_m'$ by the actinic photon irradiance (PPFD):

$$rETR = \Delta F/F_m' * PPFD$$

rETRs were plotted against irradiance of actinic light and three photosynthetic parameters, $rETR_{max}$ (i.e. maximal relative electron transport rate), α (i.e. initial slope of curve at limiting irradiance) and I_k (i.e. light saturation parameter, a crossing point between α and $rETR_{max}$) were determined according to the hyperbolic tangent model of Jassby and Platt (1976):

$$rETR = rETR_{max} * \tanh (\alpha * E_{PAR} * rETR_{max}^{-1})$$

where $rETR_{max}$ is the maximal relative electron transport rate, tanh is the hyperbolic tangent function, α is the electron transport efficiency, and E is the photon fluence rate of PAR. Curve fit was calculated with the Solver Module of MS-Excel using the least squares method comparing differences between measured and calculated data (Roleda et al., 2006a).

For measurement of Chl fluorescence kinetics, a different portable Chl fluorometer, PAM-2100 (Walz, Germany) was used. PAM-2100 still maintains similar properties of PAM-2000 but with several improved features (Heinz Walz GmbH, 2003). This PAM instrument allows to run pre-programmed experiments operated from an external personal computer (PC) using the PamWin Windows Software program (Software V 1.17, Walz, Germany). All experiments involving the Chl a fluorescence kinetics were done using this program. Prior to the start of the kinetics analysis, the values for F_o and F_m of the samples were determined in a similar manner as that done with PAM-2000 (*vide supra*). This was essential for scaling the Y-axis in F_t/F_m units and as a prerequisite for calculation of fluorescence quenching parameters. Samples were then subjected to RLC recordings on the Light Curve window of PamWin. The recording of RLC consisted of a series of illumination steps (i.e. 11 steps with inceasing red actinic light of 9.3-665 µmol m^{-2} s^{-1}), with a SP being applied at the end of each step (i.e. every 20 s)

for assessment of Chl fluorescence parameters, from which the effective PSII quantum yield (Yield, Y) and the quenching parameters were calculated.

The effective PSII quantum yield was calculated as follows (Genty et al., 1989, cited in Schreiber, 2004):

$$Y = (F_m' - F)/F_m'$$

where F_m' and F are maximal fluorescence yield reached during the last SP and fluorescence yield measured briefly before application of the last SP, respectively, both normally measured in the presence of actinic light (i.e. preilluminated or light-adapted). The photochemical quenching coefficient, qP, due to the utilization of the radiation energy in the photosynthetic apparatus, was determined as (Schreiber, 2004; Ralph and Gademann, 2005):

$$qP = (F_m' - F)/(F_m' - F_o')$$

where F_o' is minimal fluorescence yield of a preilluminated sample, determined briefly after turning off the actinic light and after several seconds of far-red illumination to assure full oxidation of PSII acceptors, and if $F_m' < F$ then qP = 0, and if $F_m' > F_m$ then qP = 1. The non-photochemical quenching coefficients, qN and NPQ, which are due to an increasing pH gradient across the thylakoid membrane were calculated as (Schreiber, 2004; Ralph and Gademann, 2005):

$$qN = 1 - [(F_m' - F_o')/(F_m - F_o)]$$

and if $F_m' > F_m$ then qN = 0, and if $F_m' > F_o$ then qN = 1, and,

$$NPQ = (F_m - F_m')/F_m'$$

and if $F_m' > F_m$ then NPQ = 0. F_m and F_o values used for qN and NPQ calculations were based on control (i.e. before irradiation).

In addition, the excitation pressure and the index of PSII susceptibility to stress were also calculated as 1-qP (Maxwell et al., 1995) and (1-qP)/NPQ (Osmond, 1994), respectively.

On the Slow Kinetics window of PamWin, light-induced changes of fluorescence parameters were plotted against time. From this, a standard dark-light Induction Curve (IC) in combination of a dark Recovery Curve (RC) were recorded. At the start of the recording, ML (~0.3 µmol m^{-2} s^{-1} red light) was switched

on. After a 60 s delay, AL (~300 µmol m^{-2} s^{-1} red light, modulated at 20 kHz) was concurrently switched on and SP (~9660 µmol m^{-2} s^{-1} white light for 0.6-0.8 s) was applied repetitively every 20 s for measurement of F_m'. Immediately after SP, a FR (~50 µmol m^{-2} s^{-1} red light) was triggered for 3 s for F_o' determination. The overall IC recordings took about 5 min at which AL illumination was terminated and RC was investigated with repetitive illumination of SP similar to that of IC but with AL off. After 10 min, SP was switched off and the recordings were terminated.

Rapid dark–light fluorescence induction curve (i.e. Kautsky effect) was recorded on the Fast Kinetics window. Rapid induction curves were determined at two sampling rate, 300 and 1000 µs/data point with total recording of 1.2 and 4 s, respectively. At sampling rate of 1000 µs/data point, after ML (~1.0 µmol m^{-2} s^{-1}) was on, F_o was determined. AL (~430 µmol m^{-2} s^{-1} red light, modulated at 20 kHz) pulse was then activated for 2 s. The recording continued for another 2 s after termination of AL to monitor the dark relaxation kinetics. A similar experimental sequence was determined at 300 µs/data point but with no relaxation kinetics recorded.

2.4 Pigments analysis

Three types of photosynthetic pigments were extracted from the algae: chlorophylls (Chl, i.e. Chls a, b and c), phycobiliproteins (i.e. R-phycoeryhtrin, R-PE and R-phycocyanin, R-PC) and carotenoids (i.e. fucoxanthin). Chl a, being the primary photosynthetic pigment was extracted from all classes of algae examined. The accessory pigments, R-PE and R-PC were extracted only from the red algae, Chl c and fucoxanthin from the brown algae and Chl b was extracted only from the green alga. The concentration of all the pigments was determined photometrically using a UVPC-2101 UV-VIS spectrophotometer (Shimadzu, Japan). The concentration of the pigments was expressed as mg pigments/g fresh weight (FW).

Chl a (except for the brown algae) and Chl b were extracted in 5 mL of dimethylformamide (DMF) for 5 days at 4˚C in darkness (Bischof et al., 2000a). After 5 days, the absorbance of the DMF extracts was measured at 664.5 and 647 nm using DMF as blank. The Chls concentration was measured using these formulae (Inskeep and Bloom, 1985):

$$\text{Chl a (mg/L)} = 12.7*A_{664.5nm} - 2.79*A_{647nm}$$

$$\text{Chl b (mg/L)} = 20.70*A_{647nm} - 4.62*_{A664.5nm}$$

The phycobiliproteins, R-PC and R-PE were extracted according to Beer and Eshel (1985) with some modifications. Algal materials of 0.014 -0.071 g were ground in liquid nitrogen and transferred to 5 mL of 0.1M phosphate buffer (pH 6.8). The extracts were then centrifuged at 1,000*xg* and 4˚C for 10 min. Absorbance of the supernatants was read at 455, 564, 592, 618 and 645 nm using 0.1M phosphate buffer as blank. The concentrations of the phycobiliproteins were determined as follow (Beer and Eshel, 1985):

$$\text{R-PE (mg/mL)} = ((A_{564}-A_{592}) - 0.2*(A_{455}-A_{592}))*0.12$$

$$\text{R-PC (mg/mL)} = ((A_{618}-A_{645}) - 0.51*(A_{592}-A_{645}))*0.15$$

Pigments from the brown algae, Chl a, Chl c and fucoxanthin were extracted according to Seely et al. (1972) with modifications. Algal blades (FW = 0.01 – 0.14 g) were added to 4 mL of dimethylsulphoxide (DMSO) in test tubes. The pigments were allowed to be extracted for 15 min in darkness. After 15 min, the samples were washed with 1 mL distilled water (dH_2O) in a beaker and the wash water was added to the DMSO extract. The samples were then added to 3 mL acetone in new test tubes. The pigments were further extracted for 2 h in darkness. After 2 h, the samples were removed and the acetone extracts were diluted in 1 mL methanol and 1 mL dH_2O. If needed, the samples were incubated again in acetone for total extraction of pigments (i.e. until the algal blade was white in colour). Absorbance for both the extracts at various wavelengths were then measured using mixtures of DMSO:dH_2O (4:1) and acetone:methanol:dH_2O (3:1:1) as blanks for DMSO and acetone extracts, respectively.

The concentrations of the pigments in the DMSO extract were calculated as follow (Seely et al., 1972):

$$\text{Chl a (g/L)} = A_{665nm}/72.8$$

$$\text{Chl c (g/L)} = (A_{631nm} + A_{582nm} - 0.297*A_{665nm})/61.8$$

$$\text{Fucoxanthin (g/L)} = (A_{480nm} - 0.772(A_{631nm} + A_{582nm} - 0.297*A_{665nm}) - 0.049*A_{665nm})/130$$

while the concentrations of the pigments in the acetone extract were calculated as follow (Seely et al., 1972):

$$\text{Chl a (g/L)} = A_{664nm}/73.6$$

$$\text{Chl c (g/L)} = (A_{631nm} + A_{581nm} - 0.3*A_{664nm})/62.2$$

$$\text{Fucoxanthin (g/L)} = (A_{470nm} - 1.239(A_{631nm} + A_{581nm} - 0.3*A_{664nm}) - 0.0275*A_{664nm})/141$$

The total content of the brown algae pigments was calculated by combining the concentrations from both the DMSO and acetone extracts.

2.5 Crude extracts preparation and protein extraction

Extraction of the photosynthetic and antioxidative enzymes was done according to Bischof and co-workers (2000a) and Rautenberger and Bischof (2006), respectively. Samples were taken from -40˚C and added into liquid nitrogen prior to extraction. All crude extracts were stored at -40˚C prior to further analyses.

2.5.1 Photosynthetic enzymes extraction

For the photosynthetic enzymes extraction, the crude extracts were prepared by grinding frozen alga material to a fine powder and transferring it into test tubes containing ice-cold extraction buffer (Bischof et al., 2000a): 0.1M Tris-HCl, 2 mM EDTA, 10 mM $MgCl_2$, 20% glycerol, 2% Triton X-100, 50 mM DTT, 100 mM Na-ascorbate and 10 mM $NaHCO_3$ at pH 7.6. For enzymes extraction in the brown algae, 2% polyvinylpolypyrrolidone (PVPP) (P6755, Fluka) was included in the extraction buffer. The extracts were then incubated in ice for 30 min before centrifugation at 16000 x*g* and 4°C for 2 min.

2.5.2 Antioxidative enzymes extraction

For antioxidative enzymes extraction, the ground algal materials were added to 50 mM potassium phosphate buffer (pH 7.0). One tablet of Complete Protease Inhibitor Cocktail (11697498001, Roche Diagnostics) was also added for every 50 mL of the buffer. Similar to photosynthetic enzymes extraction, 2% PVPP was added to the buffer intended for brown algal antioxidative enzymes extraction. The extracts were centrifuged at 16000 x*g* and 4°C for 15 min. Prior to centrifugation, the extracts were incubated on ice for 30 min.

2.6 Protein content determination

Total soluble protein (TSP) content in both forms of the crude extracts, photosynthetic and antioxidative enzymes, was determined using either a commercial Advanced Protein Assay Reagent (78006, Fluka) or Bradford reagent buffer (B6916, Sigma). The protein content was determined by measuring absorbance at 595 nm using a UVPC-2101 spectrophotometer (Shimadzu, Japan) and calculating the concentration of proteins according to a calibration curve prepared from 1 mg/mL of bovine serum albumin (A2153, Sigma).

2.7 Enzymatic assays

All enzymatic assays were determined photometrically using a UVIKON-943 Double Beam UV/VIS spectrophotometer (Bio-Tek Kontron Instruments) attached to a circulating temperature-constant bath. Assays were carried out according to Bischof and co-workers (2000a) and Gerard and Driscoll (1996) for photosynthetic enzymes assays and Aguilera and co-workers (2002a,b) for antioxidative enzymes assays. All assay mixtures were of 1 mL in volume and assays were carried out at 25˚C. Reaction mixtures were

incubated in the spectrophotometer for 3 min before the start of reaction to allow for temperature equilibration. All enzyme activities were expressed as U/mg TSP.

2.7.1 Photosynthetic enzymes assays

The assay mixture for ribulose-1,5-bisphosphate carboxylase/oxygenase (RuBisCO) activity is made up of 50 mM Hepes (pH 7.8), 10 mM $NaHCO_3$, 20 mM $MgCl_2$, 0.2 mM NADH, 5 mM ATP, 5 mM phosphocreatine, 5 units phosphocreatine kinase (C3755, Sigma), 5 units of GAPDH/PGK (G5537, Sigma) and sample loads containing 25 µL of extract. The assay mixture was then held in the spectrophotometer for temperature equilibration and absorbance was read following that, at 340 nm for 3 min (i.e. Blank). After 3 min, the reaction was started by adding ribulose-1,5-bisphosphate (RuBP) (R0878, Sigma) at final concentration of 2 mM in the cuvette (i.e. Test). The time course of $NADH_2$ oxidation was again recorded by the decrease in absorbance at 340 nm for 3 min. The activity was measured by subtracting the background oxidation of $NADH_2$ in Blanks with the measured enzyme activities in Tests using extinction coefficient of NADH of 6.22 mM^{-1} cm^{-1}.

The activity of glyceraldehyde-3-phosphate dehydrogenase (GAPDH) was also determined by the turnover of $NADH_2$ similar to that done with RuBisCO activity. The assay mixture contained 50 mM Hepes (pH 7.8), 10 mM $NaHCO_3$, 20 mM $MgCl_2$, 0.2 mM NADH, 5 mM ATP, 5 units of phosphoglycerate kinase (P7634, Sigma) and 25 µL sample load. 50 µL of 40 mM 3-phosphoglycerate (79472, Fluka) was added to start the reaction. The activity of GAPDH was measured similar to that of RuBisCO.

2.7.2 Antioxidative enzymes assays

The assay mixture for catalase (CAT) activity consisted of 50 mM potassium phosphate buffer (pH 7.0) and 40 µL of extract. The reaction was started by adding 150 µL H_2O_2 followed by monitoring the

decrease in absorbance at 240 nm for 2 min. CAT activity was calculated by subtracting from non-enzymatic reaction and using extinction coefficient for H_2O_2 of 0.0398 mM^{-1} cm^{-1}.

Ascorbate peroxidase (APX) activity was assayed by monitoring the decrease in absorbance at 290 nm for 1 min after adding 30 µL extract to 50 mM potassium phosphate buffer (pH 7.0) containing 0.1 mM H_2O_2 and 0.5 mM ascorbate. The activity was calculated by subtracting from non-enzymatic reaction and using extinction coefficient for ascorbate of 2.8 mM^{-1} cm^{-1}.

Assay mixture of glutathione reductase (GR) was 50 µL extract in a buffer containing 80 mM Tris buffer (pH 8), 1 mM EDTA, 0.1 mM NADPH, and 0.5 mM GSSG (49741, Fluka), and oxidation of NADPH was followed at 340 nm for 5 min. GR activity was calculated by subtracting from non-enzymatic reaction and using extinction coefficient for NADPH of 6.22 mM^{-1} cm^{-1}.

2.8 Sodium Dodecyl Sulphate-Polyacrylamide Gel Electrophoresis (SDS-PAGE)

Crude extracts from photosynthetic enzymes extraction were taken out from -40˚C and incubated on ice at least 30 min prior to electrophoresis. Proteins in the extracts were separated by SDS-PAGE following the methods of Laemmli (1970). The extracts were mixed with the sample/loading buffer in a ratio of 1 volume buffer to 2 volumes of extract. The volume of crude extracts used corresponds to 10-20 µg of TSP determined as in section 2.6. The samples were then vortexed and heated at ±95°C for 10 min in AccuBlock digital dry bath (Labnet Int. Inc., USA) to denature the protein. The denatured samples were again vortexed and centrifuged at 13000 rpm and 4°C for 5 min. Protein standards and samples were loaded into a 10-well precast polyacrylamide SDS gel (161-1160 Ready Gel Tris-HCl gels, BioRad Lab). The gels were made from 10-20% linear gradient resolving gel with 4% stacking gel. Protein standards used as markers were Precision Plus Protein All Blue standards from BioRad Lab. Electrophoresis was performed in Mini-PROTEAN II cells (BioRad Lab) at 200V constant until the blue band was almost at

the end of the gel. Afterwards, proteins from the gels were transferred to nitrocellulose membranes for Western blotting. Reagents used for preparation of sample and running buffers are listed in Appendix 3.

2.9 Western blotting

The gels were blotted onto nitrocellulose membranes in the Mini Trans-Blot Electrophoretic Transfer Cell system (BioRad Lab) overnight at 30V or 90 mA. The membrane, filter papers and fibre pads used in the blotting cell were soaked in transfer buffer for about 30 min prior to transfer. A gel-membrane sandwich was prepared as followed: (black part of blotting cell's cassette) fibre pad, filter paper, gel, membrane, filter paper, fibre pad (white part of cassette). A glass tube was used to remove air bubbles between gel and membrane by rolling the tube on top of filter paper placed after the membrane. The cassette was then closed firmly and placed in the tank. The tank was then filled with the rest of the transfer buffer. The lid was put on the tank, the cables were plugged in and the blotting was started. After transferring the proteins, the blot was subjected to a series of washing with TBS buffer, TBST buffer and 2% Ponceau-S solution. The membrane was blocked for non-specific binding in TBST-5% milk for 1 h at room temperature before being incubated in primary (1˚) antibody at 4˚C overnight. The blot was then subjected to another series of washing with TBST buffers before being incubated in secondary (2˚) antibody for 1 h at room temperature. After 1 h, the blot was washed with TBST buffer and incubated in alkaline phosphatase (AP) buffer and staining solutions. All washing and incubation (except with staining solutions) of the blot were done with shaking. Stained blots were dried and scanned. The list of 1˚ and 2˚ antibodies used as well as staining solutions for respective proteins detection is shown in Table 5. Preparation of buffers used in Western blotting is listed in Appendix 3.

The amount of proteins analyzed were determined using an image processing and analysis software, ImageJ (National Institutes of Health, USA) based on integrated densitometry and the values were normalized to the before irradiation (i.e. pre-irradiation or control) samples that was set to 100%.

Table 5: List of primary (1˚), secondary (2˚) antibodies and staining solutions used to detect proteins of interest in Western blotting.

Proteins detected	1˚ antibody	2˚ antibody	Staining solution
RuBisCO	1:50000 Anti-RbcL antibody (AS01 017, Agrisera)	1:500 Rabbit polyclonal to chicken IgY (H&L) (HRP) antibody (ab6753, Abcam plc)	3,3′,5,5′-Tetramethylbenzidine (TMB) solution (T0565, Sigma)
D1 protein	1:4000 Anti-PsbA antibody (AS01 016, Agrisera)	1:500 Rabbit polyclonal to chicken IgY (AP) antibody (ab6754, Abcam plc)	SIGMA*FAST* BCIP/NBT tablet (B5655, Sigma)
HSP60	1:4000 Anti-HSP60 antibody (AM01345PU-L, Acris Antibodies GmbH)	1:4000 Rabbit anti-mouse IgG (H&L) (AP) antibody (R1253AP, Acris Antibodies GmbH)	SIGMA*FAST* BCIP/NBT tablet (B5655, Sigma)
HSP70	1:10000 Anti-HSP70 global antibody (AS08 371, Agrisera)	1:3000 Goat polyclonal to rabbit IgG H&L (HRP) antibody (ab6721, Abcam plc)	3,3′,5,5′-Tetramethylbenzidine (TMB) solution (T0565, Sigma)

2.10 Statistical analyses

Values of all the parameters tested were related to 100% of pre-irradiation values, for better comparison. The values of the parameters were standardised to 1, and then arcsine-transformed (Sokal and Rohlf, 1995) to obtain homogeneity of variance (Levene Statistic). Mean values and standard deviation were determined from three replicates of each treatments (unless stated otherwise). The statistical significance of differences among means was calculated according to (where applicable) (Dytham, 2003):

1. a one-way ANOVA followed by Fischer's least significance difference (LSD) or Student-Neuman-Keuls (SNK) *post hoc* testing, and
2. a two-way ANOVA.

In each tests, a probability level of $p < 0.05$ was applied. All statistical analysis was performed using Minitab 14 (Minitab Inc., USA) and MedCalc 11 (MedCalc Software, Belgium).

3.0 RESULTS

3.1 Macroalgal responses to low photosynthetically active radiation (PAR) and high ultraviolet radiation (UVR) stress

3.1.1 Photosynthetic performance under low PAR and high UVR

The macroalgae were irradiated to different spectral ranges as listed in Table 6. These conditions are termed low photosynthetically active radiation (PAR) 1 (L_1, see MATERIALS AND METHODS section 2.2.1 for explanation) corresponding to the low background PAR irradiance emitted by the fluorescent lamps in comparison to that of the sun simulator. All algal species received similar fluence of PAR and ultraviolet radiation (UVR) except for *Laminaria digitata* and *Ulva lactuca* which were exposed to a higher fluence of PAR and a smaller fluence of UVA than the other algal species. Ratio of PAR:UVA:UVB was calculated with respect to PAR irradiance.

Table 6: Irradiances of the different spectral ranges of the fluorescent lamps applied in the experiments.

Species	PAR (μmol m^{-2} s^{-1})	UVA (W m^{-2})	UVB (W m^{-2})	Ratio of PAR:UVA:UVB
S. chordalis	21	38.9	0.93	1:9:0.2
P. palmata	21	38.9	0.93	1:9:0.2
L. digitata	24	33.8	0.93	1:7:0.2
D. dichotoma	21	38.9	0.93	1:9:0.2
U. lactuca	24	33.8	0.93	1:7:0.2

As listed in Table 7, the red algae *Solieria chordalis* and *Palmaria palmata*, are characterized by having a lower photosynthetic performance than the brown algae *Laminaria digitata* and *Dictyota dichotoma*, and the green alga *Ulva lactuca*.

Table 7: Photosynthetic parameters of the macroalgae before irradiation at low PAR and high UVR (i.e. pre-irradiation or control). Data are means ±SD values of n=9.

Species	Parameters			
	F_v/F_m [rel. unit]	$rETR_{max}$ [rel. unit]	α [rel. unit]	I_k [μmol m^{-2} s^{-1}]
S. chordalis	0.603 ± 0.01	9.28 ± 1.7	0.468 ± 0.05	20.25 ± 1.0
P. palmata	0.504 ± 0.03	15.95 ± 3.8	0.384 ± 0.01	43.25 ± 8.0
L. digitata	0.712 ± 0.02	37.76 ± 7.3	0.587 ± 0.02	64.82 ± 8.6
D. dichotoma	0.758 ± 0.01	29.00 ± 5.5	0.542 ± 0.05	59.58 ± 9.6
U. lactuca	0.732 ± 0.02	36.40 ± 9.5	0.561 ± 0.05	64.43 ± 4.1

The maximum quantum yield (F_v/F_m) and the photosynthetic parameters of the algal samples after the treatments (i.e. after 5 h irradiation or post-irradiation, and after 18 h recovery or post-recovery) are displayed in Fig. 4. The low PAR irradiance alone showed weaker effect on all the parameters than the other treatments where the values remained more or less on par with the pre-irradiation algae (Fig. 4Ai). In contrast, presence of UVR (i.e. either UVA alone as in PAR+UVA, or UVA+UVB as in PAR+UVA+UVB) greatly affected the algae. Collectively, all three classes of the algae examined showed similar degree of F_v/F_m reductions (ANOVA, SNK *post-hoc* test, p=0.741) as well as in the rate of its recovery (p=0.085). F_v/F_m of all post-irradiation algae was reduced by more than 50% of the pre-irradiation algae (Fig. 4Ai). Most of the algae were affected the strongest by PAR+UVA+UVB particularly in *P. palmata* at which PAR+UVA+UVB reduced F_v/F_m by 75% in comparison to 68% under PAR+UVA. After 18 h under the dim light for the recovery period, these percentages of *P. palmata* increased to 60% with PAR+UVA+UVB and 54% with PAR+UVA (Fig. 4Aii). A contrasting effect was shown by post-recovery *D. dichotoma* and *U. lactuca* where F_v/F_m of the algae treated with PAR+UVA+UVB increased to 53% and 67%, respectively, compared to the algae treated with PAR+UVA which increased to 74% and 85%, respectively. The remaining post-recovery algae showed signs of recovery as well (Fig. 4Aii).

A unique behaviour in the effect of UVR on the maximum relative electron transport rate ($rETR_{max}$) was observed in *L. digitata* where instead of reducing $rETR_{max}$ as displayed by the rest of the post-irradiation algae, UVR increased the values to more than 25% (Fig. 4Bi). An increase in $rETR_{max}$ was observed in *S. chordalis* (i.e. a 38% increase, the highest increase among the species), *P. palmata* (i.e. an 8% increase) and *D. dichotoma* (i.e. a 21% increase) under PAR alone as well. In the rest of the algae, PAR+UVA+UVB appeared to cause a higher reduction (or an increase in the case for *L. digitata*) than PAR+UVA. Exception, however, was observed in *S. chordalis* whereby PAR+UVA+UVB (i.e. a 75% reduction) caused less effect on $rETR_{max}$ in comparison to PAR+UVA (i.e. an 81% reduction). $rETR_{max}$ of all post-irradiation algae showed signs of recovery after 18 h under the dim light (Fig. 4Bii). For instance, a full recovery was observed in *L. digitata* for all light treatments. In addition, a delay in recovery was

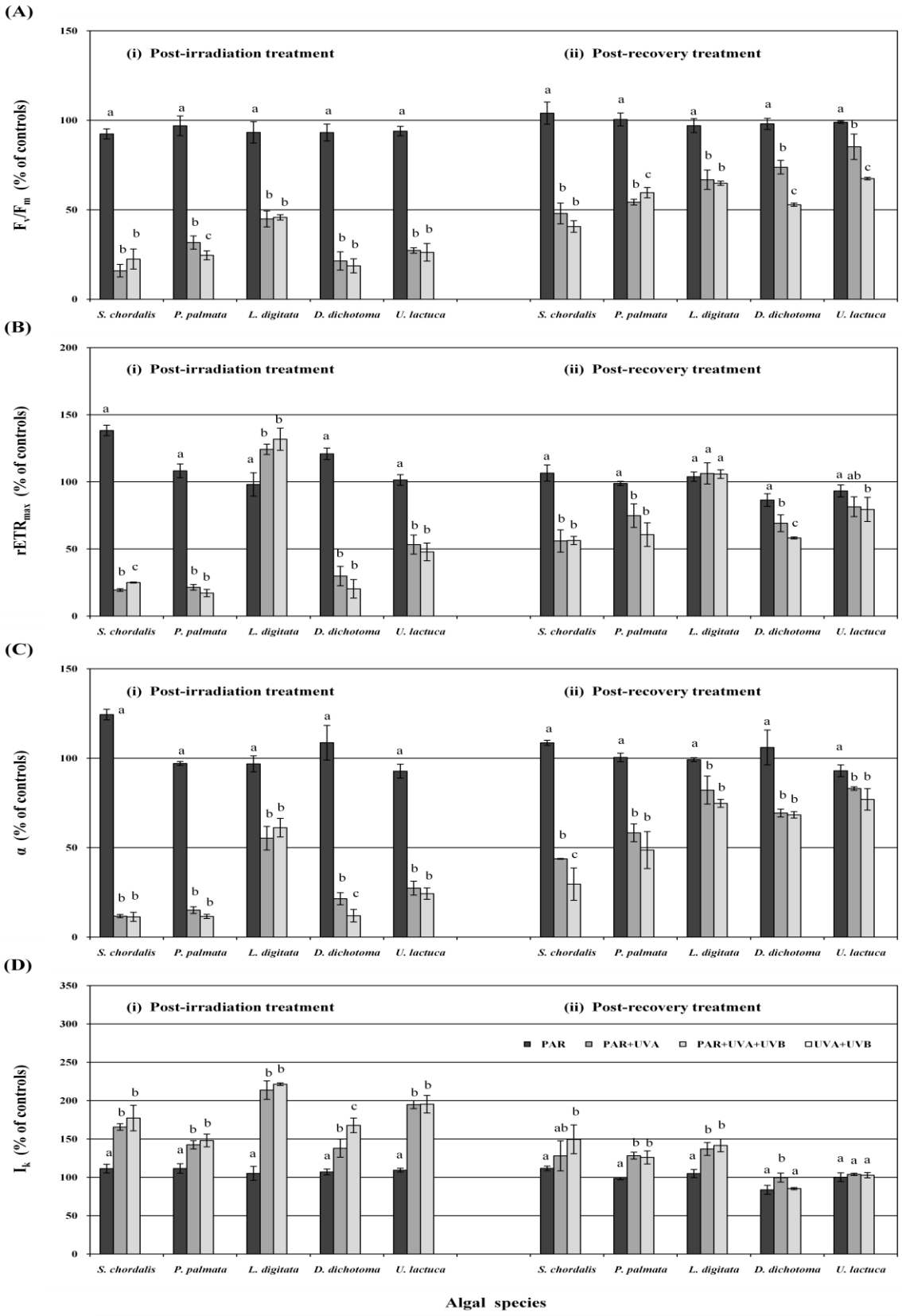

Fig. 4: Maximum quantum yield (F_v/F_m, *A*), maximum relative electron transport rate ($rETR_{max}$, *B*), photosynthetic efficiency parameter (α, *C*) and light saturation parameter (I_k, *D*) of the macroalgae after 5 h irradiation (post-irradiation, *i*) and after 18 h recovery (post-recovery, *ii*). *Black bars:* PAR only, *dark grey bars:* PAR+UVA, *light grey bars:* PAR+UVA+UVB. Different letters above bars indicate significant difference between light treatments within similar species (ANOVA, Fischer's LSD test, $p < 0.05$, n=3)

observed in PAR+UVA+UVB-treated *D. dichotoma* (i.e. $rETR_{max}$ increased to 58%) compared to PAR+UVA (i.e. increased to 69%) while $rETR_{max}$ of PAR-treated algae reduced 14% below the pre-irradiation's after the recovery period. In general, PAR+UVA recovered faster than PAR+UVA+UVB (except in *S. chordalis* and *L. digitata*).

Similar to the above parameters, the photosynthetic efficiency α, was also strongly affected by addition of UVR into the treatments (Fig. 4Ci). All post-irradiation algae showed the highest α reduction with PAR+UVA+UVB except in *L. digitata.* In particular, PAR+UVA+UVB caused an 88% reduction in α of *D. dichotoma* in comparison to that of 79% reduction with PAR+UVA. Small reduction in α was also observed in algal samples receiving only PAR with exceptions found for *S. chordalis* and *D. dichotoma* whereby α increased 24% and 9%, respectively. A delay in α recovery was observed in *S. chordalis* treated with PAR+UVA+UVB (i.e. increased to 30%) compared to PAR+UVA (i.e. increased to 45%) (Fig. 4Cii). A similar trend was observed for the other post-recovery algal species as well (Fig. 4Cii).

Unlike the previous photosynthetic parameters, an increase in I_k was observed in post-irradiation algae treated with UVR (Fig. 4Di). For instance, I_k was increased to more than double in *L. digitata* and nearly doubled in *U. lactuca* while there was a more than 50% increase in the rest of the algal species. A distinctive effect between PAR+UVA and PAR+UVA+UVB treatments was observed in *D. dichotoma* whereby PAR+UVA+UVB caused a higher increase (i.e. 68%) than PAR+UVA (i.e. 38%). I_k of all the algal samples was not affected by PAR alone, in contrast to that observed for the previous parameters. Whilst all affected *U. lactuca* showed full recovery of I_k, the remaining algae showed a delay in recovery (Fig. 4Dii). Recovery of I_k in *D. dichotoma*, however, followed two different patterns, those that received PAR+UVA showed full recovery and those that received only PAR and PAR+UVA+UVB were reduced to values below that of the pre-irradiations.

In order to determine the role of UVR to the inhibitory effect on the photosynthetic performance of the algae, changes in F_v/F_m values measured under different light treatments are plotted in a series of pairwise

comparisons (Fig. 5). Large positive values display a great additional contribution of UVR to changes in F_v/F_m. UVA and UVB synergistically caused significant inhibition of F_v/F_m in all the algae examined (Fig. 5A). Moreover, most of the inhibitory effect was contributed by UVA (Fig. 5B) with additional UVB increased the inhibition in *P. palmata* and *D. dichotoma* (Fig. 5C). However, UVB was observed to reduce the inhibition in *S. chordalis, L. digitata* and *U. lactuca*. UVA had a larger effect than UVB on the recovery of the algae while additional UVB reduced this effect in *P. palmata.*

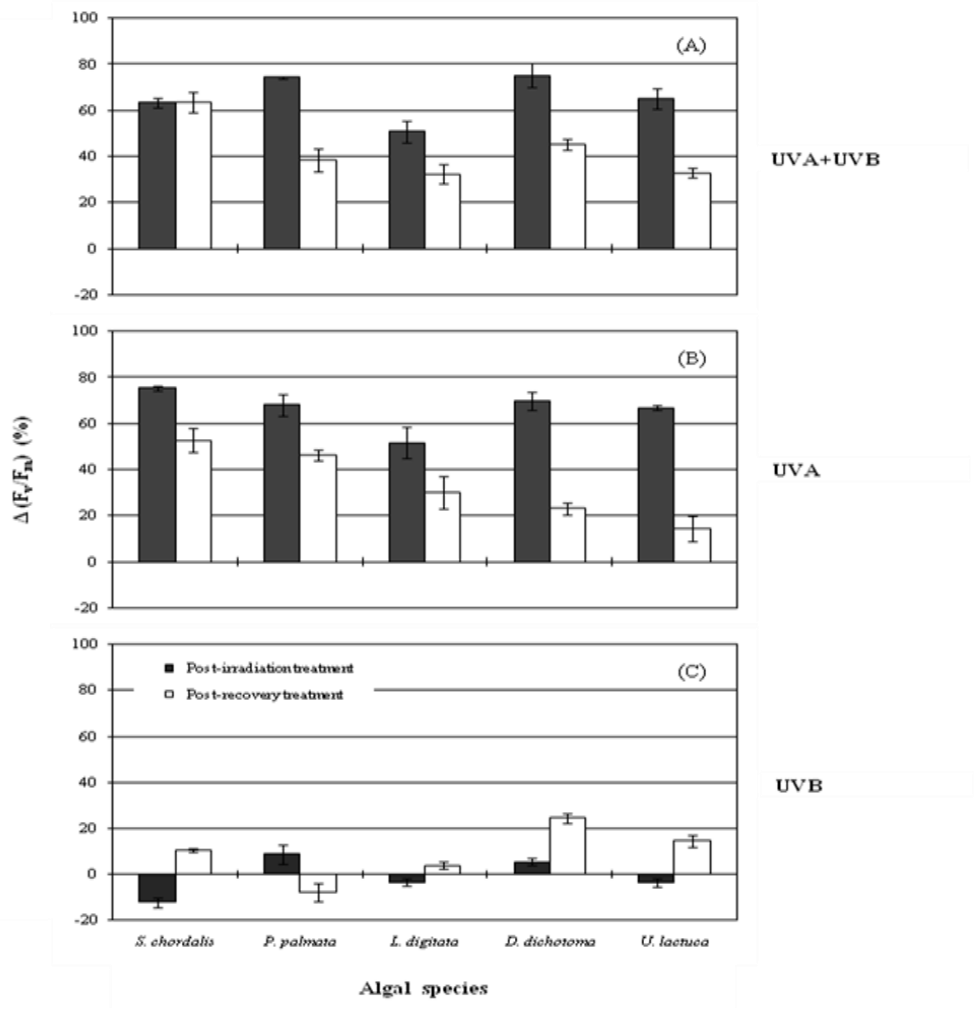

Fig. 5: Role of different wavelength ranges to the overall inhibition of photosynthetic performance in the macroalgae examined expressed as the changes in F_v/F_m values [Δ (F_v/F_m)] (in % of pre-irradiation values) measured under PAR and PAR+UVA+UVB treatment (*A*), PAR and PAR+UVA treatment (*B*), and PAR+UVA and PAR+UVA+UVB treatment (*C*). *Black bars*: after 5 h irradiation or post-irradiation; *white bars*: after 18 h recovery or post-recovery. Data are means ±SD from triplicates of each treatment.

3.1.2 Pigments content under low PAR and high UVR

Table 8 lists the concentration of the pigments extracted from the macroalgae before any treatment (i.e. pre-irradiation). Chlorophyll (Chl) a was analyzed in all the algae, the phycobiliproteins, R-phycoerythrin (R-PE) and R-phycocyanin (R-PC) were analyzed only in the red algae, Chl c and fucoxanthin were analyzed only in the brown algae, and Chl b was analyzed only in the green alga.

Table 8: Pigments content of the macroalgae before irradiation at low PAR and high UVR (i.e. pre-irradiation or control). Data are means ±SD values of n=9.

Species	Pigments content [mg pigments/g FW]					
	Chl a	Chl b	Chl c	Fucox.	R-PE	R-PC
S. chordalis	0.93 ± 0.05	–	–	–	2.37 ± 0.01	0.58 ± 0.01
P. palmata	0.87 ± 0.09	–	–	–	1.06 ± 0.003	0.35 ± 0.003
L. digitata	0.39 ± 0.02	–	0.06 ± 0.01	0.26 ± 0.03	–	–
D. dichotoma	1.09 ± 0.01	–	0.014 ± 0.00	0.78 ± 0.01	–	–
U. lactuca	1.68 ± 0.01	1.11 ± 0.01	–	–	–	–

Fucox. is fucoxanthin; R-PE is R-phycoeryhtrin; R-PC is R-phycocyanin.

In general, all the photosynthetic pigments extracted from the post-irradiation red algae showed a reduction in their content (Fig. 6). Whilst PAR alone had no effect on the pigments content, addition of UVR had a significant effect on the pigments. In *S. chordalis*, however, all treatments, with or without UVR, had similar effect on its Chl a content with about 10% reduction (Fig. 6Ai). In contrast, the content of the phycobiliproteins was strongly affected by UVR. PAR+UVA+UVB caused a significantly stronger effect on the content of R-PE (i.e. 29% reduction) than PAR+UVA (i.e. 18% reduction) (Fig. 6Aii). R-PC, on the other hand, was reduced about 25% by both PAR+UVA and PAR+UVA+UVB (Fig. 6Aiii). After 18 h under the dim light, all affected *S. chordalis* had their pigments content nearly and fully recovered except for Chl a content of PAR+UVR-affected algae which showed no recovery (Fig. 6Ai-iii). Comparatively, the content of all the pigments in *P. palmata* was significantly affected by PAR+UVR treatments with a 13%-16% reduction in Chl a (Fig. 6Bi), 27%-37% reduction in R-PE (Fig. 6Bii) and 25%-28% reduction in R-PC (Fig. 6Biii) in comparison to that of PAR alone. All affected *P. palmata*

showed a full or nearly a full recovery of their Chl a and R-PC contents but showed a delay in R-PE recovery of PAR+UVR-treated algae (Fig. 6Bi-iii).

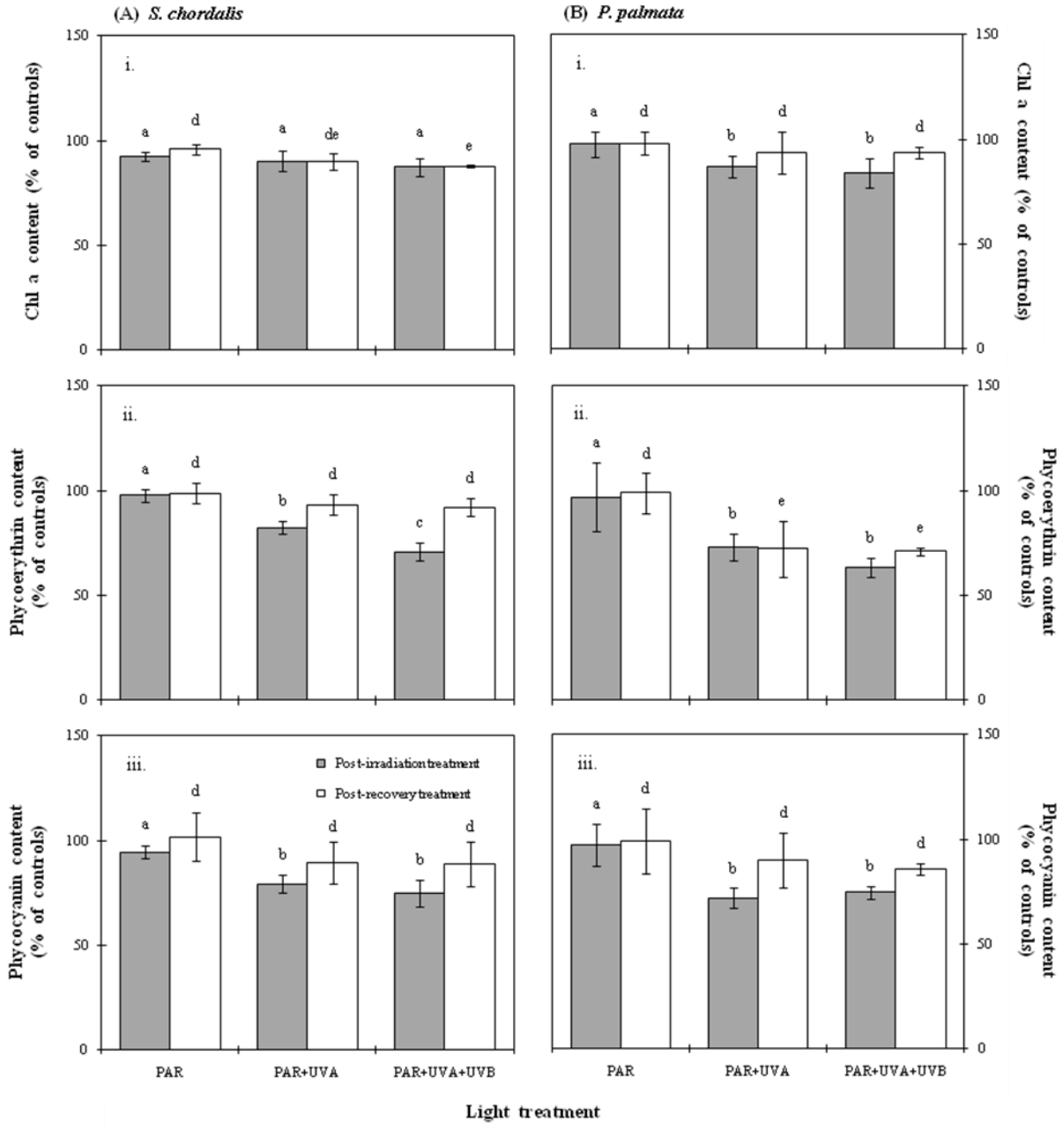

Fig. 6: Contents of chlorophyll a (*i*), R-phycoerythrin (*ii*) and R-phycocyanin (*iii*), in the red algae, *S. chordalis* (*A*) and *P. palmata* (*B*). *Grey bars*: after 5 h irradiation or post-irradiation, *white bars*: after 18 h recovery or post-recovery. Different letters above bars indicate significantly different values determined by comparison between different light treatments (ANOVA, Fischer's LSD test, $p < 0.05$, n=3).

PAR alone had no effect on the pigments content of the brown algae as well except for fucoxanthins which displayed a reducing trend (Fig. 7). When UVR was added into the treatments, there was about 17% and 32% reductions in Chl a and Chl c of *L. digitata*, respectively, in comparison to PAR alone (Fig. 7Ai-ii). There was also a reducing trend in fucoxanthins content but with no distinctive effect between all treatments (Fig. 7Aiii). All affected *L. digitata* had recovered their initial pigments content after 18 h under the dim light (Figs. 7Ai and 7Aiii) but the recovery of Chl c was delayed in PAR+UVR-treated algae compared to that of PAR (Fig. 7Aii). There was no distinctive effect between PAR and PAR+UVR treatments on Chl a and fucoxanthin contents of *D. dichotoma* but showed a reducing trend when treated under PAR+UVR (Figs. 7Bi and 7Biii). PAR+UVR, on the other hand, reduced the content of Chl c by about 17% compared to PAR alone (Fig. 7Bii). There was a delay in Chl c recovery of PAR+UVR-treated *D. dichotoma* compared to PAR-treated algae. In contrast, Chl a and fucoxanthins of affected algae nearly recovered their pre-irradiation values.

Chls content of *U. lactuca*, was also not affected by PAR alone (Fig. 8). Upon exposure to PAR+UVA and PAR+UVA+UVB, there was about 27% reduction in Chl a (Fig. 8A) and about 16% reduction in Chl b (Fig. 8B) contents compared to PAR alone. A delay in the recovery of Chl a was observed in PAR+UVR-treated algae while Chl b of affected algae showed nearly a full recovery.

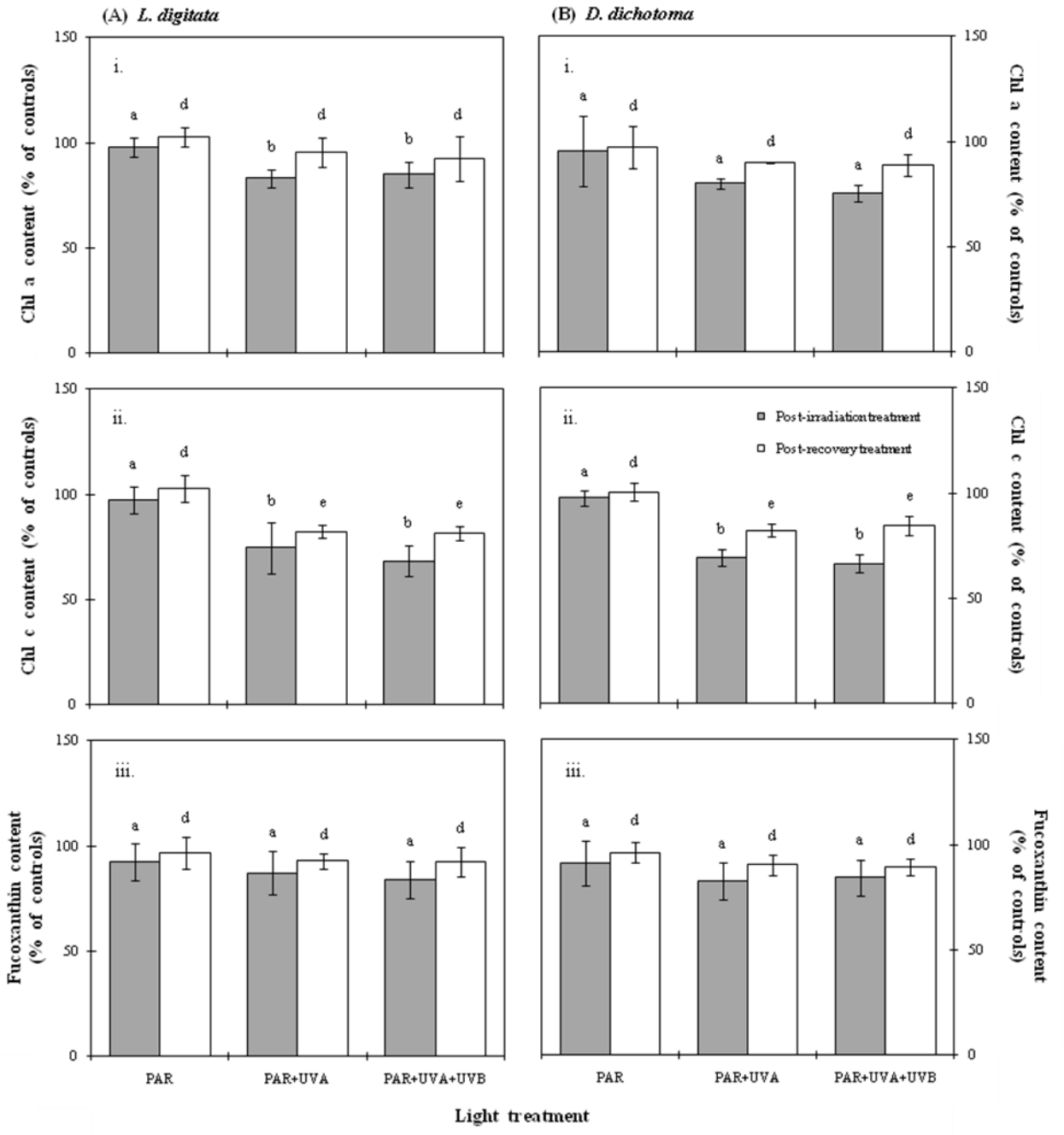

Fig. 7: Contents of chlorophyll a (*i*), chlorophyll c (*ii*) and fucoxanthin (*iii*) in the brown algae, *L. digitata* (*A*) and *D. dichotoma* (*B*). *Grey bars*: after 5 h irradiation or post-irradiation, *white bars*: after 18 h recovery or post-recovery. Different letters above bars indicate significantly different values determined by comparison between different light treatments (ANOVA, Fischer's LSD test, $p < 0.05$, n=3).

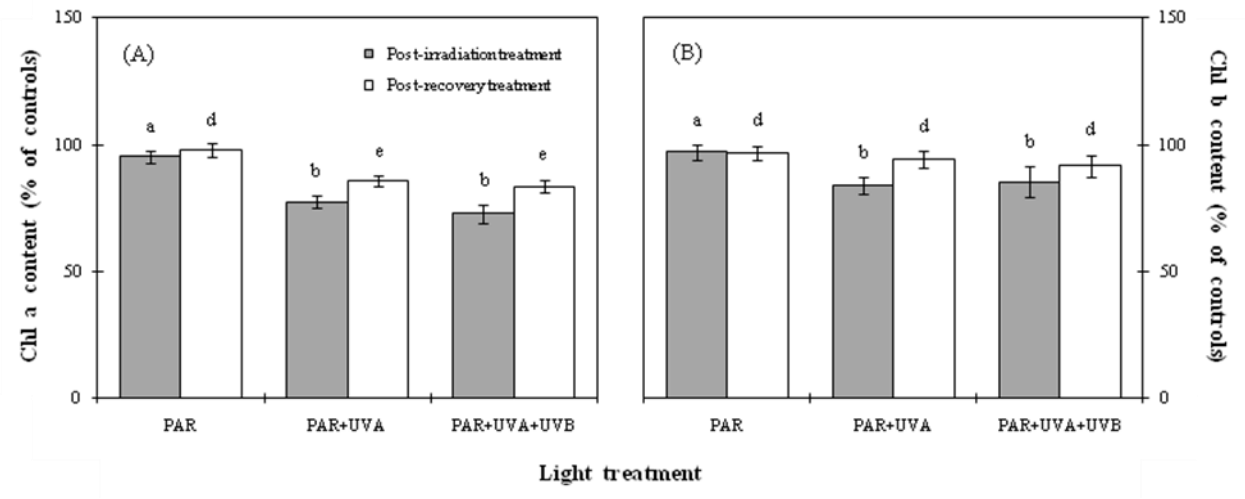

Fig. 8: Contents of chlorophyll a (*A*) and chlorophyll b (*B*) in the green alga, *U. lactuca. Grey bars:* after 5 h irradiation or post-irradiation, *white bars:* after 18 h recovery or post-recovery. Different letters above bars indicate significantly different values determined by comparison between different light treatments (ANOVA, Fischer's LSD test, $p < 0.05$, n=3).

3.1.3 Protein content under low PAR and high UVR

The content of the total soluble proteins (TSP) of the pre-irradiation macroalgae is listed in Table 9. A low amount of TSP was extracted from the brown algae due to the presence of large amount of polysaccharides which can hinder the extraction process.

Table 9: Total soluble proteins (TSP) content of the macroalgae before irradiation at low PAR and high UVR (i.e. pre-irradiation or control). Data are means ±SD values of n=3.

Species	TSP content [mg/g FW]
S. chordalis	3.07 ± 0.9
P. palmata	3.76 ± 0.6
L. digitata	1.95 ± 0.3
D. dichotoma	2.39 ± 0.3
U. lactuca	6.41 ± 1.5

The TSP content of *S. chordalis* and *D. dichotoma* was not affected by PAR alone but the content was reduced 8% in *P. palmata*, 4% in *L. digitata* and 7% in *U. lactuca* (Fig. 9A). TSP was further reduced by at least 18% of the pre-irradiations when UVR was added into the treatments. In *S. chordalis*, PAR+UVA+UVB caused a significant 27% reduction in comparison to 22% under PAR+UVA.

PAR+UVA+UVB appeared to cause the highest reduction in the remaining species. All affected algae showed signs of TSP recovery except in PAR-treated *U. lactuca* which showed no recovery (Fig. 9B). Recovery was delayed in PAR+UVA+UVB compared to PAR+UVA.

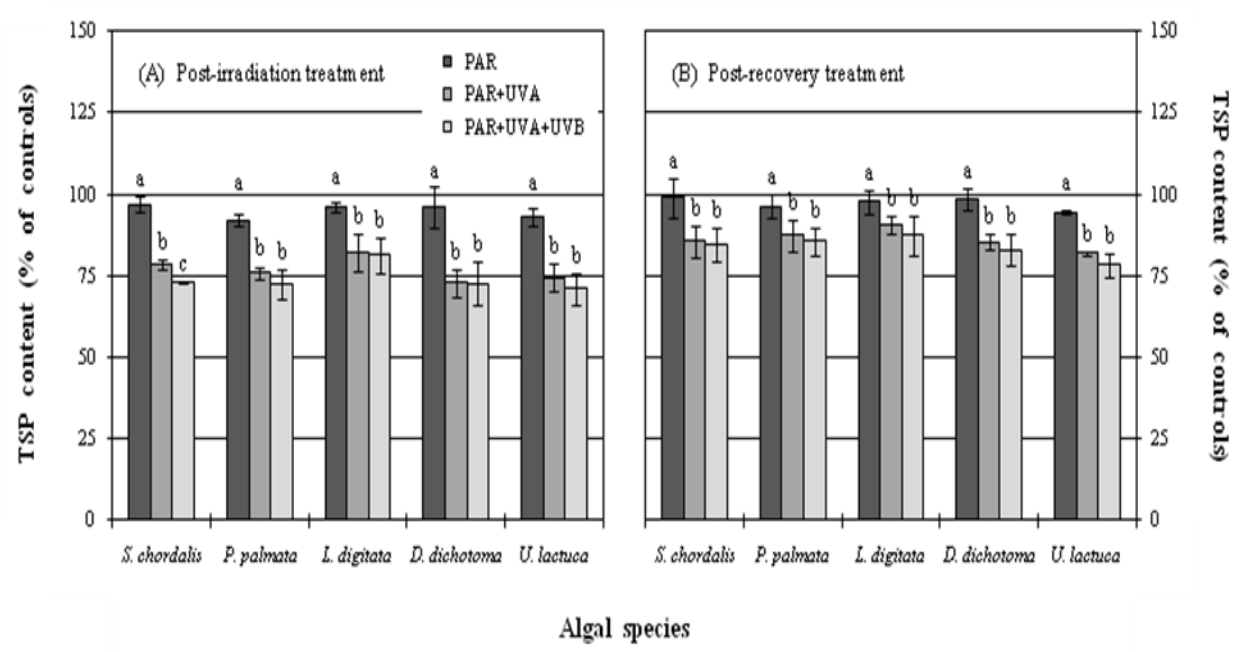

Fig. 9: Total soluble proteins (TSP) content in the macroalgae after 5 h irradiation (post-irradiation, *A*) and after 18 h recovery (post-recovery, *B*). *Black bars:* PAR, *dark grey bars:* PAR+UVA, *light grey bars:* PAR+UVA+UVB. Different letters above bars indicate significantly different values determined by comparison between different light treatments within similar species (ANOVA, Fischer's LSD test, $p < 0.05$, n=3).

3.1.4 Photosynthetic enzymes activity under low PAR and high UVR

Table 10 lists the catalytic activity of the two photosynthetic enzymes, ribulose-1,5-bisphosphate carboxylase/oxygenase (RuBisCO) and glyceraldehyde-3-phosphate dehydrogenase (GAPDH) in the pre-irradiation algae.

Table 10: Photosynthetic enzymes activity of the macroalgae before irradiation at low PAR and high UVR (i.e. pre-irradiation or control). Data are means ±SD values of n=3.

Species	Enzymes [U/mg TSP]	
	RuBisCO	GAPDH
S. chordalis	1.87 ± 0.4	0.27 ± 0.09
P. palmata	1.44 ± 0.5	0.28 ± 0.01
L. digitata	1.36 ± 0.2	0.40 ± 0.06
D. dichotoma	0.75 ± 0.5	0.13 ± 0.05
U. lactuca	1.48 ± 0.1	0.82 ± 0.04

Activity of RuBisCO was not affected by PAR alone in most of the algae examined but was reduced by 7% in *S. chordalis* (Fig. 10Ai). Addition of UVR, on the other hand, caused stronger effect than PAR alone which reduced the activity at least by 25%. PAR+UVA+UVB, for instance, caused the highest reduction in all the algal species examined. In particular, PAR+UVA+UVB caused a 37% reduction in comparison to PAR+UVA with a 20% reduction in *L. digitata*. The activity of RuBisCO was fully and almost fully recovered its pre-irradiation values in post-recovery *S. chordalis, L. digitata* and *U. lactuca* (Fig. 10Aii). A delay in recovery was observed with the PAR+UVR treatments. In particular, a distinctive effect in recovery between PAR+UVA and PAR+UVA+UVB was observed in *P. palmata* in which PAR+UVA+UVB (i.e. increased to 74%) showed a delay in recovery compared to PAR+UVA (i.e. increased to 79%).

Similar to RuBisCO, activity of GAPDH was not affected by PAR alone but the activity was strongly affected when UVR was added to the treatments with at least a 12% reduction (Fig. 10Bi). Whilst no distinctive effect was observed between PAR+UVA and PAR+UVA+UVB in any of the algae, a trend showed that the strongest effect was caused by PAR+UVA+UVB. The activity of GAPDH was fully and almost fully recovered in post-recovery *S. chordalis* and *U. lactuca* but was delayed in post-recovery *P. palmata, L. digitata* and *D. dichotoma* (Fig. 10Bii). In fact, a delay in recovery was observed in PAR+UVA-treated *L. digitata* (i.e. increased to 89%) compared to PAR+UVA+UVB (i.e. increased to 97%).

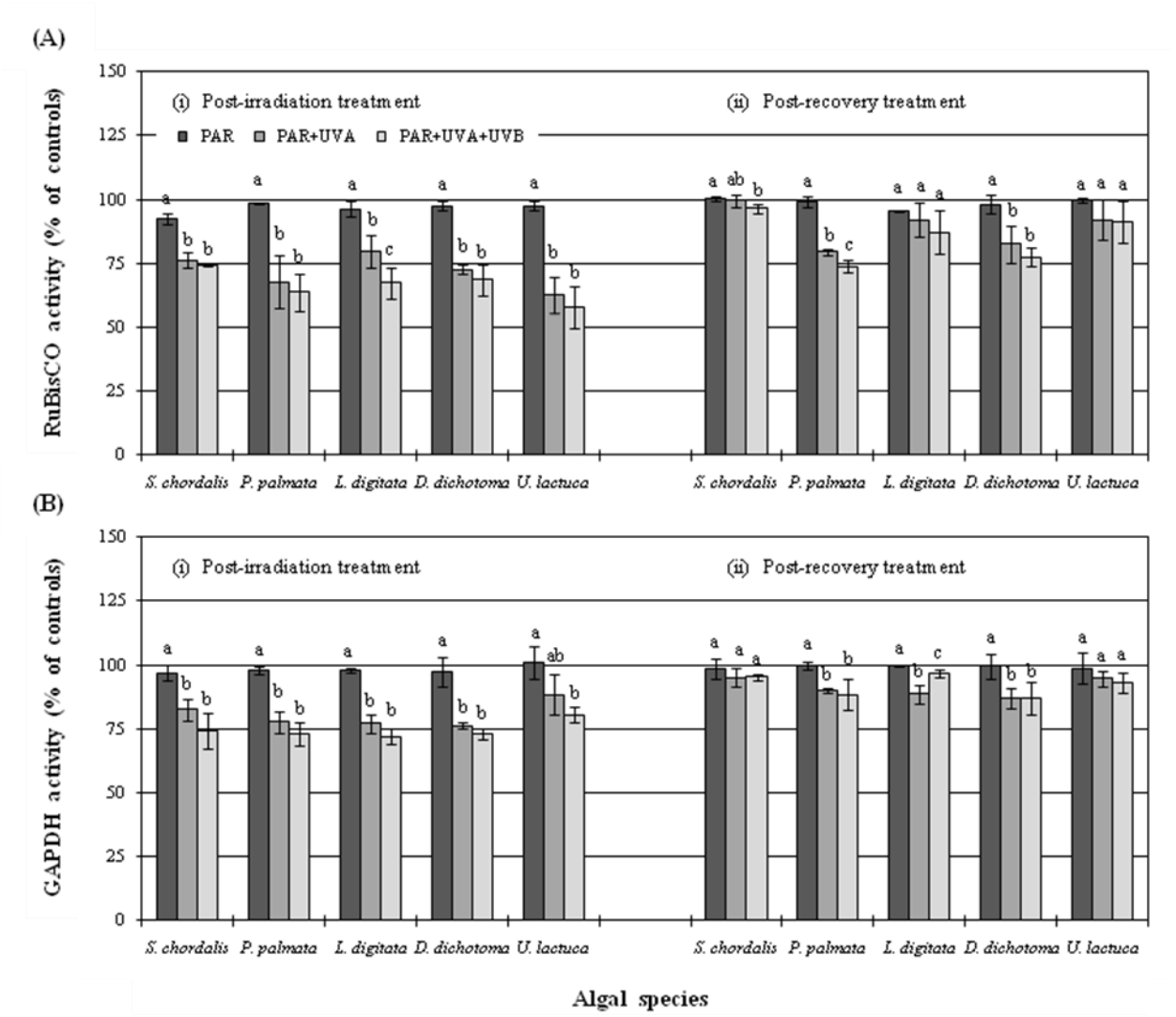

Fig. 10: Activity of ribulose-1,5-bisphosphate carboxylase/oxygenase (RuBisCO) (*A*) and glyceraldehyde-3-phosphate dehydrogenase (GAPDH) (*B*) in the macroalgae after 5 h irradiation (post-irradiation, *i*) and after 18 h recovery (post-recovery, *ii*). *Black bars:* PAR, *dark grey bars:* PAR+UVA, *light grey bars:* PAR+UVA+UVB. Different letters above bars indicate significantly different values determined by comparison between different light treatments within similar species (ANOVA, Fischer's LSD test, $p < 0.05$, n=3).

3.1.5 Antioxidative enzymes activity under low PAR and high UVR

The catalytic activity of catalase (CAT), ascorbate peroxidase (APX) and glutathione reductase (GR) in the pre-irradiation algae is listed in Table 11, in post-irradiation algae, though, the activity of these enzymes was induced in the presence of UV (Fig. 11). Moreover, the induction of these antioxidative

enzymes was also noted in PAR-treated algae. However, the extent of induction was rather small compared to that of UV.

Table 11: Antioxidative enzymes activity of the macroalgae before irradiation at low PAR and high UVR (i.e. pre-irradiation or control). Data are means ±SD values of n=3.

Species	Enzymes [U/mg TSP]		
	CAT	APX	GR
S. chordalis	0.69 ± 0.03	0.73 ± 0.04	0.20 ± 0.03
P. palmata	0.28 ± 0.09	0.57 ± 0.01	0.90 ± 0.01
L. digitata	0.75 ± 0.01	0.56 ± 0.02	0.58 ± 0.04
D. dichotoma	0.26 ± 0.01	0.69 ± 0.04	0.30 ± 0.02
U. lactuca	0.50 ± 0.04	1.04 ± 0.02	0.39 ± 0.03

CAT activity in *L. digitata,* the highest induction in all algal species examined, was increased to more than 70% under PAR+UVR (Fig. 11Ai). The lowest increase by PAR+UVR was observed in *U. lactuca* with less than 30%. In the rest of the algae, the increase by PAR+UVR was between 32% and 50%. Between the two PAR+UVR treatments, PAR+UVA+UVB appeared to cause higher increase than PAR+UVA in all post-irradiated algae except in *L. digitata.* A full recovery in CAT activity was observed in affected *S. chordalis* and *U. lactuca* while a delay in recovery was observed in affected *P. palmata, L. digitata* and *D. dichotoma* (Fig. 11Aii). Moreover, PAR+UVA+UVB-treated *L. digitata* showed a delay in recovery (i.e. reduced to 142%) compared to PAR+UVA (i.e. reduced to 114%).

The increase in APX activity by PAR+UVR in all algal species examined exceeded that of 30% in *S. chordalis, P. palmata* and *L. digitata* while in *D. dichotoma,* APX was increased by about 24% and a much smaller increase was observed in *U. lactuca* with less than 10% (Fig.11Bi). Furthermore, PAR+UVA+UVB caused a significantly higher increase in *L. digitata* (i.e. 43%) than PAR+UVA (i.e. 33%). PAR+UVA+UVB caused higher increase than PAR+UVA in *S. chordalis* and *U. lactuca* as well but not in *P. palmata* and *D. dichotoma.* The activity fully recovered to that of the pre-irradiations in affected *S. chordalis, L. digitata* and *U. lactuca* but was delayed in affected *P. palmata* and *D. dichotoma* (Fig. 11Bii).

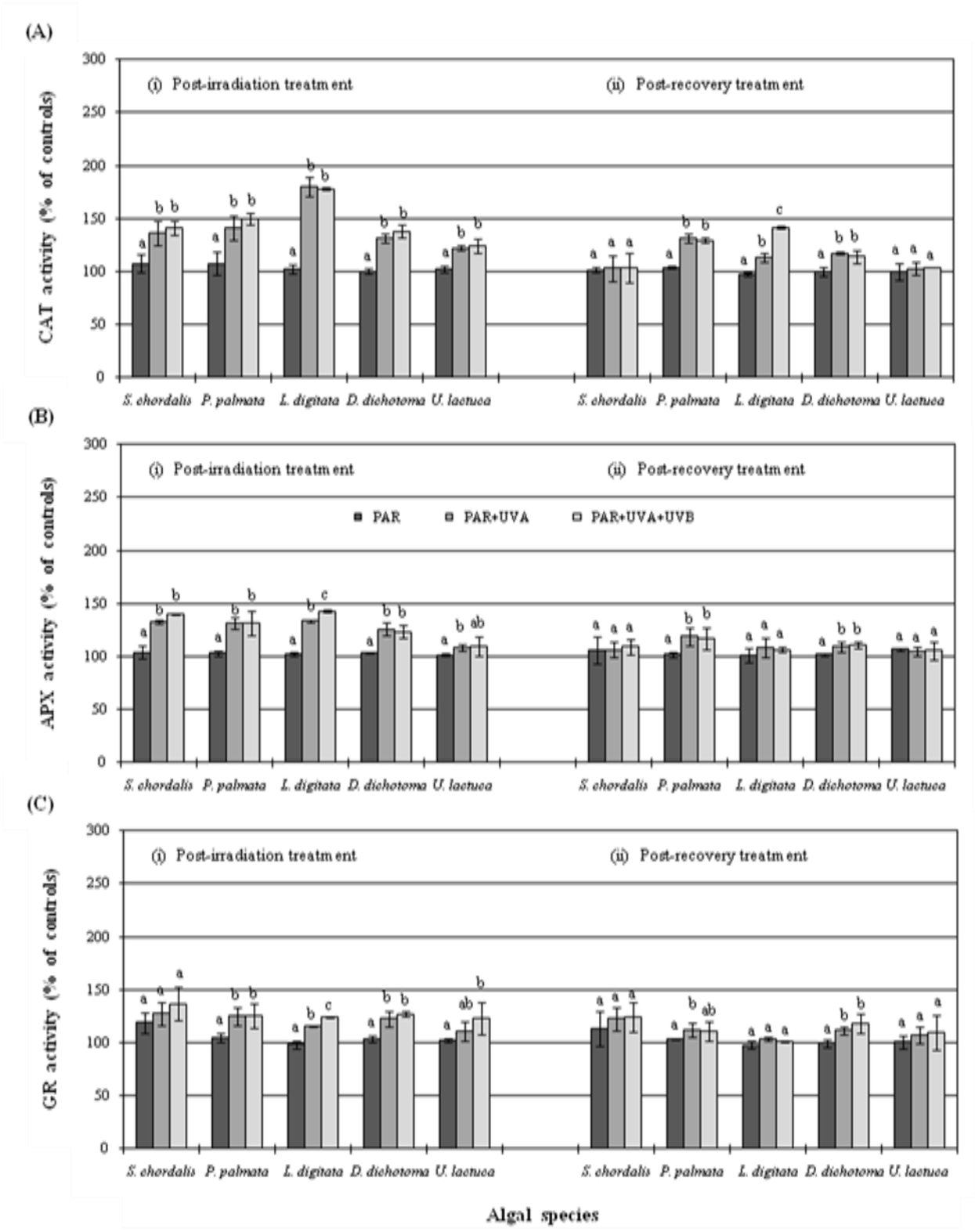

Fig. 11: Activity of catalase (CAT) (*A*), ascorbate peroxidase (APX) (*B*) and glutathione reductase (GR) (*C*) in the macroalgae after 5 h irradiation (post-irradiation, *i*) and after 18 h recovery (post-recovery, *ii*). *Black bars:* PAR, *dark grey bars:* PAR+UVA, *light grey bars:* PAR+UVA+UVB. Different letters above bars indic ate significantly different values determined by comparison between different light treatments within similar species (ANOVA, Fischer's LSD test, $p < 0.05$, n=3).

PAR+UVA+UVB caused the highest increase in GR activity of the post-irradiation algae except in *P. palmata* (Fig. 11Ci). A significantly higher increase was observed in *L. digitata* under PAR+UVA+UVB with 24% than PAR+UVA with an 16% increase. Additionally, a smaller increase in GR activity was also noticeable in PAR-treated *S. chordalis* than the other species. All affected post-irradiation algae showed signs of recovery with a full recovery observed in *L. digitata* and *U. lactuca* and a delay in recovery in *S. chordalis*, *P. palmata* and *D. dichotoma* (Fig. 11Cii).

3.1.6 Contents of RuBisCO LSU, D1 protein, HSP60 and HSP70 under low PAR and high UVR

Western blots of RuBisCO large subunit (LSU) or its antibody equivalent *RbcL* extracted from each algae and the percentage content of the protein based on the content of pre-irradiation samples are displayed in Fig. 12. On the blot, the bands corresponding to the protein *RbcL* were visible at about 52kDa (Fig. 12A). At the end of irradiation with PAR+UVR, *RbcL* was reduced by about 37% in *S, chordalis*, about 30% in *P. palmata*, about 28% in *L. digitata*, about 26% in *D. dichotoma* and about 39% in *U. lactuca* in comparison to PAR alone (Fig. 12Bi). In general, higher reduction was observed under PAR+UVA+UVB than the other treatments except in *P. palmata. RbcL* in both red algae *S. chordalis* and *P. palmata*, was also affected by PAR alone with about 6% reduction. The content of *RbcL* in all affected algae slowly recovered to that of their pre-irradiations after 18 h under the dim light (Fig. 12Bii). A delay in recovery was observed with PAR+UVA+UVB except in *P. palmata* and *U. lactuca.*

The bands corresponding to the D1 protein or its antibody equivalence *PsbA* extracted from the algae were visible at about 32kDa (Fig. 13A). It appeared that the protein was more strongly affected by PAR+UVR compared to that of *RbcL* especially in the red algae and the green alga whereby between 41% and 47% of *PsbA* was reduced (Fig. 13Bi). In the brown algae on the other hand, 18%-24% of *PsbA* was reduced. Similar to *RbcL*, PAR+UVA+UVB caused higher reduction than PAR+UVA as well. *PsbA* of *P. palmata* was also affected by PAR alone along with that of *U. lactuca* with about 5% reduction. The

content of *PsbA* protein in post-recovery algae slowly recovered to that of their pre-irradiations with a delay in recovery in PAR+UVA+UVB (Fig. 13Bii).

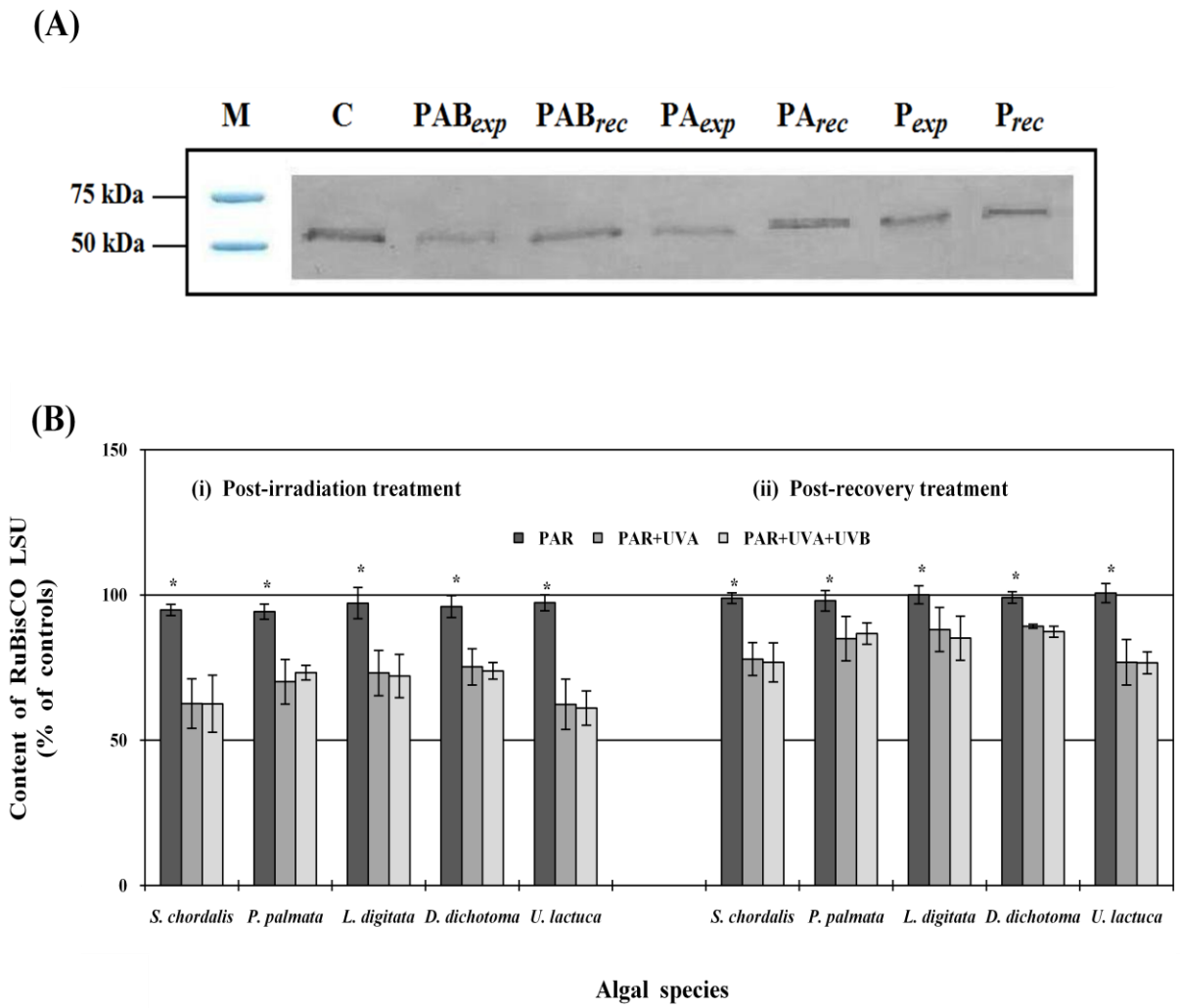

Fig. 12: An example of a western blot of RuBisCO's large-subunit (LSU) (*RbcL*) (*A*) in the macroalgae and percentage content of *RbcL* quantified from corresponding blots (*B*). *M*: protein markers showing the position of the protein on the blot with respective molecular weight on the left; *C:* pre-irradiation (i.e. control); *PAB:* PAR+UVA+UVB, *PA:* PAR+UVA, *P:* PAR, *exp:* after 5 h irradiation or post-irradiation, *rec:* after 18 h recovery or post-recovery. Data of (*B*) are means ±SD values, different asterisks above bars indicate statistically significant difference between treatments within similar species (ANOVA, Fischer's LSD test, $p < 0.05$, n=3).

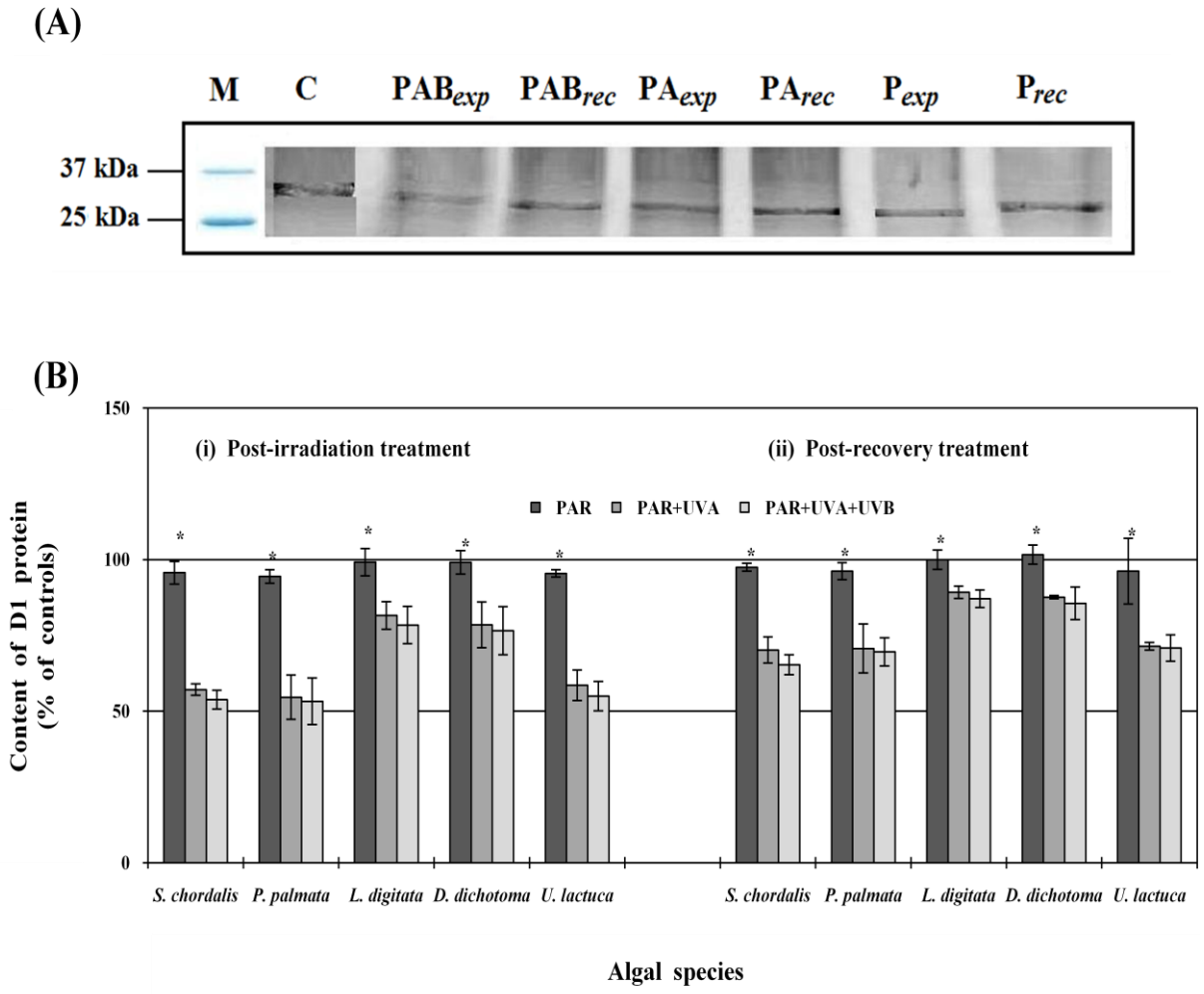

Fig. 13: An example of a western blot of D1 protein (*PsbA*) (*A*) in the macroalgae and percentage content of *PsbA* quantified from corresponding blots (*B*), details as in Fig. 12.

As the name implies, the heat shock protein 60 (HSP60) has a molecular weight of 60 kDa and hence the bands on the blots corresponding to the *Hsp60* protein were visible between 75 and 50 kDa (i.e. 60 kDa, Fig. 14A). Upon irradiation with PAR+UVR, *Hsp60* increased 50% in *S. chordalis*, *P. palmata* and *L. digitata* while in *D. dichotoma* and *U. lactuca*, the increase exceeded that of 55% and 85%, respectively (Fig. 14Bi). Higher increase was observed under PAR+UVA+UVB than PAR+UVA except in *P. palmata.* A small increase by PAR alone was also observed in *S. chordalis* and *U. lactuca*. A reduction in *Hsp60* content of post-recovery algae indicated signs of recovery. A delay in recovery was observed with PAR+UVA compared to the other treatments in *S. chordalis* and *P. palmata* and with PAR+UVA+UVB in *L. digitata* and *D. dichotoma* (Fig. 14Bii).

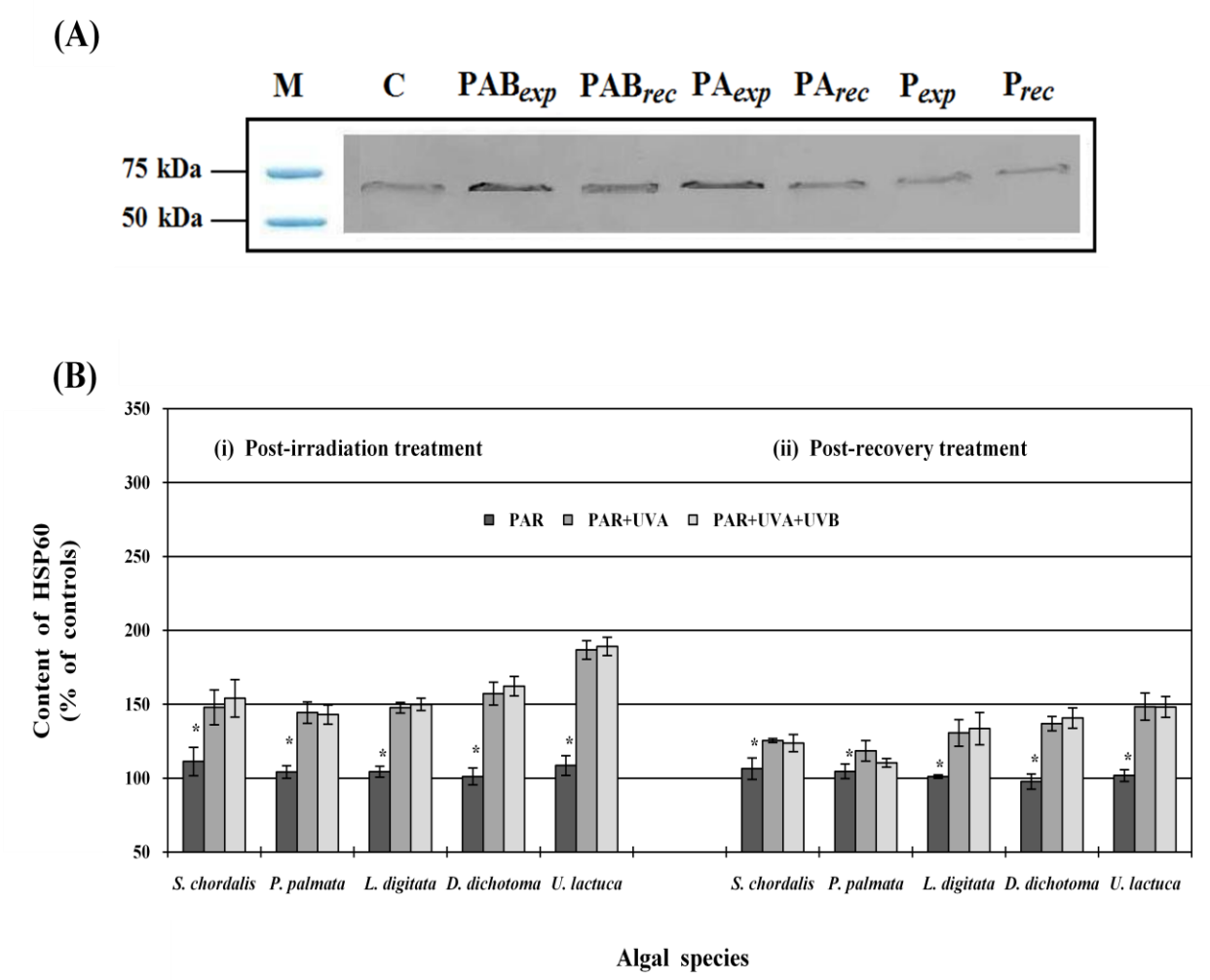

Fig. 14: An example of a western blot of the stress protein, HSP60 (*A*) in the macroalgae and percentage content of *Hsp60* quantified from corresponding blots (*B*), details as in Fig. 12.

The bands corresponding to *Hsp70* protein were visible at about 70 kDa (Fig. 15A). As with *Hsp60*, the content of *Hsp70* was increased after treatment with PAR+UVR (Fig. 15Bi). However, the increase was higher than that of *Hsp60* with the content of *Hsp70* doubled to that of the pre-irradiations. The highest increase was observed in *U. lactuca* with more than 120%. PAR+UVA+UVB caused a higher increase than PAR+UVA in *L.digitata* and *U. lactuca* but was lower than PAR+UVA in *P. palmata*. Significantly, PAR+UVA caused a higher increase (i.e. 111% increase) than PAR+UVA+UVB (i.e. 100% increase) in *S. chordalis.* In addition, PAR alone had a positive effect on *Hsp70* of *S. chordalis* but a negative effect on *D. dichotoma*. The percentage of *Hsp70* in post-recovery algae slowly reduced towards that of their pre-irradiations (Fig. 15Bii). Recovery was delayed in PAR+UVA-treated *S. chordalis* and *P. palmata*

compared to PAR+UVA+UVB and in PAR+UVA+UVB-treated *L. digitata a*nd *D. dichotoma* compared to PAR+UVA.

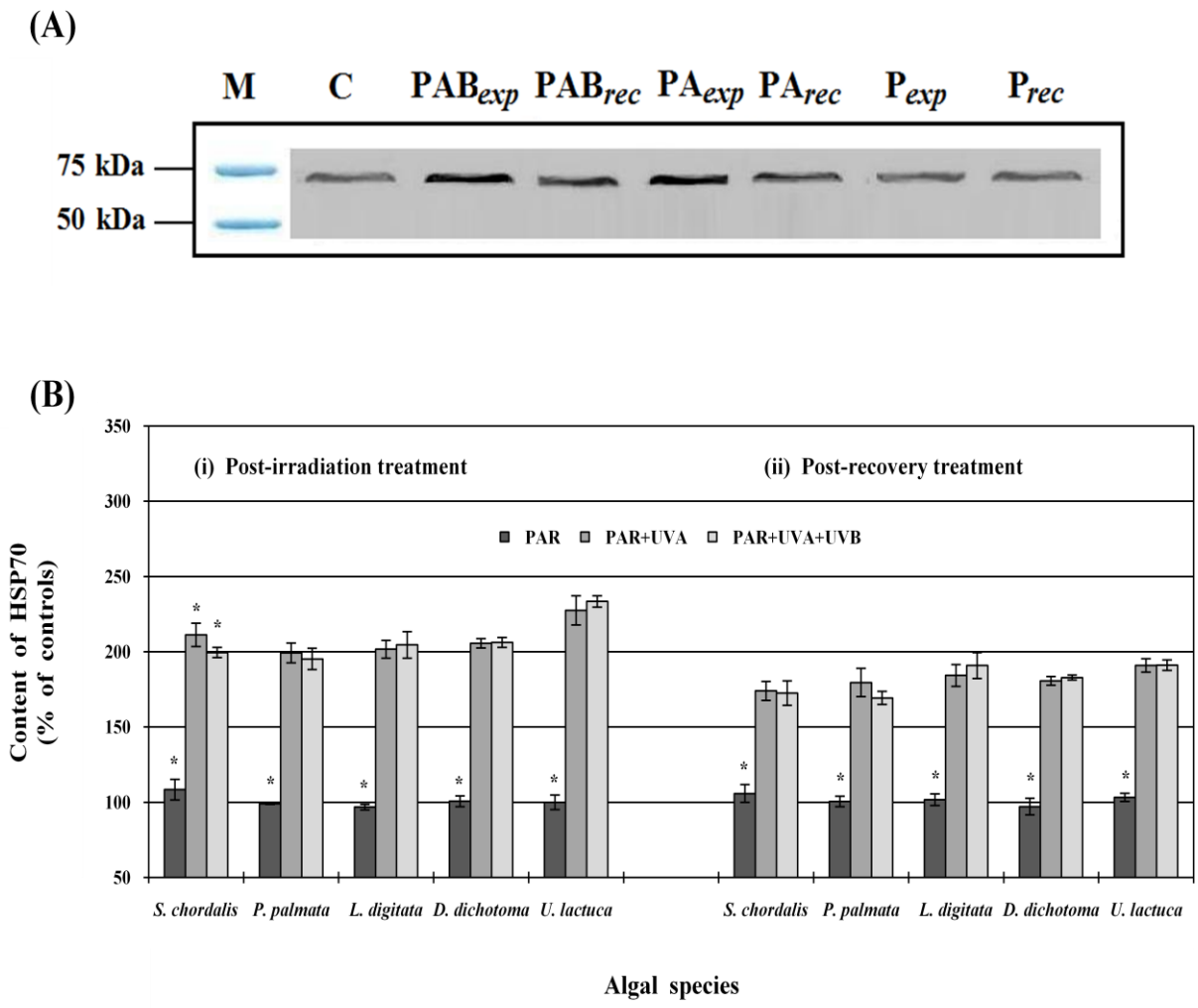

Fig. 15: An example of a western blot of the stress protein, HSP70 (*A*) in the macroalgae and percentage content of *Hsp70* quantified from corresponding blots (*B*), details as in Fig. 12.

3.1.7 Statistical comparisons for low PAR and high UVR

The effect of light treatments on the photosynthetic performance, protein content, Chl a content, RuBisCO and CAT activities was dependent on the species (Table 12A). Moreover, these parameters differed significantly when the effect of species and light treatments were measured independently. The content of R-PC, Chl c and fucoxanthin was not species-dependent but differ under different light

treatments. Similar results were also observed with GAPDH and GR activities as well as the content of RuBisCO LSU. In contrast, when the effect of light treatments was examined individually, the content of R-PE, activity of APX, content of D1 protein and the stress proteins, differed significantly. Additionally, these parameters were significantly different between species. The effect of light treatments was, however, species-independent.

Table 12: Results (*p*-values) of a two-way ANOVA's on photosynthetic parameters; protein content; pigments content; photosynthetic enzymes activity; antioxidative enzymes activity; and, content of large-subunit (LSU) of RuBisCO, D1 protein and stress proteins calculated from samples after 5 h irradiation at L_1 (i.e. post-irradiation) and after 18 h recovery periods (i.e. post-recovery).

Responses	Main effects		Interactive effect
	Species	Treatment	Species x Treatment
(A) Post-irradiation treatment:			
Photosynthetic parameters			
F_v/F_m	< 0.001 *	< 0.001 *	0.007 *
$rETR_{max}$	< 0.001 *	< 0.001 *	< 0.001 *
α	< 0.001 *	< 0.001 *	< 0.001 *
I_k	0.019 *	< 0.001 *	< 0.001 *
Protein	< 0.001 *	< 0.001 *	0.029 *
Pigments			
Chl a	0.001 *	< 0.001 *	0.004 *
[a] R-PE	0.004 *	< 0.001 *	0.101 *n.s.*
[a] R-PC	0.812 *n.s.*	< 0.001 *	0.083 *n.s.*
[b] Chl c	0.396 *n.s.*	< 0.001 *	0.784 *n.s.*
[b] Fucoxanthin	0.986 *n.s.*	< 0.001 *	0.130 *n.s.*
Photosynthetic enzymes			
RuBisCO	0.020 *	< 0.001 *	0.001 *
GAPDH	0.903 *n.s.*	< 0.001 *	0.217 *n.s.*
Antioxidative enzymes			
CAT	< 0.001 *	< 0.001 *	0.043 *
APX	< 0.001 *	< 0.001 *	0.109 *n.s.*
GR	0.079 *n.s.*	< 0.001 *	0.769 *n.s.*
LSU of RuBisCO	0.051 *n.s.*	< 0.001 *	0.384 *n.s.*
D1 protein	< 0.001 *	< 0.001 *	0.059 *n.s.*
Stress proteins			
HSP60	0.002 *	< 0.001 *	0.526 *n.s.*
HSP70	0.016 *	< 0.001 *	0.176 *n.s.*
(B) Post-recovery treatment:			
Photosynthetic parameters			
F_v/F_m	< 0.001 *	< 0.001 *	0.001 *
$rETR_{max}$	< 0.001 *	< 0.001 *	< 0.001 *
α	< 0.001 *	< 0.001 *	< 0.001 *
I_k	< 0.001 *	< 0.001 *	< 0.001 *
Protein	< 0.001 *	< 0.001 *	0.511 *n.s.*
Pigments			
Chl a	0.010 *	< 0.001 *	0.050 *n.s.*
[a] R-PE	0.001 *	< 0.001 *	0.003 *
[a] R-PC	0.006 *	< 0.001 *	< 0.001 *
[b] Chl c	0.099 *n.s.*	< 0.001 *	0.231 *n.s.*
[b] Fucoxanthin	0.088 *n.s.*	< 0.001 *	0.275 *n.s.*

(Table 12 continued...)

Photosynthetic enzymes			
RuBisCO	< 0.001 *	< 0.001 *	0.011 *
GAPDH	0.027 *	< 0.001 *	0.004 *
Antioxidative enzymes			
CAT	< 0.001 *	< 0.001 *	0.001 *
APX	0.543 *n.s.*	0.073 *n.s.*	0.016 *
GR	< 0.001 *	0.134 *n.s.*	0.104 *n.s.*
LSU of RuBisCO	0.004 *	< 0.001 *	0.348 *n.s.*
D1 protein	< 0.001 *	< 0.001 *	0.013 *
Stress proteins			
HSP60	0.015 *	< 0.001 *	0.111 *n.s.*
HSP70	0.458 *n.s.*	< 0.001 *	0.505 *n.s.*

Experimental factors are species (the 5 macroalgal species studied) and treatment (PAR, PAR+UVA and PAR+UVA+UVB). * indicates a significant value at $p < 0.05$ while *n.s.* indicates a not significant value. Data are calculated from three replicates from each experiments (see MATERIALS AND METHODS for explanation).
[a] Comparisons were made between the red algae, *S. chordalis* and *P. palmata*
[b] Comparisons were made between the brown algae, *L. digitata* and *D. dichotoma*

The recovery of photosynthetic performance, phycobiliproteins contents, photosynthetic enzymes and CAT activities as well as the content of D1 protein varied significantly among the species and the light treatments which were inter-dependent with each other (Table 12B). Recovery of protein and Chl a plus HSP60 contents, on the other hand, differed significantly among the species and the light treatments but the effect of light treatments did not rely on species. Chl c and fucoxanthin in the brown algae and HSP70 recovered significantly indifferent on species but dependent on light treatments. Additionally, the recovery effect of light treatments was not dependent on species. Contrastingly, recovery of APX and GR activities varied insignificantly with light treatments. Furthermore, recovery of APX was not species dependent. The consequence of light treatments on APX activity was dependent on species while acting independently on GR activity.

3.2 Macroalgal responses to high PAR and high UVR stress

3.2.1 Photosynthetic performance under high PAR and high UVR

The irradiation conditions of the experimental setup are listed in Table 13. These conditions are termed high PAR 1 (H_1, see MATERIALS AND METHODS section 2.2.2 for explanation) corresponding to the high background PAR irradiance emitted by the sun simulator compared to that of the fluorescent lamps. The photosynthetic characteristics of the samples before irradiation (i.e. pre-irradiation or control) are listed in Table 14.

Table 13: Irradiances of the different spectral ranges of the sun simulator applied in the experiments.

Species	PAR ($\mu mol\ m^{-2}\ s^{-1}$)	PAR ($W\ m^{-2}$)	UVA ($W\ m^{-2}$)	UVB ($W\ m^{-2}$)	Ratio of PAR:UVA:UVB
S. chordalis	704	148	37.9	1.72	100:26:1.2
P. palmata	648	136	35.2	1.35	100:26:1.0
L. digitata	677	143	36.4	1.59	100:25:1.1
D. dichotoma	611	129	35.7	1.22	100:28:0.9
U. lactuca	669	141	37.2	1.71	100:26:1.2

Table 14: Photosynthetic parameters of the macroalgae before irradiation at high PAR and high UVR (i.e. pre-irradiation or control). Data are means ±SD values of n=12.

Species	Parameters			
	F_v/F_m [rel. unit]	$rETR_{max}$ [rel. unit]	α [rel. unit]	I_k [$\mu mol\ m^{-2}\ s^{-1}$]
S. chordalis	0.636 ± 0.02	22.65 ± 4.8	0.519 ± 0.02	44.23 ± 11.5
P. palmata	0.553 ± 0.04	13.30 ± 3.7	0.577 ± 0.06	23.09 ± 7.3
L. digitata	0.749 ± 0.01	50.08 ± 8.1	0.754 ± 0.02	66.17 ± 11.1
D. dichotoma	0.689 ± 0.02	22.52 ± 3.6	0.472 ± 0.02	46.09 ± 10.8
U. lactuca	0.741 ± 0.01	62.54 ± 5.9	0.607 ± 0.04	109.32 ± 15.2

The maximum quantum yield (F_v/F_m) and the photosynthetic parameters of the post-irradiation and post-recovery algae are displayed in Fig. 16. Collectively, F_v/F_m of the brown algae were the most affected, followed by the red algae and the green alga (ANOVA, SNK *post-hoc* test, $p<0.001$) while its recovery was the fastest in the green alga ($p<0.001$). Individually, the highest reduction of F_v/F_m was observed in *L. digitata* and the lowest in *U. lactuca* ($p<0.001$). Faster recovery, however, was observed in *U. lactuca* with the slowest in *L. digitata* for the brown algae and *S. chordalis* for the red algae ($p<0.001$). F_v/F_m of the algae were strongly affected by all the light treatments with values reduced to below than 40% (Fig. 16Ai). Several trends in the F_v/F_m changes could be observed. Firstly, in *S. chordalis* (i.e. 71% reduction) and *U. lactuca* (i.e. 63% reduction), UVR alone (i.e. UVA+UVB) caused the least effect while the least effect in the remaining algal species was observed under PAR alone. Secondly, PAR+UVA caused the

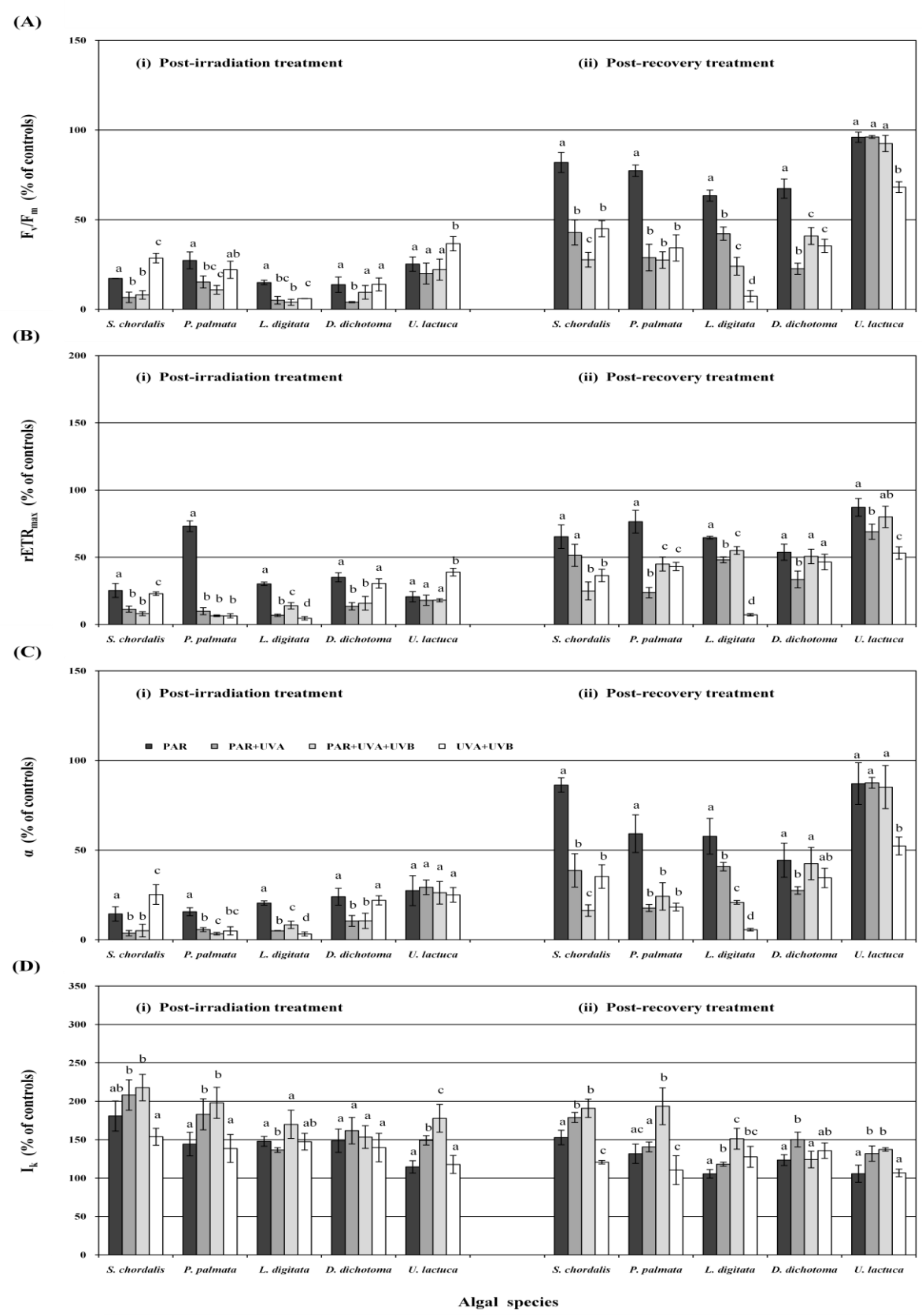

Fig. 16: Maximum quantum yield (F_v/F_m, *A*), maximum relative electron transport rate ($rETR_{max}$, *B*), photosynthetic efficiency parameter (α, *C*) and light saturation parameter (I_k, *D*) in the macroalgae after 5 h irradiation (post-irradiation, *i*) and after 18 h recovery (post-recovery, *ii*). *Black bars:* PAR only, *dark grey bars:* PAR+UVA, *light grey bars:* PAR+UVA+UVB, *white bars:* UVA+UVB. Different letters above bars indicate significant difference between light treatments within similar species (ANOVA, Fischer's LSD test, $p < 0.05$, n=3)

strongest effect in *S. chordalis, D. dichotoma* and *U. lactuca* while PAR+UVA+UVB caused the strongest effect in *P. palmata* and *L. digitata*. In particular, PAR+UVA+UVB caused less effect in *D. dichotoma* (i.e. 86% reduction) in comparison to PAR+UVA (i.e. 90% reduction). All post-recovery algae showed signs of F_v/F_m recovery (Fig. 16Aii). In most of the algae, recovery was the fastest in PAR-treated algae which increased to 82% in *S. chordalis,* 77% in *P. palmata,* 63% in *L. digitata* and 67% in *D. dichotoma*. There was a delay in recovery in *U. lactuca* treated with UVA+UVB (i.e. increased to 68%) while in the rest of the treatments, recovery was nearly completed. There was also a delay in recovery of PAR+UVA+UVB-treated *S. chordalis* and *L. digitata* (i.e. increased to 45% and 24%, respectively) compared to that of PAR+UVA-treated algae (i.e. increased to 43% and 42%, respectively). In contrast, no recovery was observed in UVA+UVB-treated *L. digitata*. Furthermore, PAR+UVA+UVB-treated *D. dichotoma* (i.e. increased to 41%) showed a faster recovery than PAR+UVA-treated algae (i.e. increased to 23%).

The maximum relative electron transport rate ($rETR_{max}$) of the algae was also strongly affected by the high irradiance treatments (Fig. 16Bi). Whilst $rETR_{max}$ of most of the algae was less affected by PAR alone with a 75% reduction in *S. chordalis*, 27% reduction in *P. palmata* and 70% reduction in *L. digitata, U. lactuca* was the least affected by UVA+UVB with a 61% reduction. PAR+UVR caused the strongest effect in all the algae except in *L. digitata* whereby UVA+UVB affected the alga the strongest with a 95% reduction. In addition, $rETR_{max}$ of *L. digitata* irradiated with PAR+UVA was reduced by 93% compared to 86% observed under PAR+UVA+UVB. There was a significantly smaller $rETR_{max}$ recovery observed in post-recovery *L. digitata* treated with UVA+UVB (i.e. an increase of 3% from post-irradiation) than the other treatments (Fig. 16Bii). Furthermore, UVA+UVB was the slowest to recover in *U. lactuca* with an increase to 53%. PAR+UVA+UVB-treated *P. palmata* (i.e. 45%), *L. digitata* (i.e. 55%) *and D. dichotoma* (i.e. 51%) showed a significantly higher $rETR_{max}$ after the recovery than their PAR+UVA equivalences (i.e. 24%, 48% and 34%, respectively). However, the effect was reversed in *S. chordalis* with $rETR_{max}$ of PAR+UVA was higher (i.e. 51%) than PAR+UVA+UVB (i.e. 25%). Post-recovery algae treated with PAR alone had the highest $rETR_{max}$ after the recovery in *P. palmata* (i.e.

77%) and *L. digitata* (i.e. 65%) in comparison to the other treatments while in the rest of the algal species, similar trend was observed but with no significant difference.

PAR alone reduced the photosynthetic efficiency (α) of *P. palmata* and *L. digitata* by 84% and 80%, respectively, the least affected among the treatments (Fig. 16Ci). UVA+UVB, on the other hand, affected *S. chordalis* the least by reducing α by 75%. Further reduction in α was observed with PAR+UVR treatments in most of the algae. Distinctive effect between PAR+UVA and PAR+UVA+UVB treatments, however, was noticeable in *P. palmata* and *L. digitata*. In *P. palmata*, PAR+UVA+UVB caused a higher reduction of α (i.e. 97% reduction) than PAR+UVA (i.e. 94% reduction) while in *L. digitata*, PAR+UVA caused a higher reduction (i.e. 95% reduction) than PAR+UVA+UVB (i.e. 92% reduction). Recovery of α in post-recovery *L. digitata* treated with UVA+UVB was the slowest among the light treatments with a significant 2% increase from the post-irradiation algae (Fig. 16Cii). There was also a delay in α recovery of *U. lactuca* treated with UVA+UVB (i.e. increased to 52%) while in the rest of the treatments, α was almost fully recovered. In *S. chordalis* and *L. digitata*, PAR+UVA (i.e. increased to 39% and 41%, respectively) showed a much faster recovery than PAR+UVA+UVB (i.e. increased to 16% and 21%, respectively) while in *D. dichotoma*, recovery in PAR+UVA+UVB (i.e. increased to 42%) was faster than PAR+UVA (i.e. increased to 27%). Furthermore, PAR-treated *S. chordalis* (i.e. increased to 86%), *P. palmata* (i.e. increased to 59%) and *L. digitata* (i.e. increased to 58%) showed the fastest to recover among the light treatments.

Unlike the other parameters, the light saturation parameter, I_k was increased by all the light treatments in the post-irradiation algae (Fig. 16Di). Several trends in the increase were observed among the algae. Firstly, the increase in post-irradiation algae treated with PAR+UVA+UVB was the highest among the treatments as observed in most of the algae. In particular, PAR+UVA+UVB showed a higher increase (i.e. 78%) than PAR+UVA (i.e. 49%) in *U. lactuca.* Secondly, the increase was less under UVA+UVB as observed by the trend in *S. chordalis, P. palmata* and *D. dichotoma*. The recovery of I_k in post-recovery algae followed several trends as well (Fig. 16Dii). Post-recovery algae treated with UVA+UVB were the

fastest to recover in *S. chordalis* (i.e. a significant reduction to 121%) and *P. palmata* while in the rest of the algae, PAR alone had the fastest recovery. PAR+UVA+UVB delayed the recovery of I_k in *P. palmata* and *L. digitata*. Furthermore, PAR+UVA+UVB (i.e. reduced to 124%) showed a significantly faster recovery than PAR+UVA (i.e. reduced to 150%) in *D. dichotoma.*

Synergistic inhibitory effect of the UVR on F_v/F_m is shown in Fig. 16Ai. Most of the UVR influence in the inhibition of F_v/F_m originated from UVA, higher in *D. dichotoma* and smaller in *U. lactuca* than the rest of the algal species (Fig. 17A). UVB on the other hand, had a larger role than UVA in the inhibition of *U. lactuca* (Fig. 17B). Moreover, UVB reduced the inhibition in *S. cordalis* and largely in *D. dichotoma.* It also appeared that UVA and UVB caused more effect on the recovery of the algae than during the inhibition except in *U. lactuca*. Additonal UVB, however, increased the recovery of F_v/F_m of *D. dichotoma.*

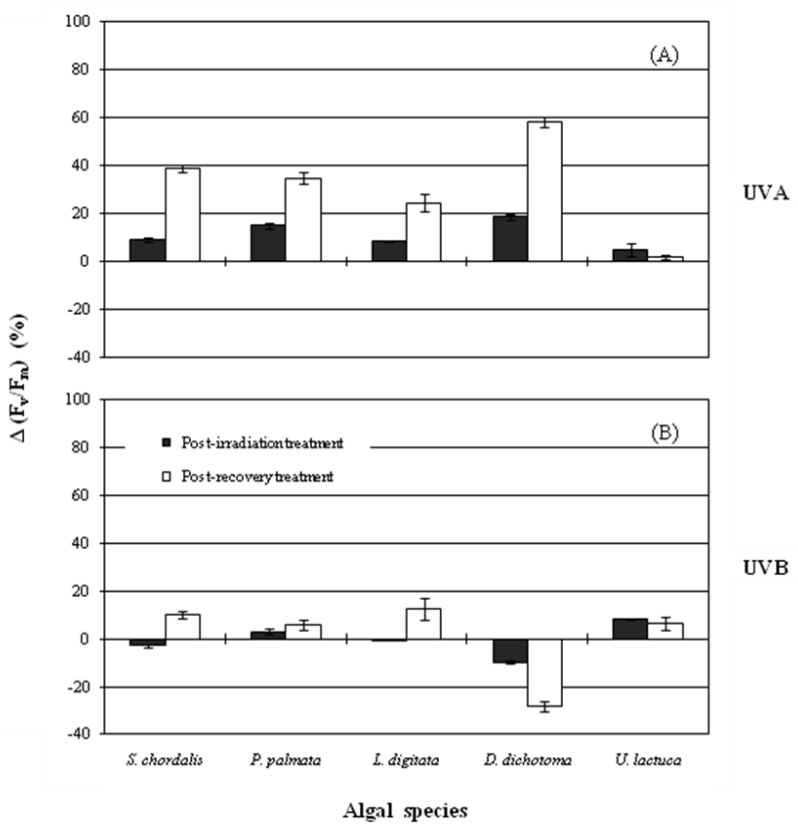

Fig. 17: Role of different wavelength ranges to the overall inhibition of photosynthetic performance in the macroalgae expressed as the changes in F_v/F_m values [Δ (F_v/F_m)] (in % of pre-irradiation values) measured under PAR and PAR+UVA treatment (*A*), and PAR+UVA and PAR+UVA+UVB treatment (*B*). *Black bars*: after 5 h irradiation or post-irradiation; *white bars*: after 18 h recovery or post-recovery. Data are means ±SD from triplicates of each treatment.

3.2.2 Pigments content under high PAR and high UVR

Pigments content of the macroalgae examined before irradiation (i.e. pre-irradiation) is listed in Table 8. In general, the content of chlorophyll (Chl) a, R-phycoerythrin (R-PE) and R-phycocyanin (R-PC) of the red algae were decreased by all the light treatments (Fig. 18). UVA+UVB appeared to cause the least reduction in Chl a content of *S. chordalis* (Fig. 18Ai). In addition, PAR alone significantly increased the content of R-PE in *S. chordalis* by about 18% (Fig. 18Aii) *w*hile there was an increasing trend observed for R-PC in this alga (Fig. 18Aiii). PAR+UVR and UVA+UVB treatments further reduced the content of R-PE and R-PC in this alga. Comparatively, PAR alone appeared to cause the least effect on Chl a (Fig. 18Bi) and R-PC (Fig. 18Biii) contents of *P. palmata* while significantly reduced R-PE to about 12% (Fig. 18Bii). Moreover, all pigments were further reduced under the PAR+UVR treatments. All post-recovery algae showed signs of recovery. There was, however, no sign of recovery for Chl a content of post-recovery *S. chordalis* treated with UVA+UVB (Fig. 18Ai). R-PE in post-recovery *S. chordalis* treated with all light treatments exceeded that of the pre-irradiations (Fig. 18Aii). Similar trend was observed in the alga for R-PC of PAR+UVA+UVB and UVA+UVB as well (Fig. 18Aiii). In post-recovery *P. palmata*, a delay in recovery was observed in PAR+UVR treatments for all pigments and generally showed a slower recovery of the pigments (Fig. 18Bi-iii) than *S. chordalis* (Fig. 18Ai-iii).

Irradiation of both the brown algae with PAR+UVR treatments had damaging effect on their Chls as well as fucoxanthins, however, with exception (Fig. 19). PAR alone caused a 13% reduction in Chl a content of *L. digitata* while there was a 19% reduction with UVA+UVB and about 28% reduction among both PAR+UVR treatments (Fig. 19Ai). In addition, PAR and UVA+UVB caused a less effect on the alga's Chl c content compared to PAR+UVR (Fig. 19Aii) while a lower fucoxanthin was observed under PAR+UVA+UVB than the other light treatments (Fig. 19Aiii). Comparatively, PAR caused a significantly lower reduction in the Chl a content of *D. dichotoma* (i.e. 20% reduction) than the other light treatments which showed a much higher reduction trend (Fig. 19Bi). Furthermore, Chl c of *D. dichotoma* was significantly less affected by UVA+UVB (i.e. 33% reduction) compared to PAR and PAR+UVR

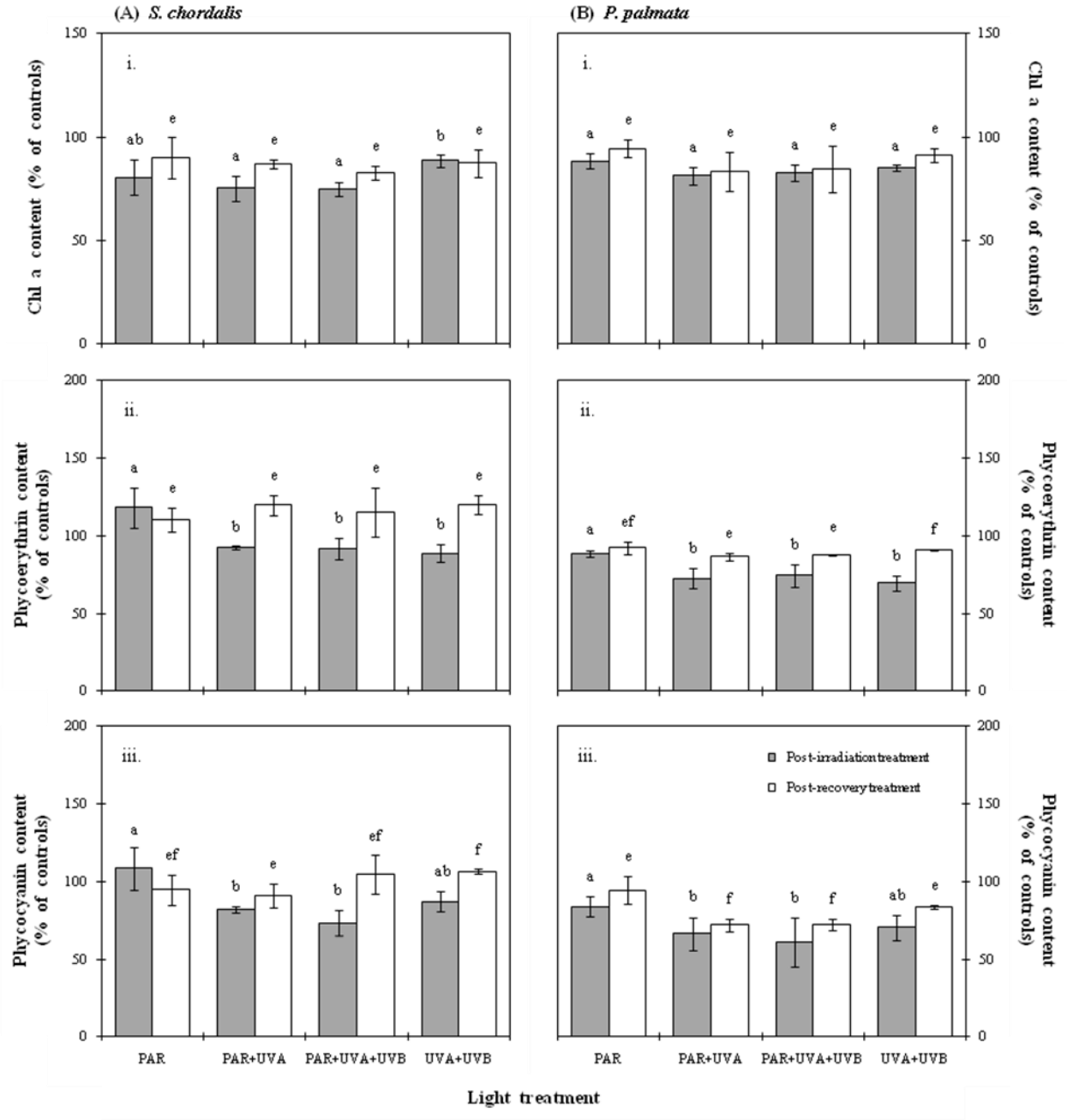

Fig. 18: Contents of chlorophyll a (*i*), R-phycoerythrin (*ii*) and R-phycocyanin (*iii*), in the red algae, *S. chordalis* (*A*) and *P. palmata* (*B*). *Grey bars*: after 5 h irradiation or post-irradiation, *white bars*: after 18 h recovery or post-recovery. Different letters above bars indicate significantly different values determined by comparison between different light treatments (ANOVA, Fischer's LSD test, $p < 0.05$, n=3).

(Fig. 19Bii). Fucoxanthin, on the other hand, showed two different trends. Whilst there was a significant reduction under PAR+UVA+UVB (i.e. 20%), an increase in fucoxanthin was observed under PAR (i.e. a significant 91% increase), PAR+UVA and UVA+UVB (Fig. 19Biii). All affected pigments in both brown

algae showed signs of recovery but to a variable extent. Basically, recovery of the pigments in both brown algae was delayed in post-recovery algae treated with PAR+UVR. Additionally, recovery of Chl c was faster in *L. digitata* while the recovery of fucoxanthin was faster in *D. dichotoma* than the other algal species.

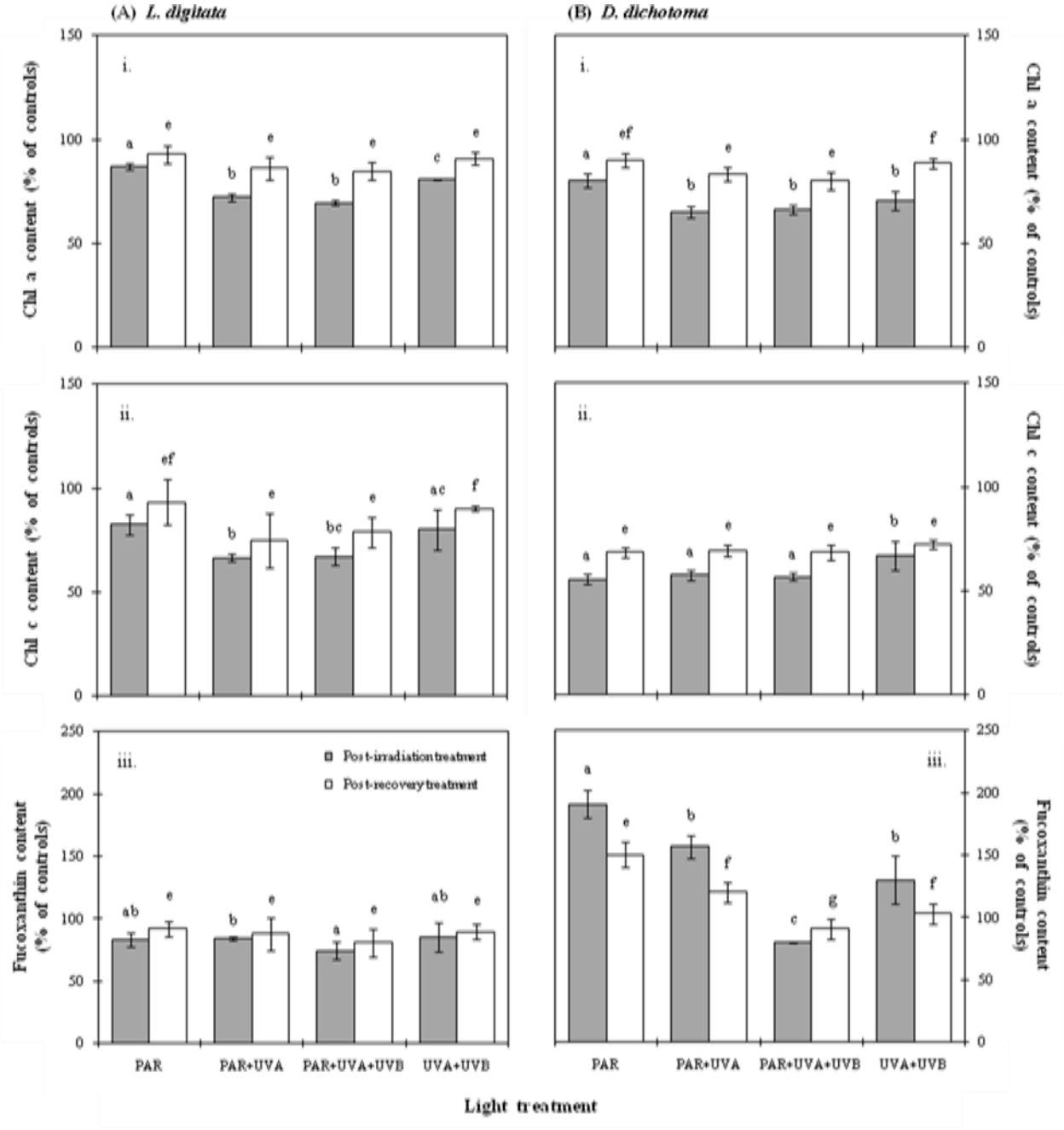

Fig. 19: Contents of chlorophyll a (*i*), chlorophyll c (*ii*) and fucoxanthin (*iii*) in the brown algae, *L. digitata* (*A*) and *D. dichotoma* (*B*). *Grey bars*: after 5 h irradiation or post-irradiation, *white bars*: after 18 h recovery or post-recovery. Different letters above bars indicate significantly different values determined by comparison between different light treatments (ANOVA, Fischer's LSD test, $p < 0.05$, n=3).

Similar to the other algal species, the Chls (i.e. Chl a and Chl b) in *U. lactuca* were found to be damaged by all the light treatments as well (Fig. 20). The reduction in the content of both the Chls followed a trend. Both Chls were less affected by either PAR and UVA+UVB compared to the PAR+UVR treatments. Recovery of both Chls was significantly faster in post-recovery algae treated with PAR (i.e. increased to 96% for both Chls) than in any other light treatments. In addition, recovery of Chl b was basically delayed compared to Chl a.

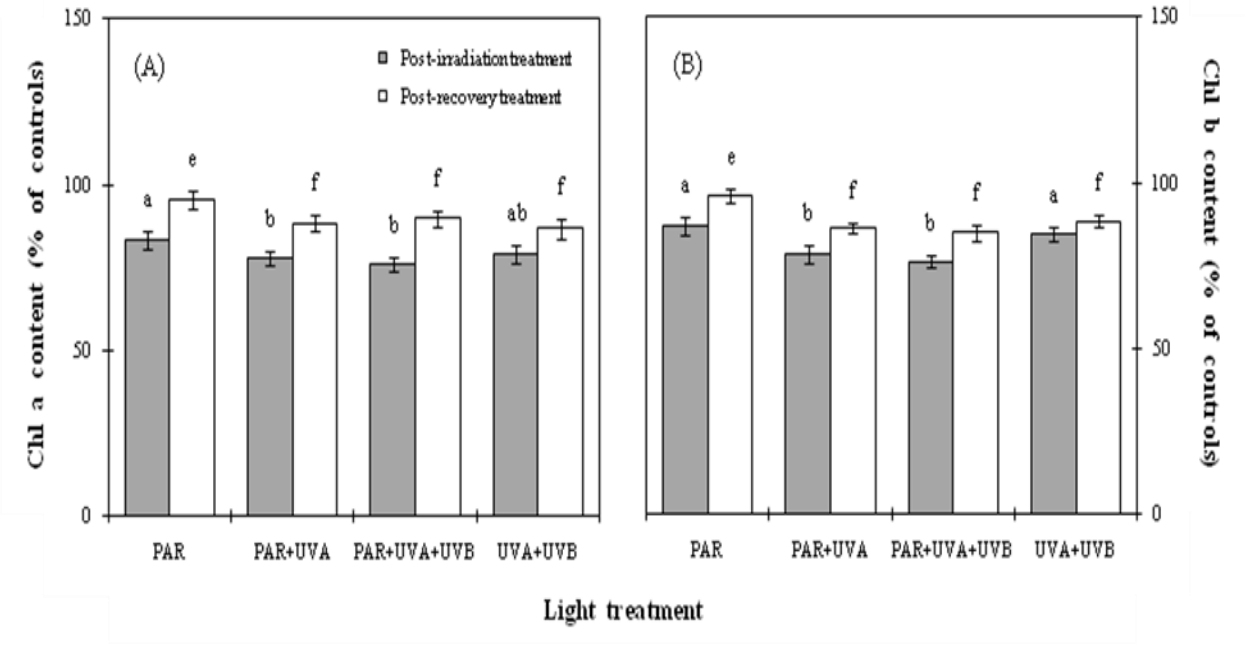

Fig. 20: Contents of chlorophyll a (*A*) and chlorophyll b (*B*) in the green alga, *U. lactuca. Grey bars:* after 5 h irradiation or post-irradiation, *white bars:* after 18 h recovery or post-recovery. Different letters above bars indicate significantly different values determined by comparison between different light treatments (ANOVA, Fischer's LSD test, $p < 0.05$, n=3).

3.2.3 Protein content under high PAR and high UVR

The total soluble proteins (TSP) content of the macroalgae before irradiation (i.e. pre-irradiation) is listed in Table 9. TSP content was reduced by at least 25% in most of the post-irradiation algae by all the light treatments (Fig. 21A). TSPs were significantly less affected by PAR as could be observed in *S. chordalis* (i.e. 23% reduction), *P. palmata* (i.e. 23% reduction) and *U. lactuca* (i.e. 24% reduction). UVA+UVB, on

the other hand, appeared to cause the highest reduction of TSP content in most of the algae. Furthermore, PAR+UVA+UVB caused stronger effect than PAR+UVA as displayed by a trend in *S. chordalis, P. palmata* and *D. dichotoma*. The slowest recovery of TSP was observed in post-recovery algae treated with UVA+UVB especially in *S.chordalis* (i.e. increased to 75%) and *U. lactuca* (i.e. increased to 62%) (Fig. 21B). In addition, the fastest to recover was the PAR-treated algae as was noticeable in *S. chordalis* (i.e. increased to 89%). *S. chordalis* irradiated with PAR+UVA showed a faster recovery (i.e. increased to 83%) than PAR+UVA+UVB (i.e. increased to 79%) as well. Other algal species showed similar trend as well.

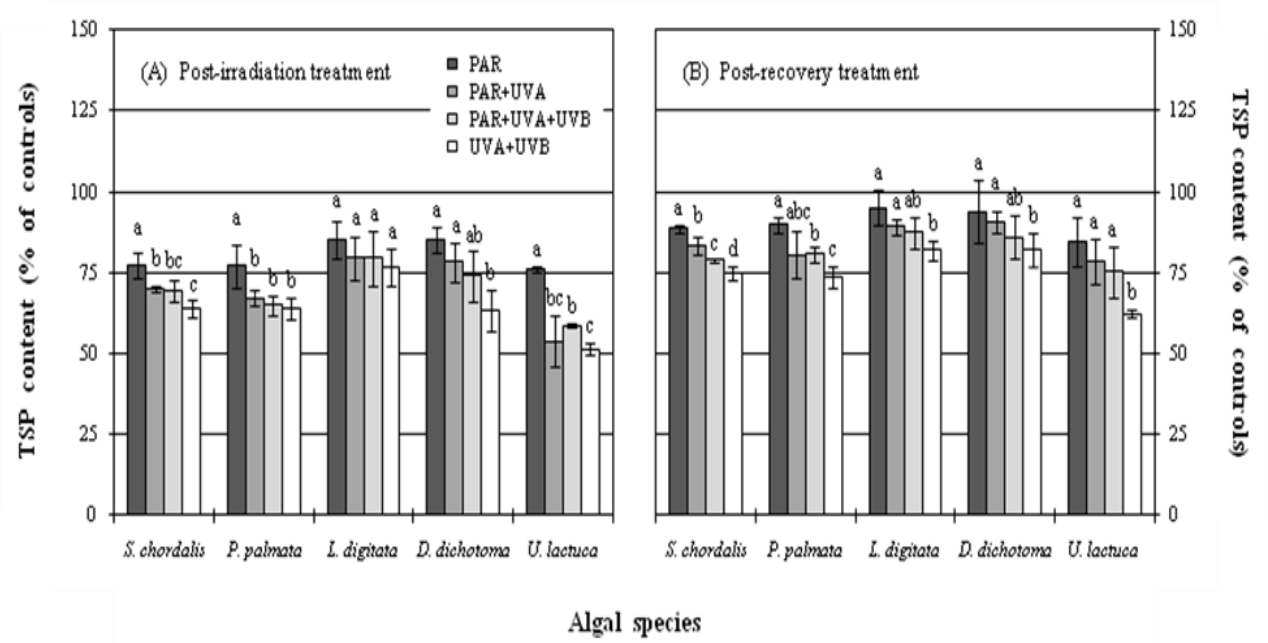

Fig. 21: Total soluble proteins (TSP) content in the macroalgae after 5 h irradiation (post-irradiation, *A*) and after 18 h recovery (post-recovery, *B*). *Black bars:* PAR, *dark grey bars:* PAR+UVA, *light grey bars:* PAR+UVA+UVB, *white bars:* UVA+UVB. Different letters above bars indicate significantly different values determined by comparison between different light treatments within similar species (ANOVA, Fischer's LSD test, $p < 0.05$, n=3).

3.2.4 Photosynthetic enzymes activity under high PAR and high UVR

The catalytic activity of ribulose-1,5-bisphosphate carboxylase/oxygenase (RuBisCO) and glyceraldehyde-3-phosphate dehydrogenase (GAPDH) in the macroalgae before irradiation (i.e. pre-irradiation) is listed in Table 15.

Table 15: Photosynthetic enzymes activity of the macroalgae before irradiation at high PAR and high UVR (i.e. pre-irradiation or control). Data are means ±SD values of n=3.

Species	Enzymes [U/mg TSP]	
	RuBisCO	GAPDH
S. chordalis	1.45 ± 0.5	0.29 ± 0.7
P. palmata	1.29 ± 0.4	0.31 ± 0.3
L. digitata	1.33 ± 0.3	0.53 ± 0.3
D. dichotoma	0.93 ± 0.4	0.17 ± 0.6
U. lactuca	1.51 ± 0.6	0.71 ± 0.7

The activity of RuBisCO was strongly affected by all the light treatments (Fig. 22Ai). The activity was reduced by 49%-68% in *S. chordalis*, 45%-55% in *P. palmata*, 40%-52% in *L. digitata*, 41%-49% in *D. dichotoma* and 25%-32% in *U. lactuca*. UVA+UVB caused a significantly less reduction compared to the other light treatments in *S. chordalis* (i.e. 49% reduction) and *U. lactuca* (i.e. 25% reduction). PAR+UVA+UVB appeared to cause the strongest effect on RuBisCO as displayed by a trend in *S. chordalis* and *P. palmata* while in the remaining algal species, the strongest effect was caused by PAR+UVA. However, PAR+UVA caused a significantly higher reduction (i.e. 49%) in *D. dichotoma* than the other light treatments. The activity of RuBisCO showed a full or almost a full recovery in *U. lactuca* (Fig. 22Aii). A delay in the recovery was observed in post-recovery algae treated with PAR+UVR. PAR+UVA+UVB for instance, had the slowest recovery among the light treatments as observed in *P. palmata* (i.e. increased to 63%) and *L. digitata* (i.e. increased to 71%).

Similarly, the activity of GAPDH was strongly affected by all the light treatments as well (Fig. 22Bi). The effect, however, was generally weaker than that observed for RuBisCO. The activity of GAPDH reduced by 31%-45% in *S. chordalis*, 22%-31% in *P. palmata*, 33%-44% in *L. digitata*, 32%-42% in *D. dichotoma* and 12%-20% in *U. lactuca*. PAR caused a significantly less reduction compared to the other light treatments as observed in *P. palmata* (i.e. 22% reduction) and *D. dichotoma* (i.e. 31% reduction). In these two algal species, UVA+UVB caused significantly lower reduction in the activity following PAR while PAR+UVR caused the highest reduction. In general, GAPDH activity in all post-irradiation algae was higher under PAR+UVA+UVB compared to PAR+UVA. However, PAR+UVA+UVB significantly caused a higher reduction in *P. palmata* (i.e. 31% reduction) than PAR+UVA (i.e. 28% reduction). The

recovery in GAPDH activity was the fastest in post-recovery algae treated with PAR alone except for *U. lactuca*, while the slowest was in PAR+UVR (Fig. 22Bii). For comparison, PAR+UVA+UVB was the slowest to recover in *S. chordalis* and *P. palmata* while PAR+UVA was the slowest to recover in *L. digitata* and *D. dichotoma*.

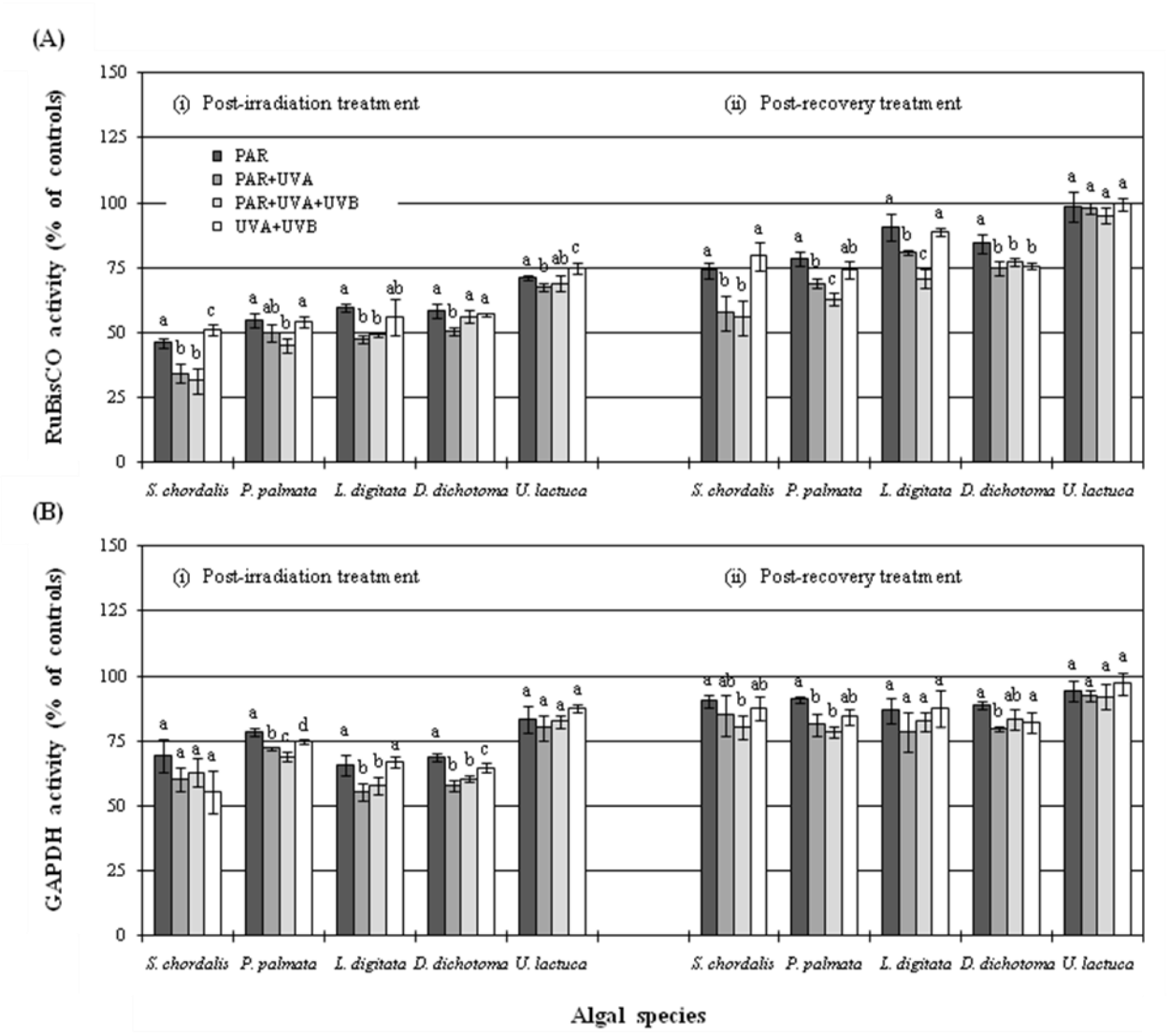

Fig. 22: Activity of ribulose-1,5-bisphosphate carboxylase/oxygenase (RuBisCO) (*A*) and glyceraldehyde-3-phosphate dehydrogenase (GAPDH) (*B*) in the macroalgae after 5 h irradiation (post-irradiation, *i*) and after 18 h recovery (post-recovery, *ii*). *Black bars:* PAR, *dark grey bars:* PAR+UVA, *light grey bars:* PAR+UVA+UVB, *white bars:* UVA+UVB. Different letters above bars indicate significantly different values determined by comparison between different light treatments within similar species (ANOVA, Fischer's LSD test, $p < 0.05$, n=3).

3.2.5 Antioxidative enzymes activity under high PAR and high UVR

The catalytic activity of the antioxidative enzymes, catalase (CAT), ascorbate peroxidase (APX) and glutathione reductase (GR) in the macroalgae before irradiation (i.e. pre-irradiation) is listed in Table 16.

Table 16: Antioxidative enzymes activity of the macroalgae before irradiation at high PAR and high UVR (i.e. pre-irradiation or control). Data are means ±SD values of n=3.

Species	Enzymes [U/mg TSP]		
	CAT	APX	GR
S. chordalis	0.41 ± 0.04	0.61 ± 0.03	0.35 ± 0.05
P. palmata	0.34 ± 0.07	0.57 ± 0.03	0.58 ± 0.03
L. digitata	0.39 ± 0.01	0.65 ± 0.02	0.49 ± 0.03
D. dichotoma	0.34 ± 0.03	0.79 ± 0.02	0.28 ± 0.01
U. lactuca	0.52 ± 0.02	1.15 ± 0.05	0.43 ± 0.06

In post-irradiation algae, the activity of the three antioxidative enzymes showed an increase (Fig. 23A-Ci). Among the antioxidative enzymes, the activity of CAT increased the most in all the algal species examined ($p<0.001$). The recovery was the fastest with CAT as well ($p=0.008$ for the red algae and $p<0.001$ for both brown and green algae). Overall increase in CAT activity was observed in the brown algae, followed by the red algae and the green alga ($p<0.001$, Fig. 23Ai). The increase in CAT activity was the smallest under PAR alone especially in *P. palmata* (i.e. 61% increase), *L. digitata* (i.e. 70% increase) and *D. dichotoma* (i.e. 66% increase). PAR+UVR caused the greatest increase especially in *S. chordalis* and *D. dichotoma* while *P. palmata* was affected the most by UVA+UVB (i.e. 81% increase). PAR+UVA caused a higher increase than PAR+UVA+UVB in most of the algae except in *U. lactuca.*

Recovery of CAT activity was the fastest in post-recovery *P. palmata* (i.e. reduced to 126%) and *D. dichotoma* (i.e. reduced to 134%) treated with PAR (Fig. 23Aii). For *L. digitata* (i.e. reduced to 131%) and *U. lactuca* (i.e. reduced to 103%), on the other hand, the fastest to recover was in UVA+UVB. A delay in recovery was observed in PAR+UVR-treated algae particularly in *S. chordalis* and *L. digitata*. In *D. dichotoma*, for example, a faster recovery was observed with PAR+UVA+UVB (i.e. reduced to 151%) than PAR+UVA (i.e. reduced to 157%).

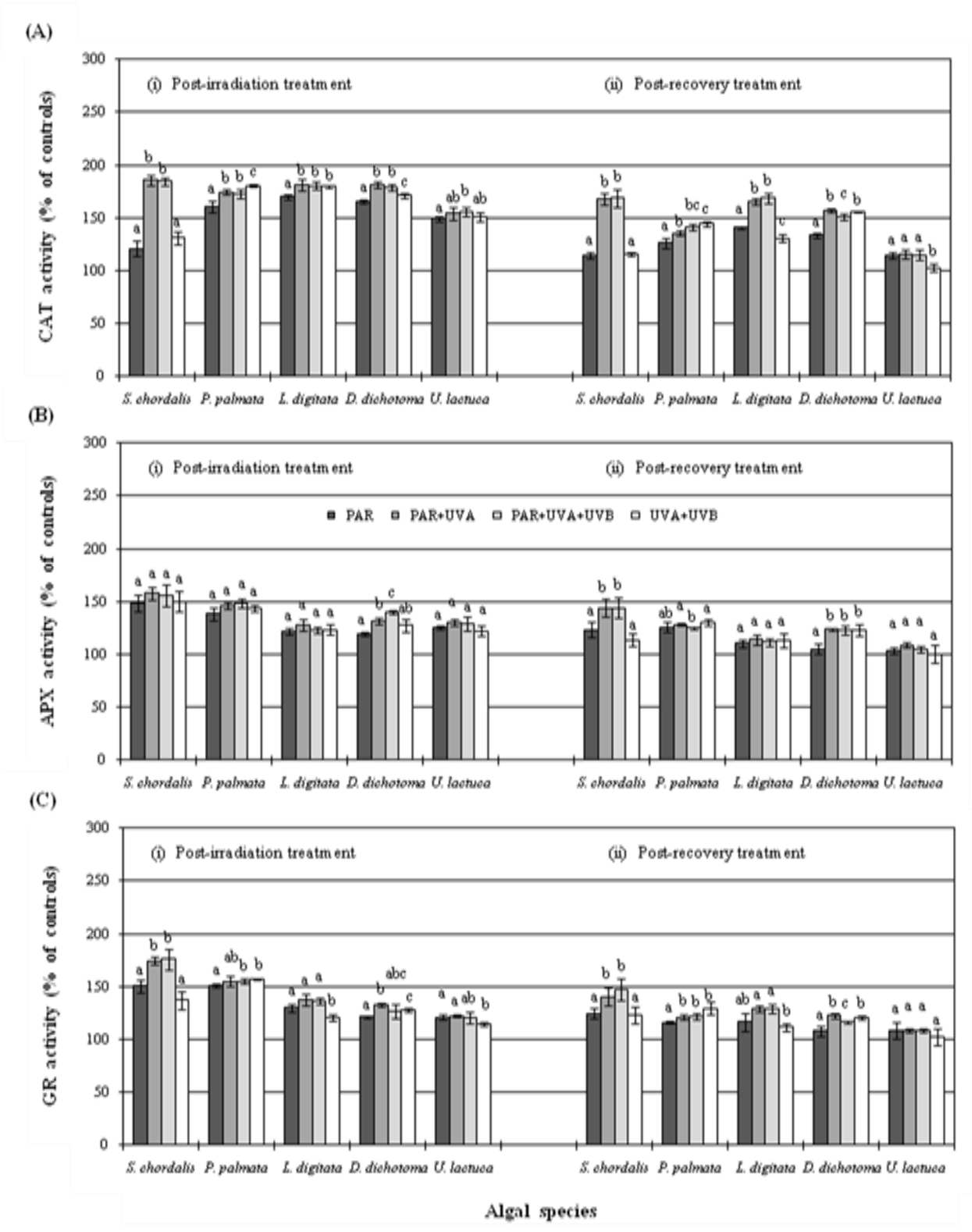

Fig. 23: Activity of catalase (CAT) (*A*), ascorbate peroxidase (APX) (*B*) and glutathione reductase (GR) (*C*) in the macroalgal species studied after 5 h irradiation (post-irradiation, *i*) and after 18 h recovery (post-recovery, *ii*). *Black bars:* PAR, *dark grey bars:* PAR+UVA, *light grey bars:* PAR+UVA+UVB, *white bars:* UVA+UVB. Different letters above bars indicate significantly different values determined by comparison between different light treatments within similar species (ANOVA, Fischer's LSD test, $p < 0.05$, n=3).

The activity of APX increased the most in the red algae, followed by the brown algae and green alga (p<0.001, Fig. 23Bi). PAR caused less increase of APX activity in most of the algae while PAR+UVA caused the highest increase in *S. chordalis, L. digitata* and *U. lactuca* while in *P. palmata* and *D. dichotoma* with PAR+UVA+UVB. In *D. dichotoma,* particularly, PAR+UVA+UVB caused a 40% increase in comparison to 31% under PAR+UVA. The activity of APX fully or almost fully recovered in all post-recovery *U. lactuca* (Fig. 23Bii). The fastest to recover in most of the post-recovery algae, especially in *D. dichotoma* (i.e. reduced to 105%), was observed in PAR while a slower recovery was observed in PAR+UVA or UVA+UVB. In *P. palmata,* the activity recovered faster in PAR+UVA+UVB (i.e. reduced to 125%) than in PAR+UVA (i.e. reduced to 128%).

Similar to APX, the activity of GR increased the most in the red algae, followed by the brown algae and the green alga (p<0.001, Fig. 23Ci). UVA+UVB caused the lowest increase in most of the algae particularly in *L. digitata* (i.e. 20% increase) and PAR+UVA caused the highest increase in *L. digitata, D. dichotoma* and *U. lactuca w*hile in *S. chordalis,* the highest increase was with PAR+UVA+UVB. Like CAT and APX, activity of GR was fully or almost fully recovered in post-recovery *U. lactuca* (Fig. 23Cii). PAR was the fastest to recover in *P. palmata* (i.e. reduced to 116%) and *D. dichotoma* (i.e. reduced to 123%). Generally, there was a delay in the recovery in PAR+UVR with GR activity of PAR+UVA+UVB reduced to a much lower value (i.e. 117%) than PAR+UVA (i.e. 123%) in *D. dichotoma.*

3.2.6 Contents of RuBisCO LSU, D1 protein, HSP60 and HSP70 under high PAR and high UVR

The content of RuBisCO LSU was reduced in the post-irradiation algae but improved later in post-recovery algae (Fig. 24B). In the red algae, for instance, *RbcL* was reduced by 27%-46% while in the green alga, *RbcL* was reduced by 37%-41% (Fig. 24Bi). In the brown algae, however, *RbcL* was reduced by a lower percentage (i.e. 14%-26%) than the other algal species. All of the algae, except *U. lactuca,* were less affected by UVA+UVB notably in *P. palmaria* (i.e. 27% reduction). In contrast, the strongest

effect on *RbcL* was observed either under PAR+UVA as in *D. dichotoma a*nd *U. lactuca* or PAR+UVA+UVB as in *P. palmata* and *L. digitata* or PAR as in *S. chordalis*. Recovery of *RbcL* was the fastest in post-recovery algae treated with PAR notably in *P. palmata* (i.e. increased to 90%) while the slowest either in PAR+UVA+UVB as in *S. chordalis, P. palmata* and *U. lactuca* or PAR+UVA as in *D. dichotoma* or UVA+UVB as in *P. palmata* and *L. digitata* (Fig. 24Bii).

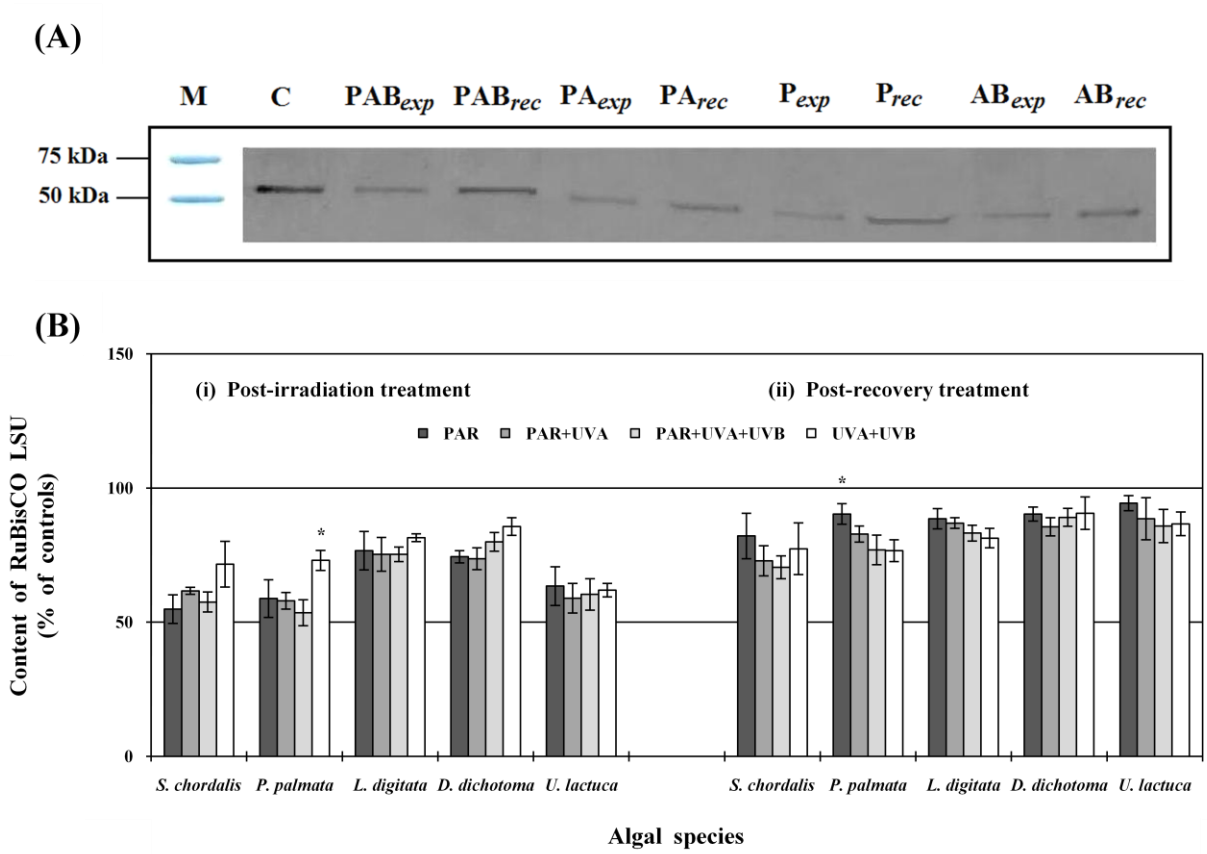

Fig. 24: An example of a western blot of RuBisCO large-subunit (LSU) (*RbcL*) (*A*) in the macroalgae and percentage content of *RbcL* quantified from corresponding blots (*B*). *M*: protein markers showing the position of the protein on the blot with respective molecular weight on the left; *C:*before irradiation (i.e. pre-irradiation, control); *PAB:* PAR+UVA+UVB, *PA:* PAR+UVA, *P:* PAR, *AB:* UVA+UVB, *exp:* after 5 h irradiation or post-irradiation, *rec:* after 18 h recovery or post-recovery. Data of (*B*) are means ±SD values, different asterisks above bars indicate statistically significant difference between treatments in similar species (ANOVA, Fischer's LSD test, $p < 0.05$, n=3).

The content of D1 protein (Fig. 25A) was strongly affected by PAR+UVR treatments as well (Fig. 25B). The least reduction in *PsbA* was measured under PAR in *S. chordalis, P. palmata* (i.e. with a significant 31% reduction) and *D. dichotoma* (Fig. 25Bi). In comparison, the least reduction of *PsbA* was measured under UVA+UVB in *L. digitata* and *U. lactuca*. The highest reduction was generally observed under

PAR+UVR except in *L. digitata*. PAR+UVA caused the highest reduction in *S. chordalis* and *D. dichotoma* while PAR+UVA+UVB caused the highest reduction in *P. palmata a*nd *U. lactuca.* In all post-recovery algal species, PAR had the highest content of *PsbA* with a significant value of 78% in both *S. chordalis* and *P. palmata,* and 97% in *L. digitata* (Fig. 25Bii). A delay in *PsbA* recovery was observed in PAR+UVA+UVB in all of the algal species except *L. digitata* and *D. dichotoma* with a significant increased to 55% in *P. palmata.* In *D. dichotoma,* there was a delay in *PsbA* recovery of PAR+UVA compared to PAR+UVA+UVB.

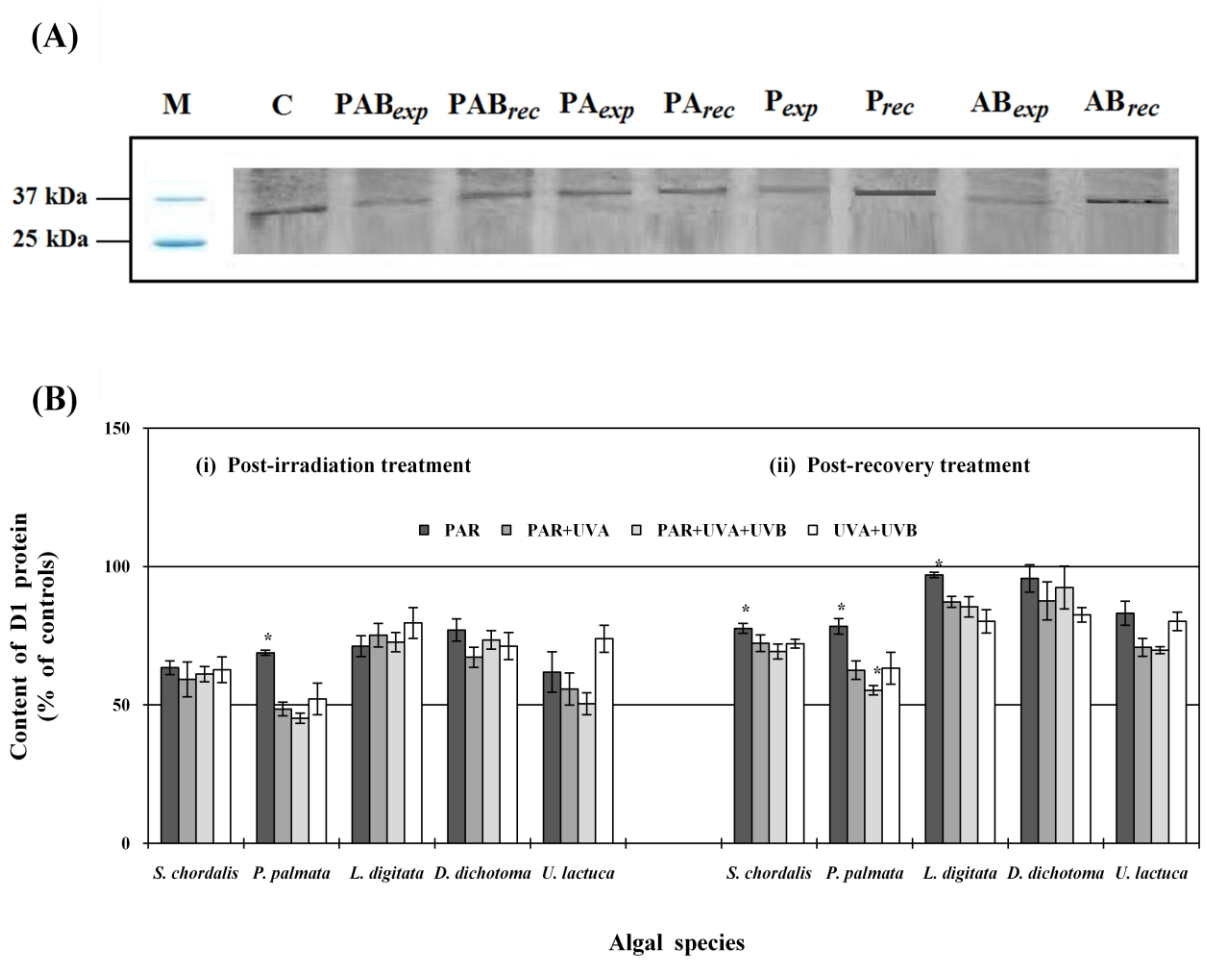

Fig. 25: An example of a western blot of D1 protein (*PsbA*) (*A*) in the macroalgae and percentage content of *PsbA* quantified from corresponding blots (*B*), details as in Fig. 24.

Unlike *RbcL* and *PsbA*, the content of the stress protein HSP60 was induced in the post-irradiation algae but eventually reduced in post-recovery algae (Fig. 26B). The increase in *Hsp60* after the irradiation varied among the algal species but followed several trends (Fig. 26Bi). *Hsp60* of *U. lactuca* increased to

values more than double of their pre-irradiations under all light treatments which were the highest among the algal species. The highest increase among the light treatments in most of the algal species was observed either under PAR+UVA+UVB as in *S. chordalis* and *U. lactuca* or in PAR+UVA as in *P. palmata* or UVA+UVB as in *L. digitata* while the lowest under UVA+UVB with a significant value of 46% observed in *D. dichotoma*. However, in *L. digitata* the lowest increase was observed under PAR with a significant value of 43%. In most of the post-recovery algae, the fastest recovery of *Hsp60* was observed in PAR notably in *L. digitata* (i.e. reduced to 115%) and *D. dichotoma* (i.e. reduced to 118%) while *S. chordalis* showed a full recovery (Fig. 26Bii). Exception, however, was observed in *U. lactuca* with the fastest to recover was in UVA+UVB. A delay in recovery was observed in PAR+UVA+UVB as shown by *S. chordalis* and *U. lactuca* while in *P. palmata* and *D. dichotoma*, recovery was slower in PAR+UVA than PAR+UVA+UVB.

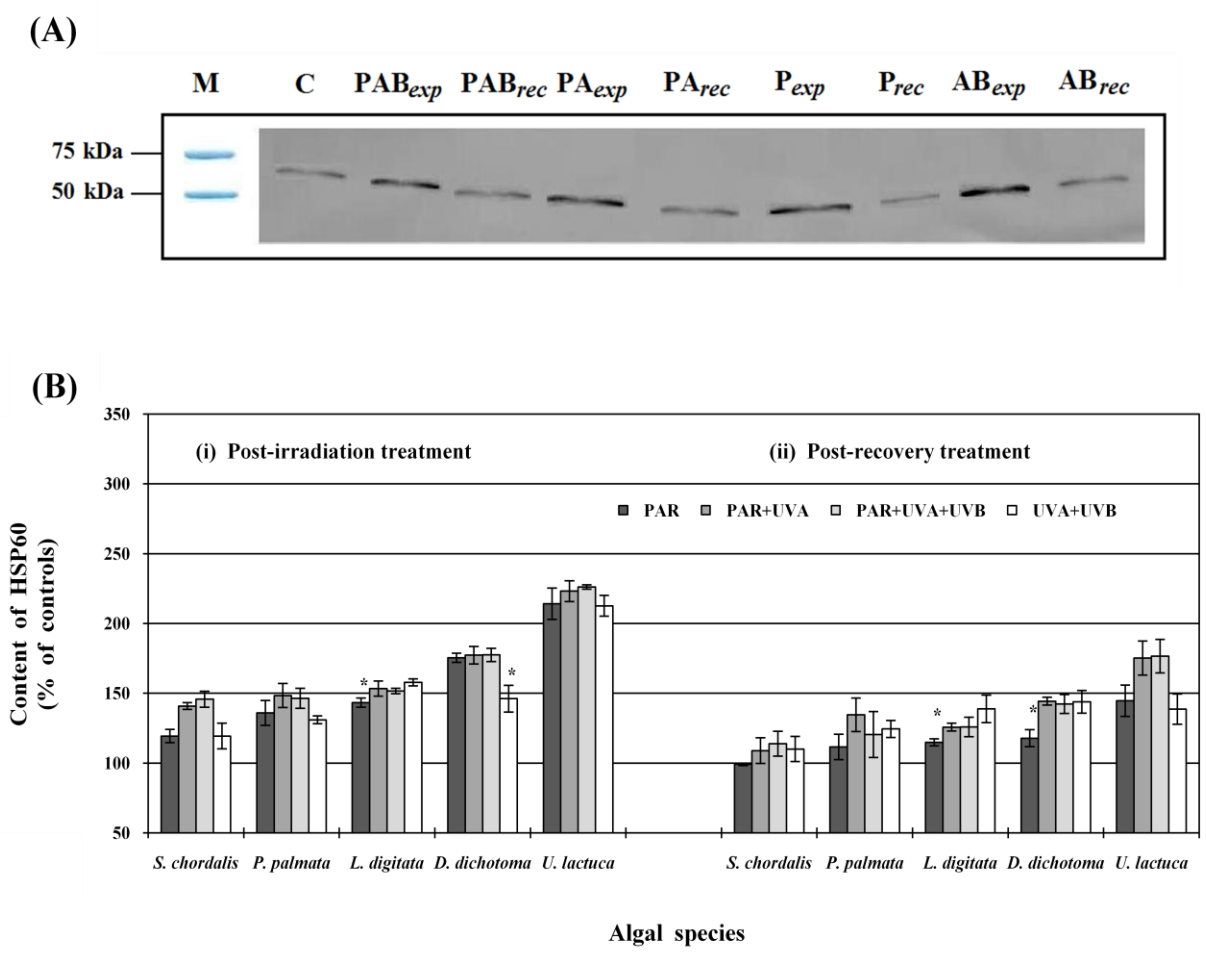

Fig. 26: An example of a western blot of the stress protein, HSP60 (*A*) in the macroalgae and percentage content of *Hsp60* quantified from corresponding blots (*B*), details as in Fig. 24.

The content of *Hsp70* in all post-irradiation algae increased more than 2-fold of their pre-irradiations (Fig. 27Bi). The increase in *Hsp70* was the lowest under PAR in *S. chordalis* (i.e. with a significant 132% increase), *L. digitata* and *U. lactuca* or under UVA+UVB in *P. palmata*. In comparison, most algal species showed the highest increase under PAR+UVR treatments. This trend was particularly noticeable in *U. lactuca* with more than 170% increase. *Hsp70* of *L. digitata* was strongly affected by PAR+UVA+UVB while in *P. palmata* and *D. dichotoma*, the highest increase was under PAR+UVA. In addition, the highest increase of *Hsp70* in *S. chordalis* and *P. palmata* was measured under UVA+UVB. At the end of the recovery period, *Hsp70* degraded the fastest in PAR notably in *D. dichotoma* (i.e. content reduced to 181%) but with exception observed in *U. lactuca* (Fig. 27Bii). In *U. lactuca*, UVA+UVB showed the fastest recovery of *Hsp70* (i.e. concentration reduced to a significant 157%). A delay in the recovery was observed either in post-recovery *S. chordalis*, *L. digitata* and *D.dichotoma* treated with UVA+UVB or in post-recovery *P. palmata* treated with PAR+UVA or in post-recovery *U. lactuca* treated with PAR+UVA+UVB.

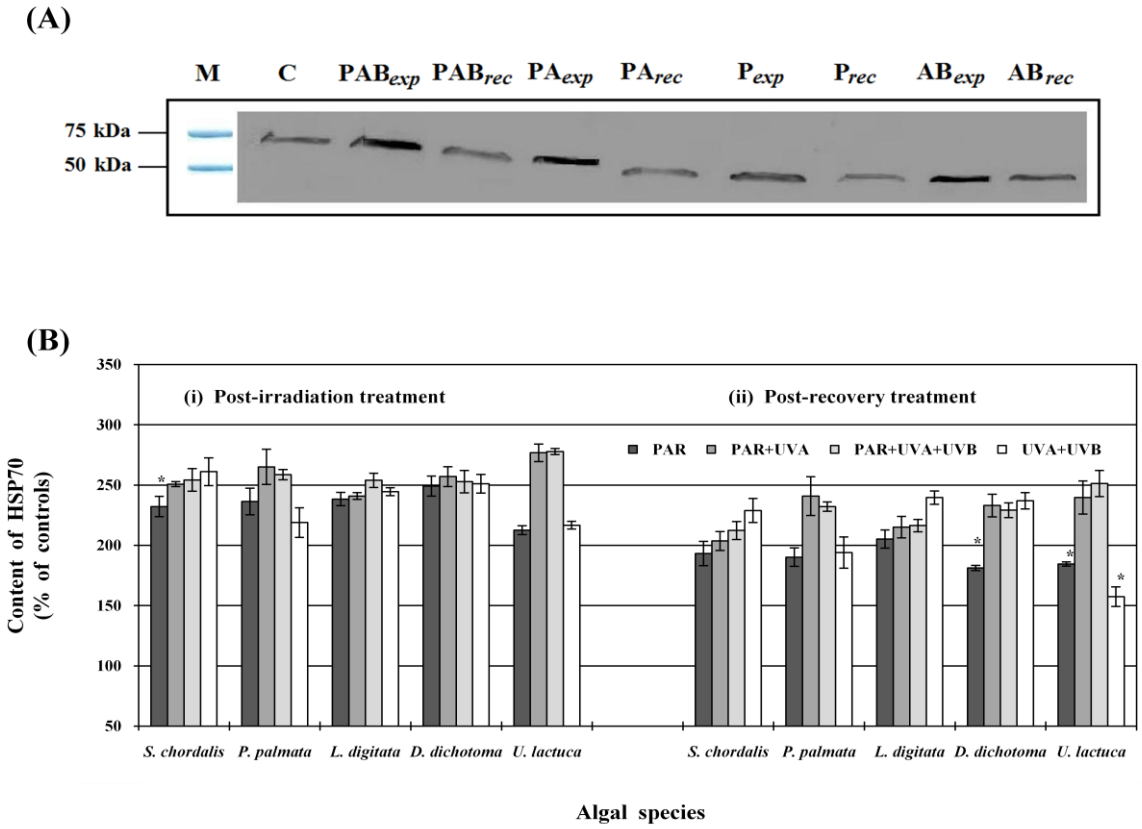

Fig. 27: An example of a western blot of the stress protein, HSP70 (*A*) in the macroalgae and percentage content of *Hsp70* quantified from corresponding blots (*B*), details as in Fig. 24.

3.2.7 Statistical comparisons for high PAR and high UVR

All photosynthetic parameters; Chl a and Chl c contents; both the photosynthetic enzymes activity; CAT and GR activity; and, the content of D1 protein and both the stress proteins differed significantly when either species or light treatments were measured independently and the effect of light treatments on the above-mentioned parameters was dependent on species (Table 17A). In comparison, the effect of light treatments on proteins, R-PC and fucoxanthin contents; APX activity; and, content of RuBisCO LSU was not dependent on species but differed significantly when either factor was examined separately. Furthermore, R-PE content of the post-irradiated red algae differed significantly among the species while the light treatments caused no significant difference.

Table 17: Results (*p*-values) of a two-way ANOVA's on photosynthetic parameters; protein content; pigments content; photosynthetic enzymes activity; antioxidative enzymes activity; and, the content of large-subunit (LSU) of RuBisCO, D1 protein and stress proteins from samples calculated after 5 h irradiation at H_1 (i.e. post-irradiation) and after 18 h recovery periods (i.e. post-recovery).

Responses	Main effects		Interactive effect
	Species	Treatment	Species x Treatment
(A) Post-irradiation treatment:			
Photosynthetic parameters			
F_v/F_m	< 0.001 *	< 0.001 *	< 0.001*
$rETR_{max}$	< 0.001 *	< 0.001 *	< 0.001 *
α	< 0.001 *	< 0.001*	0.002 *
I_k	< 0.001 *	< 0.001*	< 0.001*
Protein	< 0.001 *	< 0.001 *	0.396 *n.s.*
Pigments			
Chl a	< 0.001 *	< 0.001 *	0.001 *
[a] R-PE	< 0.001 *	0.159 *n.s.*	0.006 *
[a] R-PC	< 0.001 *	< 0.001 *	0.321 *n.s.*
[b] Chl c	< 0.001 *	< 0.001 *	0.002 *
[b] Fucoxanthin	< 0.001 *	< 0.001 *	0.802 *n.s.*
Photosynthetic enzymes			
RuBisCO	< 0.001 *	< 0.001 *	< 0.001 *
GAPDH	< 0.001 *	< 0.001 *	0.014 *
Antioxidative enzymes			
CAT	< 0.001 *	< 0.001 *	< 0.001 *
APX	< 0.001 *	0.001 *	0.509 *n.s.*
GR	< 0.001 *	< 0.001 *	< 0.001 *
LSU of RuBisCO	< 0.001 *	< 0.001 *	0.098 *n.s*
D1 protein	< 0.001 *	< 0.001 *	< 0.001 *
Stress proteins			
HSP60	< 0.001 *	< 0.001 *	< 0.001 *
HSP70	0.005 *	< 0.001 *	< 0.001 *
(B) Post-recovery treatment:			
Photosynthetic parameters			
F_v/F_m	< 0.001 *	< 0.001 *	0.019 *
$rETR_{max}$	< 0.001 *	< 0.001 *	< 0.001 *

(Table 17 continued...)

α	< 0.001*	< 0.001*	< 0.001*
I_k	< 0.001*	< 0.001*	0.284 *n.s.*
Protein	< 0.001 *	< 0.001 *	0.784 *n.s.*
Pigments			
Chl a	0.163 *n.s.*	< 0.001 *	0.767 *n.s.*
[a] R-PE	0.413 *n.s.*	0.229 *n.s.*	0.604 *n.s.*
[a] R-PC	0.001 *	0.004 *	0.033 *
[b] Chl c	< 0.001 *	< 0.001 *	< 0.001 *
[b] Fucoxanthin	0.163 *n.s.*	0.115 *n.s.*	0.057 *n.s.*
Photosynthetic enzymes			
RuBisCO	< 0.001 *	< 0.001 *	< 0.001 *
GAPDH	< 0.001 *	< 0.001 *	0.580 *n.s.*
Antioxidative enzymes			
CAT	< 0.001 *	0.001 *	0.008 *
APX	< 0.001 *	< 0.001 *	< 0.001 *
GR	< 0.001 *	< 0.001 *	0.001 *
LSU of RuBisCO	< 0.001 *	< 0.001 *	0.575 *n.s*
D1 protein	< 0.001 *	< 0.001 *	0.102 *n.s*
Stress proteins			
HSP60	< 0.001 *	< 0.001 *	0.282 *n.s*
HSP70	< 0.001 *	< 0.001 *	< 0.001 *

Experimental factors were species (the 5 macroalgal species studied) and treatment (PAR, PAR+UVA, PAR+UVA+UVB, UVA+UVB). * indicates a significant value at $p<0.05$ while *n.s.* indicates a not significant value. Data are calculated from three replicates from each experiment (see MATERIALS AND METHODS for explanation).

[a] Comparisons were made between the red algae, *S. chordalis* and *P. palmata*

[b] Comparisons were made between the brown algae, *L. digitata* and *D. dichotoma*

Most of the parameters analyzed were significantly different among species for the post-recovery algae (Table 17B) excluding that of the photosynthetic pigments. Likewise, most of the parameters behaved differently among the light treatments. The effect on the recovery of most parameters by the different light treatments was also dependent on species.

3.3 Effects of PAR and UVR stress on chlorophyll (Chl) a fluorescence kinetics

3.3.1 Irradiation conditions

Table 18 lists the irradiances applied in the study of chlorophyll (Chl) a fluorescence kinetics. The algae were irradiated under the fluorescent lamps, which will be termed L_{1B} with respect to the low background PAR irradiance as in section 3.1 and in the sun simulator, which will be termed H_{1B} with respect to the

high background PAR irradiance as in section 3.2. However, the ratio of PAR:UVA:UVB with respect to PAR was generally higher at L_1 (Table 6) and H_1 (Table 13, except that measured in *S. chordalis* and *U. lactuca* which showed a lower ratio at H_1 than at H_{1B}) compared to L_{1B} and H_{1B}, respectively (Table 18). Examples of fluorescence traces are displayed in Fig. 47 for rapid light curves (RLC) and Fig. 48 for light-dark relaxation kinetics (Appendix 4).

Table 18: Irradiances of the different spectral ranges applied for fluorescence kinetics.

Setup	Species	PAR (μmol m^{-2} s^{-1})	PAR (W m^{-2})	UVA (W m^{-2})	UVB (W m^{-2})	Ratio of PAR:UVA:UVB
L_{1B}	*S. chordalis*	23	-	50.9	1.23	1:11:0.3
	P. palmata	23	-	50.9	1.23	1:11:0.3
	L. digitata	23	-	50.9	1.23	1:11:0.3
	D. dichotoma	23	-	50.9	1.23	1:11:0.3
	U. lactuca	23	-	50.9	1.23	1:11:0.3
H_{1B}	*S. chordalis*	568	120	31.5	1.27	100:26:1.1
	P. palmata	536	113	30.7	1.30	100:27:1.2
	L. digitata	550	116	34.1	1.43	100:29:1.2
	D. dichotoma	557	117	34.1	1.47	100:29:1.3
	U. lactuca	582	123	33.4	1.41	100:27:1.1

3.3.2 F_v/F_m

The extent of photoinhibition and recovery of the macroalgae before the Chl fluorescence kinetics analysis was determined by the changes in the maximum quantum yield (F_v/F_m). F_v/F_m of the macroalgae before the treatment (i.e. pre-irradiation), after the 5 h irradiation (i.e. post-irradiation) and after 18 h recovery (i.e. post-recovery) treatments are displayed in Fig. 28. Generally, the algae were weakly affected by the presence of low PAR irradiance (L_{1B}) (Fig. 28Ai) in comparison to the relatively high PAR irradiance (H_{1B}) (Fig. 28Aii). Additionally, the low PAR irradiance alone, showed no or less effects on the algae (Fig. 28Ai) while the high PAR alone showed a stronger effect (Fig. 28Aii). In contrast, PAR+UVR had the strongest effect especially at H_{1B}. It appeared that F_v/F_m of most of the algae was strongly affected by PAR+UVA+UVB at L_{1B} except in *S. chordalis*. PAR+UVA+UVB caused the strongest effect at H_{1B} as well except in *P. palmata* and *D. dichotoma.* PAR+UVA significantly caused a higher F_v/F_m reduction in *D. dichotoma* (i.e. 80%) than PAR+UVA+UVB (i.e. 75%) at H_{1B}. UVA+UVB

had the least effect in most of the algae particularly in *L. digitata* (i.e. 32% reduction) and *D. dichotoma* (i.e. 50% reduction). In *P. palmata* at H_{1B}, PAR caused a significantly less reduction (i.e. 51%) compared to the other light treatments.

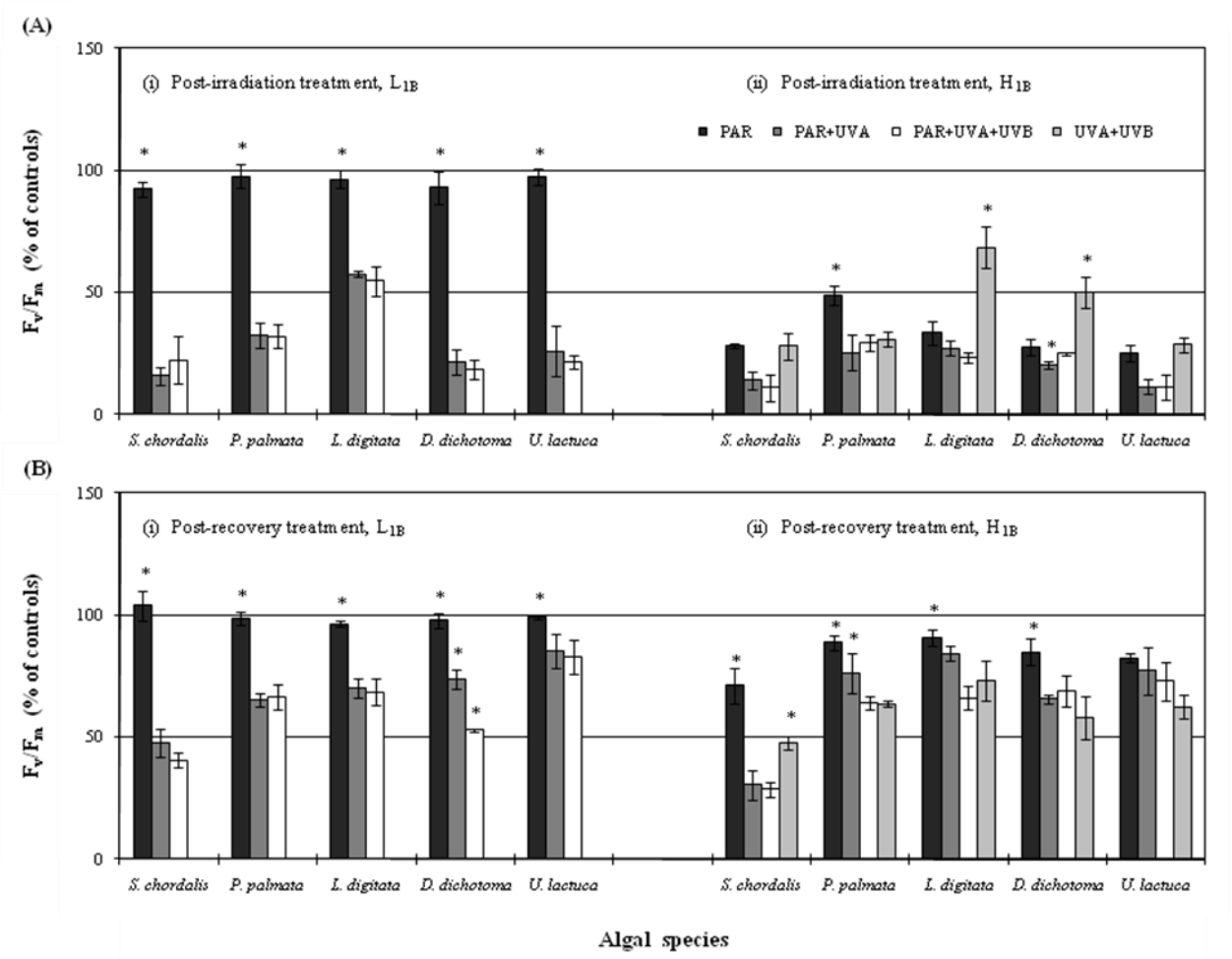

Fig. 28: Maximal quantum yield (F_v/F_m) of the macroalgae after 5 h irradiation under different light treatments (post-irradiation, *A*) and after 18 h recovery under dim light (post-recovery, *B*). *i:* L_{1B} (23 µmol m^{-2} s^{-1} PAR, 51 Wm^{-2} UVA, 1.2 Wm^{-2} UVB), *ii:* H_{1B} (536-582 µmol m^{-2} s^{-1} PAR, 31-34 Wm^{-2} UVA, 1.3-1.5 Wm^{-2} UVB), *black bars:* PAR, *dark grey bars:* PAR+UVA, *white bars:* PAR+UVA+UVB, *light grey bars:* UVA+UVB. Data are means ±SD values. Asterisks signify statistically significant difference between light treatments within similar species (ANOVA, Fischer's LSD test, $p < 0.05$, n=3).

F_v/F_m of all post-recovery algae showed signs of recovery but with varied extent. Algae irradiated at L_{1B}, mostly recovered faster with PAR+UVA (except *P. palmata*) than PAR+UVA+UVB (Fig. 28Bi). This effect was particularly noticeable in *D. dichotoma* where PAR+UVA increased F_v/F_m to 74% in comparison to 53% with PAR+UVA+UVB. At H_{1B}, PAR showed the fastest recovery with the values

increased to 71% in *S. chordalis*, 89% in *P. palmata*, 91% in *L. digitata* and 85% in *D. dichotoma* while *U. lactuca* showed a similar trend but was not significant (Fig. 28Bii). UVA+UVB was the slowest to recover as observed by a trend in *P. palmata, D. dichotoma* and *U. lactuca w*hile PAR+UVA+UVB was the slowest to recover in *S. chordalis* and *L. digitata*.

3.3.3 Rapid Light Curve (RLC)

In order to describe the response of the macroalgae to a range of light levels, a rapid light curve (RLC) was recorded. For the purpose of simplifications, results for RLC were represented by algae irradiated with PAR+UVA+UVB at H_{1B} (i.e. post-irradiation treatment) since the algae reacted very strongly to this treatment based on the changes in F_v/F_m (Fig. 28). Furthermore, RLCs of the other light or irradiance treatments showed similar patterns or shapes as these treatments but to variable extent. Post-irradiation algae treated with PAR at L_{1B}, which showed no or small changes in F_v/F_m, however, displayed similar RLC patterns as the pre-irradiations. Figures 29A, 30A, 31A, 32A and 33A show the fluorescence yield curves recorded during a RLC for the pre-irradiation algae. The fluorescence yield curves for these algae were essentially similar. The fluorescence yield, F increased rapidly for the first few actinic irradiances and remained elevated until it started to level off at higher actinic irradiances. In the red algae *S. chordalis* and *P. palmata*, F increased 156% (Fig. 29A) and 131% (Fig. 30A) from the beginning until the end of RLC recordings, respectively. The increase, however, was much higher in the rest of the algal species. In *L. digitata, D. dichotoma* and *U. lactuca*, the increase was 222% (Fig. 31A), 270% (Fig. 32A) and 360% (Fig. 33A), respectively. The fluorescence during the saturation pulses, F_m', on the other hand, slowly declined at lower actinic irradiances and eventually levelled off at higher actinic irradiances. In *S. chordalis, P. palmata* and *U. lactuca*, F_m' was reduced 32% (Fig. 29A), 33% (Fig. 30A) and 13% (Fig. 33A), respectively. However, in the brown algae, *L. digitata* and *D. dichotoma*, F_m' increased for the first three actinic irradiances but declined thereafter (Figs. 31-32A). The decline was 31% in *L. digitata* and

22% in *D. dichotoma*. As actinic irradiances increased, F and F_m' approached each other resulting in a small ΔF signal (i.e. differences between F and F_m').

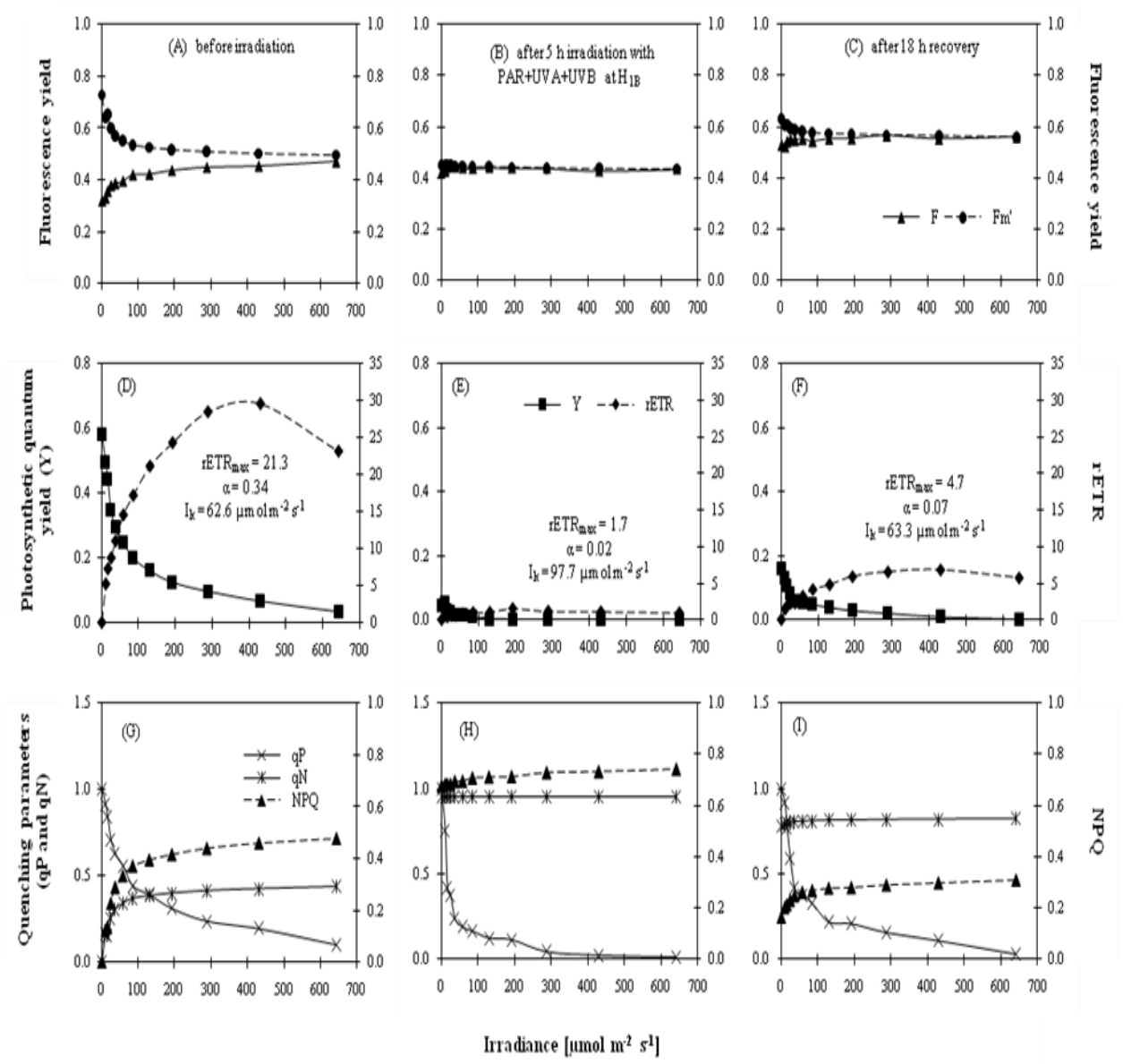

Fig. 29: Derived parameters of rapid light curves (RLC) from *S. chordalis* before irradiation (pre-irradiation, *A, D* and *G*), after 5 h irradiation with PAR+UVA+UVB at H_{1B} (post-irradiation, *B, E* and *H*), and after 18 h recovery under dim light (post-recovery, *C, F* and *I*). *A, B* and *C:* fluorescence yield (F) and maximum light-adapted fluorescence yield (F_m') as a function of actinic light irradiance, *D, E* and *F*: effective quantum yield (Y) and relative electron transport rate (rETR) as a function of actinic irradiance, *G, H* and *I*: quenching coefficients associated with the RLC, photochemical quenching (qP), non-photochemical quenching (qN) and Stern–Volmer non-photochemical quenching (NPQ) as a function of actinic light irradiance; *triangles with straight lines:* F, *circles with dashed lines:* F_m', *squares:* Y, *diamonds:* rETR, *crosses:* qP, *asterisks:* qN, *triangles with dashed lines:* NPQ. Note: The photosynthetic parameters from rETR vs. irradiance plot are derived from fitted curves according to that of Jassby and Platt (1976), see MATERIALS and METHODS for explanation.

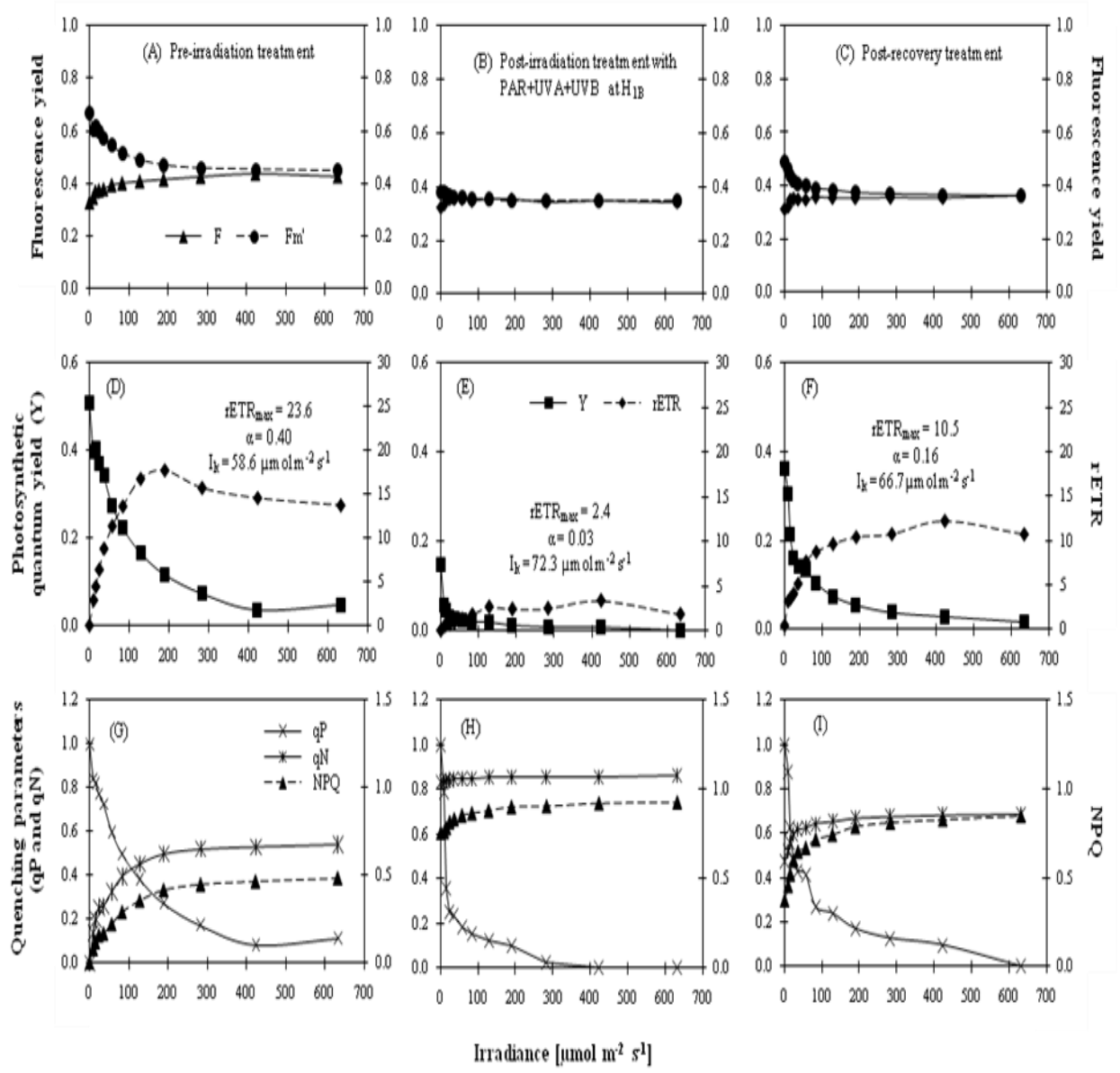

Fig. 30: Derived parameters of rapid light curves (RLC) from *P. palmata* before irradiation (pre-irradiation, *A*, *D* and *G*), after 5 h irradiation with PAR+UVA+UVB at H_{1B} (post-irradiation, *B*, *E* and *H*), and after 18 h recovery under dim light (post-recovery, *C*, *F* and *I*), details as in Fig. 29.

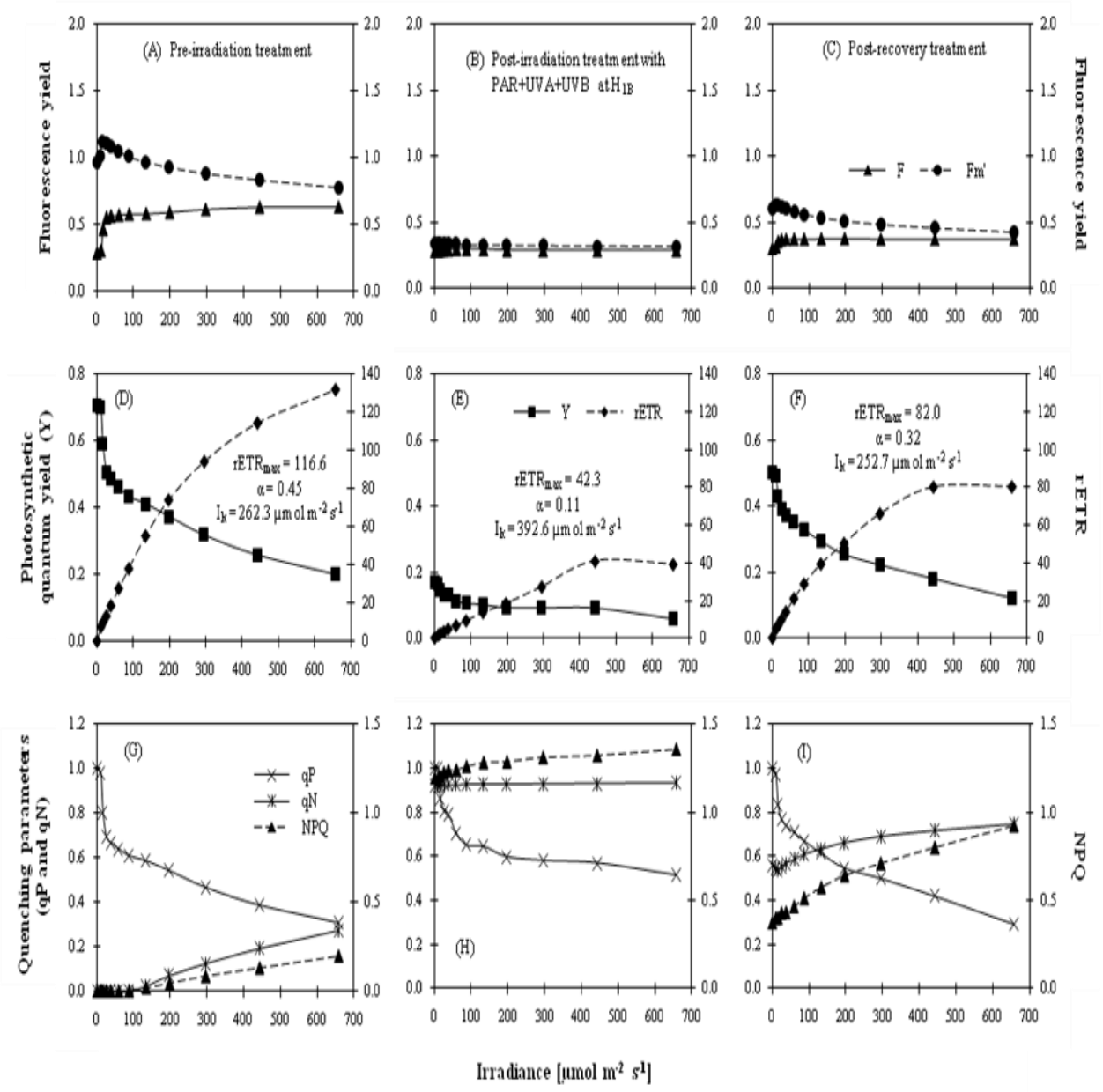

Fig. 31: Derived parameters of rapid light curves (RLC) from *L. digitata* before irradiation (pre-irradiation, *A*, *D* and *G*), after 5 h irradiation with PAR+UVA+UVB at H_{1B} (post-irradiation, *B*, *E* and *H*), and after 18 h recovery under dim light (post-recovery, *C*, *F* and *I*), details as in Fig. 29.

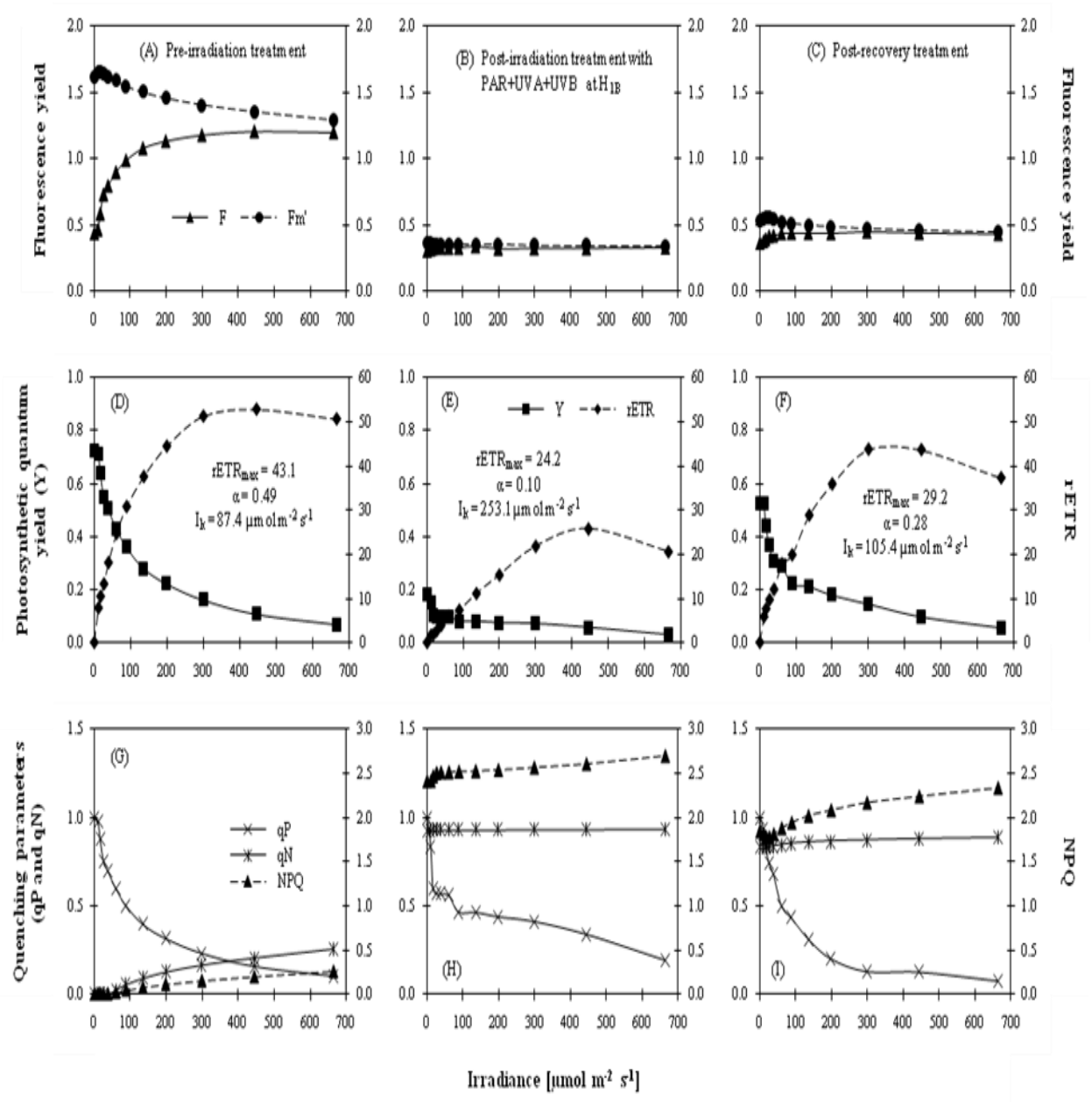

Fig. 32: Derived parameters of rapid light curves (RLC) from *D. dichotoma* before irradiation (pre-irradiation, *A, D* and *G*), after 5 h irradiation with PAR+UVA+UVB at H_{1B} (post-irradiation, *B, E* and *H*), and after 18 h recovery under dim light (post-recovery, *C, F* and *I*), details as in Fig. 29.

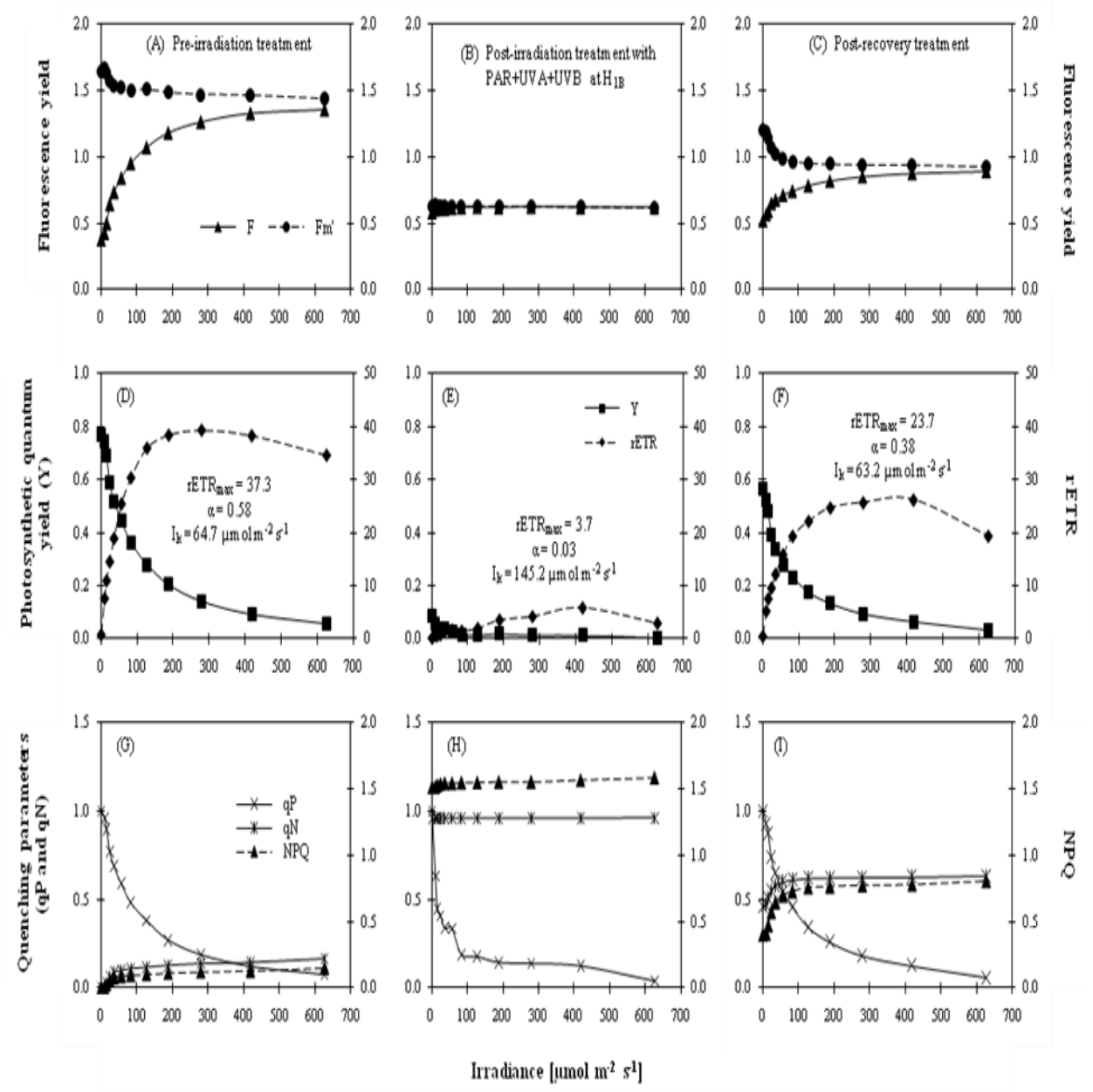

Fig. 33: Derived parameters of rapid light curves (RLC) from *U. lactuca* before irradiation (pre-irradiation, *A*, *D* and *G*), after 5 h irradiation with PAR+UVA+UVB at H_{1B} (post-irradiation, *B, E* and *H*), and after 18 h recovery under dim light (post-recovery, *C, F* and *I*), details as in Fig. 29.

A small ΔF signal at the beginning of the RLC recording was observed in all post-irradiation algae. This was due to the rapid approachment of F and F_m' which started at smaller values than the pre-irradiation algae (Figs. 29-33B). In *S. chordalis,* for instance, ΔF of the pre-irradiation algae (Fig. 29A) at the beginning of recording was 0.41 which reduced to 0.03 in the post-irradiation algae (Fig. 29B). At some

point during the recording, ΔF is so small that these two fluorescence parameters appeared to converge with one another as displayed in the figures for the red algae (Figs. 29-30B). Thus, the degree of changes in both the fluorescence parameters in post-irradiation algae was somewhat much smaller than the pre-irradiation algae. In post-irradiated *S. chordalis*, F increased 103% and F_m' reduced 4% (Fig. 29B). Comparatively, F increased 107% and F_m' reduced 9% in *P. palmata* (Fig. 30B), 92% and 8% in *L. digitata* (Fig. 31B), 108% and 4% in *D. dichotoma* (Fig. 32B) and 107% and 2% in *U. lactuca* (Fig. 33B). The fluorescence curves of the post-recovery algae started to improve a bit where the ΔF signal at low actinic irradiances became large again (Figs. 29-33C).

Initially, all the algae were healthy as shown by the effective quantum yield (Y): 0.58 for *S. chordalis*, 0.51 for *P. palmata*, 0.71 for *L. digitata*, 0.73 for *D. dichotoma* and 0.77 for *U. lactuca* (Figs. 29-33D). As the actinic irradiances increased, Y steadily declined to values close to 0. In *S. chordalis*, Y was reduced to 0.04, 0.05 in *P. palmata*, 0.20 in *L. digitata*, 0.07 in *D. dichotoma* and 0.06 in *U. lactuca*. At the end of the post-irradiation treatments, the initial Y of the algae showed a reduction relative to that of the pre-irradiations. The initial Y was 0.05 for *S. chordalis*, 0.15 for *P. palmaria*, 0.17 for *L. digitata*, 0.18 for *D. dichotoma* and 0.09 for *U. lactuca* (Figs. 29-33E). At the end of RLC recordings, these values were reduced to 0.00 in both *S. chordalis* and *P. palmata*, 0.06 in *L. digitata*, 0.03 in *D. dichotoma* and 0.01 in *U. lactuca*. The initial Y increased to 0.16 for *S. chordalis*, 0.36 for *P. palmata*, 0.50 for *L. digitata*, 0.52 for *D. dichotoma* and 0.56 for *U. lactuca*, in post-recovery algae (Figs. 29-33F). Y steadily declined thereafter to 0.00 in *S. chordalis*, 0.02 in *P. palmata*, 0.12 in *L. digitata*, 0.06 in *D. dichotoma* and 0.03 for *U. lactuca* at the highest actinic irradiance.

The plot of rETR as a function of the actinic irradiance showed the classical shape of a photosynthesis-irradiance (P-I) curve with a linear rise at lower light irradiance followed by a plateau at higher light irradiances (Figs. 29-33D). At even higher irradiance, rETR showed a decline as displayed by the rETR plot of all the algal species at actinic irradiance between 430 and 640 μmol m^{-2} s^{-1} (i.e. between the 11^{th} and 12^{th} steps) (Figs. 29-30D and 32-33D). Exception, however, was observed in *L. digitata* (Fig. 31D).

In post-irradiation algae, the convexity of the curve was reduced 13 times in *S. chordalis,* 10 times in *P. palmata,* 3 times in *L. digitata,* 2 times in *D. dichotoma* and 10 times in *U. lactuca* (Figs. 29-33E) from the pre-irradiation algae. In the post-recovery algae, the convexity of the curves increased again to 3 times in *S. chordalis,* 4 times in *P. palmata,* 2 times in *L. digitata,* 1 time in *D. dichotoma* and 6 times in *U. lactuca* of the post-irradiation, slowly resembling that of the pre-irradiation (Figs. 29-33F).

From the rETR plot, the maximum relative electron transport rate ($rETR_{max}$), the photosynthetic efficiency parameter (α) and the light saturation parameter (I_k) were determined. For instance, in pre-irradiation *S. chordalis*, the $rETR_{max}$ was 23.1, α was 0.34 and I_k was 62.5 µmol m^{-2} s^{-1} (Fig. 29D). In the post-irradiation algae, the value was reduced to 8% for $rETR_{max}$ and 6% for α, while I_k was increased 156% (Fig. 29E). The parameters slowly improved at the end of the post-recovery period whereby $rETR_{max}$ and α increased to 22% and 21%, respectively, while I_k was reduced to 101% compared to the post-irradiation treatment (Fig. 29F). Similar patterns in changes of $rETR_{max}$, α and I_k were observed in the rest of pre-irradiation (Figs. 30-33D), post-irradiation (Figs. 30-33E) and post-recovery (Figs. 30-33F) algal species. The values of the parameters are listed in the corresponding figures.

Quenching coefficients plotted as a function of actinic irradiance showed a steady decline in qP and a clear increase in qN and NPQ with increasing irradiance (Figs. 29-33G-I). qN started at 0 in the pre-irradiation algae (Figs. 29-33G) but the value increased by more than 90% in the post-irradiation algae (Figs. 29-33H) but was reduced again in the post-recovery algae (Figs. 29-33I). Similar patterns were observed for NPQ as well. In *S. chordalis,* for instance, qN started at a value of 0.95 and NPQ started at 0.68 for the post-irradiation treatment and these values were reduced to 0.78 for qN and 0.17 for NPQ at the end of post-recovery treatment (Fig. 29H-I). In addition, post-irradiated *P. palmata* showed an increased to 0.83 for qN and 0.75 for NPQ while qN reduced to 0.47 and NPQ reduced to 0.37 in post-recovery (Fig. 30H-I). Post-irradiated *L. digitata,* on the other hand, showed an increased to 0.92 for qN and 1.20 for NPQ while qN reduced to 0.56 and NPQ reduced to 0.38 in post-recovery (Fig. 31H-I). Furthermore, post-irradiated *D. dichotoma* showed an increased to 0.93 for qN and 2.42 for NPQ while

qN reduced to 0.84 and NPQ reduced to 1.84 in post-recovery (Fig.32H-I). Finally, post-irradiated *U. lactuca* showed an increased to 0.96 for qN and 1.51 for NPQ while qN reduced to 0.46 and NPQ reduced to 0.41 in post-recovery (Fig.33H-I).

Conversely, qP which started at 1, was steadily reduced to 0.10 in *S. chordalis*, 0.12 in *P. palmata*, 0.31 in *L. digitata*, 0.10 in *D. dichotoma* and 0.07 in *U. lactuca* at the highest actinic irradiance for the pre-irradiation algae (Figs. 29-33G). In comparison, these values were lower in the post-irradiated red and green algae but were higher in the post-irradiated brown algae. qP was reduced to values close to 0 in the red algae with a value of 0.01 in *S. chordalis* and 0.00 in *P. palmata* (Figs. 29-30H). qP in *U. lactuca* was reduced to 0.04 (Fig. 33H) while in the brown algae *L. digitata a*nd *D. dichotoma*, qP was reduced to 0.51 and 0.19, respectively (Figs. 31-32H). For the post-recovery algae, the reduction of qP showed little improvement in *S. chordalis* with the value increased to 0.03 but remained similar to that of post-irradiation for *P. palmata* (Figs. 29-30I). qP at the highest actinic irradiance increased to 0.29 in *L. digitata*, 0.08 in *D. dichotoma*, and 0.06 in *U. lactuca* for the post-recovery algae (Figs. 31-33I).

In order to estimate the relative changes to the photosystem II (PSII) reduction state, the excitation pressure index, 1-qP of the algae at the end of RLC (i.e. at the highest actinic irradiance) was measured. The maximum excitation pressure is achieved when 1-qP=1 while no excitation pressure when 1-qP=0. In addition, the susceptibility of PSII to stress index, (1-qP)/NPQ was measured as well, to assess the contribution of photochemical and non-photochemical quenching in relation to photoinactivation of PSII. High index value indicates high susceptibility to stress. As an example, 1-qP and (1-qp)/NPQ of algae irradiated with PAR+UVA+UVB at H_{1B} are shown here. Similar patterns were observed in other light and irradiance treatments but to a varied extent. As displayed in Fig. 34A, the excitation pressure in pre-irradiation algae was high (i.e. between 0.69 and 0.93). 1-qP was further increased in post-irradiated *S. chordalis* (i.e. 10% increase), *P. palmata* (i.e. 13% increase) and *U. lactuca* (i.e. 4% increase) but was reduced in *L. digitata* (i.e. 15% reduction) and *D. dichotoma* (i.e. 10% reduction). In fact, maximum excitation pressure was achieved in *P. palmata* and was nearly achieved in *S. chordalis*. In post-recovery

treatment, the values slightly reduced in *S. chordalis* and *U. lactuca* but were increased in *L. digitata* and *D. dichotoma*. The excitation pressure was still at its maximum in post-recovery *P. palmata*.

The (1-qP)/NPQ index of the pre-irradiation algae was generally the highest in the green alga, followed by the brown algae and red algae (Fig. 34B). In post-irradiation algae, the values reduced by 29% in *S. chordalis*, 41% in *P. palmata*, 89% in *L. digitata*, 91% in *D. dichotoma* and 90% in *U. lactuca.* Post-recovery algae had a higher susceptibility index than the post-irradiation algae but was still much lower than the pre-irradiation algae. Exception, however, was observed in *S. chordalis* where the value increased more than the pre-irradiation.

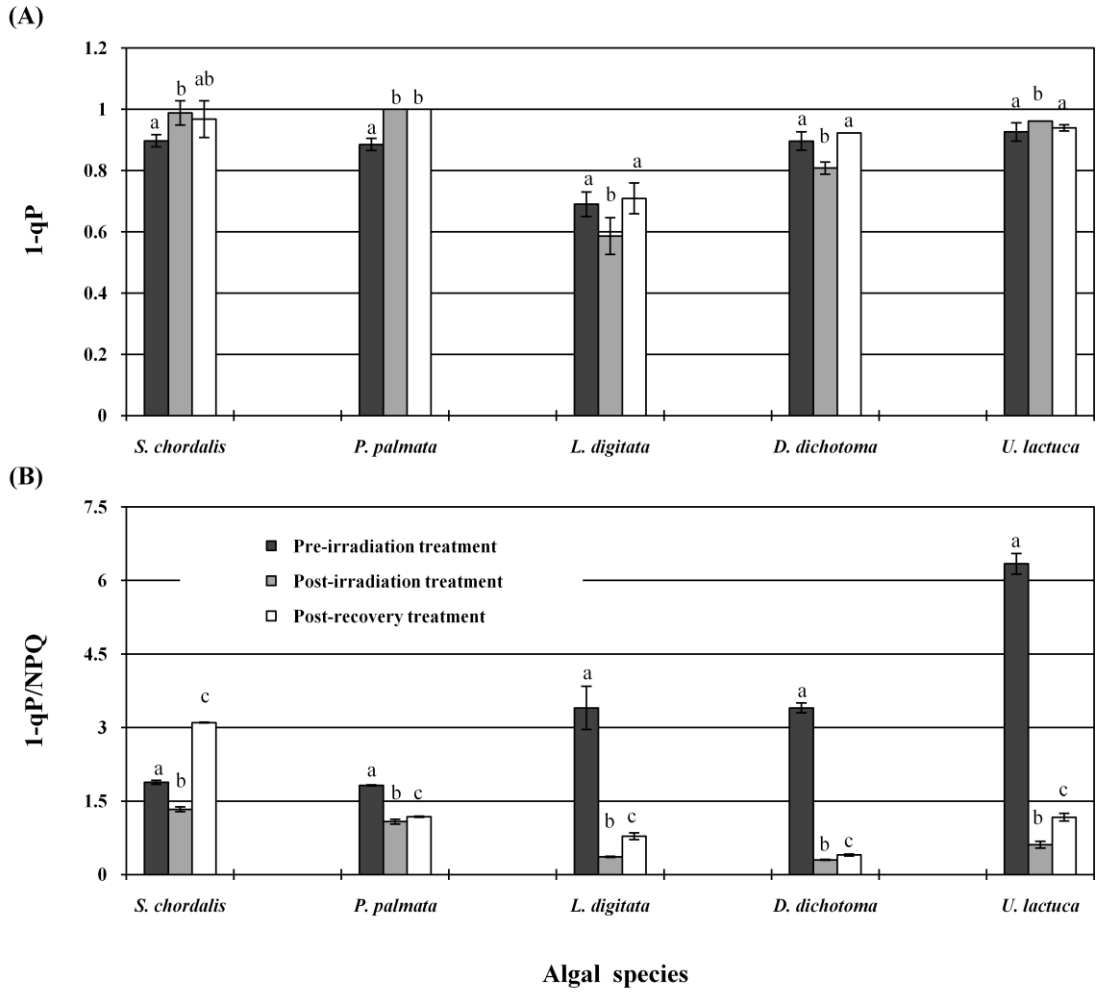

Fig. 34: The excitation pressure index [(1-qP)] (*A*) and the susceptibility of PSII to stress index [(1-qP)/NPQ] (*B*) of the macroalgae before irradiation (i.e. pre-irradiation, *black bars*), after 5 h irradiation with PAR+UVA+UVB at H_{1B} (i.e. post-irradiation, *grey bars*) and after 18 h recovery under dim light (i.e. post-recovery, *white bars*). Data are means±SD values of n=3. Different letters above bars indicate significant difference between treatments within similar species (ANOVA, Fischer's LSD test, $p < 0.05$, n=3).

3.3.4 Light-dark relaxation kinetics

Recording of light-dark relaxation kinetics was carried out immediately after RLC to gain additional information on how the macroalgal photosystems recover from light exposure. The algae were initially subjected to light or induction phase which showed the response of the algae to light and then the dark or relaxation phase was recorded to determine the relaxation of various components of the non-photochemical quenching (see MATERIALS AND METHODS section 2.3 for further explanation). The parameters in the light phase shown in Figs. 35, 36 and 37 followed that of RLC but the parameters are plotted against time instead of light irradiance. Therefore, during the light or induction phase, Y and qP declined steadily while qN and NPQ increased with increasing time. Twenty seconds after the actinic light was switched off, Y showed a slow but steady increase while qP rapidly increased to the maximum 1 (with exceptions). qN and NPQ, on the other hand, showed a 'relax' pattern whereby they slowly declined with time.

The starting effective quantum yield, Y, of the light phase (see MATERIALS AND METHODS section 2.3 for conditions) in pre-irradiated *S. chordalis, P. palmata, L. digitata*, *D. dichotoma* and *U. lactuca,* was 0.22 (Fig.35A), 0.15 (Fig. 35B), 0.38 (Fig. 36A), 0.16 (Fig. 36B) and 0.17 (Fig. 37A), which declined to 0.02 (Fig. 35C), 0.02 (Fig. 35D), 0.13 (Fig. 36C), 0.04 (Fig. 36D) and 0.02 (Fig. 37B) in the post-irradiated and increased again to 0.06 (Fig. 35E), 0.07 (Fig. 35F), 0.25 (Fig. 36E), 0.10 (Fig. 36F) and 0.10 (Fig. 37C) in the post-recovery algae, respectively. In all cases, Y steadily declined afterwards until the end of the light phase and the values reached close to 0 especially in the post-irradiation red and green algae.

In the light phase, the curve of qP followed that of Y with a slow but steady decline (Figs. 35-37). In pre-irradiated *S. chordalis*, qP declined from 0.47 to 0.36 (Fig. 35A) while qP declined from 0.48 to 0.38 in *P. palmata* (Fig. 35B), from 0.54 to 0.48 in *L. digitata* (Fig. 36A), from 0.23 to 0.19 in *D. dichotoma* (Fig. 36B) and from 0.25 to 0.21 in *U. lactuca* (Fig. 37A) during the light phase. In post-irradiation algae

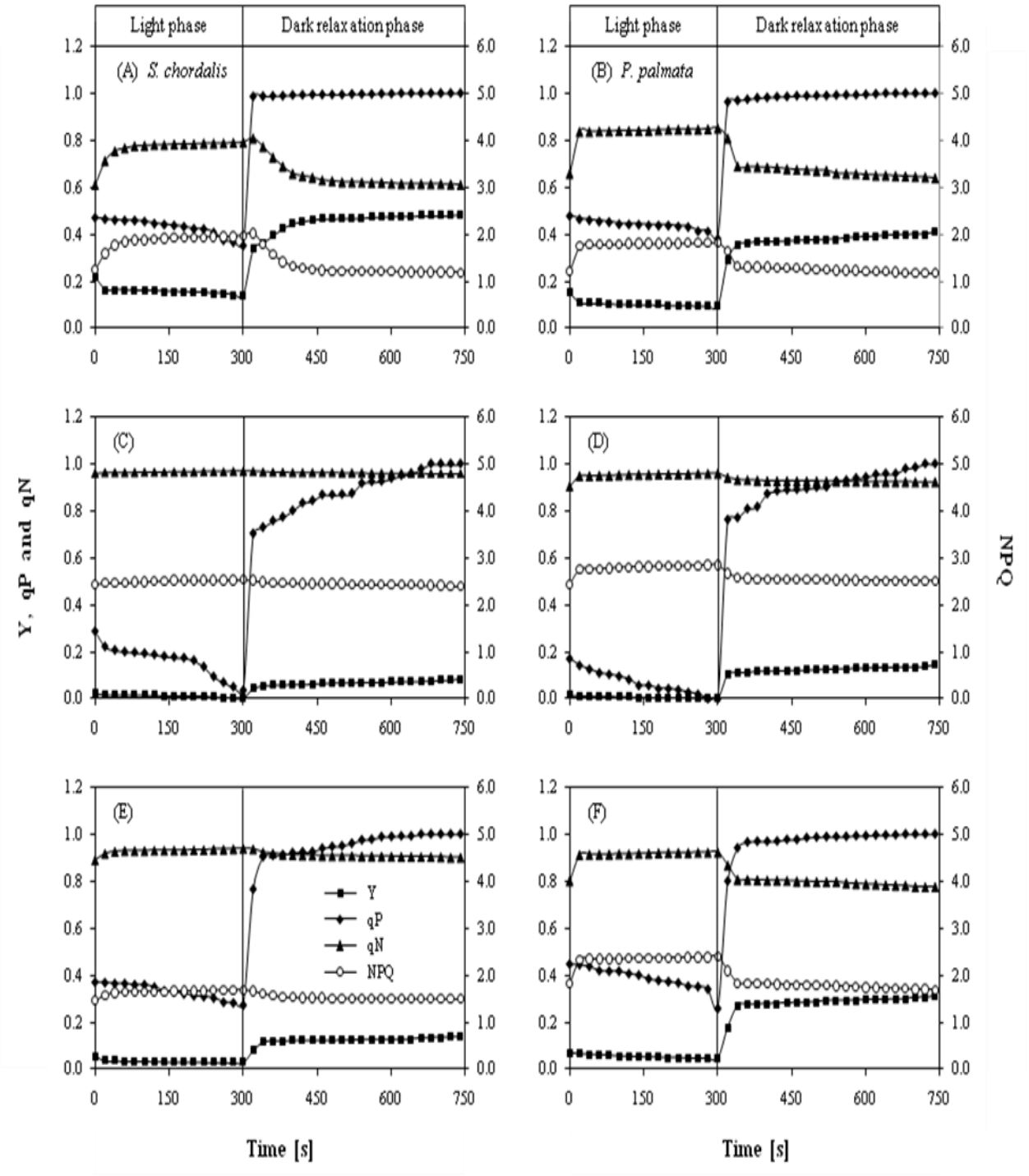

Fig. 35: Light-dark relaxation kinetics with quenching analysis measured in the red algae *S. chordalis* (*A,C* and *E*) and *P. palmata* (*B, D* and *F*) before irradiation (pre-irradiation, *A, B*), after 5 h irradiation with PAR+UVA+UVB at H_{1B} (post-irradiation, *C, D*) and after 18 h recovery under dim light (post-recovery, *E, F*). *Squares*, effective quantum yield, Y; *diamonds*, photochemical quenching, qP; *triangles*, non-photochemical quenching, qN, *open circles:* Stern-Volmer non-photochemical quenching, NPQ.

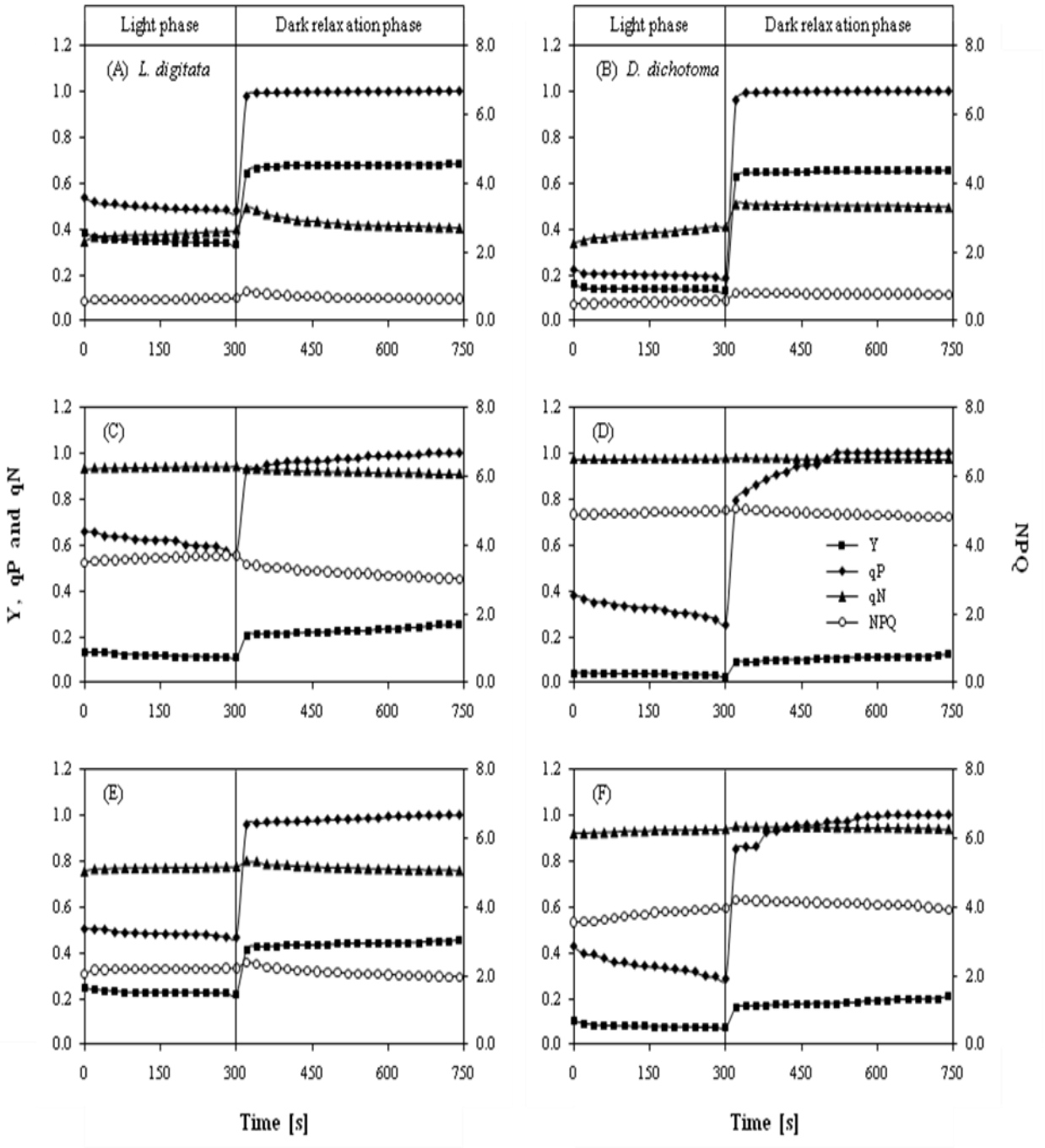

Fig. 36: Light-dark relaxation kinetics with quenching analysis measured in the brown algae *L. digitata* (*A*,*C* and *E*) and *D. dichotoma* (*B*, *D* and *F*) before irradiation (pre-irradiation, *A*, *B*), after 5 h irradiation with PAR+UVA+UVB at H_{1B} (post-irradiation, *C*, *D*) and after 18 h recovery under dim light (post-recovery, *E*, *F*), details as in Fig. 35.

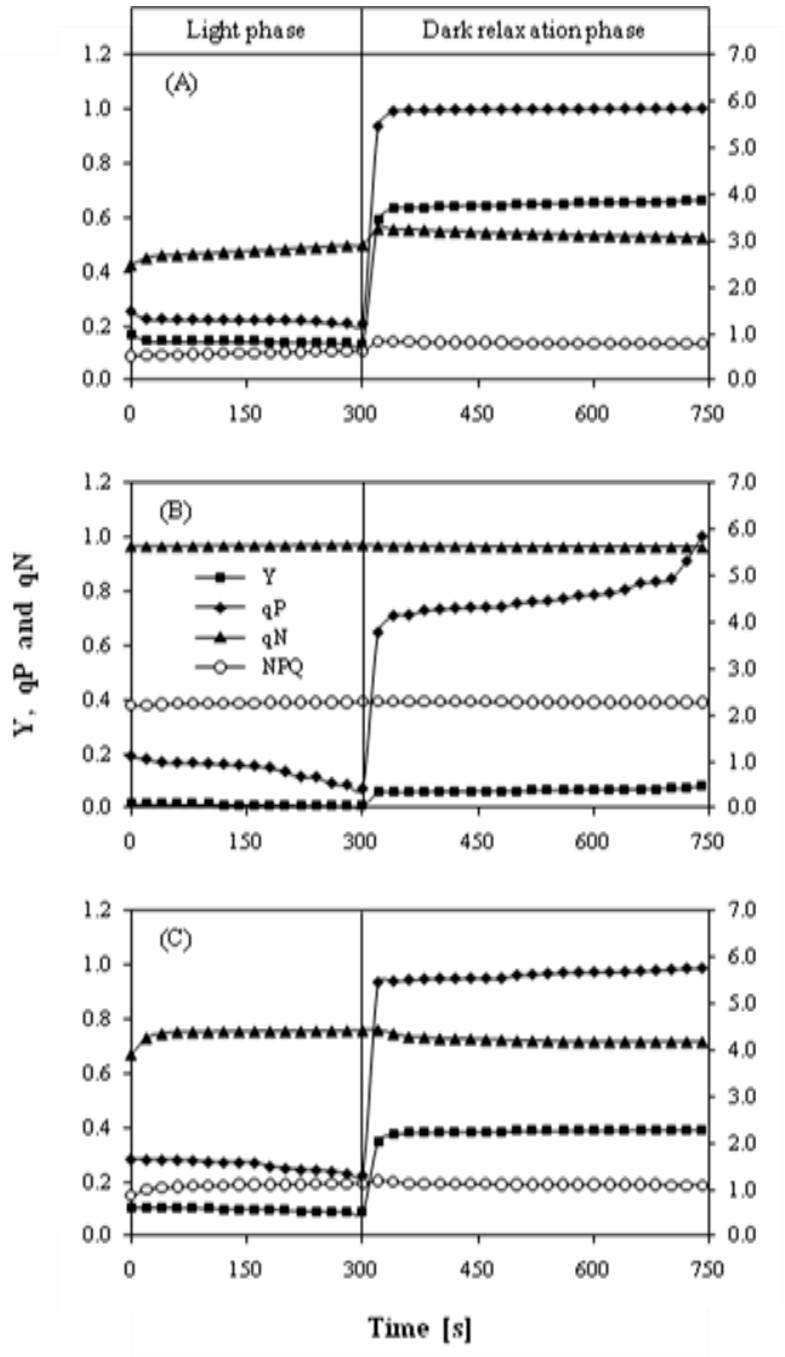

Fig. 37: Light-dark relaxation kinetics with quenching analysis measured in the green alga *U. lactuca* before irradiation (pre-irradiation, *A*), after 5 h irradiation with PAR+UVA+UVB at H_{1B} (post-irradiation, *B*) and after 18 h recovery under dim light (post-recovery, *C*), details as in Fig. 35.

(Figs. 35-36C-D and 37B), qP declined from 0.29 to 0.03 in *S. chordalis*, from 0.17 to 0.00 in *P. palmata*, from 0.66 to 0.56 in *L. digitata*, from 0.38 to 0.26 in *D. dichotoma* and from 0.19 to 0.07 in *U. lactuca*. In the post-recovery algae (Figs. 35-36C-F and 37C), on the other hand, qP declined from 0.37 to 0.27 in *S.*

chordalis, from 0.45 to 0.26 in *P. palmata*, from 0.51 to 0.47 in *L. digitata*, from 0.43 to 0.28 in *D. dichotoma* and from 0.28 to 0.22 in *U. lactuca.*

In contrast, the increase in qN during the light phase of the pre-irradiation algae was rapid in the red algae (Fig. 35A-B) but was slow and steady in the brown algae (Fig. 36A-B) and green alga (Fig. 37A). Initial qN during the light phase was 0.61 in *S. chordalis* (Fig. 35A), 0.66 in *P. palmata* (Fig. 35B), 0.35 in *L. digitata* (Fig. 36A), 0.34 in *D. dichotoma* (Fig. 36B) and 0.43 in *U. lactuca* (Fig. 37A) which increased to 0.79, 0.81, 0.40, 0.41 and 0.50 at the end of RLC, respectively. All post-irradiated algae (Figs. 35-36C-D and 37B) showed a slow and steady increase in qN, from 0.96 to 0.97 in *S. chordalis*, from 0.91 to 0.96 in *P. palmata*, from 0.93 to 0.94 in *L. digitata*, from 0.97 to 0.98 in *D. dichotoma* and from 0.96 to 0.97 in *U. lactuca*. In the post-recovery algae (Figs. 35-36E-F and 37C), the degree of increased was larger again and the curve resembled that of pre-irradiation with an increase from 0.89 to 0.94 in *S. chordalis*, from 0.80 to 0.92 in *P. palmata*, from 0.75 to 0.78 in *L. digitata*, from 0.92 to 0.94 in *D. dichotoma* and from 0.67 to 0.76 in *U. lactuca*.

The curve for NPQ followed that of qN but to a different extent. There was also a rapid increase in NPQ of pre-irradiation red algae but a slow and steady increase in the brown algae as well as green alga. NPQ in these algae started at 1.24 in *S. chordalis* (Fig. 35A), 1.23 in *P. palmata* (Fig. 35B), 0.56 in *L. digitata* (Fig. 36A),0.48 in *D. dichotoma* (Fig. 36B) and 0.51 in *U. lactuca* (Fig. 37A) which increased to 1.98, 1.83, 0.68, 0.60 and 0.64, respectively. NPQ increased from 2.45 to 2.53 in *S. chordalis*, from 2.44 to 2.84 in *P. palmata*, from 3.50 to 3.70 in *L. digitata*, from 4.90 to 5.00 in *D. dichotoma* and from 2.20 to 2.29 in *U. lactuca* at the end of post-irradiation treatment (Figs. 35-36C-D and 37B). NPQ in the post-recovery algae (Figs. 35-36E-F and 37C), on the other hand, was increased from 1.46 to 1.69 in *S. chordalis*, from 1.83 to 2.40 in *P. palmata*, from 2.05 to 2.23 in *L. digitata*, from 3.56 to 3.97 in *D. dichotoma* and from 0.86 to 1.13 in *U. lactuca*.

Despite of the pre- and post-irradiation and post-recovery treatments, Y rapidly increased on the onset of the dark or relaxation phase and remained elevated until it reached a steady level in the course of recording. In the pre-irradiated algae (Figs. 35-36A-B and 37A), Y increased from 0.14 to 0.49 in *S. chordalis*, from 0.10 to 0.41 in *P. palmata*, from 0.34 to 0.68 in *L. digitata*, from 0.13 to 0.66 in *D. dichotoma* and from 0.13 to 0.66 in *U. lactuca*. Comparatively, in the post-irradiation algae (Figs. 35-36C-D and 37B), Y increased from 0.00 to 0.08 in *S. chordalis*, from 0.00 to 0.15 in *P. palmata*, from 0.11 to 0.25 in *L. digitata*, from 0.02 to 0.12 in *D. dichotoma* and from 0.01 to 0.08 in *U. lactuca*. In the post-recovery (Figs. 35-36E-F and 37C), Y increased from 0.03 to 0.14 in *S. chordalis*, from 0.05 to 0.31 in *P. palmata*, from 0.22 to 0.45 in *L. digitata*, from 0.07 to 0.21 in *D. dichotoma* and from 0.09 to 0.39 in *U. lactuca*.

After 20 s into the dark phase, qP of the pre-irradiation algae rapidly increased to above 0.95 in all the species (Figs. 35-37) and the value steadily increased until it reached the maximum value 1. The increase, however, was slow in post-irradiation algae (Figs. 35-36C-D and 37B) which took some time to reach the maximum value. qP of the post-recovery algae more or less followed that of the pre-irradiation algae (Figs. 35-36E-F and 37C).

Contrastingly, qN showed a declining pattern during the course of the dark phase. In the pre-irradiation red algae, qN declined from 0.81 to 0.61 in *S. chordalis* (Fig. 35A) and from 0.92 to 0.78 in *P. palmata* (Fig. 35B) which rapidly relaxed within the first 120 s and 40 s into the dark phase, respectively, and steadily declined afterwards. In the brown and green algae, on the other hand, qN was increased after 20 s and steadily declined afterwards. qN declined from 0.49 to 0.41 in *L. digitata* (Fig. 36A) and from 0.51 to 0.50 in *D. dichotoma* (Fig. 36B) and from 0.56 to 0.53 in *U. lactuca* (Fig. 37A). Comparatively, in the post-irradiation algae (Figs. 35-36C-D and 37B), qN declined from 0.97 to 0.96 in *S. chordalis*, from 0.96 to 0.92 in *P. palmata*, from 0.94 to 0.91 in *L. digitata*, from 0.98 to 0.97 in *D. dichotoma* and from 0.97 to 0.96 in *U. lactuca*. In the post-recovery algae (Figs. 35-36E-F and 37C), on the other hand, qN declined from 0.94 to 0.90 in *S. chordalis*, from 0.92 to 0.78 in *P. palmata* (i.e. with a rapid decline visible after 40

s), from 0.80 to 0.76 in *L. digitata*, from 0.95 to 0.94 in *D. dichotoma* and from 0.76 to 0.72 in *U. lactuca*. The last three species also showed an initial increase after 20 s and steadily declined afterwards.

The curves of NPQ followed that of qN. However, the relaxation of NPQ was more pronounced than that of qN. In the pre-irradiation algae (Figs. 35-36A-B and 37A), NPQ declined from 2.02 to 1.19 in *S. chordalis*, from 1.83 o 1.18 in *P. palmata*, from 0.86 to 0.64 in *L. digitata*, from 0.81 to 0.77 in *D. dichotoma* and from 0.83 to 0.78 in *U. lactuca*. In comparison, in the post-irradiation algae (Figs. 35-36C-D and 37B), NPQ declined from 2.53 to 2.40 in *S. chordalis*, from 2.84 to 2.51 in *P. palmata*, from 2.35 to 1.93 in *L. digitata*, from 5.06 to 4.83 in *D. dichotoma* and from 2.29 to 2.27 in *U. lactuca*. Additionally, in the post-recovery algae (Figs. 35-36E-F and 37C), qN declined from 1.69 to 1.49 in *S. chordalis*, from 2.40 to 1.69 in *P. palmata*, from 1.64 to 1.33 in *L. digitata*, from 4.20 to 3.97 in *D. dichotoma* and from 1.18 to 1.10 in *U. lactuca*.

3.3.5 Rapid induction kinetics

The rapid induction kinetics shows the involvement of several components of PSII redox system. The rapid induction curve of the algae at 1000 µs/data point is displayed in Fig. 38. During the recording, an induction phase (the first 2 s) as well as dark relaxation kinetics (the last 1 s) were determined (see MATERIALS AND METHODS section 2.3 for experimental conditions). In the induction phase, based on a report by Lazár (1999), at least two distinct rise components were noticeable, from O to I_2 and from I_2 to M (i.e. a transient maximum) as shown by the arrows on the curve for pre-irradiation *U. lactuca* (Fig. 38D). In between, there was a shoulder, designated by D (Fig. 38D). Other pre-irradiated algae did not show this trend due to the signal to noise ratio which obscuring the curve (Fig. 38A-C). Irradiation with PAR+UVA+UVB at H_{1B} strongly decreased the fluorescence (i.e. fluorescence signal between O and M) and completely quenched the O-I_2 and I_2-M phases. In post-recovery *U. lactuca*, the fluorescence was still

low but I_2 and D phases were more pronounced. After the actinic light was switched off (i.e. in the relaxation phase, the last 1 s of recording), the fluorescence rapidly declined in *P. palmata* (Fig. 38A) but

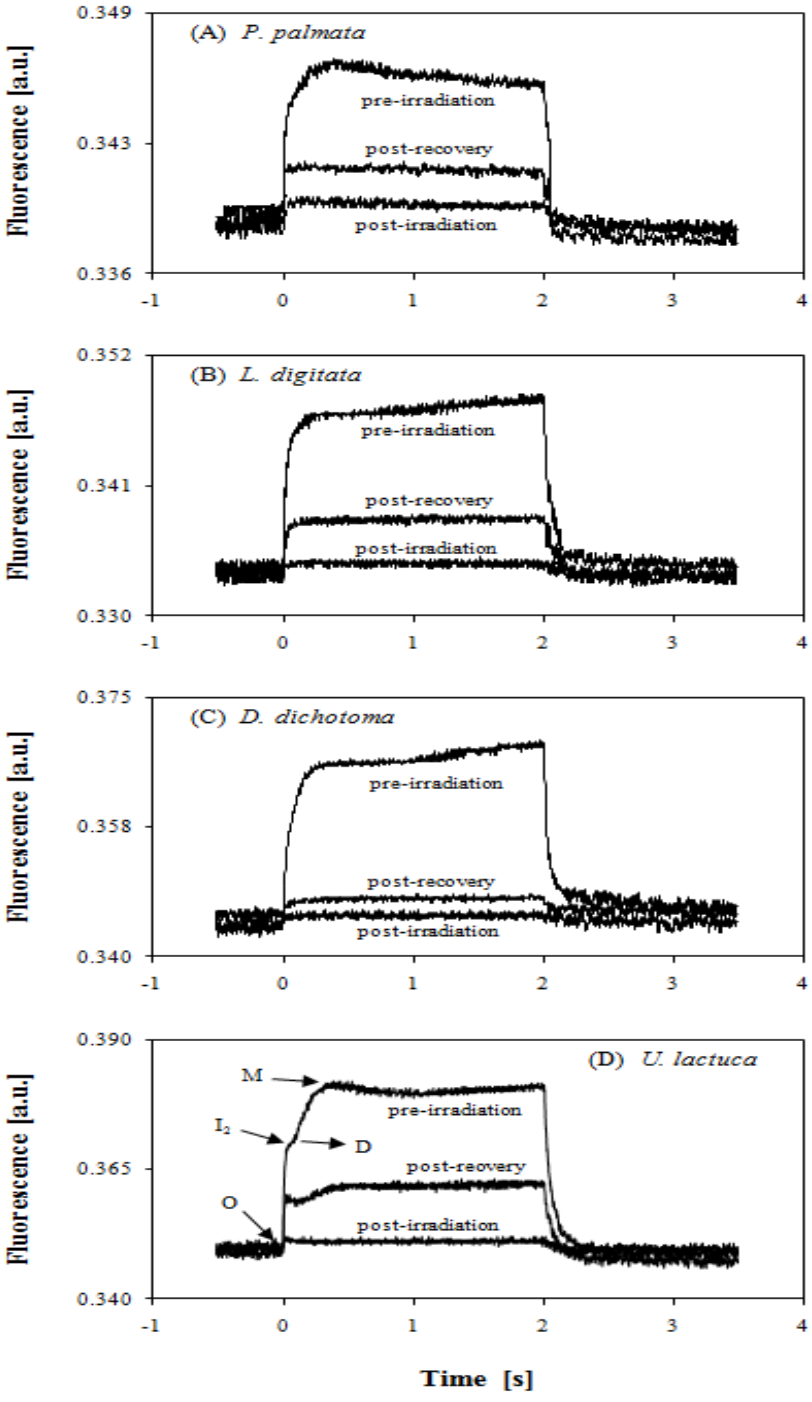

Fig. 38: Rapid induction and relaxation kinetics at 1000 µs/data point measured in *P. palmata* (*A*), *L. digitata* (*B*), *D. dichotoma* (*C*) and *U. lactuca (D*). Recordings were made before the irradiation (i.e. pre-irradiation), after 5 h irradiation with PAR+UVA+UVB at H_{1B} (i.e. post-irradiation) and after 18 h recovery under dim light (i.e. post-recovery). The curves are normalized to the same initial amplitude. (The O-I_2-D-M markers are based on Lazár, 1999 and Roháček and Barták, 1999).

was increased in *L. digitata* (Fig. 38B) and *D. dichotoma* (Fig. 38C) while there was first a decline then a small increase afterwards for *U. lactuca* (Fig. 38D). These changes showed that it took less than 1 s for the photosynthetic apparatus to regain its function. However, it took longer than 1 s for the photosynthetic apparatus to recover in all post-irradiation and post-recovery algae since there was only a steady level of fluorescence observed.

The polyphasic rise in the induction phase should be even better separated at a higher sampling rate of 300 µs/data point by plotting logarithmically as shown by *U. lactuca* in Fig. 39. In this example, the polyphasic rise was divided to several steps: O to J, J to I, I to P as observed in the induction curve of pre-irradiated algae. After post-irradiation treatment, the steps were quenched, leaving a monophasic rise (i.e. from O to J to P). However, after the recovery, the curve regained its pre-irradiation form but at a smaller scale.

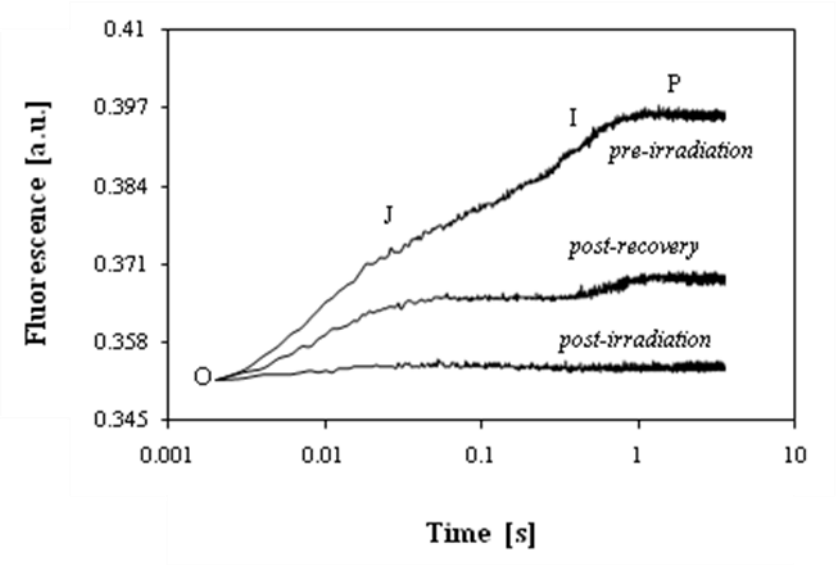

Fig. 39: Rapid induction and relaxation kinetics at 300 µs/data measured in *U. lactuca* plotted logarithmically. Recordings were made in pre-irradiated algae (i.e. control), after 5 h irradiation with PAR+UVA+UVB at H_{1B} and after 18 h recovery under dim light. The curves are normalized to the same initial amplitude. (The O-J-I-P markers are based on Boisvert et al., 2006).

3.4 Photosynthetic performance of macroalgae irradiated with variable UVR

These experiments were carried out to determine the response of the macroalge to variable irradiances of ultraviolet radiation (UVR, UVA and UVB) but to a constant photosynthetically active radiation (PAR).

3.4.1 Low PAR and variable UVR

The irradiation conditions for the experiments are listed in Table 19. The setups from henceforth are termed low PAR 2 (i.e. L_2) and low PAR 3 (i.e. L_3) (see MATERIALS AND METHODS section 2.2.1 for explanation) corresponding to the low background PAR irradiance emitted by the fluorescent lamps in comparison to that of the sun simulator. Ratio of PAR:UVA:UVB was calculated with respect to PAR.

Table 19: Irradiances of the different spectral ranges in the fluorescent lamps experimental setups.

Species	Setup	Radiation conditions	Ratio of PAR:UVA:UVB
S. chordalis, *L. digitata* and *U. lactuca*	L_2	18 µmol m^{-2} s^{-1} PAR + 13.6 W m^{-2} UVA + 0.38 W m^{-2} UVB	1:4:0.1
S. chordalis, *L. digitata* and *U. lactuca*	L_3	21 µmol m^{-2} s^{-1} PAR + 25.5 W m^{-2} UVA + 0.79 W m^{-2} UVB	1:6:0.2

The photosynthetic parameters of the macroalgae before irradiation (i.e. pre-irradiation) are listed in Table 20. The measurements for post-irradiation and post-recovery algae are standardized to 100% of these values.

Table 20: The maximal quantum yield (F_v/F_m) and photosynthetic parameters determined from rETR vs. actinic light curve in the macroalgae before irradiation at low PAR and variable UVR (i.e. pre-irradiation or control). Data are means ±SD values of n=9.

Species	Photosynthetic parameters			
	F_v/F_m [rel. units]	$rETR_{max}$ [rel. units]	α [rel. units]	I_k [µmol m^{-2} s^{-1}]
S. chordalis	0.588 ± 0.03	15.60 ± 5.7	0.443 ± 0.06	35.54 ± 5.3
L. digitata	0.701 ± 0.03	46.46 ± 9.6	0.572 ± 0.07	82.06 ± 7.4
U. lactuca	0.700 ± 0.04	31.65 ± 3.1	0.508 ± 0.07	71.08 ± 9.3

Generally, no notable effect of PAR alone on the photosynthetic parameters was oberved in all the algae examined at L_2 (Fig. 40). However, when UVR was added into the treatments, the algae were strongly

affected. The maximum quantum yield (F_v/F_m) of *S. chordalis* irradiated with both PAR+UVR treatments, for instance, was reduced by more than 70% while in *L. digitata* and *U. lactuca*, F_v/F_m was reduced by more than 40% and 50%, respectively (Fig. 40Ai). In addition, PAR caused about 7% reduction of F_v/F_m in *L. digitata*. F_v/F_m was increased to more than 80% in both PAR+UVR-treated *L. digitata* and *U. lactuca* after the recovery period (Fig. 40Aii). In particular, F_v/F_m of PAR+UVA-treated *S. chordalis* recovered faster than PAR+UVA+UVB with the value increased to 79% compared to 70%.

Similar to F_v/F_m, the maximum relative electron transport rate ($rETR_{max}$) was not affected by PAR alone in all the algae including *L. digitata* (Fig. 40Bi). In addition, it appeared that PAR+UVR treatments had no effect on $rETR_{max}$ of *L. digitata* as well even though PAR+UVA+UVB showed an increasing trend. In contrast, PAR+UVR reduced the $rETR_{max}$ of *U. lactuca* by about 37%. Individually, PAR+UVA+UVB caused a 68% reduction of the $rETR_{max}$ in *S. chordalis* compared to a 59% reduction with PAR+UVA. All post-irradiated algae showed signs of recovery with values increased to more than 80% at the end of post-recovery treatment (Fig. 40Bii).

The photosynthetic efficiency parameter, α, was seemingly affected the strongest by PAR+UVA+UVB. Reduction was 72-74% in *S. chordalis*, 23-33% in *L. digitata* and 46-51% in *U. lactuca* under both the PAR+UVR treatments (Fig. 40Ci). PAR alone, on the other hand, caused no effect on α. The α of PAR+UVR-affected *L. digitata* showed a full recovery but appeared to reduce slightly in PAR (Fig. 40Cii). In *S. chordalis* and *U. lactuca*, α of PAR+UVR-affected algae showed an increase to values higher than 75% after the recovery period. Furthermore, α of PAR-affected *S. chordalis* was increased to 106% after the recovery.

Unlike the above parameters, the light saturation parameter, I_k, was increased after the irradiation with PAR+UVR while there was no effect after irradiation with PAR alone (Fig. 40Di). In *S. chordalis, L. digitata* and *U. lactuca*, I_k was increased by 39%-41%, 31%-56% and 19%-27% after irradiation with PAR+UVR treatments, respectively. The highest increase was observed with PAR+UVA in *S. chordalis*

and with PAR+UVA+UVB in *L. digitata* and *U. lactuca.* After the recovery period, I_k of PAR+UVR-affected *L. digitata* and *U. lactuca* showed a full recovery while there appeared to be a delay in recovery for *S. chordalis* (Fig. 40Dii).

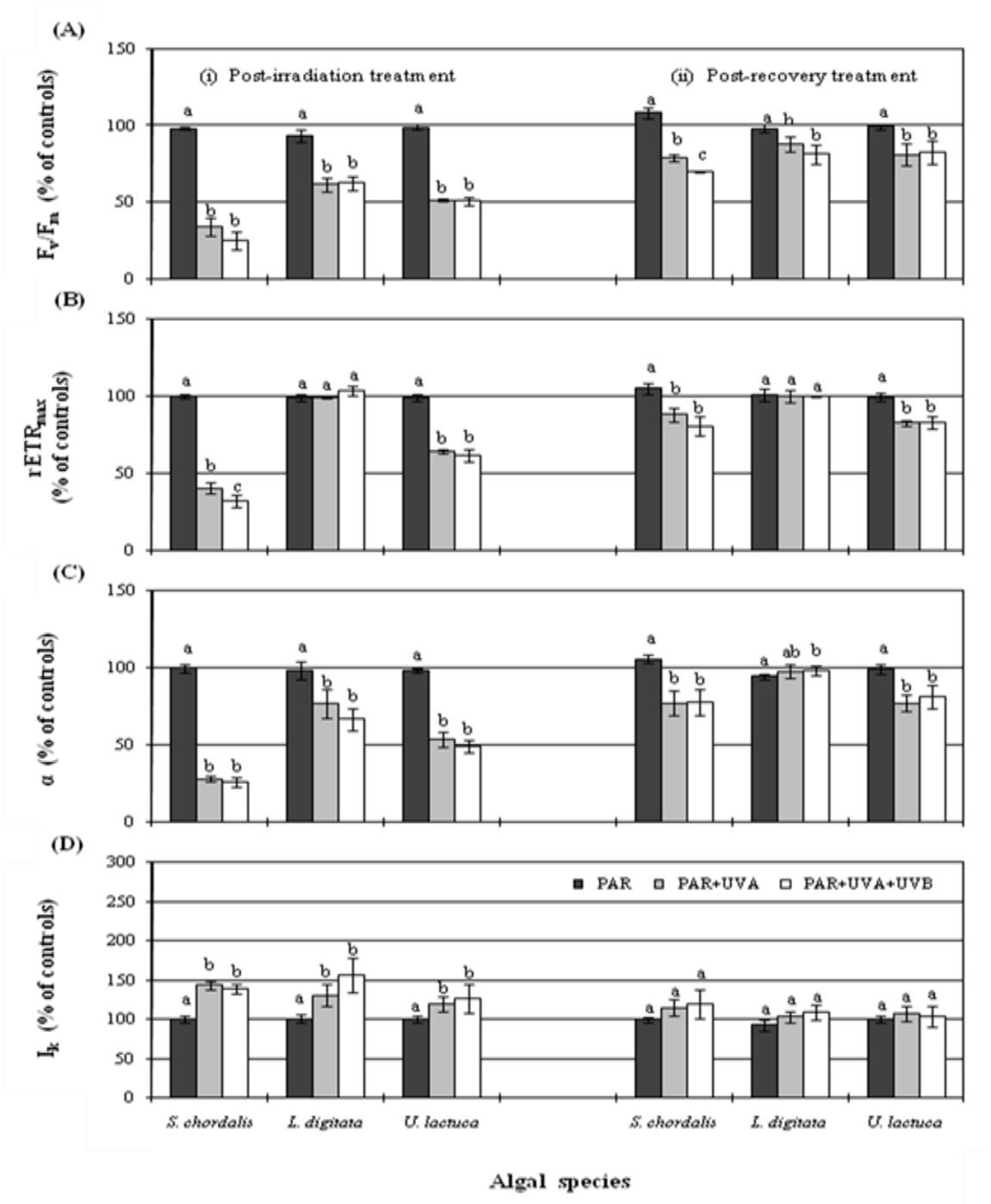

Fig. 40: Maximum quantum yield (F_v/F_m, *A*), maximum relative electron transport rate ($rETR_{max}$, *B*), photosynthetic efficiency (α, *C*) and light saturation parameter (I_k, *D*) of *S. chordalis*, *L. digitata* and *U. lactuca* after 5 h irradiation at 18 µmol m^{-2} s^{-1} PAR, 13.6 Wm^{-2} UVA and 0.4 Wm^{-2} UVB (L_2, post-irradiation, *i*) and after 18 h recovery under dim light (post-recovery, *ii*). *Black bars:* PAR, *grey bars:* PAR+UVA, *white bars*: PAR+UVA+UVB. Data are means ±SD values. Different letters above bars indicate significant difference between different light treatments within similar species (ANOVA, Fischer's LSD test, $p < 0.05$, n=3).

The F_v/F_m of the algae irradiated at higher fluence of UVR than L_2 (i.e. at L_3) (Fig. 41Ai) was reduced to a higher values than at L_2 (Fig. 40Ai) in *L. digitata* (ANOVA, SNK *post-hoc* test, $p<0.001$) and *U. lactuca* ($p<0.001$) but not in *S. chordalis* ($p=0.095$). When comparison was made between L_1 and L_3, it appeared that higher reduction was observed at L_1 in *S. chordalis* ($p=0.215$) but higher at L_3 in *L. digitata* ($p=0.328$) and *U. lactuca* ($p=0.271$). PAR alone at L_3 showed no effect on *L. digitata* and *U. lactuca* but slightly increased F_v/F_m of *S. chordalis* (Fig. 40Ai). After irradiation with PAR+UVR, F_v/F_m of *S. chordalis* and *L. digitata* was reduced by more than 74% and 55%, respectively. Furthermore, PAR+UVA+UVB caused less reduction in *U. lactuca* (i.e. 71% reduction) compared to that of PAR+UVA (i.e. 86% reduction). Equal rate of F_v/F_m recovery was observed in post-recovery algae between both the irradiance conditions (i.e. L_2 and L_3) ($p=0.086$ for *S. chordalis*, $p=0.115$ for *L. digitata* and $p=0.519$ for *U. lactuca*). However, when compared between L_1, L_2 and L_3, recovery was much faster at lower UV irradiance (i.e. L_2 and L_3) in *S. chordalis* ($p<0.001$), *L. digitata* ($p<0.001$) and *U. lactuca* ($p=0.387$). At L_3, recovery was faster in PAR+UVA-treated *S. chordalis* (i.e. increased to 74%) than PAR+UVA+UVB (i.e. increased to 63%) (Fig. 41Aii). There was a slower recovery in PAR+UVA+UVB-treated *L. digitata* (i.e. increased to 84%) as well, compared to that of PAR+UVA which attained full recovery. F_v/F_m of PAR+UVR-treated *U. lactuca*, on the other hand, increased to values higher than 75% after the recovery period.

PAR+UVR treatments reduced $rETR_{max}$ of algae irradiated at L_3 (Fig. 41Bi) to a much higher values than L_2 (Fig. 40Bi) as well. $rETR_{max}$ was reduced by more than 65% in *S. chordalis* and by more than 45% in *U. lactuca*. However, opposite effect was observed in *L. digitata* whereby $rETR_{max}$ was increased by more than 18% after irradiation with PAR+UVR Furthermore, PAR alone increased $rETR_{max}$ of *U. lactuca* by 4%. After the recovery period, $rETR_{max}$ of affected *L. digitata* showed a full recovery while $rETR_{max}$ of PAR+UVR-affected *S. chordalis* and *U. lactuca w*as increased to values higher than 75% and 80%, respectively (Fig. 41Bii).

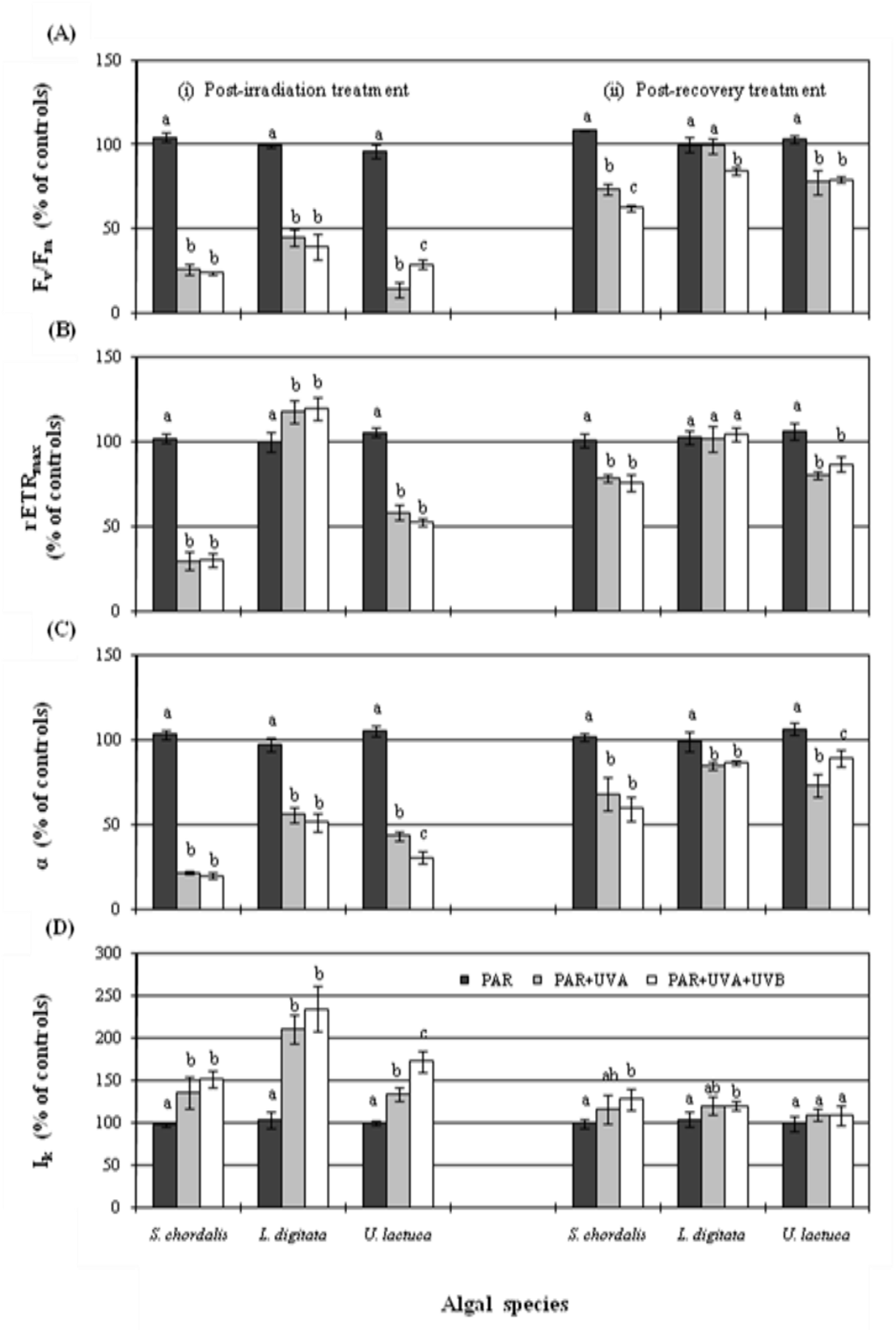

Fig. 41: Maximum quantum yield (F_v/F_m, *A*), maximum relative electron transport rate ($rETR_{max}$, *B*), photosynthetic efficiency (α, *C*) and light saturation parameter (I_k, *D*) of *S. chordalis*, *L. digitata* and *U. lactuca* after 5 h irradiation at 21.3 µmol m^{-2} s^{-1} PAR, 25.5 Wm^{-2} UVA and 0.8 Wm^{-2} UVB (L_3, post-irradiation, *I*) and after 18 h recovery under dim light (post-recovery, *II*), details as in Fig. 40.

Comparatively, α was reduced by more than 78% in *S. chordalis* and by more than 44% in *L. digitata* after irradiation with PAR+UVR at L_3 (Fig. 41Ci). A distinctive effect between the two PAR+UVR treatments was observed in *U. lactuca* whereby PAR+UVA+UVB caused more reduction in α (i.e. 69% reduction) than PAR+UVA (i.e. 56% reduction). In *U. lactuca,* α was slightly increased by PAR alone. PAR+UVA+UVB showed a faster recovery of α in *U. lactuca* (i.e. increased to 89%) than PAR+UVA (i.e. increased to 74%) while PAR-affected algae did not show any recovery (Fig. 41Cii). The α in PAR+UVR-affected *S. chordalis* and *L. digitata* recovered to values higher than 55% and 85%, respectively.

After irradiation with PAR+UVR treatments, I_k of the algae increased to more than 35% in *S. chordalis* and to more than doubled their control values in *L. digitata* (Fig. 41Di). In *U. lactuca,* PAR+UVA+UVB caused a higher increase in I_k (i.e. 73% increase) than PAR+UVA (i.e. 34% increase). All affected algae showed signs of recovery with I_k in *U. lactuca* was fully recovered while a delay in recovery was observed in *S. chordalis* and *L. digitata* (Fig. 41Dii).

3.4.2 High PAR and variable UVR

The irradiation conditions for the experiments are listed in Table 21. Henceforth, the setups are termed high PAR 2 (i.e. H_2) and high PAR 3 (i.e. H_3) (see MATERIALS AND METHODS section 2.2.2 for explanation) corresponding to the high background PAR irradiance emitted by the sun simulator in comparison to that of fluorescent lamps. Generally, the algae were exposed to a fixed PAR, a lower UVA and a higher UVB at H_2 than at H_3 (Table 21). Ratio of PAR:UVA:UVB was calculated with respect to PAR.

The photosynthetic parameters of the macroalgae before irradiation (i.e. pre-irradiation or control) are listed in Table 22. As for L_2/L_3, the measurements for post-irradiation and post-recovery algae are standardized to 100% of these values.

Table 21: Irradiances of the different spectral ranges in the sun simulator experimental setups.

Setup	Species	PAR ($\mu mol\ m^{-2}\ s^{-1}$)	PAR ($W\ m^{-2}$)	UVA ($W\ m^{-2}$)	UVB ($W\ m^{-2}$)	Ratio of PAR:UVA:UVB
H_2	*S. chordalis*	476	100	7.0	0.42	100:7:0.4
	P. palmata	498	105	6.6	0.38	100:6:0.4
	L. digitata	496	104	7.0	0.41	100:7:0.4
	D. dichotoma	540	114	10.0	0.59	100:9:0.5
	U. lactuca	501	105	13.4	0.68	100:13:0.6
H_3	*S. chordalis*	489	103	19.2	0.22	100:19:0.2
	P. palmata	475	100	17.1	0.19	100:17:0.2
	L. digitata	496	104	19.0	0.22	100:18:0.2
	D. dichotoma	522	110	20.8	0.29	100:19:0.3
	U. lactuca	512	108	20.0	0.25	100:19:0.2

Table 22: The maximal quantum yield (F_v/F_m) and photosynthetic parameters determined from rETR vs. actinic light curve in the macroalgae before irradiation at high PAR and variable UVR (i.e. pre-irradiation or control). Data are means ±SD values of n=12.

Species	Photosynthetic parameters			
	F_v/F_m [rel. units]	$rETR_{max}$ [rel. units]	α [rel. units]	I_k [$\mu mol\ m^{-2}\ s^{-1}$]
S. chordalis	0.583 ± 0.02	45.16 ± 7.0	0.426 ± 0.03	106.55 ± 18.5
P. palmata	0.482 ± 0.04	11.36 ± 2.4	0.407 ± 0.06	28.52 ± 6.8
L. digitata	0.744 ± 0.02	62.77 ± 5.0	0.516 ± 0.06	124.59 ± 17.6
D. dichotoma	0.687 ± 0.02	48.39 ± 4.2	0.466 ± 0.05	106.69 ± 18.9
U. lactuca	0.736 ± 0.02	35.38 ± 7.8	0.574 ± 0.04	69.78 ± 7.8

At H_2, UVA+UVB caused the least reduction of F_v/F_m in all the algal species examined with a 25% reduction in *S. chordalis*, 37% in *P. palmata,* 22% in *L. digitata,* 18% in *D. dichotoma* and 35% in *U. lactuca* (Fig. 42Ai). Following UVA+UVB was PAR alone with 58% reduction in *S. chordalis,* 60% in *P. palmata,* 76% in *L. digitata* and 68% in *U. lactuca.* In *D. dichotoma,* however, similar trend was observed but was not significant. The highest F_v/F_m reduction was observed with PAR+UVR treatments. PAR+UVA+UVB caused a significantly higher reduction in *P. palmata* (i.e. 81%) than PAR+UVA (i.e. 78%) while PAR+UVA caused a significantly higher reduction in *D. dichotoma* (i.e. 79%) and *U. lactuca* (i.e. 80%) than PAR+UVA+UVB (i.e. 73% and 76%, respectively). F_v/F_m of all affected *D. dichotoma*

and *U. lactuca* showed a full or nearly a full recovery (Fig. 42Aii). There was a delay in the recovery with PAR+UVR-affected *S. chordalis*, *P. palmata* and *L. digitata*, especially in *P. palmata* where F_v/F_m in PAR+UVA+UVB increased to a lower 47% compared to the other light treatments. In general, F_v/F_m recovery was fast in UVA+UVB especially in *P. palmata* which increased to a significant 88%, followed by PAR alone.

Similar to F_v/F_m, UVA+UVB caused the least effect on $rETR_{max}$ with a 25% reduction in *S. chordalis*, 30% reduction in *P. palmata*, 3% reduction in *L. digitata* and 33% reduction in *U. lactuca* (Fig. 42Bi). However, there was a 12% increase in *D. dichotoma* after irradiation with UVA+UVB. PAR alone caused the next least effect with a 57% reduction in *S. chordalis*, 51% reduction in *P. palmata*, 60% reduction in *L. digitata* and 58% reduction in *U. lactuca*. In *D. dichotoma*, this effect was not significant. The strongest effect was caused by the PAR+UVR treatments. In *S. chordalis*, $rETR_{max}$ was reduced by 71% under PAR+UVA+UVB and a higher reduction was observed under PAR+UVA (i.e. 78%). The opposite effect was observed in *P. palmata w*ith an 83% reduction under PAR+UVA+UVB and a 73% reduction under PAR+UVA. In the other species, PAR+UVA caused the highest reduction. There was a slower recovery of $rETR_{max}$ in PAR+UVA-affected *S. chordalis* and *D. dichotoma* (i.e. increased to 65% and 75%, respectively) than the other light treatments which increased to values higher than 75% and 85%, respectively (Fig. 42Bii). In contrast, PAR+UVA+UVB-affected *P. palmata* showed the slowest recovery with an increase to 36% compared to more than 55% in other light treatments. Furthermore, $rETR_{max}$ of *L. digitata* was increased to values higher than their pre-irradiations with an increase to 149% in PAR, and, to 120% in both PAR+UVA+UVB and UVA+UVB but was 8% lower than the pre-irradiations in PAR+UVA.

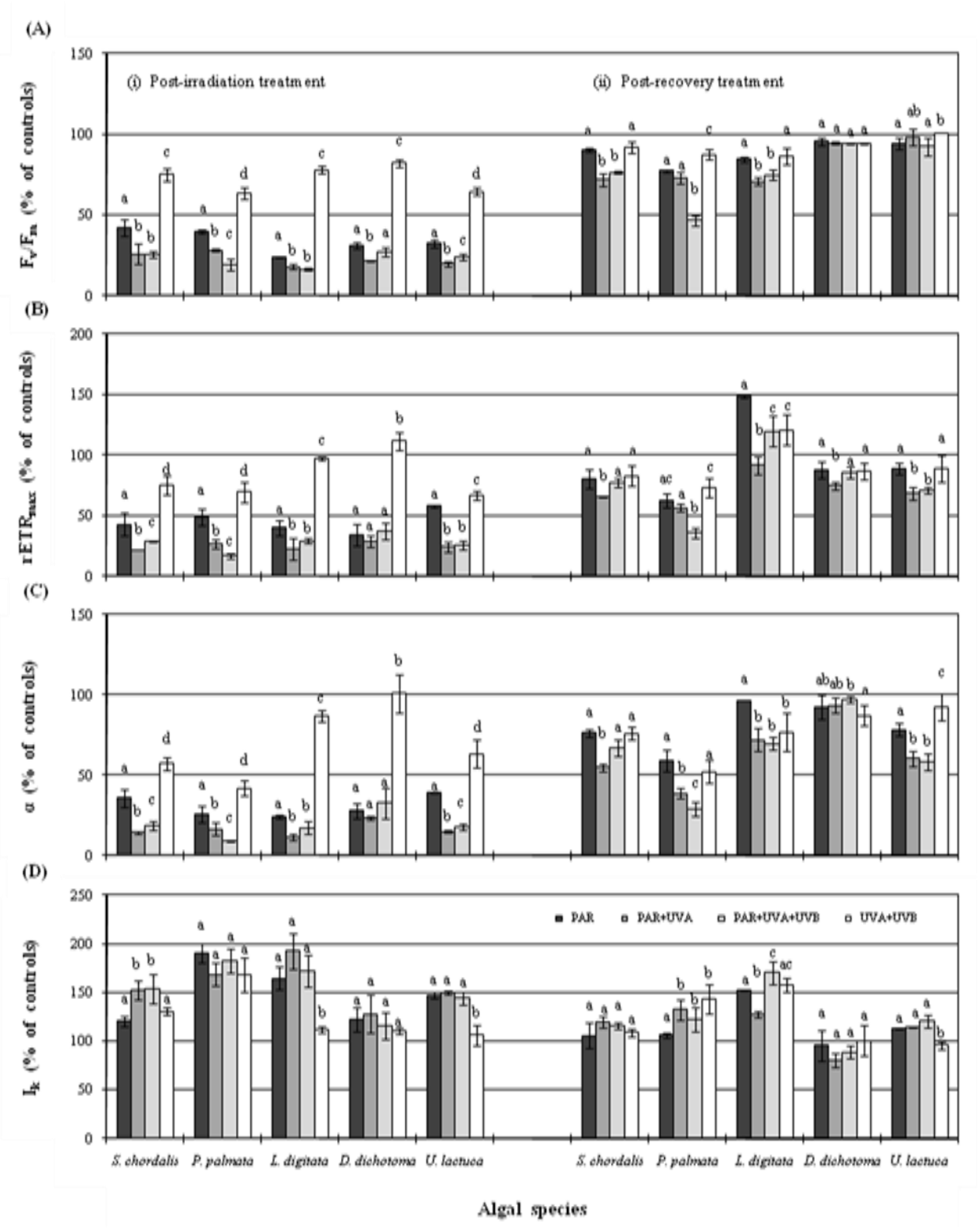

Fig. 42: Maximum quantum yield (F_v/F_m, *A*), maximum relative electron transport rate ($rETR_{max}$, *B*), photosynthetic efficiency (α, *C*) and light saturation parameter (I_k, *D*) of *S. chordalis, P. palmata, L. digitata, D. dichotoma* and *U. lactuca* after 5 h irradiation at 476-540 µmol m^{-2} s^{-1} PAR, 6.6-13.4 Wm^{-2} UVA and 0.4-0.7 Wm^{-2} UVB (H_2, post-irradiation, *i*) and after 18 h recovery under dim light (post-recovery, *ii*). *Black bars:* PAR, *dark grey bars:* PAR+UVA, *light grey bars*: PAR+UVA+UVB, *white bars:* UVA+UVB. Data are means ±SD values. Different letters above bars indicate significant difference between different light treatments within similar species (ANOVA, Fischer's LSD test, $p < 0.05$, n=3).

The trend in F_v/F_m and $rETR_{max}$ changes was displayed by α as well (Fig. 42Ci). UVA+UVB reduced α of *S. chordalis* by 43%, *P. palmata* by 58%, *L. digitata* by 13% and *U. lactuca* by 37% but appeared not to affect *D. dichotoma.* In addition, PAR alone caused a 64% reduction in *S. chordalis,* 74% reduction in *P. palmata,* 76% reduction in *L. digitata a*nd 61% reduction in *U. lactuca.* PAR+UVA+UVB caused the strongest effect in *P. palmata* with a 91% reduction while PAR+UVA caused the strongest effect in *S. chordalis* and *U. lactuca w*ith an 85% reduction in both algal species. In *D. dichotoma,* it appeared that PAR+UVA caused the strongest effect, followed by PAR and PAR+UVA+UVB. A delay in α recovery was observed in PAR+UVA-affected *S. chordalis* which increased to 55% compared to more than 65% in other light treatments (Fig. 42Cii). On the other hand, PAR+UVA+UVB-affected *P. palmata* showed a delay in recovery (i.e. increased to 29%) compared to PAR+UVA (i.e. increased to 39%). In *U. lactuca,* UVA+UVB showed the fastest recovery (i.e. increased to 93%), followed by PAR (i.e. increased to 79%) and PAR+UVR treatments. All affected *D. dichotoma* and PAR-affected *L. digitata* showed nearly a full recovery while recovery in PAR+UVR- and UVA+UVB-affected *L. digitata* was delayed.

Contrastingly, PAR+UVR treatments caused a 50% increase in I_k of *S. chordalis* while PAR alone caused the least effect, followed by UVA+UVB (Fig. 42Di). I_k was increased between 68% and 90% and between 11% and 28% in post-irradiation *P. palmata* and *D. dichotoma*, respectively. UVA+UVB caused the least increase in *L. digitata* with 12% while in the rest of the light treatments, I_k increased by more than 65%. In addition, whilst I_k was increased the least by UVA+UVB in *U. lactuca* with only 6%, in the rest of the light treatments, I_k was increased by about 50%. All post-recovery algae showed signs of recovery except for *L. digitata* under PAR+UVA+UVB (Fig. 42Dii). A delay in I_k recovery was observed in PAR-affected *P. palmata* (i.e. reduced to 106%), PAR+UVA-affected *L. digitata* (i.e. reduced to 128%) and UVA+UVB-affected *U. lactuca* (i.e. reduced to 96%). Furthermore, I_k in PAR+UVR-affected *D. dichotoma* was reduced to ca. 85% after the recovery period.

Interestingly, most of the algae showed a higher reduction of F_v/F_m at H_3 (Fig. 43Ai) than H_2 (Fig. 42Ai) after post-irradiation treatment with additional UV. This was noticeable with *S. chordalis* (p=0.019), *D.*

dichotoma (p=0.040) and *U. lactuca* (p<0.001). In contrast, *L. digitata* showed a higher reduction at H_2 than H_3 (p=0.045) while a similar trend was also observed with *P. palmata* but with insignificant difference (p=0.310). When compared with H_1 (Fig. 16Ai), reduction was higher at H_1 than H_3 in *S. chordalis* (p<0.001) and *D. dichotoma* (p=0.003) but was lower at H_1 than H_3 in *U. lactuca* (p=0.001). Furthermore, H_1 caused higher reduction than H_2 for *L. digitata* (p<0.001) and *P. palmata* (p=0.001). Similar to H_2, the least effect was still caused by UVA+UVB at H_3 but with a 40% reduction in *S. chordalis*, 29% reduction in *L. digitata*, 32% in *D. dichotoma* and 45% in *U. lactuca.* The next least effect was observed with PAR alone with a 69% reduction in *S. chordalis*, 72% in *L. digitata*, 73% in *D dichotoma* and 77% in *U. lactuca.* PAR+UVR treatments caused the strongest effect on F_v/F_m of the algae. The effect was stronger under PAR+UVA in *S. chordalis* (i.e. 83% reduction) and *U. lactuca* (i.e. 96% reduction) than under PAR+UVA+UVB (i.e. 77% and 92% reductions, respectively) while PAR+UVA+UVB was stronger in *D. dichotoma* (i.e. 83% reduction) than under PAR+UVA (i.e. 77% reduction). F_v/F_m recovery was faster at H_3 than H_2 in *S. chordalis* (p<0.001), *P. palmata* (p=0.468) and *U. lactuca* (p=0.993) while H_2 showed faster recovery than H_3 in *L. digitata* (p=0.049) and *D. dichotoma* (p<0.001). In addition, PAR+UVA+UVB had the slowest F_v/F_m recovery in *S. chordalis* which increased to 43% while PAR+UVA was the slowest in *U. lactuca* which increased to 72%. UVA+UVB was the fastest to recover which increased to 82% in *S. chordalis*, 95% in *P. palmata*, 90% in *L. digitata*, 97% in *D. dichotoma* and 98% in *U. lactuca*. The next to recover following UVA+UVB was PAR alone which increased to 72% in *S. chordalis*, 79% in both *P. palmata* and *L. digitata*, and 92% in *D. dichotoma.* However, PAR+UVA+UVB was the next to recover in *U. lactuca* which increased to 92%.

The $rETR_{max}$ of *L. digitata* was increased by 9% when irradiated with UVA+UVB at H_3 (Fig. 43Bi). In *D. dichotoma*, UVA+UVB caused no effect on $rETR_{max}$ but a 38% reduction in *S. chordalis* and 23% reduction in *U. lactuca.* In *S. chordalis*, the highest reduction was observed under PAR+UVA with 84%. It appeared that PAR+UVA caused the highest reduction in *P. palmata a*nd *L. digitata* as well but the highest reduction in *D. dichotoma* and *U. lactuca* was under PAR+UVA+UVB. In addition, PAR alone caused a 76% reduction in *U. lactuca*, the least affected after UVA+UVB. All affected *P. palmata*

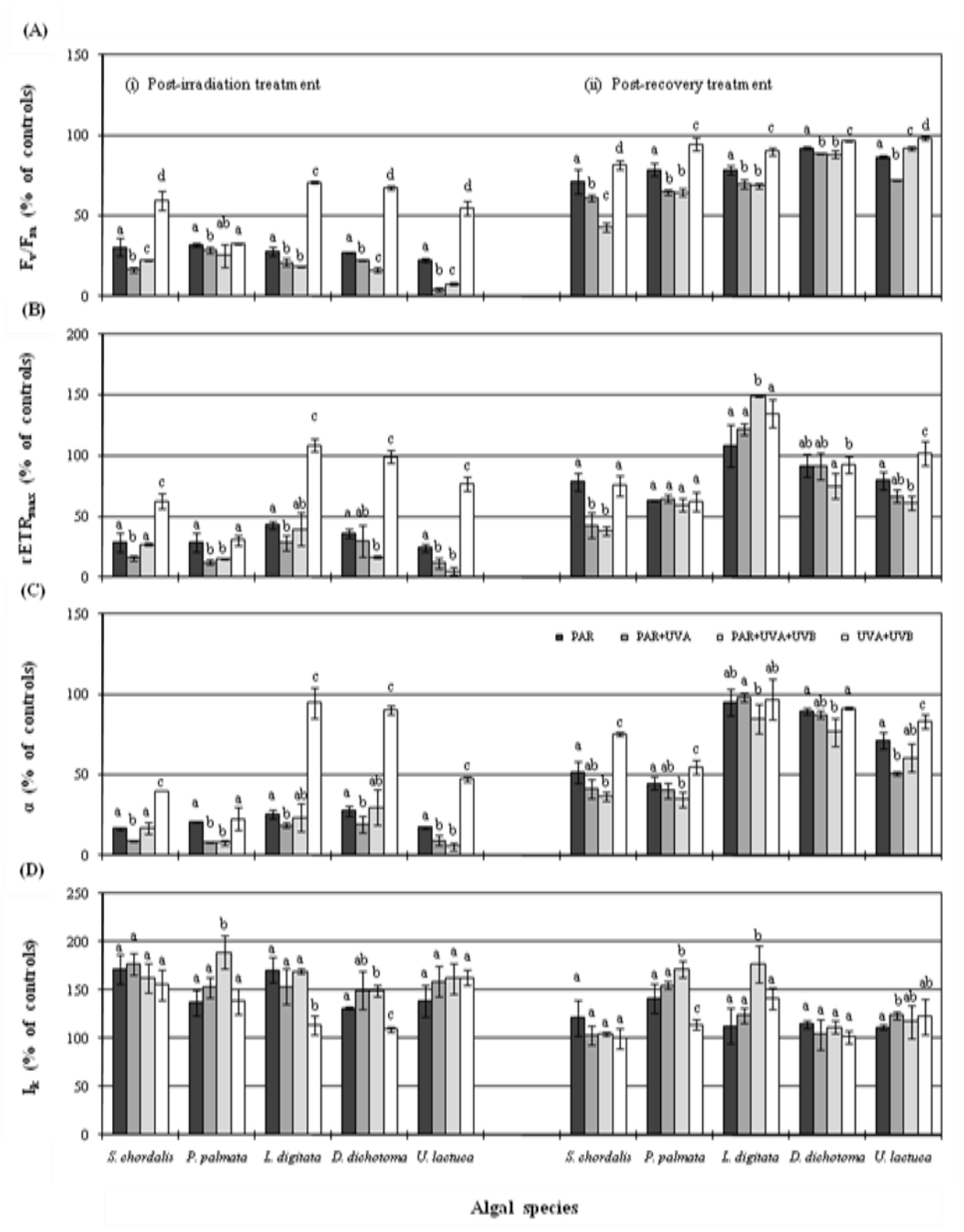

Fig. 43: Maximum quantum yield (F_v/F_m, *A*), maximum relative electron transport rate ($rETR_{max}$, *B*), photosynthetic efficiency (α, *C*) and light saturation parameter (I_k, *D*) of *S. chordalis, P. palmata, L. digitata, D. dichotoma* and *U. lactuca* after 5 h irradiation at 475-522 µmol m^{-2} s^{-1} PAR, 17.0-20.8 Wm^{-2} UVA and 0.2-0.3 Wm^{-2} UVB (H_3, post-irradiation, *I*) and after 18 h recovery under dim light (post-recovery, *II*), details as in Fig. 42.

showed an increase of $rETR_{max}$ to values higher than 60% after the recovery period (Fig. 43Bii). In *S. chordalis,* PAR+UVR showed a slower recovery than PAR and UVA+UVB. In *D. dichotoma,* all light treatments showed a tendency to a full $rETR_{max}$ recovery except in PAR+UVA+UVB. Whilst UVA+UVB showed a full recovery in *U. lactuca,* other light treatments showed a delay in recovery. Contrastingly, $rETR_{max}$ of *L. digitata* increased to values exceeding that of their pre-irradiations especially with PAR+UVA+UVB which increased to 150%.

UVA+UVB caused the least effect on α of the algae as well (Fig. 43Ci). There was a 60% reduction in *S. chordalis,* 5% reduction in *L. digitata,* 9% reduction in *D. dichotoma* and 53% reduction in *U. lactuca* after irradiation with UVA+UVB. In *S. chordalis,* α was the strongest affected by PAR+UVA with a 91% reduction, followed by PAR and PAR+UVA+UVB. *P. palmata* showed the strongest effect with PAR+UVR treatments, followed by PAR and UVA+UVB. In *U. lactuca,* the strongest effect was observed with PAR+UVR treatments as well, followed significantly by PAR with an 82% reduction.

Furthermore, a trend was observed in the brown algae *L. digitata* and *D. dichotoma* whereby PAR+UVA showed the strongest effect on α, followed by other light treatments. Recovery of α was the fastest with UVA+UVB especially in *S. chordalis, P. palmata* and *U. lactuca* which increased to 75%, 55% and 83%, respectively (Fig. 43Cii). In general, recovery was the slowest with PAR+UVR treatments followed by PAR while most of affected *L. digitata* and *D. dichotoma* had their α fully or nearly fully recovered.

I_k of *S. chordalis* increased by more than 50% after irradiation with all light treatments with the least under UVA+UVB, followed by PAR+UVA+UVB, PAR and PAR+UVA (Fig. 43Di). In *P. palmata,* PAR+UVA+UVB caused the highest increase with 90%, followed by PAR+UVA, PAR and UVA+UVB. UVA+UVB caused the least increase in *L. digitata* and *D. dichotoma* with 14% and 10%, respectively, followed by PAR+UVR and PAR in *L. digitata* and the opposite in *D. dichotoma*. In addition, PAR caused the least increase in I_k of *U. lactuca* followed by PAR+UVR and UVA+UVB. The slowest recovery of I_k in *S. chordalis* appeared to be in PAR while in the rest of light treatments, full recovery

was attained (Fig. 43Dii). In *P. palmata*, I_k recovered the fastest under UVA+UVB which was reduced to 114% and the slowest was observed under PAR+UVA+UVB which was reduced to 171%. There appeared to be a delay in recovery under PAR+UVA but a faster recovery under PAR compared to the other light treatments in *U. lactuca*. All affected *D. dichotoma* either fully recovered or nearly fully recovered. Contrastingly, I_k of PAR+UVA+UVB-affected *L. digitata* showed an increasing trend after the recovery period. However, when compared with the post-irradiation algae, there was no significant difference. In addition, PAR was the fastest to recover in *L. digitata*, followed by PAR+UVA and UVA+UVB.

4.0 DISCUSSION

4.1 Impact of PAR and UVR on photosynthetic performance

The maximal quantum yield (F_v/F_m) has been frequently used to monitor plant's health (Maxwell and Johnson, 2000). A drop in this value indicates that the plant is under stress or experiencing photoinhibition (Cordi et al., 1997). Under non-stressed conditions, red algae typically possess F_v/F_m in the range of 0.5 to 0.6 while brown algae and green algae in the range of 0.6 to 0.7 and 0.7 to 0.8, respectively (D. Hanelt, personal commun.). Low F_v/F_m in the brown algae may be due to chlororespiration (Buschel and Wilhelm 1993, cited in Franklin and Forster 1997) or, in the red algae case, to fluorescence contributions from phycobiliproteins (Franklin and Forster, 1997). F_v/F_m of the pre-irradiated algal samples is within this range, implying that the algae are not stressed at the start of the treatments. Photoinhibition has been proposed as a strategy of photoprotection against high irradiance (Osmond, 1994; Hanelt, 1996) and is mostly related to the degree and extent of damage and its recovery. A dramatic decline in F_v/F_m after post-irradiation treatment indicates that the algae are strongly photoinhibited. The decline in F_v/F_m is higher in post-irradiated algae at H_1 (i.e. average reduction of 74%-92%) than at L_1 (i.e. average reduction of 39%-56%). Recovery, however, was faster at L_1 than at H_1. This suggests that the mechanism of photoinhibition in the algae is triggered when the algae are transferred from low light to high light conditions.

Ecophysiological studies have suggested that the physiological responses of macroalgae to UVB are associated with their zonation pattern. A survey of the UV tolerance of marine rhodophytes from tropical habitats showed that UV exposure caused less pronounced effects in intertidally occurring species than in subtidal species (van de Poll et al., 2001). In addition, photoinhibition was more pronounced in deep water algae than in surface algae with the latter recovered fast while the former showed incomplete or non-existent recovery (Häder et al., 1998b). Hence, in my study, the upper-middle sublittoral *Laminaria digitata* is more photoinhibited and recovered slower than the intertidal or eulittoral *Ulva lactuca* and

Solieria chordalis on exposure to H_1. However, these results also delineate the facts that algae subjected to high irradiances have higher photoinhibition and recovery capacity than those inhabiting shaded sites (Figueroa and Gómez, 2001), and, UVB is potentially detrimental for photosynthesis when algae are maintained close to the surface (Gómez et al., 2005).

It has been known that PAR irradiance accounts for a great fraction of photoinhibition of photosynthesis in macroalgae, whereas a considerable fraction is due to short wavelength solar UV (Hanelt, 1998; Bischof et al., 1999; Dring et al, 2001; van de Poll et al., 2001). Furthermore, the effects of UV take a longer time to be reversed than those involving PAR (Häder et al., 1998b; Hanelt, 1998; Bischof et al., 1999; Häder et al., 2001b). These effects can be observed at H_1 (Fig. 16Ai) where the high PAR alone causes rapid reduction in F_v/F_m while at L_1, no or smaller effect by the low PAR alone is observed (Fig. 4Ai). Further reduction in F_v/F_m is also observed when UV is included into the treatments either at H_1 or L_1 suggesting a role of UVR in photoinhibition of the algae (as also been shown in Figs. 5 and 17). The low light intensity as in L_1, which itself causes no or smaller effect, confers protection against UVB damage by enhancing protein repair capacity (Sicora et al., 2003), hence, less F_v/F_m reduction than H_1. With high light intensity as in H_1, the protective effect becomes insignificant (Sicora et al., 2003) as shown by higher F_v/F_m reduction under PAR+UVA+UVB than under PAR alone or UVA+UVB in some algae (Fig. 16Ai). This may be due to partial inhibition of the protein repair capacity by reactive oxygen species (ROS) induced by high light illumination (Nishiyama et al., 2001; Nishiyama et al., 2006). In addition, PAR can synergistically accelerate the damage to photosystem II (PSII) caused by UV as well (Babu et al., 1999).

Recovery of F_v/F_m in PAR-affected algae at H_1 is faster than in PAR+UVR and UVR alone while recovery is more rapid in algae with PAR than without PAR (Figs. 4A and 16A). This can be explain by the necessity of light for repair or recovery mechanisms (Shelly et al., 2003; Roleda et al., 2004b; Aguilera et al., 2008) since PAR is required to drive ATP synthesis which is needed for repair or recovery (Shelly et al., 2003). According to Franklin and Forster (1997), photoinhibition induced by PAR is more

related to the down-regulation process of PSII while UVB-induced photoinhibition seems to be caused by direct damage of proteins or DNA. In addition, recovery in UVR treated algae requires additional protein synthesis and this process is slower (Franklin and Forster, 1997). UVB and UVA inactivate PSII much more efficiently than PAR (Friso et al., 1995; Ivanov et al., 2000; Vass et al., 2002) while UV-induced inactivation of PSII can be efficiently reversed under PAR (Aro et al., 1993; Adir et al., 2003). UV also induces the repair of PSII but its efficiency is not as great as that of PAR. Thus, UV may allow rapid inactivation of PSII in the absence of equally rapid repair (Zsiros et al., 2006). Hence, a higher reduction of F_v/F_m under PAR+UVR than PAR alone. However, the activity of UV-photoinhibited PSII is restored *in vivo via* a similar repair process that restores the activity of PSII after PAR photoinhibition (Greenberg et al., 1989; Melis et al., 1992).

The results from my study are in line with several findings observed in other algae as well. For instance, Figueroa and co-workers (2003), on the study of the effect of artificial UVR and PAR on two species of the genus *Ulva* observed that the algae exhibit lower photoinhibition under low PAR plus UVR than observed under high PAR. In a study by Fredersdorf and Bischof (2007) on the effect of varying PAR intensities in combination with constant UV irradiances on the green alga *U. lactuca*, they found that the strongest inhibition of F_v/F_m was observed under high PAR and UV. They also observed that recovery was slowed down under high PAR conditions in combination with UV in comparison to algae exposed under UV exclusion. Adverse effects of UVB on photosynthesis of *Ulva* canopies under field conditions were only observed with high levels of PAR as well (Bischof et al., 2002b). In addition, F_v/F_m of three species of *Laminaria* and three subtidal red algal species were reduced to minimal values after 4 h exposure to full spectrum of natural sunlight (i.e. PAR+UVA+UVB), PAR, PAR+UVA, UVA+UVB and UVA alone, with F_v/F_m of the more tolerant *Laminaria* spp. and *Phyllophora pseudoceranoides* were higher after exposure to UVR alone compared to that of PAR with or without UV (Dring et al., 2001). However, recovery in all the species was more rapid in UVA+UVB and UVA alone than those that include PAR. This behaviour is also displayed by most of the algae irradiated at either H_2 (Fig. 42A) or H_3 (Fig. 43A) suggesting that the algae are tolerant to a lower UV irradiance than that of H_1 (Fig. 16A).

Interestingly, most of the algae exhibit higher tolerance at H_2 than at H_3 since H_2 contains higher UVB but lower UVA than H_3 (Table 21). With the results, Dring and co-workers (2001) concluded that the high irradiances of PAR in the natural sunlight were responsible for the photoinhibition while UVR did not contribute significantly to photoinhibition.

A slow or delay in recovery may indicate photodamage while fast recovery indicates photoprotection (Hanelt et al., 1997). The former is termed chronic photoinhibition and the latter is termed dynamic photoinhibition. Chronic photoinhibition leads to inactivation or damage to D1 protein of PSII in which recovery and repair mechanisms may take many hours or days (Osmond, 1994). Dynamic photoinhibition, on the other hand, is regarded as a mechanism for protecting photosynthesis under conditions of high PAR and UV (Hanelt et al., 1997) and is defined as an internal down-regulation process of PSII in order to increase the dissipation of excess absorbed energy allowing the recovery of photosynthetic activity when the excess energy is removed (Osmond, 1994). For instance, an absence of recovery after 24 h under the shade in the red alga *Gelidium sesquipedale* under high PAR, PAR+UVA and PAR+UVA+UVB was observed by Gómez and Figueroa (1998) suggesting that this alga suffered chronic photoinhibition compared to *Gelidium latifolium* which recovered its photosynthesis between 80% to 100% under the shade conditions. In a study by Aguilera and co-workers (2008), it was observed that *Porphyra* species were photoregulated against the damaging effects of UVR in photosynthesis through dynamic photoinhibition in response to UVA stress, and through chronic photoinhibition after exposure to UVB. Comparatively, all affected algae in my study are photoregulated against UV and high or low PAR by dynamic photoinhibition except for *L. digitata* under UVA+UVB at H_1 which suffers chronic photoinhibition (Fig. 16A). The data obtained from *L. digitata* can also be an example where under conditions of enhanced UVB radiation, algae in shallow sites show marked photoinhibition and rapid recovery of photosynthesis (dynamic photoinhibition), whereas algae from deeper locations can suffer photodamage (chronic photoinhibition) as reviewed by Figueroa and Gómez (2001).

Whilst the photosynthetic efficiency of the algae is inhibited, the photosynthetic apparatus of the algae may not be damaged because the algae can still recover from the UV stress. This can be observed particularly in *U. lactuca* where its F_v/F_m is inhibited by UVA and UVB at H_1 but almost fully recovered after the post-recovery treatment (Fig. 16A). Furthermore, in this alga, additional high light treatment plus UVA+UVB (Fig. 16Ai) does not cause a stronger photoinhibition than under the respective low light condition (Fig. 4Ai) indicating that *U. lactuca* is well adapted to high levels of PAR. Similar findings were reported in the red alga *Palmaria decipiens* as well (Poppe et al., 2002).

The course of recovery differs from L_1 and H_1 and with or without additional UV suggesting the effects of increased UV are different from photoinhibitory effect of high light. However, equal recovery rate between PAR and PAR+UVR as observed in *U. lactuca* at H_1 (Fig. 16Aii) and *Dictyota dichotoma* at H_3 (Fig. 43Ai), on the other hand, may indicate presence of a complex synergistic effects involved in inhibition (Shelly et al., 2003). Similar or slightly higher rates of photoinhibition as observed in samples exposed under PAR+UVA, for example, in *S. chordalis*, *D. dichotoma* and *U. lactuca* at H_1 (Fig. 16Ai), in *S. chordalis*, *D. dichotoma* and *U. lactuca* at H_2 (Fig. 42Ai) as well as in *S. chordalis* and *U. lactuca* at H_3 (Fig. 43Ai), compares to that of PAR+UVA+UVB can be of ecological relevance since the intensity of UVA spectral range in the natural sunlight is at least 10 times more than UVB and, UVA cannot be attenuated by the ozone layer (Holm-Hansen et al., 1993; Dring et al., 1996; Figueroa et al., 2003). A study performed with Antarctic phytoplankton has demonstrated that at least half of the damage caused by solar radiation between 290 and 400 nm is induced by the UVA range (Holm-Hansen et al., 1993). Furthermore, Cullen and co-workers (1992, cited in Turcsányi and Vass, 2000) stated that even under strong ozone depletion, UV damage is dominated by the UVA range (40–50% inhibition) with only a small effect induced by UVB (10% inhibition). Thus, UVA can be damaging to the algae as that of UVB.

Studies done by Turcsányi and Vass (2000) and Vass and co-workers (2002) had shown that the primary attack of UVA on PSII was also the oxygen-evolving complex with similar mechanisms as that induced by UVB but different from that induced by PAR. In addition, strong inhibitory effect of UVA on the PSII

donor side may trigger the so-called donor-side induced damaging mechanism of PAR, and thereby also enhance photodamage by PAR under the conditions of natural sunlight (Turcsányi and Vass, 2000). Thus, there is a possibility that UVA may exert similar effect on PSII as UVB but different from that of PAR. UVA irradiation, which fully inactivates PSII in a minute, does not induce significant damage to DNA and other cellular components (Zsiros et al., 2006). In fact, UVA and blue light had the capability of reversing the damage of DNA and hence can contribute to the fast recovery of the algae from DNA damage. UVA being less energetic than UVB is less likely to be absorbed by the proteins as well (Davies, 2003). Hence, a faster recovery was observed under PAR+UVA-affected algae than that of PAR+UVA+UVB in most of the algae at either L_1 (Fig. 4Aii) or H_1 (Fig. 16Aii).

Another interesting phenomenon can be observed in *D. dichotoma* at H_1. In this alga, PAR+UVA causes more pronounced photoinhibition than PAR+UVA+UVB but PAR+UVA+UVB recovers significantly rapid than PAR+UVA (Fig. 16Ai). A significant delay in F_v/F_m recovery of PAR+UVA compares to PAR+UVA+UVB is also observed in *Palmaria palmata* irradiated at L_1 (Fig. 4Ai) and *U. lactuca* irradiated at H_3 (Fig. 43Ai) while a similar trend is observed in *S. chordalis* and *L. digitata* at H_2 (Fig. 42Ai). These results suggest that UVB seems to cause an ameliorating effect on certain algae under certain conditions. According to Hanelt and Roleda (2009), the UVB ameliorating effect is demonstrated by the lower F_v/F_m recovery kinetics under PAR+UVA in comparison to that of PAR+UVA+UVB. Similar observations in *D. dichotoma* had been reported by Flores-Moya and co-workers (1999) and in *Dictyota* spp. by Hanelt and Roleda (2009) with both studies were done *in situ*. In both studies, a stronger photoinhibition was observed under PAR+UVA and PAR+UVA+UVB than under PAR but recovery was delayed when UVB was filtered out from the full spectrum radiation. Moreover, in *Dictyota* spp., PAR+UVA+UVB or PAR+UVA caused a stronger effect than the sum of the effects of each waveband alone (Hanelt and Roleda, 2009) which also coincide with my results (Fig. 16Ai). In addition to *Dictyota* spp., ameliorating effect of UVB was observed in the green alga *Halimeda discoidea* and in the brown alga *Turbinaria turbinata* by Hanelt and Roleda (2009); and, in several aquatic freshwater plants of New Zealand lakes (Hanelt et al., 2006) as well.

The above phenomenon is quite interesting since UVB compared to UVA is regarded as being more energetic and had been known to cause damaged to many important biological macromolecules. Kinetics studies show that photoprotective processes and recovery of photosynthesis occur concomitantly during the inhibition phase so that an increase or better induction of this process may cause a decrease in the level of photoinhibition (Osmond, 1994; Hanelt, 1998) Therefore, it seems that UVB had induced or even involved in the repair mechanism during the irradiation. Recovery would be better under full solar radiation (i.e. PAR+UVA+UVB) if UVB supports repair or photoprotective processes (Sicora et al., 2003). In the studies done by Flores-Moya and co-workers (1999), Hanelt and co-workers (2006) and Hanelt and Roleda (2009), the ameliorating effect of UVB was observed in the macrophytes that were previously adapted to a high UV environment and the studies were conducted at high PAR and UV ratio. Hanelt and Roleda (2009) stated that macrophytes which inhabit a much lower natural irradiation did not generally display such effect. However, results obtained from my study delineate this since *D. dichotoma* and *U. lactuca* used in the study are originally collected from the coastal waters of Helgoland and *P. palmata* from Sylt, located in the temperate region and further cultivated in a temperature controlled room under low light. Yet, *D. dichotoma* is irradiated in the sun simulator under high PAR:UV ratio. Similarly, *U. lactuca* is irradiated in the sun simulator but at a lower UVB irradiance. *P. palmata*, on the other hand, is irradiated in the laboratory at low PAR and high UV ratio using artificial radiation from fluorescent lamps.

All the pre-irradiated algae examined are characterized as having a high photosynthetic efficiencies (α) and low light saturation parameter (I_k) values (Tables 7 and 14). These photosynthetic characteristics are typical for low light adapted (Weykam et al., 1996; Hanelt et al., 2003) or shade-adapted algae (Necchi Jr., 2004; Gómez et al., 2005). Thus, upon irradiation to high irradiance, these algae will encounter pronounced photoinhibition as shown by reductions in F_v/F_m. The photosynthetic parameters are further discussed in section 4.6.

A report by Bautista and Necchi Jr. (2008) stated that algae usually follow one of two basic photoacclimation strategies: one involves an alteration in the size of photosynthetic units (PSU) and the other of changing the number of PSU. An alteration in the PSU number and a fixed PSU size are revealed by an increase in P_{max} (=ETR_{max}) plus low α and high I_k which is a typical acclimation strategy of plants acclimated to long-term exposure under high irradiance while the acclimation strategy in the short-term experiment consisted of changing the PSU size, with fixed number of PSUs, as revealed by similar P_{max} but high α and low I_k under low irradiance (Ramus, 1981, cited in Bautista and Necchi Jr., 2008). In the former case, more light is needed to saturate photosynthesis as indicated by the high I_k and in the latter, less light is required to saturate photosynthesis (low I_k) indicating a more efficient PSUs. According to Han (2002), the increase in number of PSU enhances the initial slope, α and P_{max} while the increase in size of PSU improves photosynthetic efficiency only at low irradiance. Thus, the post-irradiated algae may have adapted to the light treatments at either L_1 or H_1 by decreasing their PSU number while having a fixed PSU size as indicated by a decrease in $rETR_{max}$, a lower α and a higher I_k than the pre-irradiated algae (Fig. 16B-D). In addition, both *S. chordalis* and *D. dichotoma* may have adapted to the low PAR alone by increasing the PSU number with much higher $rETR_{max}$ and α, as well as a slight increase in I_k than the pre-irradiation algae (Fig. 4B-D). *L. digitata*, on the other hand, seems to alter their PSU size in response to PAR alone at L_1 while altering their PSU number in response to PAR+UVR. Comparatively, phytoplankton in stable low light regime, for example, tend to follow the increase in PSU size strategy, while in unstable low light regime, phytoplankton are readily exposed to high irradiance and prefer the increase in number of PSU strategy (Han, 2002).

Relative electron transport rate (rETR) is an approximation of the rate of electrons pumped through the ETC (Beer et al., 2001, cited in Ralph and Gademann, 2005). In addition, changes in $rETR_{max}$ are also attributed to changes in the Calvin cycle enzymes (e.g. ribulose-1,5-bisphosphate carboxylase/oxygenase, RuBisCO) activity and concentration, and in components of the photosynthetic electron transport chain (Raven and Geider, 2003; Cruz and Serôdio, 2008) while the photosynthetic efficiency (α) is known to be regulated by changes in chlorophyll (Chl) content (Sand-Jensen, 1988, cited in Han et al., 2003).

Differences in the initial slope (α) of photosynthesis reflect differences in the light harvesting capabilities and thus differences in the size and/or numbers of PSUs and/or efficiency of electron transport in the PSU (Beach et al., 1995). The α values are a measure for the efficiency of the photosynthetic apparatus to absorb photons in the irradiance-limited range of the photosynthesis-irradiance (P-I) curve (*vide infra*). Thus, changes in α point to the disturbance or even damage of the light harvesting systems (Holzinger et al., 2004). I_k on the other hand, is related to quenching where photochemical quenching dominates below the I_k (i.e. at irradiance < I_k) and non-photochemical quenching dominates above I_k (i.e. at irradiance > I_k) (Ralph and Gademann, 2005). Furthermore, I_k values were not correlated to morpho-functional attributes, and, thus, algae set their optimal photosynthetic performance in response to the light environment (Franklin et al., 1996, cited in Gómez et al., 2004).

Therefore, it might be that the decrease in $rETR_{max}$ of the post-irradiated algae (Figs. 4B and 16B) is due to the lower activity or concentration of the Calvin cycle enzymes (Figs. 10 and 22) or a smaller number of active reaction centres (i.e. PSU number) compared to the pre-irradiation algae. A low photosynthetic efficiency α (Figs. 4C and 16C) indicates light is less efficiently absorbed due to decrease or damage to Chls or other photosynthetic pigments, or poor energy transfer in the light harvesting complex (LHC) (Figs. 6-8 and 18-20), thus, a smaller number of PSUs will be served which subsequently affect the light saturation parameter, I_k. A high value of I_k (Figs. 4D and 16D) shifts the light saturation for photosynthesis to a higher irradiance so that higher energy is needed to saturate photosynthesis, excess energy absorbed can be used for photochemistry, minimising the occurrence of photodamage. High I_k also indicates inefficient PSUs. An increase in $rETR_{max}$ and I_k and a decrease in α of *L. digitata* at low PAR irradiance under the UVR treatments (Fig. 4B-D) compares to that of pre-irradiated indicate that the alga can still maintain high photosynthetic activity even under UV. Similar behaviour is also observed in *L. digitata* irradiated at L_3 (Fig. 4I) but not at L_2 (Fig. 4O).

In *Porphyra umbilicalis*, a decrease in the percentage of change of the linear slope and ETR_{max} estimated from ETR vs. irradiance curves was induced by UV during the light phase (Aguilera et al., 2008). A

particularly strong UV effect on α values of P-I curves was reported in *P. palmata* and *Odontalia dentata* which in turn increase I_k while ETR_{max} was more or less unaffected in these two red algal species (Holzinger et al., 2004). Exposure to 24 h of PAR+UVA+UVB, for instance, led to a rapid decrease in α and ETR_{max} while increasing I_k to almost 5 times in *P. palmata* compared to the PAR control plants (Holzinger et al., 2004). In a study on an Antarctic marine benthic diatom community, the highest ETR_{max} was observed under 8 hr of PAR alone which decreased with PAR+UVA and PAR+UVA+UVB treatments. In addition, no photoinhibition was observed at the highest actinic light treatment even though photosynthesis was already saturated at lower irradiance. Photosynthetic capacity (ETR_{max} and α) increased under higher PAR treatment compared to the control, which was maintained under low PAR conditions (Wulff et al., 2008).

4.2 Impact of PAR and UVR on photosynthetic pigments

Photosynthetic pigments such as Chls and carotenoids primarily absorb in the visible (VIS) region but their composition can be significantly altered by exposure to UVR *in vivo* and *in vitro* (Strid and Porra, 1992). In my study, loss of Chls, phycobiliproteins and the carotenoid fucoxanthin in the post-irradiated algae is observed. The pigments lost are greater under radiation with additional UVR than under radiation without UVR which indicates that one of the direct attacks of UVR is on the pigments. A reduction in the quantum efficiency of photosynthesis and loss of energy transfer from light-harvesting pigments (fucoxanthin, Chl a, and Chl c) to PSII indicate that the major light-harvesting complex of *Macrocystis pyrifera*, the fucoxanthin-Chl protein complex (FCPC), was another site of UV damage (Clendennen et al., 1996). Thus, during prolonged exposure to high PAR or UVR, two important processes occur in leaves or chloroplasts – photoinhibition which is explained above and photobleaching or photo-oxidation of photosynthetic pigments. However, according to Jones and Kok (1966, cited in Vincent and Neale, 2000), pigment bleaching occurs at a much slower rate than reduction of photosynthetic capacity. Furthermore, in PSII photodamage reactions, inactivation of PSII reaction centres by light absorbed by

Chls only occurs when the light-induced activation of oxygen-evolving complex (OEC) is completed (Ohnishi et al., 2005). Hence, it is observed that the loss of the pigments in my study does not exceed that of 20% while F_v/F_m is reduced by more than 70% especially at H_1 (Fig. 16Ai).

Photobleaching is a process whereby a bulk of photosynthetic pigments is lost. Photobleaching of pigments by PAR and UV had been reported for Chls (Merzlyak et al., 1996; Cordi et al., 1997; Olszówka et al., 2003; Santabarbara, 2006; Zvezdanović et al., 2009), phycobiliproteins (Lao and Glazer, 1996; Cordi et al., 1997; Rinalduccci et al., 2006) and carotenoids (Cordi et al., 1997; Olszówka et al., 2003; Santabarbara, 2006). The accessory pigments such as phycobiliproteins and carotenoids are impaired first than the Chls upon exposure to photoinhibitory conditions (Cordi et al., 1997; Poppe et al., 2002; Häder et al., 2003a; Santabarbara, 2006). Similar results are observed in my study as well whereby the content of the phycobiliprotein R-phycoerythrin (PE) in *P. palmata* is significantly lower than Chl a after post-irradiation treatment at H_1 (Fig. 18Bi-ii, ANOVA, SNK *post-hoc* test, p=0.009). Additionally, the content of carotenoid fucoxanthin in *L. digitata* is significantly low compares to Chl a at H_1 as well (Fig. 19Ai,iii, p=0.009). Among the Chls, Chl a is damaged faster than Chl b (Strid et al., 1990; Olszówka et al., 2003) as can be observed with *U. lactuca* irradiated under PAR+UVA and PAR+UVA+UVB at L_1 which had their Chl a content significantly reduced to a lower value than their Chl b content after the post-irradiation treatment (Fig. 8, p<0.001). Furthermore, Chl c_1 is more sensitive than Chl a (Roleda et al., 2004a). In *D. dichotoma,* for instance, the content of Chl c is significantly lower than Chl a after the post-irradiation treatment at H_1 (Fig. 19Bi-ii, p<0.001).

High PAR and enhanced UV irradiances have significantly reduced Chl content in higher plants and algae (Strid et al., 1990; Post and Larkum, 1993; Cordi et al., 1999; Bischof et al., 2002b; Choi and Roh, 2003; Hellbling et al., 2004; Roleda et al., 2004a). For example, a reduction in Chl content and photosynthetic rates was noticeable in the Antarctic green alga, *Prasiola crispa* after 4 weeks in the presence of enhanced UVB (Post and Larkum, 1993). An irreversible damage to Chl a and accessory pigments as indicated by a 60% decrease in thallus absorptance and lack of F_v/F_m recovery was observed in *P.*

palmata treated outdoor with elevated UVB (Cordi et al., 1999). A continuous decrease of Chl a content was also observed in the red algae *Callithamnion gaudichaudii* compared to the other Patagonian red algal species after exposure to full solar radiation for 46 h (Hellbling et al., 2004). Furthermore, exposure to unfiltered solar radiation caused a drastic loss of Chl a and b content in *Ulva* canopies of southern coast of Spain compared to the other treatments (Bischof et al., 2002b). Finally, sporophytes of *Laminaria ochroleuca* had lower Chl c_1 content after exposure to PAR+UVA+UVB compared to PAR alone (Roleda et al., 2004a).

Pigment damage can result from one or more of these mechanisms: direct absorbance of energy and subsequent photochemical degradation; by photosensitizer action; and by oxygen radical production in addition to singlet oxygen (Vincent and Neale, 2000). In the Chl case, it can be due to all of these mechanisms. Chl is very efficient in absorbing light and has the additional advantage that the excited states are long-lived enough to allow conversion of the excitation energy into an electrochemical potential *via* charge separation. If the energy is not efficiently used or energy is absorbed in excess, as in the case of high PAR irradiance, the spins of the electrons in the excited state can rephase and give rise to a lower energy excited state: the Chl triplet (^{3}Chl) state. The ^{3}Chl state reacts with oxygen to produce the very reactive singlet oxygen ($^1O_2$) if no efficient quenchers are close by (Krieger-Liszkay et al., 2008). During the process, Chl may become damaged or can elicit damage to neighbouring molecules from the production of highly toxic ROS (Lesser, 2006). Even though Chls are not an efficient UV-absorbers, they are still able to absorb UVR (Johnson and Day, 2002; Zevzdanović et al, 2009). The absorption of UVR by Chls, through several complex mechanisms can also lead to production of ROS (Vass et al., 2007). The increase in the antioxidative enzymes as observed in my study is an evident for the build up of oxidative stress in the algae which may originate from these actions of Chls (*vide infra*).

In addition to the direct absorption of excess PAR and in some extent UVR, several other mechanisms may explain the reduction of Chls observed in the algae examined. For instance, the synthesis of Chls can be degraded or repressed by UVB (Choi and Roh, 2003). Furthermore, UVB radiation can influence the

genetic regulation of the Chl-binding protein leading to Chl destruction (Strid and Porra, 1992). Cordi and colleagues (1997) and Santabarbara (2006), on the other hand, relate the reduction of Chls content along with other photosynthetic pigments with the loss and destabilization of the thylakoid membrane structure. The irradiation of Chl solutions with PAR and UV results in the irreversible breakdown of Chl, accompanied by the appearance of a number of intermediate and final products (Hynninen, 1991). Fluorescent products, for instance, most probably arise from the cyclic tetrapyrrol–porphyrin structure of Chl (Karukstis, 1991, cited in Zvezdanović et al., 2009) which will open up during photobleaching. Absorption spectra of Chl solutions from the algae extracts from my study using dimethylformamide have also been measured but with no apparent changes in terms of the formation of photoproducts have been observed, except with the apparent decrease in the 'blue' (B) and 'red'(Q) bands of the spectrum (data not shown). The Q-band is a sensitive indicator for Chl changes since it is exhibited by only the Chl and not the carotenoids (Zvezdanović et al., 2009).

Phycobiliproteins, as its name implies, are protein-based pigments and since UVR has been known to attack proteins, phycobiliproteins are therefore sensitive to UVR. In fact, phycobiliproteins will be destroyed 20-times faster than the DNA bases. Nevertheless, this is to be expected since the phycobiliproteins act as a shield to DNA (Lao and Glazer, 1996). UVR directly attack the aromatic amino acids in the protein moiety and damage the bilins leading to photochemical degradation (Lao and Glazer, 1996). Besides, the damaged bilins can induce the reaction between the chromophore with atmospheric oxygen and lead to production of free radicals (Rinalducci et al., 2006). This suggests that bilins act as photosensitizers in the phycobilisomes. In a separate experiment, exposure of isolated intact phycobilisomes of cyanobacteria to illumination with strong white light (3500 μmol m^{-2} s^{-1} PAR) gave rise to the formation of free radicals, presumably, $^1O_2$ and O_2^- formed from direct reaction between a triplet state of phycobiliproteins with molecular oxygen (Rinalducci et al., 2008). Therefore, the decrease in PE and R-phycocyanin (PC) observed in both the red algae of my study can also be due to the role of phycobiliproteins as photosensitizers (similar to that of Chls) as evident from the increase in antioxidative enzymes (*vide infra*).

Negative effects of UV on phycobiliproteins had also been reported by other researchers. For instance, a decline in the amount of PE and PC was observed in three marine red algae, *Callithamnion byssoides*, *Ceramium rubrum* and *Corallina officinalis* with the degree of bleaching of phycobiliproteins was more pronounced and less recovery in the samples that received unfiltered solar radiation than PAR alone (Häder et al., 2003a). Significant decreases in the concentrations of PE and PC were also demonstrated in *P. palmata* after exposure to elevated UVB (Cordi et al., 1999). In *P. decipiens*, PE and PC were initially decreased in samples exposed to additional UVB (i.e. after 4 h) in comparison to PAR and PAR+UVA but increased after prolonged exposure to UVB (i.e. after 8 h exposure) (Poppe et al., 2002). They suggested that protective mechanism in response to UV-induced damage of membrane structures and function, especially the photosynthetic apparatus, was activated in this red alga. Uncoupling of antenna pigments, hence, a decrease in energy transfer between phycobilisomes, might be a photoadaptive mechanism to protect PSII from photodamage after high exposure to high levels of PAR and UVR (Lorenz et al., 1997; Aguirre-von-Wobeser et al., 2000). Furthermore, phycobilisomes have been recently reported to having protective mechanisms involving the non-photochemical quenching as well (Kirilovsky, 2007). This may explain why there is an increase in PE and PC contents of post-irradiated *S. chordalis* under PAR alone at H_1 (Fig. 18Aii-iii).

Most studies done on pigments analysis involving fucoxanthin showed a decline in concentration after initial exposure to UV. In two different diatoms, for instance, concentrations of fucoxanthin appeared to decrease after 4 h exposure under PAR+UVR (Wulff et al., 2008) and after 16 days of low and high UVB conditions (Zudaire and Roy, 2001). However, in the latter study, the concentration of fucoxanthin slightly increased between the 16 and 22 days, followed by a decrease back to initial or slightly lower values. A significant reduction in fucoxanthin content was observed in sporophytes of *L. ochroleuca* exposed to PAR+UVA+UVB compared to that of PAR alone (Roleda et al., 2004a). UVB-induced shifts of fucoxanthin content in favour of hexanoyloxyfucoxanthin and cis-fucoxanthin were observed in the phytoplankton *Emiliania huxleyi* (Buma et al., 2000). Fucoxanthin as carotenoids in general, is involved in many aspects of photosynthesis, notably light absorption and energy transfer to the reaction centre and

protection of the photosynthetic apparatus from damage (Mimuro and Katoh, 1991). In my study, a decline in the content of fucoxanthin is also observed in both the post-irradiated brown algae under UVR at L_1 (Fig. 7A-Biii). At H_1, fucoxanthin is further decreased in *L. digitata* (Fig. 17Aiii) but the overall content of fucoxanthin is increased in *D. dichotoma* (Fig. 17Biii). However, a decrease in fucoxanthin is observed with additional UVB in *D. dichotoma* at H_1 suggesting that UVB suppressed the synthesis of fucoxanthin and may impair the pigment instead. UVB-induced H_2O_2 may affect the gene expression of *Lhcb*, which encodes the light-harvesting complex proteins (Mackerness et al., 2001). An increase in fucoxanthin of *D. dichotoma* at H_1 may be due to the induction in the synthesis of the pigment in response to the high PAR and UVA. In addition to its role in energy transfer, fucoxanthin exhibits many other biological activities, such as an antioxidant (Yan et al., 1999; Sachindra et al., 2007; Heo et al., 2008) and as a protective role in H_2O_2-induced cell damage (Heo et al., 2008). A protective role of fucoxanthin against UVB had been reported by Heo and Jeon (2009), such as in the case of *D. dichotoma* at H_1, however, not against UVB but against high PAR and UVA.

Furthermore, in brown algae and diatoms, decreases in the ratio of fucoxanthin to Chl a are observed with decreasing irradiances indicating two separate functions of fucoxanthin, a light-harvesting functions at low irradiances and a protective functions at high irradiances (Dring, 1992). This is shown by *D. dichotoma* irradiated under PAR alone at H_1 where its fucoxanthin content is higher than Chl a (i.e. high fucoxanthin to Chl a ratio, Fig. 19Bi,iii) compares to a low fucoxanthin to Chl a ratio at L_1 (Fig. 7i,iii). Hence, at H_1, fucoxanthin may exhibit a protective role while at L_1, it acts as a light-harvesting pigment. In high irradiances, some fucoxanthins are uncoupled from the photosynthetic apparatus, thus less energy is absorbed by the fucoxanthin and transferred to Chl a to be used in photosynthesis (Dring, 1992). This will protect the photosynthetic apparatus from excessive irradiances.

4.3 Impact of PAR and UVR on D1 protein and photosynthetic enzymes

Excessive light energy causes impairment of the electron transport through PSII (Vass et al., 1992). Impairment of the ETC can lead to overproduction of ROS which includes $^1O_2$ and H_2O_2. Chls and other pigments including phycobiliproteins, as explained above, can act as photosensitizers. As a result, the steady state level of cellular ROS is disrupted, which in turn will result in a condition known as oxidative stress. Moreover, high PAR and enhanced UVB have been shown to generate oxidative stress in macroalgae (for e.g. Aguilera et al., 2002b; Shiu and Lee, 2005; Lee and Shiu, 2009). Proteins can be photo-oxidized by ROS (Davies and Truscott, 2001; Davies, 2003). In addition, some chromophoric amino acids can absorb in the UV range. Hence, decreases in the overall content of the total soluble proteins (TSP) are noticeable in all the macroalgae examined particularly under UVR at both L_1 (Fig. 9A) and H_1 (Fig. 21A). Decreases in TSP are observed with PAR alone at H_1 as well but at L_1, no or smaller reduction in TSP is observed. Concurrent to the changes in TSP at L_1 by PAR alone, there is no or small increase in antioxidative enzymes (Fig. 11). Strong losses of soluble proteins were also observed in *Ulva* subcanopies exposed to unfiltered natural solar radiation and filtered PAR+UVA+UVB with less apparent losses observed under PAR+UVA and PAR alone (Bischof et al., 2002b). *Ulva* receiving only UVA+UVB, however, did not show adverse effects on the proteins. Exposure to UV also resulted in the loss of TSP in two deep-water algae, *Laminaria solidungala* and *Phycodrys rubens* but not in shallow-water algae, *Monostroma arcticum, P. palmata* and *Alaria esculenta* (Bischof et al., 2000a). Comparatively, it appears that *U. lactuca*, which inhabits the intertidal zone showed higher loss of TSPs than *L. digitata*, an upper-middle sublittoral alga at both L_1 (Fig. 9A) and H_1 (Fig. 21A) which is in contrast to that observed by Bischof and colleagues (2000a). The loss of TSP in these algae is also in contrast to the fact that *L. digitata* is more photoinhibited than *U. lactuca*. The reason may lie on the different extraction method used since brown algae contain high amount of polysaccharides on its cell wall which can hinder TSP extraction. In addition, the protein content in thalli of a red alga, *Polysiphonia arctica* was reduced to below 2 mg per g dry weight from 18 mg g dry weight in concurrent to increasing

concentrations of H_2O_2 indicating that proteins in this alga are severely affected by presence of H_2O_2 (Dummermuth et al, 2003).

PSII, the critical component of the photosynthetic machinery is inactivated by strong light (Kok, 1956, cited in Ohnishi et al., 2005). In earlier accepted hypotheses (i.e. donor and acceptor side inhibition), excess light energy produces ROS and/or over-reduction of Q_A resulting in photodamage to PSII (Vass et al., 1992; Melis, 1999). D1 protein of the PSII complex has both donor and acceptor side roles in electron transport through PSII. Hence, the proximity of D1 to powerful oxidants with potential to form highly reactive radicals may explain the vulnerability of D1 to damage by excess light (Long et al., 1994). All the algae examined in my study, for instance, show a reduction in D1 protein after irradiation with high PAR alone (Fig. 25B). High activities of antioxidative enzymes are also observed in these algae indicating the presence of high ROS (Fig. 23). It is believed that ROS accelerates the photodamage of PSII by inhibiting the repair of the damage to PSII but not by accelerating the damage directly (Nishiyama, 2001; Nishiyama et al., 2006). ROS induced by absorption of excessive light energy, for example, inhibit the *de novo* synthesis of D1 protein and most of the other proteins in the cyanobacterium *Synechocystis* sp. (Nishiyama, 2001; Allakhverdiev and Murata, 2004).

Studies also show that UV-induced impairment of photosynthesis resembles that of PAR-induced photoinhibition, being associated with enhanced degradation of the D1, and to a lesser extent, the D2 proteins (Vass et al. 1992; Friso et al., 1994a,b; Friso et al., 1995; Chaturvedi and Shyam, 2000; Turcsányi and Vass, 2000; Xiong, 2001; Tyystjärvi, 2008). Hence, a decrease in D1 content (Figs. 13 and 23) is also observed in algae irradiated with PAR+UVA and PAR+UVA+UVB but with larger effect than PAR alone. The larger effect in PAR+UVR than PAR treatments can be explained by the distinct mechanism employed by the mixed irradiances in the amplified degradation of D1 and D2 proteins from that involve in degradation by PAR or UV alone (Babu et al., 1999). This amplified degradation is found to be tightly coupled with the redox status of PSII which is not observed in degradation driven by either PAR or UVB alone (Melis, 1999; Babu et al., 1999).

Breakdown of D1 protein or photodamage occurs when the rate of its damage exceeds that of the rate of its repair (Aro et al., 1993; Hanelt, 1996). The repair of PSII under environmental stress is the critical step that determines the outcome of the photodamage–repair cycle (Allakhverdiev and Murata, 2004). Thus, the D1 turnover is a fast process, taking place in a wide range of light conditions and it is reasoned that the rapid turnover of the D1 protein represents one of the strategies for protection of PSII from extensive photodamage, especially when the light is stressful for plants (Anderson et al., 1997; Vass et al., 2007). According to Asada (1999), the breakdown of the D1 protein acts as ‘‘emergency sacrifice’’ at high irradiances as a means of reducing incoming light energy when other photoprotective strategies fail to protect photosystem I (PSI) from irreversible damage. Non-functional, D1-containing PSII centres appear to accumulate rather than being rapidly degraded and repaired under photon irradiance higher than growth, acting as centres for energy dissipation (Krause and Weis, 1991). Thus, as D1 protein synthesis is inhibited (i.e. resulting in accumulation of non-functional D1 as evident from loss of D1, Figs. 13 and 25), F_v/F_m decreases (Figs. 4A and 16A) and non-photochemical quenching qN and NPQ increases (Figs. 29-33G-I, *vide infra*) similarly reported by Ji and Jiao (2000). Ji and Jiao (2000) also concluded that the turnover capacity of D1 protein is an important physiological basis for tolerance of photoinhibition.

Newly synthesized D1 protein occurs continuously, independent of damage but a dynamic relationship exists between photodamage and repair. The interaction between these two processes determines whether there will be adverse effect on photosynthesis. If the chloroplast cannot keep up with repairing the damaged D1 leading to its accumulation, the productivity of photosynthesis will decline and a condition popularly known as chronic photoinhibition will entail. In particular, chronic photoinhibition results in the imbalance between photodamage and repair of the photodamaged PSII (e.g., degradation and resynthesis of the key protein, D1, of the PSII) (Osmond, 1994). Chronic photoinhibition has been observed under UVA+UVB in *L. digitata* irradiated at H_1 as evident from F_v/F_m which did not show any recovery (Fig. 16A). The content of D1 protein in this alga is reduced to 80% after irradiation and does not improved after 18 h under the dim light (Fig. 25B). Thus, it seems that UV alone had induced a permanent damage to PSII of *L. digitata*.

A small reduction in D1 protein level (Figs. 13Bi and 25Bi) when PSII activity reduces greatly (i.e. F_v/F_m, Figs. 4Ai and 16Ai) after PAR+UVA+UVB irradiation in the algae suggest the role of UVB during the synthesis of D1 protein. In contrast to photodamage by PAR, where mainly the D1 subunit is damaged and repaired, UVB damages both D1 and D2 proteins to almost the same extent and the repair process includes *de novo* synthesis of both subunits (Sass et al., 1997) which is an essential step in repair of UVB-induced damage (Chaturverdi and Shyam, 2000). The *de novo* protein synthesis of UV-induced damage of PSII during repair requires transcription of DNA encoding D1 and D2 reaction centre subunits. Since DNA can be damaged by UVB, accumulation of damaged DNA can hamper the transcription process and retard the protein-synthesis-dependent repair of PSII (Sicora et al., 2006). Furthermore, it appears that UVB induces multiple lesions in the vicinity of the PSII complex and impairs the post translational processes which in turn become rate limiting factors for the repair of PSII (Chaturverdi and Shyam, 2000). Contrastingly, UVB-induced transcription of *PsbA* genes which encode the D1 protein had been demonstrated by the cyanobacterium *Synechocystis* (Máté et al., 1998). This may explain the appearance of a faster recovery observed in PAR+UVA+UVB-affected *D. dichotoma* in comparison to PAR+UVA at H_1 (Fig. 25Bii). However, this mechanism may only be successful as long as UVB does not induce strong damage to DNA which can impair the gene expression. Opposite effect of that observed in *D. dichotoma* is displayed by other species especially in *P. palmata* indicating that the UVB radiation used in the experiments may have caused an impairment of *PsbA* gene expression instead (Fig. 25Bii).

UVA, on the other hand, has been reported to degrade D1 and to a lesser extent of D2 proteins and can cause damage to PSII *via* similar ways as that caused by UVB but the damaging weight is smaller (Turcsányi and Vass, 2000). In addition, repair of UVA-induced photoinactivation follows similar mechanisms as that induced by PAR or UVB (Zsiros et al., 2006). In comparison to UVB, UVA does not cause significant damage to DNA and other cellular components (Zsiros et al., 2006), and hence, faster recovery or repair process is observed with PAR+UVA than with PAR+UVA+UVB (Figs. 13Bii and 25Bii) even though PAR+UVA caused higher reduction in D1 protein than PAR+UVA+UVB in some species.

The restoration of lost D1 (and D2) proteins requires light as well (Sass et al., 1997; Bergo et al., 2003). The absence of light during translation will lead to an increased accumulation of polysome-bound D1 translation intermediates, indicating that light is required for efficient elongation of the D1 protein. In addition, light is also required for efficient incorporation of the D1 protein into the PSII core complex. In darkness, the newly synthesized D1 protein accumulated predominantly as unassembled protein (van Wijk and Eichacker, 1996). Light is also required for the removal of UVB-induced degradation of D1 protein and synthesis of new D1 (Bergo et al., 2003). Absence of PAR during the post UVB exposure in *Dunaliella tertiolecta* results in lack of recovery indicating that PAR is needed for repair by directly or indirectly affecting the ATP synthesis (Shelly et al., 2003). Thus, recovery of D1 protein is faster in post-irradiated algae receiving PAR than that receiving radiation without PAR (Figs. 25Bii). However, since the damage-repair cycle involves other processes, the interruption of D1 and D2 proteins synthesis by UVB may not be the only limiting factor for the rapid process of recovery induced by PAR (Chaturverdi and Shyam, 2000). Tolerance of the photosynthetic apparatus to UVB is therefore, associated with a strong capacity for recovery from the UVB-induced damage and this capacity is related to the D1 turnover-mediated repair cycle (Chaturverdi and Shyam, 2000). Both *L. digitata* and *D. dichotoma*, for instance, show a higher degree of D1 recovery than any other species examined suggesting a high tolerance to L_1 (p=0.012) or H_1 (p<0.001) (Figs. 13Bii and 25Bii).

Whilst post-irradiated algae under PAR+UVR show loss of D1 protein, the lost subunit is simultaneously restored in post-recovery algae (i.e. under dim light). At H_1 (Fig. 25B), the recovery of D1 protein is fast under PAR and PAR+UVR indicating that presence of PAR during the inhibitory phase is required for recovery (*vide supra*). Furthermore, recovery of D1 protein in post-irradiated algae under PAR+UVR at L_1 (Fig. 13B) also indicates that repair can proceed even under low light conditions. However, a delay in recovery by PAR+UVA+UVB compares to other light treatments may also indicates some degree of UVB-induced damage might have occurred during the irradiation. In addition, the loss of D1 protein in post PAR+UVA and PAR+UVA+UVB irradiation at H_1 is significantly higher than L_1 in *P. palmata* (p=0.038), *L. digitata* (p=0.039) and *D. dichotoma* (p=0.011). The damage rate has been found to be

increased with increasing PAR fluxes (Shelly et al., 2003, for e.g. refer to D1 inhibition and recovery between L_1 and H_1) since PAR synergistically accelerates the damage to PSII caused by UVB (Babu et al., 1999). Additionally, UVB decreases the rate of D1 synthesis and PSII repair as well (Barbato et al., 2000; Bouchard et al., 2005).

RuBisCO is the most abundant proteins found in plants comprising up to 50% of the total soluble protein (Ellis, 1979). Thus, the reduction in the TSP (Figs. 9 and 21) of the algae may mainly result from the reduction of the enzyme's protein. Furthermore, the decrease in activity of RuBisCO is partly caused by the degradation of its subunits (Jordan et al., 1992; Allen et al., 1997; Bischof et al., 2000a; Keiller et al., 2003). However, the reduction in the activity of RuBisCO (Figs. 10A and 22A) is greater than that observed for TSP or the composition of RuBisCO large subunits (LSU, Figs. 12B and 24B). High light or UV irradiation can cause disruption of the enzyme's holoenzyme and, consequently, may reduce the maximum rate of carbon assimilation by the enzyme under conditions where it would normally be fully activated (Jordan et al., 1992; Aro et al., 1993). The reduction in the activity of RuBisCO as well as RuBisCO LSU composition after irradiation with UV observed in my study are in line with the findings among others, by Bischof and co-workers (2000a, 2002b) in the macroalgae as well as Takeuchi and co-workers (2002), Choi and Roh (2003) and Keiller and co-workers (2003) in higher plants.

For instance, activity of RuBisCO was decreased by 20%-38% among the post-irradiated algae at L_1 (Fig. 10Ai) while the reduction is higher at H_1 (Fig. 22Ai) after 5 h exposure to the light treatments with *U. lactuca* and *S. chordalis* are strongly affected at L_1 and H_1, respectively. Comparatively, a 55% reduction in RuBisCO activity was observed in five macroalgae including *P. palmata* at the end of 72 h exposure under artificial radiation of fluorescent lamps with *P. rubens* shown to be the most affected with no activity after 24 h (Bischof et al., 2000a). Analysis of SDS gels showed that the decrease in activity was partly due to the degradation of the enzyme. Reduction in RuBisCO LSU is observed in my study as well which may suggest that the decline in activity is partly due to loss of LSU (Figs. 12Bi and 24Bi). A significant loss of RuBisCO LSU was observed within the first two subcanopy layers of *Ulva* exposed to

PAR+UVA+UVB and only a slight decrease under PAR+UVA and PAR alone (Bischof et al., 2002b). Even though there is insignificant changes observed, PAR+UVA+UVB seems to have the strongest effect on the RuBisCO LSU of the algae examined especially at L_1 suggesting the role of UVB in activation of RuBisCO activity (Fig. 12Bi). In addition, Bischof and colleagues (2002b) also concluded that the activity of RuBisCO in the algae was impaired only when UVR was accompanied by PAR. In comparison, algae under UVA+UVB did not exhibit any reduction in RuBisCO content. The authors attributed this to the low ROS generated by the algae. However, this is opposite to that found in my study where a reduction in RuBisCO as well as high ROS production (as shown by increases in the antioxidative enzymes) are observed in all the algae including *U. lactuca* irradiated under UVA+UVB (Fig. 22A).

Contrasting results as above were observed in *U. lactuca* exposed to natural solar radiation (Bischof et al., 2002a). An increase in the overall activity of RuBisCO was observed in algae exposed to PAR alone and PAR+UVA with higher elevation found in the former while algae exposed to full solar radiation remained on par with the initials throughout the experiment. These observed activities were also reflected in the concentration of LSU analysed by SDS-PAGE followed by Western blotting. Nevertheless, these results also showed that RuBisCO activity was low under UVB and that the gene expression of *RbcL* (codes for RuBisCO LSU) was suppressed under UVB. Even though activation of RuBisCO increases with increasing light intensity, it seems that the activity of RuBisCO in *C. reinhardtii* was negatively affected when the cells were transferred from low light to high light (Yosef et al., 2004). Similar results are also observed for RuBisCO activity of all the algae which is strongly affected when the low-light adapted algae (*vide supra*) are exposed to high irradiance of H_1. The reason for this may be due to the dramatic arrest in the synthesis of LSU caused by oxidative stress (Yosef et al., 2004).

Loss of RuBisCO can be the result of either light or UV induced destruction of the protein or reduced synthesis due to down-regulation of gene expression (Wilson et al., 1995; Mackerness et al., 1999; Takeuchi et al., 2002; Choi and Roh, 2003; Cohen et al., 2005). In addition, UVB affects the

carboxylating efficiency of RuBisCO by changing its activity and by degrading RuBisCO (Jordan et al., 1992; Allen et al., 1997; Keiller et al., 2003). In RuBisCO, there are no UVB-absorbing cofactors except for Trp which is the only amino acid that can absorb in the range of UVB radiation (Wilson et al., 1995). Trps are present in the active sites of RuBisCO as well as at the interfaces between LSU and small subunit (SSU) within the holoenzyme (Knight et al., 1990, cited in Wilson et al., 1995). Absorption of the radiation by Trp results in triplet Trp which will react with oxygen and subsequently formed photoproducts including N-formylkynurenine (Nfk). Nfk is a significant photosensitizer and is better in generating $^1O_2$ than Trp itself (Igarashi et al., 2007). Photolysis of Trp results in the disassembly of the RuBisCO holoenzyme, hence, the inactivation of the enzyme.

Cohen and colleagues (2005) examined the inhibitory effect of oxidative stress on RuBisCO assembly and on expression of its subunits and observed that the translation of RuBisCO LSU is almost completely inhibited during oxidative stress leading to a halt in the holoenzyme assembly. The inhibition of the translation might be due to the structural change in the nascent LSU chains caused by oxidation of the thiol groups by oxidative stress generated *in vivo* by light. In addition, newly synthesized SSU that are encoded by the nucleus are also rapidly degraded (Cohen et al., 2005; Knopf and Shapira, 2005). Synthesis of LSU and reassembly of both subunits will resume after oxidative stress ceases (Cohen et al., 2005). Thus, the increase in LSU content in post-recovery algae is observed in parallel with reductions of antioxidative enzymes (Figs. 11 and 23). When both LSU and SSU assemble, RuBisCO holoenzymes can be activated again and carboxylating activity of RuBisCO will resume, hence an increase in activity is observed in post-irradiated algae. Additionally, PAR-affected algae show faster recovery in activity of RuBisCO than the other treatments. Increased PAR protects the mRNA transcripts to some extent which becomes apparent at the level of the RuBisCO proteins (Jordan et al., 1992). The protection may be caused by increased efficiency of photo-repair mechanisms or by the provision of more energy and is likely to be important in moderating the UVB effect under natural daylight conditions (Jordan et al., 1992).

As with RuBisCO, GAPDH is also sensitive to UV, oxidative stress and since GAPDH activation requires light, it is also sensitive to high light intensity. Hence, reduction in the activity of GAPDH was observed in algae exposed to radiation containing high UVR (especially with additional UVB) and high PAR and activity of GAPDH decreases more at H_1 than L_1 (Figs. 10B and 22B). Recovery is mostly faster at H_1 than at L_1 as well. Voss and co-workers (2007), for instance, studied the effect of different spectral irradiances on GAPDH. While UVA led to a decrease in free thiol content which concomitantly resulted in loss of enzyme's activity and only at high doses resulted in aggregation and fragmentation, effects of UVB were more precise. UVB acted on specific amino acids such as arginine, proline and tyrosine as well as can formed aggregation and fragmentation of the enzyme even at low dose.

The content of GAPDH in five species of macroalgae was decreased after prolonged exposure to artificial radiation of 20 µmol m^{-2} s^{-1} PAR, 8 Wm^{-2} UVA and 0.8 Wm^{-2} UVB (Bischof et al., 2000a). While initially within the 36 h, GAPDH activity was not affected in the green alga *M. arcticum*, a small decreased in the enzyme activity (i.e. 83% of control) was observed after 72 h. For the rest of the algae, the activity dropped 10%, 15%, 25% and 40% of initial values within the 1st or 2nd h of exposure in *P. palmata, A. esculenta, L. solidungula* and *P. rubens*, respectively. Activity of a cytosolic GAPDH of *Arabidopsis thaliana* dropped to 81% compared to the control in the presence of 0.1 mM H_2O_2 while increasing the concentration of H_2O_2 to 0.5 mM caused the enzyme to completely lose its activity (Hancock et al., 2005). Furthermore, adding 10 mM of reduced glutathione (GSH) to the 0.1 mM H_2O_2-inhibited GAPDH, restored the enzyme's activity to 76% of control but activity was not recovered in 0.5 mM H_2O_2-inhibited GAPDH when similar concentration of glutathione (GSH) was added. In conclusion, GAPDH becomes inactivated in the presence of H_2O_2 and the inactivation of the enzyme is reversible by the addition of reductants such as GSH. These results can also be correlated with the results obtained from my study whereby the activity of GAPDH is reduced with concomitant increase in the antioxidative enzymes which shows signs of oxidative stress (Figs. 11 and 23). Reduction of 5'-IAF-labelled (5'-IAF is 5'-iodoacetamide fluorescein) GAPDH on 1D PAGE gel after pretreatment of GAPDH with 10 mM H_2O_2 and subsequent treatment with 100 µM 5'-IAF, a fluorescent tagging derivative which can react with

reduced thiol groups, revealed that H_2O_2 affect the thiol groups of the enzyme (Hancock et al., 2005). As been mentioned earlier, thiol groups are prone to oxidation by ROS, and hence decreased the ability of GAPDH to bind 5'-IAF. In addition, the impairment of GAPDH (and other Calvin cycle enzymes) may itself generate ROS due to the over-reduction of the photosynthetic electron transport chain since GAPDH is involved in the regeneration of ribulose bisphosphate and reducing power, $NADP^+$ (Xu et al., 2008).

GAPDH is activated by the thioredoxin f system. In the presence of light, some electrons reduced thioredoxin f which in turn reduces GAPDH to break the thiol bridge and the enzyme becomes active (Sharkey, 2000). It had been reported that thioredoxin f can be glutathionylated. Protein S-glutathionylation *in vitro* can be triggered by protein thiol oxidation by ROS followed by reaction with glutathione (GSH) or by thiol-disulfide exchange with glutathione disulfide (oxidized glutathione, GSSG) (Dalle-Donne et al., 2003). Glutathionylation decreased the activity of thioredoxin f under enhanced ROS production and thus leads to decreased inactivation of target enzymes such as GAPDH which in turn will slow down the Calvin cycle (Michelet et al., 2005). Once ROS have been detoxified, there presumably exists a system to deglutathionylate the thioredoxin f and the other glutathionylated proteins. However, this is yet to be discovered (Michelet et al., 2005). Hence, this may also explain the reduction of GAPDH activity with concomitant increase in antioxidative enzymes observed in my study.

Impairment of the Calvin cycle enzymes such as RuBisCO and GAPDH has been shown to suppress the repair of PSII by inhibiting the light-dependent synthesis of PSII proteins *de novo* (Takahashi and Murata, 2005). A decrease in energy utilization caused by interruption of the Calvin cycle does not induce the oxidative damage of D1 protein but inhibited the synthesis of the D1 protein and other related proteins required for D1 protein reassembly at the post-transcriptional level. Takahashi and Murata (2006) on further experiments found out that supply of 3-phosphoglycerate (3-PGA) generated by the Calvin cycle is important for the synthesis of D1 protein. It appears that 3-PGA accepts electrons from NADPH and decreases the amount of ROS which can inhibit the synthesis of proteins. Thus, interruption of Calvin

cycle is expected to inhibit the synthesis of proteins involved in the repair cycle after photodamage. This is shown in my study by the induction of antioxidative enzymes indicating high ROS formation which in turn inhibit the Calvin cycle as shown by the decline in activity and concentration of RuBisCO (as well as GAPDH). As a consequence, this will inhibit synthesis of D1 protein, and hence, a decline in D1 content and overall photosynthetic activity of the algae. An alternative supply of 3-PGA is from the oxygenation reaction of RuBisCO *via* the photorespiratory pathway. Thus, photorespiration can help to mitigate inhibition of the synthesis of D1 protein. This is also the case for all the algae in my study where it has been observed that catalase (CAT), an antioxidative enzyme that detoxify H_2O_2 in the peroxisome is higher than the other two enzymes analysed indicating that photorespiration is activated in the post-irradiated algae (Figs. 11A and 23A, *vide infra*).

The results obtained from my study also indicate that RuBisCO is more sensitive to high PAR and high UVR (i.e. H_1) exposure than GAPDH ($p<0.001$). Similar results are reported by Bischof and his colleagues (2002b) and they attributed this to the complex holoenzyme structure of RuBisCO and the complex regulation of its activity in comparison to GAPDH (Portis, 1992; Andersson and Backlund, 2008). The reduction of enzymes involved in primary carbon metabolism may also indicates redirection of carbon resources into other pathways, such as those involved in repair or protection processes (Xu et al., 2008), for instance, photorespiratory pathway as explained above or inducing the production of stress proteins (*vide infra*).

4.4 Induction of antioxidative enzymes by PAR and UVR stress

As been mentioned above, production of ROS occurs under stress conditions during exposure to excessive light (Hideg et al., 2000; Nishiyama et al., 2001; Hernández et al., 2006; van de Poll et al., 2009) or UVR (Aguilera et al., 2002b; Bischof et al., 2003; Shiu and Lee, 2005; Lee and Shiu, 2009; van de Poll et al., 2009). If accumulation of ROS exceeds the capacity of enzymatic and non-enzymatic

antioxidant systems the photosynthetic apparatus is further damaged due to destruction of proteins (as in D1 protein, RuBisCO and GAPDH), lipids and nucleic acids (Choo et al., 2004; Häder and Sinha, 2005), which can lead to cell death (Collén and Pedersén, 1996; Franco et al., 2009). Thus, the ecological success of an organism depends on how well and efficient the organism employ mechanisms that can detoxify ROS (Aguilera et al., 2002b).

Data obtained in my study show that presence of UVR greatly induced the antioxidative enzymes such as catalase (CAT), ascorbate peroxidase (APX) and glutathione reductase (GR) in all the algae examined indicating that the algae are experiencing oxidative stress. High irradiation with PAR or UVR alone also causes a significant induction in the enzymes but to a lower extent than those with PAR plus UVR. Furthermore, low irradiance of PAR alone affects GR activity in the red alga *S. chordalis* indicating that the low PAR has caused a small degree of ROS accumulation in this alga (Fig. 11). A significant reduction in GR and SOD activities are observed in the green alga *Acrosiphonia penicilliformis* when solar UVR was cut off in the field, indicating low oxidative stress in the absence of UVR (Aguilera et al., 2002b) while APX, CAT and peroxidase were increased in correlation with H_2O_2 generated from low UVB-flux (Shiu and Lee, 2005).

Build-up of ROS in cells initiates signalling response to induce gene expression of antioxidative enzymes (Strid et al., 1994; Hernández et al., 2006). For instance, UVB disrupts the balance between the production and removal of H_2O_2 in *Ulva fasciata* and the accumulation of H_2O_2 initiates the signalling responses leading to the induction of enzymatic antioxidant defence systems in the alga (Shiu and Lee, 2005). Additionally, as pointed out by Hideg and co-workers (2000), the production of $^1O_2$ is a unique characteristic of acceptor side photoinhibition by excess PAR alone while Shiu and Lee (2005) reported that O_2^- is the first ROS generated by UVB. Exposure to UVB in combination with PAR may also induce formation of $^1O_2$ but according to Hideg and co-workers (2000), this is only observed in severely damaged leaves after long irradiation and is accompanied by membrane lipid peroxidation. Thus, excess PAR and UV alone or PAR plus UV may initiate different signalling responses to detoxify the ROS. In

addition to $^1O_2$ and O_2^-, H_2O_2 and hydroxyl radicals can also be produced within the cells. Different from H_2O_2 metabolism, $^1O_2$ is efficiently quenched by β-carotene, tocopherol or plastoquinone. If not quenched, it can trigger the up-regulation of genes, which are involved in the molecular defence response of photosynthetic organisms against photo-oxidative stress (Krieger-Liszkay et al., 2008) such as genes that expressed the antioxidative enzymes.

Higher induction of the antioxidative enzymes is observed at H_1 than at L_1 with the red algae exhibiting the highest overall inductions of the enzymes (p<0.001) suggesting that these algae are experiencing higher oxidative stress than the other algal classes. Activities of several antioxidative enzymes including APX, GR and CAT are observed to be much lower in *Triticum aestivum* L. seedlings grown under low-light conditions than in those grown under high-light conditions. Activities of all these enzymes significantly increased within 24 h of transfer of the low-light-grown seedlings to the high-light regime. The results suggest that the increase in enzyme activities was an adaptive response of the plants to higher amounts of active oxygen species generated at higher light intensities (Mishra et al., 1995). Thus, the increases in activity of CAT, APX and GR observed in the algae are the results of an adaptive response of the algae to high or low PAR and high UV.

Individually, the red alga *S. chordalis* which inhabits the eulittoral region, exhibits higher activity in the antioxidative enzymes than the middle sublittoral brown alga *L. digitata* after exposure to H_1 (p=0.037). Similarly, the antioxidative enzymes are higher in the upper sublittoral red alga *P. palmata* than *L. digitata* as well (p=0.011). These results are in accordance to that obtained by Aguilera and co-workers (2002b) with several Arctic marine macroalgae collected on field and concluded that eulittoral and upper sublittoral Arctic marine macroalgae showed higher antioxidant enzyme activities than species from lower sublittoral. However, two red algae from subtropical region, namely *Gelidium amansii* and *Ptercladiella capillacea* showed a reverse reaction on exposure to UVB. *G. amansii* which inhabits lower subtidal region exhibits higher antioxidative enzymes, thus, experiencing greater oxidative stress than *P. capillacea* which inhabits upper subtidal region (Lee and Shiu, 2009). In comparison, *P. palmata* in my

study has a higher concentrations of antioxidative enzymes than *S. chordalis* after the post-irradiation treatment with additional UVB at H_1 but with no significant differences (p=0.581). Furthermore, lower antioxidant enzyme activities are measured in the green alga *U. lactuca* compares to the others after exposure to H_1 (p<0.001) indicating that the alga can tolerate with the changing environment conditions. This can be attributed to the high antioxidative enzymes in the pre-irradiated algae (Table 16). Aguilera and co-workers (2002b) also observed that Arctic marine green algae generally show higher antioxidant enzyme activities than the brown or red algae.

The increase in the activity of GR is to regenerate GSH needed for the reduction of dehydroascorbate (DHA) to ascorbic acid (AsA). AsA is then used as a substrate in APX activity. APX has been considered as the main H_2O_2 scavenging enzymes in the cytosol and chloroplast (Asada, 1992). According to Shiu and Lee (2005), the first ROS generated by UVB is the superoxide anions (O_2^-). O_2^- can be converted to H_2O_2 by a dismutation process by the enzyme superoxide dismutase (SOD). CAT, on the other hand, is also one of the enzymes that can detoxify H_2O_2 but is important in peroxisomes for scavenging H_2O_2 created by photorespiration (Asada, 1992). Thus, in the case of my study, an increase in all the three antioxidative enzymes can be correlated to an increase in the H_2O_2 and since CAT activity is the highest induced by all the algal classes particularly under the high PAR and high UVR conditions (H_1, p=0.008 for red algae, p<0.001 for brown and green algae), perhaps that the oxidative stress during the experiments was mainly caused by photorespiration.

Photorespiration is one of the alternative electron sinks to reduce the over-reduction of electron carriers which can excite PSII to photoinhibition (Melis, 1999; Niyogi, 2000). It is believed that consumption of photochemical energy, such as ATP and NADPH, through the photorespiratory pathway helps avoid the photo-oxidative damage to PSII *via* the acceptor-side photoinhibition by $^1O_2$ (Osmond and Grace, 1995; Osmond et al., 1997). For instance, the photorespiratory pathway helps avoid inhibition of the synthesis of D1 protein, which is important for the repair of photodamaged PSII upon interruption of the Calvin cycle (Takahashi et al., 2007, *vide supra*). Thus, it appears that all the algal classes examined in my study

employ the photorespiratory pathway in order to mitigate photodamage to PSII from the inhibitory conditions of H_1 and L_1. Another mechanism that can act as electron sinks is the water-water cycle (Asada, 1999; Niyogi, 2000). In the water-water cycle, electrons generated by oxidation of water at PSII are used to reduce O_2 to water at PSI *via* O_2^- and H_2O_2, thus helping to scavenge ROS in the chloroplast (Asada, 1999; Asada, 2006). In addition to this function, the water-water cycle can also dissipates excess excitation energy by the generation of proton gradient across the thylakoid membrane (Asada, 1999; Asada, 2006). GR and APX are the two main enzymes involved in this pathway. Therefore, the algae examined may also employ this mechanism to detoxify H_2O_2 that is accumulated in the chloroplast. As Collén and Davidson (1999) as well as Dummermuth and co-workers (2003) pointed out, the key element in reactive oxygen metabolism might be the balance between production and protection in individual compartments, such as peroxisomes and chloroplasts rather than protection integrated over the entire cell.

Similar results were also demonstrated by a 2-fold increased in CAT activity compared to that of APX in *Cladophora glomerata* incubated under 600 µmol m^{-2} s^{-1} PAR in the laboratory (Choo et al., 2004). Nevertheless, in the field samples, APX activity was observed to be higher than CAT activity in *C. glomerata* (Choo et al., 2004) and in the brown alga *Fucus* spp. (Collén and Davison, 1999) and the green alga *Ulva rigida* (Collén and Pedersén, 1996) as well, suggesting APX as the main scavenging enzyme for H_2O_2.

When UVR or high PAR is not a burden anymore, H_2O_2 ceased to accumulate and excess H_2O_2 has been quenched, thereby slowing down the activity of the protective antioxidative system. Thus, a recovery in the antioxidative enzymes is observed under the dim light (Figs. 11 and 23). Concomitant to the reductions in the antioxidative enzymes activity, there are recovery of F_v/F_m, D1 protein, RuBisCO and GAPDH activity and TSPs. For instance, higher ability of *U. lactuca* to completely recover from the light stress may be due to the higher ability of this alga to induce antioxidative enzymes to detoxify the ROS which can induce more damage to PSII if left unchecked.

4.5 Induction of stress proteins by PAR and UVR stress

Upon irradiation to high PAR and high UVR conditions (i.e. at H_1), the algae show signs of photoinhibition (Fig. 16). The algae, among others, have lost their functional D1 protein (Fig. 25), lost their RuBisCO LSU (Fig. 24) which is accompanied by reduction in the enzyme's activity (Fig. 22A), reduction in GAPDH activity (Fig. 22B), lost some of their TSPs (Fig. 21) and show signs of pigment damage, for e.g. Chl and phycobiliproteins (Figs. 18-20). Concomitantly, the level of heat shock proteins or stress proteins, HSP60 (Fig. 26) and HSP70 (Fig. 27) accumulate during the same irradiation period. These changes are noticeable particularly when UV is included into the treatments. Whilst low PAR alone shows no or small changes, high UV in combination with the low PAR (i.e. at L_1) shows a stronger effect (Figs. 14-15) but the effect is of a smaller scale than H_1.

The patterns in the changes of the stress proteins observed in my study are comparable to other studies as well. For instance, *Hsp70* gene expression appeared to be up-regulated in very high light-resistant mutants compared to the wild-type strains of the green alga, *Chlamydomonas reinhardtii* after treatment to a very high light intensity (Förster et al., 2006). Upon a shift of *Dunaliella salina* cultures from low light to high light, a significant transient accumulation of HSP70B mRNA transcripts was observed as well (Yokthongwattana et al., 2001). There is, however, a scarce information on the responses of HSPs to UVR in macroalgae but has been reported in other aquatic organisms. For instance, in a study by Bischof and co-workers (2002b) involving *Ulva*, a green alga, elevated concentrations of chaperonin 60 (CPN60, a homolog to HSP60) were observed within the canopies of this alga exposed under filtered PAR, PAR+UVA, PAR+UVA+UVB and UVA+UVB but not under unfiltered solar radiation. An induction of HSP levels by UV has been demonstrated in UV-sensitive diatoms (Döhler et al., 1995). Marine copepod, *Acartia tonsa* receiving 4 h of high full solar radiation and PAR+UVA exhibited 4 and 3.5-fold increased in HSP70 levels, respectively, compared to the dark controls (Tartarotti and Tores, 2009). Higher levels of HSP70 were also detected in sea urchin embryos exposed to UVB (Bonaventura et al., 2005; Bonaventura et al., 2006).

There is a tight correspondence between the synthesis of stress proteins with the loss or damage of proteins indicating an efficient communication between the chloroplast and nucleus. For instance, Chl biosynthesis precursors can act as chloroplast-originating signals which trigger a signal transduction pathway leading to synthesis of inducible forms of stress proteins (Kropat et al., 1997). Under irradiance-stress, there is a build-up of excitation pressure at PSII, triggering a slow-down in the rate of Chl synthesis possibly generating an excess of Chl biosynthesis intermediates and precursors in which the latter can spill out from chloroplast and thus serve in the signal transduction pathway (Yokthongwattana et al., 2001). It has also been reported that UVB can repress the synthesis of Chl leading to the above conditions (Choi and Roh, 2003). The reduction in Chl a and Chl b contents observed in the algae may also be due to repression of Chl synthesis by UVB as well. Hence, this may links the increase in the stress proteins observed in my study with the concomitant reduction in the Chl content.

In addition, as stated in the 'abnormal protein hypothesis of stress protein induction' coined by Anathan and colleagues in 1986 (cited in Bierkens et al., 2000), damaged proteins in the cell can trigger the activation of stress genes. Oxidative stress is also one of the factors that can induce the synthesis of HSPs since ROS has long been known to damage biological molecules (Freeman et al., 1999). A high induction of 18 members of the HSPs families is observed in *A. thaliana* cells exposed to H_2O_2 stress (Scarpeci et al., 2008). A short-term acclimation of *Ectocarpus siliculosis*, a brown alga, to oxidative stress conditions resulted in transcriptomic changes displaying up-regulation of four genes coding for HSPs (Dittami et al., 2009). It has also been suggested that the response of stress proteins to UVR and PAR is through the generation of ROS (i.e. oxidative stress conditions) (Sierra-Rivera et al., 1993, cited in Freeman et al., 1999). Hence, the increase in HSP60 and HSP70 observed in my study by UVR and high PAR may be induced by the oxidative stress build-up in the cells of the algae as evident from the induction of the antioxidative enzymes.

Stress proteins are rapidly induced by cells experiencing disturbances in cellular homeostasis caused by proteotoxic stressors (in this case, high PAR and high UVR). Some stress proteins are constitutive (for

e.g. HSP70 and HSP60), they are present at low concentrations under normal conditions and play essential roles in cellular protein homeostasis by acting as molecular chaperones (Sharkey and Schrader, 2006). They act in the assembly and folding of proteins by engaging in transient attachment to target proteins as well as in the transport of nuclear-encoded precursors into chloroplasts (Bierkens, 2000; Jackson-Constan et al., 2001). With stress, however, the levels of constitutive stress proteins rise and inducible forms (for e.g. HSP60) begin to be synthesised (Sharkey and Schrader, 2006). The rise in constitutive and inducible HSPs is apparently associated with the denaturation and/or aggregation of normal cellular proteins, a condition known as proteotoxicity. Under proteotoxic conditions, HSPs take on additional but related functions to molecular chaperoning, by preventing the denaturation of proteins and holding them in the state of folding or assembly to facilitate repair and promoting the degradation of abnormal proteins (Bierkens, 2000). This will help in repairing the denatured proteins and protecting others from damage allowing the cells to recover and survive under the stress. Hence, by the induction of the stress proteins as observed in my study in concurrent with the loss of several photosynthetic proteins (e.g. D1 protein, RuBisCO, GAPDH and others that are mentioned at the beginning), prevents further damage and helps in the repair process. Consequently, the algae will be able to recover and survive under the high PAR and UVR stress. This also indicates the triggers of efficient protective mechanism which is induced by the stressors.

Data obtained from my study shows that the stress proteins HSP60 and HSP70 are greatly induced by addition of UVR into the treatment. High PAR and UVR alone induced the production of the stress proteins as well. Inductions are much higher at H_1 than at L_1 ($p<0.001$). This may be due to higher breakdown of proteins occurring under H_1 than L_1. In general, HSP70 is induced more than HSP60 at both H_1 and L_1 ($p<0.001$). This may be due to a wider range of HSP70 functions compared to HSP60 which will be discussed below. The green alga *U. lactuca* shows the highest HSP60 induction in comparison to that of red and brown algae at H_1 ($p<0.001$) as well as at L_1 ($p<0.001$). HSP70 is equally induced in all the algae at H_1 ($p=0.615$) but at L_1, the highest induction of HSP70 is observed in *U.*

lactuca (p<0.001). The highest induction observed in *U. lactuca* may explain why *U. lactuca* has the fastest recovery in its photosynthetic activity as indicated by almost a full recovery in F_v/F_m (Fig. 16A).

The best understood and extensively studied HSP system is the HSP70 family. HSP70 and its homologs are expressed in response, among others, to heat (Ireland et al., 2004; Henkel and Hoffmann, 2008), high light (Yokthongwattana et al., 2001; Förster et al., 2006), heavy metal (Lewis et al., 2001), temperature (Vayda and Yuan, 1994; Fu et al., 2009) and UVR (Häkkinen et al., 2004) stresses. Expression of HSP70 in a wide array of stresses suggests that organisms may employ the same HSPs in different manners to solve the problems encountered in their habitats. These patterns are observed since production of HSPs incurs significant costs along with significant benefits (Coleman et al., 1995). Role of HSP70 (and its isoforms/homologs) in the function and protecting the photosynthetic machinery from various environmental stresses had been reported by several scientists.

For instance, direct evidence of the involvement of HSP70 in resistance to photoinhibition was presented in *C. reinhardtii* (Schroda et al., 1999, 2001). Overexpression of HSP70B (i.e. an isoform of HSP70) in response to light stress reduces photoinactivation of PSII and enhances recovery, whereas underexpression causes the opposite effect (Schroda et al., 1999, 2001). Moreover, alga with overexpressed HSP70B had low high-light induced damage than the underexpressed alga (Schroda et al., 2001). This can be seen in the green alga *U. lactuca* which shows overexpression of HSP70 (Fig. 27B) and high rate of photosynthetic activity recovery (Fig. 16Aii). Initially, it was proposed that HSP70B acts by preventing the destruction of inactivated reaction centres and promoting the synthesis of new centres (Schroda et al., 1999). Further studies led Schroda and co-workers (2001) to assume that the overexpressed HSP70 prevent the degradation of D1 protein by recognizing the altered confirmation at the Q_B-binding site, reverting the D1 to its functional state since degradation is not to happen. In addition, HSP70 might also bind to PSII and stabilize the damaged complex until the coordinated D1 degradation and synthesis can occur. Since D1 cannot be recycled, insufficient HSP70 might lead to rapid degradation of D1 and destabilization of PSII. When PSII falls apart, all its component is also degraded and

reconstitution requires *de novo* synthesis of D1 and reassembly of PSII units. On the other hand, in *D. salina*, binding of a HSP70B to an exposed hydrophobic region of photodamaged D1 resulted in the formation of the PSII repair intermediate (Yokthongwattana et al., 2001). This may explain the loss and recovery of D1 protein in the algae (Fig. 25B) with concomitant increase in HSP70 level (Fig. 27B). Additionally, by acting as a molecular chaperone and as a constituent component of the repair intermediate HSP70 may also afford conformational protection to the disassembled PSII-core complex be of importance in the regulation of the repair process (Yokthongwattana et al., 2001). This may be critical in green algae since the latter lack a photodamage dependent D1 phosphorylation which occurs in higher plants (Kettunen et al., 1996). Thus, this may explain why the composition of HSP70 is higher in *U. lactuca* than any other algal classes examined.

As mentioned earlier, UVB have negative effects on RuBisCO by disrupting the interactions between both its LSU and SSU leading to disassembly of the holoenzyme. The disassembly and aggregation of the holoenzyme subunits trigger the production of HSP60 (or CPN60) which prevent improper aggregation of LSU by protecting the exposed hydrophobic surfaces (Schneider et al., 1992). In addition, CPN60 also plays a role in the ATP-dependent refolding of denatured RuBisCO (Bertsch et al., 1992) and in reassembly of fully denatured RuBisCO subunits into holoenzyme *in vitro* (Yong et al., 2006). Presence of HSP70 in the reassembly process greatly increased the content of reassembled RuBisCO as well (Yong et al., 2006). These comparable results may explain the role of HSP60 and HSP70 in the recovery of RuBisCO LSU observed in the post-recovery algae (Fig. 12B and 24B). In addition, the mechanisms employed by HSP60 in coping with the different forms of polypeptide chains had been demonstrated by Naletova and co-workers (2006) with GAPDH. Thus, this shows that HSP60 may also helps in the recovery of GAPDH as displayed by the post-recovery algae (Figs. 13B and 25B).

4.6 Impact of PAR and UVR on Chl a fluorescence kinetics

The ratio of F_v/F_m is used to estimate the maximum quantum yield of Q_A reduction, i.e., PSII photochemistry. A low value of F_v/F_m usually means that the leaf or plants are under stressed or is photoinhibited (*vide supra*). According to Maxwell and Johnson (2000), a change in F_v/F_m is due to a change in the efficiency of non-photochemical quenching. This is reflected by the association of a decrease in F_m and an increase in F_o with a decrease in F_v/F_m (Baker, 2008). A decrease in F_m is a sign of an increase in non-photochemical quenching (qN) process (Baker, 2008) while an increase in F_o is associated to photoinactivation and loss of PSII reaction centres (Bradbury and Baker, 1981; Osmond, 1994). Thus, stressing photosynthetic tissues in the light can result in increases in non-photochemical quenching processes, which can often be accompanied by photoinactivation, which in turn will lead to oxidative damage and loss of PSII reaction centres (Aro et al., 1993). For example, in *L. digitata,* F_m and F_o of pre-irradiated alga are 0.97 and 0.28, respectively, but these values are reduced to 0.34 for F_m and 0.29 for F_o in post-irradiation under PAR+UVA+UVB at H_1. A reduction in F_m in this alga resulting in an increase of qN to 0.92 while a higher F_o results in an increase in photoinactivation, decrease from 0.71 to 0.17 F_v/F_m (Fig. 28Aii) and an increase in qN from 0 to 0.92 (Fig. 31G-H). After the post-recovery period, F_m and F_o rise to 0.61 and 0.30 with a simultaneous increase from 0.17 to 0.50 in F_v/F_m (Fig. 28Bii) and a decrease in qN to 0.56 (Fig. 31I).

As with F_v/F_m, changes in the quenching parameters in response to actinic irradiances and time can be determined with the fluorescence yield/signal. For instance, a change in the effective quantum yield, Y (or sometimes referred as Φ_{PSII}) is due to the change between F and F_m'. The increase in F is presumably associated with closure of PSII centres (White and Critchley, 1999). With increasing irradiances, number of PSII centres which are closed increases as well and when all are essentially closed, F does not increase further. This can be seen in the F curves of the pre-irradiated algae (Figs. 29-33A). An increase in F also indicates that a greater proportion of PSII centres becomes inactivated. A high F normally links with the build-up of proton gradient across the thylakoid membrane (ΔpH) due to the insufficient sink capacity to

remove most of the electrons. Since ΔpH is used as driving force for ATP production which in turn will be used by the Calvin cycle activity, increment and elevation of F indicates that the sample has a reduce sink for the electrons, thus, little CO_2 fixation is occurring (Ralph and Gademann, 2005). On the other hand, if F did not significantly increase (i.e. remained constant), there was no source or sink limitation to the photochemical pathway.

A rapid decline in F_m' (similar to that of F_m), on the other hand, indicates well-developed mechanism for energy dissipation associated with non-photochemical quenching, qN or NPQ while an equally smaller decline in F_m' implies limited capacity for qN or NPQ (Ralph and Gademann, 2005). Thus, from the pattern in F_m' curves of the pre-irradiated algae (Figs. 29-33A), it can be said that all the algae had a limited capacity for qN due to a small decline in F_m' (i.e. less than 35% reduction). According to Dau (1994), the F_m' level is affected by qN but not by photochemical quenching qP, suggesting that the quenching of F_m' is the characteristic of qN. Judging from the patterns in the RLC of the pre-irradiated algae and compares to that of a low-light adapted seagrass *Z. marina* leaf (Ralph and Gademann, 2005), it can be assumed that the algae in my study are low-light adapted since they exhibit an elevated F and a small decline in F_m' (as also been shown by the photosynthetic parameters). Therefore, it is to be expected that these algae will encounter pronounced photoinhibition when subjected to continuous high light.

Among the algae examined, *U. lactuca* appears to be more affected by PAR+UVA+UVB at H_1 than the other algae. For the pre-irradiated alga, *U. lactuca* exhibits a high elevated F and a small reduction in F_m' (Fig. 33A). These values suggest that *U. lactuca* has a lower capacity for electrons sink and a lower capacity for qN (Fig. 33G) than the other algae and is thus, more prone to photoinhibition. In fact, F_v/F_m of this alga drops to more than 85% after post-irradiation compares to less than 80% in the other species (Fig. 28Aii). In comparison, *P. palmata* is the least prone to photoinhibition by PAR+UVA+UVB at H_1 by having a lower elevated F and higher reduction of F_m' (Fig. 30B) with a higher qN (Fig. 30H) than the other algal species, resulting in a 71% reduction in F_v/F_m (Fig. 28).

As irradiance increases, F and F_m' approach each other and the fluorescence signal, ΔF becomes small, hence, decreases in Y are observed. The changes are more pronounced in the post-irradiated algae where ΔF becomes small even at low irradiance (Figs. 29-33B) with low values of Y (Figs. 29-33E). Even though both F_v/F_m and Y measures photosynthetic efficiency, Y is different from F_v/F_m since it estimates the efficiency at which light absorbed by PSII is used in photochemistry and is usually measured under light-adapted conditions (Maxwell and Johnson, 2000; Baker, 2008). As irradiance increases, Y steadily declines suggesting a limited capacity for photochemical energy usage (i.e. increase in F and PSII centres closure) while at the same time, heat dissipation mechanism is triggered (i.e. a decrease in F_m'). In this way, occurrence of photodamage can be minimised. The value of initial Y (i.e. at start of RLC, Figs. 29-33D) of the pre-irradiated algae is normally lower than their F_v/F_m equivalence (Fig. 28) due to the intrinsic effect of non-photochemical quenching reducing the light-adapted quantum yield (Beer et al., 2001, cited in Ralph and Gademann, 2005). When ETC is disrupted, inactivated or damaged (for e.g. during photoinhibition), a low initial Y is displayed as in the post-irradiated algae (Figs. 29-33E). The capacity for photochemical usage in these algae can even become nil at high irradiances as shown by the red algae (Figs. 29-30E).

Y when multiply with irradiance will give the relative electron transport rate (rETR), which is an approximation of the rate of electrons pumped through ETC (Beer et al, 2001, cited in Ralph and Gademann, 2005). The plot of rETR as a function of irradiance of the algae resembles that of traditional P-I curve with three distinct regions: the light limited, the light saturated and the photoinhibited region. The rise of the curve (α) in the light limited region is proportional to efficiency of light capture; a plateau is reached in the light saturated region where the capacity of the ETC limits photosynthesis and maximum photosynthetic occurs ($rETR_{max}$); and, a decline in the photoinhibited region at even higher irradiance which can be linked to, in the RLC case, dynamic down-regulation of PSII (White and Critchley, 1999; Schreiber, 2004). However, in my study, no related measurement is done on the photoinhibited region. In addition, an interception between α and $rETR_{max}$ will give the minimum saturating irradiance, I_k which is related to quenching where at irradiance below I_k, qP is dominating while at irradiance above I_k, qN is

dominating (Henley, 1993). All the three regions of RLC are displayed in the pre-irradiated algae (Figs. 29-30A and 32-33A) except for *L. digitata* which do not show the photoinhibited region (Fig. 31A). Unlike the other algae, *L. digitata* is able to maintain a greater level of photosynthetic activity indicated by a high $rETR_{max}$ and less acute α with a slow and steady decline of Y (Fig. 31D). Furthermore, in this alga, rETR does not decline after saturation (I_k = 262.3 µmol m^{-2} s^{-1}) implying that the actinic irradiance is significantly greater than saturation and is not dissipated, thus, can cause photoinhibitory damage (White and Critchley, 1999). After post-irradiation, α and $rETR_{max}$ becomes small while I_k is high (Figs. 29-33E, *vide supra*). The effect is more pronounced in the red and green algae in comparison to that of the brown algae. The changes in the parameters indicate that the post-irradiated algae have lower efficiency to capture light, have lower photosynthetic activity and need higher energy to saturate photosynthesis than their pre-irradiation equivalences. These characteristics are signs showing that the ETC is disrupted, inactivated or damaged (i.e. as in photoinhibition).

By examining qP and qN at the end of RLC we can determine the extent to which alga has been able to cope with excess irradiance. qP gives an indication of the proportion of reaction centres that are open (i.e. indicates the oxidation state of Q_A) (Maxwell and Johnson, 2000). For qp= 1, all Q_A are assumed to be in an oxidized state and for qp =0, all Q_A are assumed to be in a reduced state (Dau, 1994). Furthermore, a change in qP is due to the closure of reaction centres, resulting in saturation of photosynthesis (Maxwell and Johnson, 2000). Thus, as irradiance increases, qP declines steadily where proportion of reduced Q_A is increased as well as observed for all pre- and post-irradiated, and post-recovery algae. According to Melis (1999), photodamage will occur with a low probability when Q_A is oxidized and excitation energy is utilized in electron transport while a significantly high probability for photodamage occurs when the condition shifts the redox state of Q_A from oxidized to reduced during illumination. Therefore, in order to minimise the occurrence of photodamage, qP should decline to values higher than 0 (Figs. 29-33G). In the post-irradiated algae, qP in some species rapidly changes from a fully oxidized state to a fully reduced state as irradiance increases, indicating that some degree of photodamage has occurred. This effect is more pronounced in the red and green algae (Figs. 29-30H and 33H). In the brown algae particularly *L.*

digitata, on the other hand, qP slowly and steadily declines to values higher than that of the pre-irradiated algae suggesting that the algae is tolerant to the high PAR+UVA+UVB stress impinging on them (Figs. 31-32H).

The parameters qN and NPQ can be used interchangeably since both relates to the energy dissipation of PSII reaction centres. However, NPQ (or the Stern-Volmer quenching) is more sensitive to energy dissipation within the antennae matrix (where the energy dependent dissipation occurs and contains xanthophyll [X]), while it is relatively insensitive to lower values of qN which is mainly associated with thylakoid membrane energization (Schreiber, 2004). The protective mechanisms of qN and NPQ are thought to occur by (a) decreasing the lifetime of ^{1}Chl to minimize generation of $^1O_2$ in the PSII LHC and reaction centre, (b) preventing overacidification of the lumen and generation of long-lived $P680^+$, and (c) decreasing the rate of O_2 reduction by PSI (Niyogi, 1999). qN or NPQ is correlated with Y. As Y decreases with increasing irradiance, more electrons accumulate at the acceptor side of PSII. qN and NPQ are triggered so as to remove these excess energy as heat and is regarded as a protective or down-regulation mechanism of PSII (see Niyogi, 1999; Müller et al., 2001; Govindjee, 2002; Holt et al., 2004 and Ivanov et al., 2008 for reviews). Thus, an increase in qN or NPQ is observed with increasing irradiance. In the post-irradiated algae, qN and NPQ are already developing within the chloroplast at the beginning of RLC (Figs. 29-33H) but is non-existent in the pre-irradiated algae (Figs. 29-33G) suggesting that the algae is experiencing photoinhibition. In the pre-irradiated brown algae, qN and NPQ develop only after irradiance exceeds that of 40 µmol m^{-2} s^{-1} for *D. dichotoma* (Fig. 30G) and 87 µmol m^{-2} s^{-1} for *L. digitata* (Fig. 29G) while at the same time there is a decline in Y and qP. Both the brown algae are therefore, prone to photoinhibitory damage at below the respective irradiances. This is evident from the post-irradiated algae where qN and NPQ are 92-93% and 120-242% higher than the pre-irradiated algae, respectively (Figs. 29-30H).

In plants and algae, the light-regulated and reversible induction of NPQ is thought to occur through the interconversion of the light harvesting xanthophylls (Xs) to the energy quenching equivalents *via* a so-

called X cycle. This will allow a reversible switch of photosynthetic light-harvesting complexes between a light-harvesting state under low light and a dissipative state under high light. In violaxanthin (V) cycle, for instance, high light induces the drop in lumen pH which activates the enzyme V de-epoxidase and converts V to zeaxanthin (Z) *via* anteraxanthin (A). Concurrently, PsbS, a PSII protein, becomes protonated. The Z associated with PSII is an efficient quencher of excitation energy in the PSII antenna and the rate of heat loss from PSII increases. When light intensity decreases, deprotonation of PsbS occurs and zeaxanthin epoxidase converts Z back to V (Baker, 2008). Conversely, at low light that is limiting for photosynthesis, V is associated with the PSII antenna and PSII has a low rate of heat loss. Hence, low qN is observed at irradiances below I_k and high qN when irradiance exceeds I_k.

A role of Z in protection of photodamaged and disassembled PSII reaction centres was studied in the green alga *D. salina* (Jin et al., 2003). Results support the notion that Z is a component of the PSII repair process. Upon photodamaged, Z was formed *in situ* and stays in association with the disassembled and photochemically inert PSII-core until the repair of the affected PSII centres permit the return of individual units into the pool of functional PSII. Z is then converted back to V at the end of PSII damage and repair cycle in wild-type strain. The conversion of V to A to Z had been correlated with dynamic photoinhibition and recovery of photosynthesis in *D. dichotoma* as well (Uhrmacher et al., 1995).

In green and brown algae, V cycle is the major photoprotective mechanism used. However, in the red algae, the presence of carotenoids involved in the protective mechanism is contradictory. Schubert and Garcia-Mendoza (2006) in an attempt to correlate the Rhodophyta phylogeny with carotenoids profiles found that a common profile is observed up to the level of order. Furthermore, the authors also observed that the main difference between the carotenoid profiles is related to the X that represents the major carotenoid. In some species, lutein (Lut) is the major carotenoid while in others it is either Z or A. The presence of V that are X cycle related pigments is also found in four out of 12 orders analysed. Even though no carotenoid contents analysis was done on *S. chordalis* or *P. palmata* in my study, there seems to be some sort of X cycle induced as evident from the increase in NPQ. If comparison is made based on

similar orders, i.e. Gigartinales (Schubert and Garcia-Mendoza, 2006) for *S. chordalis* and similar genus, i.e. *Palmaria* (Marquadt and Hanelt, 2004) for *P. palmata*, the major carotenoid is Lut. In Lut-epoxide cycle, a monoepoxide form of lutein is converted to lutein by high light (Garcia-Plazaola et al., 2007). In addition to X-cycle pigments (A and Z which are derived from beta-carotene), alpha-carotene derived Xs such as Lut which are structural components of the subunits of the LHC, contribute to the dissipation of excess absorbed light energy and the protection of *C. reinhardtii* from photo-oxidative damage. Lut is present constitutively in the LHCs and may function in NPQ mainly at high $[H^+]$ (Niyogi et al., 1997).

A lower value of NPQ observed in the red algae after the irradiation compared to that of the brown and green algae suggests that the X cycle does not play a key role in protection against overexcitation of PSII. In fact, the red algae can employ other mechanisms which can protect the PSII centres from excessive light such as state-transitions (Delphin et al., 1996) without involving the X cycle pigments. The feedback regulation of light-harvesting by qN, on the other hand, is triggered by the decrease in pH within the thylakoid lumen which functions as an immediate signal of excessive light (Müller et al., 2001). Thus, an increase in qN is observed with increasing irradiance since more electrons accumulate at the acceptor side of PSII, hence, an increase in H^+ and a decrease in pH. It is also observed that the red algae are more sensitive to the drop in pH with a higher maximum qN achievable than the other algae examined (Figs. 29-33G).

Dark relaxation kinetics allows the various components of NPQ to be differentiated. On the basis of the time constants, one can classify the fast, energy-dependent quenching (qE: time constant less than 100s), the intermediate quenching (qT: minutes), and the slowly relaxing, photoinhibitory quenching (qI: hours to days) (Rascher and Nedbal, 2006; refer Fig. 48, Appendix 4 for typical fluorescence trace displaying the various components of NPQ). Additionally, qE is dependent on the formation of ΔpH across the thylakoid membrane generated by the light dependent translocation of H^+ and the accompanying acidification of the lumen (Horton et al., 1996). Moreover, qT is said to be predominant under low light illumination whereas qE and qI are involved mainly in the high light illumination (Lazár, 1999).

According to Ralph and Gademann (2005) the speed of NPQ to return to zero in darkness is an indicator of the photosynthetic apparatus tolerance to high light. A slow recovery indicates damage (i.e. qI) may have occurred during the recordings and it will take time to repair the PSII centres and associated proteins. A slow relaxation of NPQ is observed in the brown (Fig. 36A-B) and green (Fig. 37A) algae but there is a rapid relaxation of NPQ within 100 s in *S. chordalis* (Fig. 35A) and 40s in *P. palmata* (Fig. 35B) which correlates to the relaxation of qE. However, there is a majority of the NPQ still remains and this can be linked to qI. In the post-irradiated algae, on the other hand, most of the NPQ is due to qI (Figs. 35-36C-D and 37B). Furthermore, there is a slow recovery of Y as well implying that RLC may have cause a degree of non-reversible photodamage to these algae (Figs. 29-33E, Ralph and Gademann, 2005).

In general, quenching coefficient plotted as a function of irradiance in my study shows a clear increase in qN and NPQ with increasing irradiance and a steady decline in qP and Y. Similar patterns are also observed for the red algae *Corallina elongata* (Häder et al., 1997a), *Peyssonnelia squamata* (Häder et al., 1998c), *P. umbilicalis* (Häder et al., 1999), *C. officinatis* (Häder et al., 2003b), *C. gaudichaudii* and *Ceramium* sp. (Häder et al., 2004); and for the green algae *Caulerpa prolifera* (Häder et al., 1997b) and *Ulva (Enteromorpha) linza* (Häder et al., 2001a). Long-term effects of full-spectrum solar radiation, solar radiation without UVB, and solar radiation without total UV (UVA+UVB) were studied in intertidal *U. rigida* (Altamirano et al., 2000). After 7 days, high values of F_v/F_m, $\Delta F/F_m$' and qP were observed in the absence of UVB while samples in the presence of UVB exhibited significantly high qN values. After 20 days, F_v/F_m, $\Delta F/F_m$' and qP were decreased in the absence of UVB while qN was increased in all treatments. They suggested that greater photoinhibition was observed under UVB as indicated by increased in qN and the alga shows different adaptation between the 7 and 20 incubation days. A decrease in the effective quantum yield in the presence of UVR may indicate an internal down-regulation process, such as dynamic photoinhibition, in order to increase the dissipation of excess absorbed energy (Häder et al., 2001a). Furthermore, the decrease in NPQ ability showed a correlation to D1 breakdown and photoinhibition. The recovery to a high NPQ ability followed closely the recovery of D1 protein and the

photosynthetic electron transport (Carr and Björk, 2007) which has also been demonstrated by the algae examined in my study.

For instance, in a study by Runcie et al. (2008) on deep-water algae, qN was not developed in *Ulva expansa* and *Microdictyon umbilicatum*, even at their depth limit, although qP declined markedly at 100 m. While the high irradiance of RLC caused a decline in the photochemical capacity of the algae, there was little capacity to activate any photoprotective mechanism as evident by an increase in qN. Therefore, the green algae were poorly suited in coping with irradiances in excess of that experienced at depth exceeding 100 m. In contrast, the red and brown algae responded differently to RLCs with an increase in qN and decrease in qP with increasing depth. These algae were able to activate protective mechanisms to ameliorate the presumably damaging effect of the irradiance in addition to a decline in capacity to photosynthesize. Thus, these algae are better suited than the green algae by retaining the protective capacity which is apparently lost by the deeper green algae. In comparison, all the algae examined in my study exhibit high ability in activating the protective mechanism since there was a rapid decline in qP with a high increase in qN (and NPQ) as actinic irradiance increases, especially in the red algae (Figs. 29-30).

Excitation pressure builds up in PSII whenever photon absorption and delivery exceeds the capacity of metabolism to consume ATP and NADPH (Franklin et al., 2003). Changes in PSII excitation pressure are reflected in alterations in the redox state of PSII, which can be monitored *in vivo* by the parameter 1-qP (Huner et al., 1996). Thus, 1-qP is the measure of the proportion of reaction centres that are closed and is approximately equal to $[Q_A^-]/]Q_A]+[Q_A^-]$ (Huner et al., 1996). Increase in excitation pressure will then reflect the overreduction of Q_A. If there are no changes in the capacity to utilize the absorbed energy, energy balance is thus disrupted creating an energy imbalance. Energy imbalance builds up as irradiance increases during RLC. Large 1-qP value is observed with the pre-irradiated algae at the end of RLC (Fig. 34A) except in *L. digitata* suggesting that in *L. digitata*, substantial amount of energy is still being used in photosynthesis when it is already saturated in the other algae. This is further evidenced by the steady and

slow decline of Y and its rETR is still active even at the highest irradiance. Thus, there is a low build up of excitation pressure. After post-irradiation treatment, *L. digitata* shows a lower 1-qP than the pre-irradiated algae indicating that this alga is more tolerant to the high irradiance compares to the other algae examine. Photodamage will occur with a low probability when Q_A is oxidized and excitation energy is utilized in electron transport (Melis, 1999) while a significantly high probability for photodamage occurs when the condition shifts the redox state of Q_A from oxidized to reduced during illumination, such as when forward electron flow is slowed down or blocked and excitation energy dissipates *via* charge-recombination reactions in a non-assimilatory process (Melis, 1999). If this is the case, then *L. digitata* is less vulnerable to photodamage than the other algae.

The imbalance in energy due to the redox state of Q_A can act as a signal to activate photoprotective mechanism such as dynamic photoinhibition (Wilson et al., 2006). In fact, over-reduction of Q_A from the increase in 1-qP can be counterbalanced by NPQ as characterized by the susceptibility of PSII to light stress or (1-qP)/NPQ (Schubert et al., 2006). (1-qP)/NPQ is an intrinsic ability of PSII to balance qP and NPQ (Shen et al., 1996) and tends to increase as PSII reaction centres are closed but decreases when photoprotective mechanism of NPQ is enhanced (Park et al., 1996; Schubert et al., 2006). A higher (1-qP)/NPQ value is observed in the pre-irradiated brown and green algae compared to that of the red algae due to the large 1-qP and a slow onset of NPQ (Fig. 34B). However, after the post-irradiation treatment, NPQ is more enhanced in the brown and green algae resulting in a smaller (1-qP)/NPQ than the red algae. Furthermore, it also appears that the brown and green algae are better adapted to the irradiance because their NPQ is larger relative to the photoinactivation of PSII (i.e. 1-qP) (Fig. 34A). Among the species, *L. digitata* initially has a low 1-qP and a slow onset of NPQ. However, after the post-irradiation treatment, *L. digitata* display a reduced 1-qP but an enhanced NPQ. Not only *L. digitata* is well adapted to the changing irradiance, it is better prepared as well. Furthermore, increasing protection of functional PSIIs as photon exposure increases (accompanied by greater accumulation of energy-dissipative inactive PSIIs) as demonstrated with high 1-qP but low (1-qP)/NPQ suggested that nonfunctional PSIIs are able to confer protection to remaining connected functional PSII cores (Park et al., 1996).

The rapid induction and relaxation kinetics provide information on the light-driven reduction and dark-reoxidation of different pools of PSII acceptors. Basically, FI curve is characterized by the increase in fluorescence from the basic level, F_o or O, to the maximal one, F_m or P(or M), *via* a sequence of three steps: O-I_1, I_1-I_2 and I_2-P(M) (Fig. 38D, Schreiber, 2004) or their equivalence O-J, J-I and I-P (Fig. 39; Lazár, 1999; Boisvert et al., 2006). Roháček and Barták (1999), on the other hand, had also included two other steps, the K and D steps, generating the O-K-J-I-D-P kinetics where the D-step is noticeable in pre-irradiated and post-recovery *U. lactuca*. From P, the fluorescence will slowly decay to F_t, a minimum fluorescence at the end of FI curve (i.e. the last 1 s of Fig. 38) (Roháček and Barták, 1999). In the Chl-F induction curve (Figs. 38D and 39), the first phase (J) is thought to correspond to the photoaccumulation of reduced Q_A (or $Q_A^-Q_B$) and has been denoted the photochemical phase (Strasser et al., 1995; Lazár, 1999; Tomek et al., 2001; Heredia and de Las Rivas, 2003; Schreiber, 2004). The I-step reflects the photoaccumulation of $Q_A^-Q_B^-$ forms while the P(or M)-step has been associated with the photoaccumulation of $Q_A^-Q_B^{2-}$ forms and both constitute the slow thermal phase(s) (Strasser et al.. 1995; Tomek et al., 2001; Heredia and de Las Rivas, 2003; Schreiber, 2004). The photochemical and thermal phases are clearly displayed by the pre-irradiation *U. lactuca* indicating a functioning photosynthetic apparatus (Fig. 38D). In the other algal classes examined, no clear polyphasic rise is visible. This may be due to the disruption from the signal to noise ratio which obscures the kinetics (Fig. 38A-C). In addition, the kinetics produced may also differ between the algae since different algal classes have different construction of photosynthetic apparatus.

Upon irradiation to PAR+UVA+UVB at H_1, the fluorescence signal in the algae dramatically decreases and completely quenched the second rise (i.e. J-I-P phases) indicating photoaccumulation of reduced Q_A. The quenching of the thermal phases may also be due to strong qN quenching (possibly by high qI) observed in the algae as also shown by the RLC (Figs. 29-33H, *vide supra*) and light-dark relaxation kinetics (Fig. 37, *vide supra*). A relationship between the thermal phases and removal of NPQ caused by the reduction of plastoquinone molecules bound to Q_B has been proposed by some authors (Yaakoubd et al., 2002; Boisvert et al., 2006). In post-recovery algae, the fluorescence signal increases again but the

polyphasic rise is still not visible indicating a slow recovery of photosynthetic activity within the apparatus and PAR+UVA+UVB may has caused some degree of photodamage. In post-recovery *U. lactuca*, however, a significant decrease in I_2-D phase becomes more apparent than in its pre-irradiation equivalence (Fig. 38D). A decrease or a plateau between I_2 and D is caused by oxidation of Q_A and electron transport from Q_A to Q_B with an equal rate between reduction and reoxidation is represented by the plateau (Roháček and Barták, 1999). Additionally, the kinetics of post-recovery *U. lactuca* at 300 µs/data resembles that of the pre-irradiation indicating signs of photosynthetic activity recovery within the photosynthetic apparatus of the alga (Fig. 39).

The fluorescence decay can be distinguished by two distinct phases (unfortunately, not visible in any of the pre-irradiated algae displayed in Fig 38) (Papageorgiou et al., 2007). According to Papageorgiou and co-workers (2007), the principal causes of the decrease from P to T are related to a gradual re-oxidation of Q_A by PSI (qP), the energization of the thylakoid membrane due to proton translocation (qE) and a state transition (qT). In addition, the fluorescence decay has also been linked to changes in the rate of carbon metabolism and oxygen evolution (Lazár, 1999 and ref. therein). In the post-irradiated and post-recovery algae, a steady level of fluorescence with no fluorescence decay was observed. This condition may be contributed by the photoinhibitory quenching of qN (i.e. qI) since this type of quenching depresses the fluorescence in light (*vide supra*) and is not reversed by the dark rest (Papageorgiou et al., 2007). Häder and co-workers (2001a) stated that a fast decay may indicate that it took less than 1 s until the photosynthetic ETC to operate smoothly. This can be seen by the relaxation kinetics displayed by the pre-irradiated *P. palmata* (Fig. 38A). Similar patterns in the rapid induction and relaxation kinetics had been demonstrated for the red algae *C. elongata* (Häder et al., 1997a), *P. umbilicalis* (Häder et al., 1999), *C. officinalis* (Häder et al., 2003b), *Ceramium* sp. and *C. gaudichaudii* (Häder et al., 2004); and, the green algae *C. prolifera* (Häder et al., 1997b) and *E. linza* (Häder et al., 2001a) as well.

5.0 CONCLUSION

In conclusion, the results show that the macroalgae are strongly affected by the high light effects of photosynthetically active radiation (PAR) and ultraviolet radiation (UVR). The algae are indeed affected by UVB even under the conditions with low background PAR. Dramatic decline in F_v/F_m and slower recovery kinetics in algae irradiated with additional UVB suggest that the algae suffer a permanent damage to their photosynthetic apparatus. Furthermore, lower contents of the photosynthetic pigments, lower contents of D1 protein, lower activity of ribulose-1,5-bisphosphate carboxylase/oxygenase (RuBisCO) and loss of its large subunits (LSU), lower activity of glyceraldehyde-3-phosphate dehydrogenase (GAPDH) as well as lower photosynthetic performance observed in these algae after UVB irradiation indicate that the damage may have occurred at various parts of the photosynthetic machinery. However, these physiological patterns are observed as a result of a short-term adaptation of the macroalgae to the UVB irradiance of the sun simulator or of the fluorescent lamps. The extent of the above physiological effects may differ when measured at the algae's natural growth sites although the permanent inhibition may still be observed. Furthermore, in nature, the algae are usually adapted to lower UV irradiance than that applied in the experiments. The natural solar spectrum exhibits ratios of energy distribution over the different wavelength ranges of PAR:UVA:UVB = 100:10:0.6 at the surface of the earth (Franklin and Forster, 1997). Thus, the results collected may represent an adverse effect of UVB due to increase in photon fluence rate which accompanies the thinning of the ozone layer observed in natural conditions. All the algae examined will encounter strong photoinhibition but are still able to adapt and recover from the stress.

In addition to the above observations, a supporting effect of UVB in the recovery and repair mechanisms of the algae is also noticeable in some of the species. This effect is observed with algae that are previously adapted to low-light and has also been observed under the fluorescent lamps which emit low PAR but high UVB. These observations, therefore, are in contrast to several previous reports. The supporting effect is observed with a faster recovery in algae that receive full spectrum radiation than algae

which receives full spectrum excluding UVB. This recovery pattern is reflected in various physiological effects analyzed. Most of the algae examined can tolerate lower UVB flux and even exhibit the supporting effect of UVB at ratio of PAR:UVA:UVB closer to that of the natural conditions. Higher inhibition by UVA than UVB observed in some of the species is also of an ecological importance since in natural conditions, solar radiation contains more UVA than UVB and UVA is not significantly attenuated by the ozone layer.

The ability for the macroalgae to quickly adapt to and tolerate the high UVB flux is an important factor to determine the survival of the macroalgae under the present natural conditions, i.e. the thinning of the ozone layer. Different species may respond differently to this harmful radiation which has been demonstrated by the algae in this study. In general, an induction of antioxidative enzymes and the stress proteins as well as the triggering of the xanthophylls cycle *via* non-photochemical quenching mechanism observed with additional UVB will help to protect the algae from further damage and indirectly play a role in the repair and recovery of the algae. While some species respond by inducing more antioxidative enzymes to detoxify the reactive oxygen species, or inducing more stress proteins to keep check with the damaged proteins, others may remove the excess energy rapidly through heat (i.e. dynamic photoinhibition). Some sort of indirect link between the stress proteins and photoinhibition and its recovery has been demonstrated by the algae. However, the direct link between these two factors is not elucidated in this study. Therefore, the role of the stress proteins in photoinhibiton needs to be addressed further especially for the macroalgae since to my knowledge there is not much information available on the response of stress proteins to UV collected from the macroalgae compares to that from higher plants or other aquatic organisms.

Macroalgae exposed to solar PAR and UVR show a number of responses, which can be related to species-specific sensitivity as well as to the radiation environment in which they live. *Laminaria digitata,* for instance, inhabits the upper-middle sublittoral zone of the marine ecosystem and is submitted to drastic changes in light environment. Therefore, higher reductions in F_v/F_m are observed in this alga

especially under high PAR and UV irradiances. The higher inhibition may be partly due to the less developed photoprotective mechanisms in this alga compared to the other algal species. In comparison, *Ulva lactuca w*hich inhabits the intertidal zone is adapted to an environment of harsh extremes and thus is well-prepared and well-adapted to the high PAR and UV of this study. A complete recovery is almost attained within the measured period under the dim light in this alga. The red algae *Solieria chordalis* and *Palmaria palmata,* and the brown alga *Dictyota dichotoma* which inhabit the intertidal or upper sublittoral zone are also strongly affected by UV as well but at the same time are able to adapt to the high PAR and UV conditions.

In addition to the physiological responses of the algae to the prevailing conditions as stated above, morphological characteristics of the algae can also contribute to the adaptation. For instance, the brown algae are able to protect itself by having a thick thallus as with *L. digitata* (Johansson and Snoeijs, 2002), by having outer cell layers that can act as a shield to the inner layer providing longer pathlength for UV absorption (Häder et al., 1998b), by changing its phaeoplasts arrangement to reduce amount of light absorbed (Hanelt and Nultsch, 1990) and by producing phlorotannins as sunscreen (Wiencke et al., 2004). The red algae induce the production of UV-absorbing pigments such as mycosporine-like amino acids (MAAs, Kräbs et al., 2002; Helbling et al., 2004). Furthermore, the red algae contain phycobiliproteins that can act as ‘light-quality’ and ‘chromatic’ adapters which help the algae to cope with drastic changes in light fields (Talarico and Maranzana, 2000). MAAs can also be found in the green alga (Gröniger et al., 2000).

For future research, further experimentations should be done focusing more on the molecular acclimation mechanisms of the algae, such as interaction between the supporting effects of UVB observed and gene expression, and involvement of DNA repair during the inhibitory and recovery phases. The impact of UVB on ultrastructural changes should also be elucidated. As in their natural habitats the algae will encounter various other environmental factors, the interactive effects between these factors and UVB should be addressed. Finally, the analysis of the proteomes of the algae can give insight of the underlying

mechanisms governing the integrated physiological responses of the algae to UVB. In addition, this approach may help us to understand the modes of action and identify novel ecotoxicological biomarkers (Nesatyy and Suter, 2007).

6.0 REFERENCES

Aarti PD, Tanaka R, Tanaka A (2006) Effects of oxidative stress on chlorophyll biosynthesis in cucumber (*Cucumis sativus*) cotyledons. Physiologia Plantarum 128:186-197.

Adir N, Zer H, Shochat S, Ohad I (2003) Photoinhibition – a historical perspective. Photosynthesis Research 76:343-370.

Aguilera J, Bischof K, Karsten U, Hanelt D, Wiencke C (2002a) Seasonal variation in ecophysiological patterns in macroalgae from an Arctic fjord: II. Pigment accumulation and biochemical defence systems against high light stress. Marine Biology 140:1087-1095.

Aguilera J, Dummermuth A, Karsten U, Schrieck R, Wiencke C (2002b) Enzymatic defences against photooxidative stress induced by ultraviolet radiation in Arctic marine macroalgae. Polar Biology 25:432-441.

Aguilera J, Figueroa FL, Häder D-P, Jiménez C (2008) Photoinhibition and photosynthetic pigment reorganisation dynamics in light/darkness cycles as photoprotective mechanisms of *Porphyra umbilicalis* against damaging effects of UV radiation. Scientia Marina 72:87-97.

Aguirre-von-Wobeser E, Figueroa FL, Cabello-Pasini A (2000) Effect of UV radiation on photoinhibition of marine macrophytes in culture systems. Journal of Applied Phycology 12:159–168.

Allakhverdiev SI, Murata N (2004) Environmental stress inhibits the synthesis *de novo* of proteins involved in the photodamage–repair cycle of photosystem II in *Synechocystis* sp. PCC 6803. Biochimica et Biophysica Acta 1657:23-32.

Allen DJ, McKee IF, Farage PK, Baker NR (1997) Analysis of limitation to CO_2 assimilation on exposure of leaves of two *Brassica napus* cultivars to UVB. Plant, Cell and Environment 20:633-640.

Altamirano M, Flores-Moya A, Figueroa FL (2000) Long-term effects of natural sunlight under various ultraviolet radiation conditions on growth and photosynthesis of intertidal *Ulva rigida* (Chlorophyceae) cultivated *in situ.* Botanica Marina 43:119-126.

Alves PLCA, Magalhaes ACN, Barja PR (2002) The phenomenon of photoinhibition of photosynthesis and its importance in reforestation. The Botanical Review 68:193-208.

Anderson JM (2001) Does functional photosystem II complex have an oxygen channel? FEBS Letters 488:1–4.

Anderson, JM, Park Y-I, Chow WS (1997) Photoinactivation and photoprotection of photosystem II in nature. Physiologia Plantarum 100:214-223.

Andersson I, Backlund A (2008) Structure and function of Rubisco. Plant Physiology and Biochemistry 46:275-291.

Apel K, Hirt H (2004) Reactive oxygen species: Metabolism, oxidative stress and signal transduction. Annual Review of Plant Biology 55:373-399.

Aro E-M, Virgin I, Andersson B (1993) Photoinhibition of photosystem II. Inactivation, protein damage and turnover. Biochimica et Biophysica Acta 1143:113-134.

Asada K (1992) Ascorbate peroxidase — a hydrogen peroxide-scavenging enzyme in plants. Physiologia Plantarum 85:235–241.

Asada K (1999) The water–water cycle in chloroplasts: scavenging of active oxygens and dissipation of excess photons. Annual Review of Plant Physiology and Plant Molecular Biology 50:601–639.

Asada K (2006) Production and scavenging of reactive oxygen species in chloroplasts and their functions. Plant Physiology 141:391-396.

Babu T, Jansen M, Greenberg B, Gaba V, Malkin S, Mattoo A, Edelman M (1999) Amplified degradation of photosystem II D1 and D2 proteins under a mixture of photosynthetically active radiation and UVB radiation: Dependence on redox status of photosystem II. Photochemistry and Photobiology 69:553–559.

Baker NR (2008) Chlorophyll fluorescence: A probe of photosynthesis *in vivo*. Annual Review of Plant Biology 59:89-113.

Barbato R, Bergo E, Szabò, Vecchia FD, Giacometti GM (2000) Ultraviolet B exposure of whole leaves of barley affects structure and functional organization of photosystem II. Journal of Biological Chemistry 275:10976-10982.

Barbato R, Frizzo A, Friso G, Rigoni F, Giacometti GM (1995) Degradation of the D1 Protein of Photosystem-II reaction centre by Ultraviolet-B radiation requires the presence of functional manganese on the donor side. European Journal of Biochemistry 227:723-729.

Barber J, Andersson B (1992) Too much of a good thing: Light can be bad for photosynthesis. Trends in Biochemical Sciences 17:61-66.

Bautista AIN, Necchi Jr O (2008) Photoacclimation in a tropical population of *Cladophora glomerata* (L.) Kützing 1843 (Chlorophyta) from southeastern Brazil. Brazilian Journal of Biology 68:129-136.

Beer S, Eshel A (1983) Determining phycoerythrin and phycocyanin concentration in aqueous crude extracts of red algae. Australian Journal of Marine and Freshwater Research 36:785-792.

Beer S, Larsson C, Poryan O, Axelsson L (2000) Photosynthetic rates of *Ulva* (Chlorophyta) measured by pulse amplitude modulated (PAM) fluorometry. European Journal of Phycology 35:69-74.

Bennoun P (2001) Chlororespiration and the process of carotenoid biosynthesis. Biochimica et Biophysica Acta 1506:133-142.

Bergo E, Segalla A, Giacometti GM, Tarantino D, Soave C, Andreucci F, Barbato R (2003) Role of visible light in the recovery of photosystem II structure and function from ultraviolet B stress in higher plants. Journal of Experimental Botany 54:1665-1673.

Bertsch U, Soll J, Seetharamt R, Viitanent PV (1992) Identification, characterization, and DNA sequence of a functional "double" groES-like chaperonin from chloroplasts of higher plants. Proceedings of the National Academy of Science USA 89:8696-8700.

Bierkens JGEA (2000) Applications and pitfalls of stress-proteins in biomonitoring. Toxicology 153:61-72.

Bischof K, Hanelt D, Tüg H, Karsten U, Brouwer PEM, Wiencke C (1998a) Acclimation of brown algal photosynthesis to ultraviolet radiation in Arctic coastal waters (Spitsbergen, Norway). Polar Biology 20:388-395.

Bischof K, Hanelt D, Wiencke C (1998b) UV radiation can affect depth-zonation of Antarctic macroalgae. Marine Biology 131:597-605.

Bischof K, Hanelt D, Wiencke C (1999) Acclimation of maximal quantum yield of photosynthesis in the brown alga *Alaria esculenta* under high light and UV radiation. Plant Biology 1:435-444.

Bischof K, Hanelt D, Wiencke C (2000a) Effects of ultraviolet radiation on photosynthesis and related enzymes reactions of marine macroalgae. Planta 211:555-562.

Bischof K, Janknegt PJ, Buma AGJ, Rijstenbil JW, Peralta G, Breeman AM (2003) Oxidative stress and enzymatic scavenging of superoxide radicals induced by solar UV-B radiation in *Ulva* canopies from southern Spain. Scientia Marina 67:353-359.

Bischof K, Kräbs G, Hanelt D, Wiencke C (2000b) Photosynthetic characteristics and mycosporine-like amino acids under UV radiation: a competitive advantage of *Mastocarpus stellatus* over *Chondrus crispus* at the Helgoland shoreline? Helgoland Marine Research 54:47–52.

Bischof K, Kräbs G, Wiencke C, Hanelt D (2002a) Solar ultraviolet radiation affects the activity of ribulose-1,5-bisphosphate carboxylase-oxygenase and the composition of photosynthetic and xanthophyll cycle pigments in the intertidal green alga *Ulva lactuca* L. Planta 215: 502–509.

Bischof K, Peralta G, Kräbs G, van de Poll WH, Pérez-Lloréns JL, Breeman AM (2002b) Effects of solar UVB radiation on canopy structure of *Ulva* communities from southern Spain. Journal of Experimental Botany 53:2411-2421.

Boisvert S, Joly D, Carpentier R (2006) Quantitative analysis of the experimental O-J-I-P chlorophyll fluorescence induction kinetics. Apparent activation energy and origin of each kinetic step. FEBS Journal 273:4770-4777.

Bonaventura R, Poma V, Costa C, Matranga V (2005) UVB radiation prevents skeleton growth and stimulates the expression of stress markers in sea urchin embryos. Biochemical and Biophysical Research Communications 328:150–157.

Bonaventura R, Poma V, Russo R, Zito F, Matranga V (2006) Effects of UVB radiation on development and hsp70 expression in sea urchin cleavage embryos. Marine Biology 149:79–86.

Booth CR, Madronich S (1994) Radiation amplification factors: improved formulation accounts for large increases in ultraviolet radiation associated with Antarctic ozone depletion. In: Weiler CS, Penhale

PA (eds.) Ultraviolet Radiation in Antarctica: Measurements and Biological Effects. American Geophysical Union, Washington: pp. 39–42.

Bouchard JN, Campbell DA, Roy S (2005) Effects of UVB radiation on D1 protein repair cycle of natural phytoplankton communities from three latitudes (Canada, Brazil and Argentina). Journal of Phycology 41:273-286.

Bradbury M, Baker NR (1981) Analysis of the slow phases of the *in vivo* chlorophyll fluorescence induction curve. Changes in the redox state of photosystem II electron acceptors and fluorescence emission from photosystems l and II. Biochimica et Biophysica Acta 63:542-551.

Britt AB (2004) Repair of DNA damage induced by solar UV. Photosynthesis Research 81:105-112.

Brouwer PEM, Bischof K, Hanelt D, Kromkamp J (2000) Photosynthesis of two Arctic macroalgae under different ambient radiation levels and their sensitivity to enhanced UV radiation. Polar Biology 23:257-264.

Brown DB, Peritz AE, Mitchell DL, Chiarello S, Uitto J, Gasparro FP (2000) Common fluorescent sunlamps are inappropriate substitute for sunlight. Photochemistry and Photobiology 72:340-344.

Buma AGJ, van Oijen T, van de Poll W, Veldhuis MJW, Gieskes WWC (2000) The sensitivity of *Emiliania huxleyi* (Prymnesiophyceae) to ultraviolet-b radiation. Journal of Phycology 36:296-303.

Cabello-Pasini A, Aguirre-von-Wobeser E, Figueroa FL (2000) Photoinhibition of photosynthesis in *Macrocystis pyrifera* (Phaeophyceae), *Chondrus crispus* (Rhodophyceae) and *Ulva lactuca* (Chlorophyceae) in outdoor culture systems. Journal of Photochemistry and Photobiology B: Biology 57:169–178.

Carell T, Burgdorf LT, Kundu LM, Cichon M (2001) The mechanism of action of DNA photolyases. Current Opinion in Chemical Biology 5:491–498.

Carr H, Björk M (2007) Parallel changes in non-photochemical quenching properties, photosynthesis and D1 levels at sudden, prolonged irradiance exposures in *Ulva fasciata* Delile. Journal of Photochemistry and Photobiology B: Biology 87:18–26.

Chaturvedi R, Shyam A (2000) Degradation and *de novo* synthesis of D1 protein and *psb*A transcript in *Chlamydomonas reinhardtii* during UVB inactivation of photosynthesis. Journal of Biosciences 25:65–71.

Choi BY, Roh KS (2003) UVB radiation affects chlorophyll and activation of Rubisco by Rubisco activase in *Canavalia ensiformis* L. leaves. Journal of Plant Biology 46:117-121.

Choo K, Snoeijs P, Pedersén M (2004) Oxidative stress tolerance in the filamentous green algae *Cladophora glomerata* and *Enteromorpha ahlneriana*. Journal of Experimental Marine Biology and Ecology 298:111-123.

Clendennen SK, Zimmerman RC, Powers DA, Alberte RS (1996) Photosynthetic response of the giant kelp *Macrocystis pyrifera* (Phaeophyceae) to ultraviolet radiation. Journal of Phycology 32:614-620.

Cohen I, Knopf JA, Irihimovitch V, Shapira M (2005) A proposed mechanism for the inhibitory effects of oxidative stress on Rubisco assembly and its subunit expression. Plant Physiology 137:738–746.

Coleman JS, Heckathorn SA, Hallberg RL (1995) Heat-shock proteins and thermotolerance: Linking molecular and ecological perspectives. Trends in Ecology and Evolution 10:305-306.

Collén J, Davison IR (1999) Reactive oxygen metabolism in intertidal *Fucus* spp. (Phaeophyceae). Journal of Phycology 35:62–69.

Collén J, Pedersén M (1996) Production, scavenging and toxicity of hydrogen peroxide in the green seaweed *Ulva rigida*. European Journal of Phycology 31:265-271.

Cordi B, Depledge MH, Price DN, Salter LF, Donkin ME (1997) Evaluation of chlorophyll fluorescence, *in vivo* spectrophotometric pigment absorption and ion leakage as biomarkers of UV-B exposure in marine macroalgae. Marine Biology 130:41-49.

Cordi B, Hyde P, Donkin ME, Price DN, Depledge MH (1999) Evaluation of *in vivo* thallus absorptance and chlorophyll fluorescence as biomarkers of UV-B exposure and effects in marine macroalgae from different tidal levels. Marine Environmental Research 48:193-212.

Cruz S, Serôdio J (2008) Relationship of rapid light curves of variable fluorescence to photoacclimation and non-photochemical quenching in benthic diatom. Aquatic Botany 88:256-264.

Dahlback A (2002) Ozone depletion and UV radiation in the Arctic. In: Hessen DO (ed.) UV Radiation and Arctic Ecosystems, Ecological Studies Vol. 153. Springer, Berlin: pp. 1-22.

Dalle-Donne I, Rossi R, Giustarini D, Colombo R, Mizani A (2003) Actin S-glutathionylation: Evidence against a thiol-disulphide exhange mechanism. Free Radical Biology and Medicine 35:1185-1193.

Dau H (1994) Short-term adaptation of plants to changing light intensities and its relation to photosystem II photochemistry and fluorescence emission. Journal of Photochemistry and Photobiology B: Biology 26:3-27.

Davies MJ (2003) Singlet oxygen-mediated damage to proteins and its consequences. Biochemical and Biophysical Research Communications 305:761-770.

Davies MJ, Truscott RJ (2001) Photo-oxidation of proteins and its role in cataractogenesis. Journal of Photochemistry and Photobiology B: Biology 63:114-125.

Day TA, Howells BW, Rice WJ (1994) Ultraviolet absorption and epidermal-transmittance spectra in foliage. Physiologia Plantarum 92:207-218.

Delphin E, Duval J-C, Etienne A-L, Kirilovsky D (1996) State transitions or ΔpH-dependent quenching of photosystem II fluorescence in red algae. Biochemistry 35:9435–9445.

Demmig-Adams B, Adams WW, Barker DH, Logan BA, Bowling DR, Verhoeven AS (1996) Using chlorophyll fluorescence to assess the fraction of absorbed light allocated to thermal dissipation of excess excitation. Physiologia Plantarum 98:253–264.

Diffey BL (2002) Sources and measurement of ultraviolet radiation. Methods 28:4-13.

Dittami SM, Scornet D, Petit J-L, Ségurens B, Da Silva C, Corre E, Dondrup M, Glatting K-H, König R, Sterck L, Rouzé P, Peer Y, Cock JM, Boyen C, Tonon T (2009) Global expression analysis of the brown alga *Ectocarpus siliculosis* (Phaeophyceae) reveals large-scale reprogramming of the transcriptome in response to abiotic stress. Genome Biology 10:R66.

Döhler G, Hoffmann M, Stappel U (1995) Pattern of proteins after heat shock and UVB radiation of some temperate diatoms and the Antarctic *Odontella weisflogii*. Botanica Acta 108:93-98.

Douady D, Rousseau B, Berkaloff C (1993) Isolation and characterization of PSII core complexes from a brown alga, *Laminaria saccharina.* FEBS Letters 324:22-26.

Douglas SE, Raven JA, Larkum AWD (2003) The algae and their general characteristics. In: Larkum AWD, Douglas SE, Raven JA (eds.) Photosynthesis in Algae. Kluwer Academic Publishers, The Netherlands: pp. 1-10.

Dring MJ (1992) Photosynthesis in the sea. In: The Biology of Marine Plants. Cambridge University Press, Cambridge: pp. 43-66.

Dring MJ, Wagner A, Boeskov J, Lüning K (1996) Sensitivity of intertidal and subtidal red algae to UVA and UVB radiation, as monitored by chlorophyll fluorescence measurements: Influence of collection depth and season, and length of irradiation. European Journal of Phycology 31:293-302.

Dring MJ, Wagner A, Lüning K (2001) Contribution of the UV component of natural sunlight to photoinhibition of photosynthesis in six species of subtidal brown and red seaweeds. Plant, Cell and Environment 24:1153–1164.

Dummermuth AL, Karsten U, Fisch KM, König GM, Wiencke C (2003) Responses of marine macroalgae to hydrogen-peroxide stress. Journal of Experimental Marine Biology and Ecology 289:103-121.

Dunlap WC, Yamamoto Y (1995) Small-molecule antioxidants in marine organisms: antioxidant activity of mycosporine-glycine. Comparative Biochemistry and Physiology B 112:105-114.

Dytham C (2003) Choosing and Using Statistics: A Biologist's Guide, 2nd edn. Blackwell Publishing, UK. 248 p.

Ellis RJ (1979) Most abundant protein in the world. Trends in Biochemical Sciences 4:241-244.

Falshaw R, Furneaux RH, Stevenson DE (1998) Agars from nine species of red seaweed in the genus *Curdiea* (Gracilariaceae, Rhodophyta). Carbohydrate Research 308:107-115.

Feder ME, Hofmann GE (1999) Heat-shock proteins, molecular chaperones and the stress response: Evolutionary and ecological physiology. Annual Review of Physiology 61:243-282.

Ferreira RMB, Franco E, Teixeira ARN (1996) Covalent dimerization of ribulose bisphosphate carboxylase subunits by UV radiation. Biochemical Journal 318:227-234.

Figueroa FL, Gómez I (2001) Photosynthetic acclimation to solar UV radiation of marine red algae from the warm-temperate coast of southern Spain: A review. Journal of Applied Phycology 13:235-248.

Figueroa FL, Nygård C, Ekelund N, Gómez I (2003) Photobiological characteristics and photosynthetic UV responses in two *Ulva* species (Chlorophyta) from southern Spain. Journal of Photochemistry and Photobiology B: Biology 72:35–44.

Flores-Moya A, Hanelt D, Figueroa F-L, Altamirano M, Viñegla B, Salles S (1999) Involvement of solar UV-B radiation in recovery of inhibited photosynthesis in the brown alga *Dictyota dichotoma* (Hudson) Lamouroux. Journal of Photochemistry and Photobiology B: Biology 49:129-135.

Förster B, Mathesius U, Pogson BJ (2006) Comparative proteomics of high light stress in the model alga *Chlamydomonas reinhardtii*. Proteomics 6:4309–4320.

Franco R, Sánchez-Olea R, Reyes-Reyes EM, Panayiotidis MI (2009) Environmental toxicity, oxidative stress and apoptosis: Ménage à Trois. Mutation Research/Genetic Toxicology and Environmental Mutagenesis 674:3-22.

Franklin LA, Forster RM (1997) The changing irradiance environment: consequences for marine macrophyte physiology, productivity and ecology. European Journal of Phycology 32:207-232.

Franklin LA, Osmond CB, Larkum AWD (2003) Photoinhibition, UV-B and algal photosynthesis. In: Larkum AWD, Douglas SE, Raven JA (eds.) Photosynthesis in Algae. Kluwer Academic Publishers, The Netherlands: pp. 351-384.

Fredersdorf J, Bischof K (2007) Irradiance of photosynthetically active radiation determines ultraviolet-susceptibility of photosynthesis in *Ulva lactuca* L. (Chlorophyta). Phycological Research 55:295–301.

Freeman ML, Borrelli MJ, Meredith MJ, Lepock JR (1999) On the path to the heat shock response: Destabilization and formation of partially folded protein intermediates, a consequence of protein thiol modification. Free Radical Biology and Medicine 26:737-745.

Friso G, Barbato R, Giacometti GM, Barber J (1994a) Degradation of D2 protein due to UV-B irradiation of the reaction centre of photosystem II. FEBS Letters 339:217-221.

Friso G, Spetea C, Giacometti GM, Vass I, Barbato R (1994b) Degradation of the photosystem II reaction centre D1-protein induced by UVB radiation in isolated thylakoids. Identification and characterization of C- and N-terminal breakdown products. Biochimica et Biophysica Acta 1184:78-84.

Friso G, Vass I, Spetea C, Barber J, Barbato R (1995) UVB-induced degradation of the D1 protein in isolated reaction centres of photosystem II. Biochimica et Biophysica Acta 1231:41-46.

Fu W, Yao J, Wang X, Liu F, Fu G, Duan D (2009) Molecular cloning and expression analysis of a cytosolic Hsp70 gene from *Laminaria japonica* (Laminariaceae, Phaeophyta). Marine Biotechnology 11:738-747.

Gao K, Guan W, Helbling EW (2007) Effects of solar ultraviolet radiation on photosynthesis of the marine red tide alga *Heterosigma akashiwo* (Raphidophyceae). Journal of Photochemistry and Photobiology B: Biology 86:140-148.

García-Plazaola JI, Matsubara S, Osmond CB (2007) The lutein epoxide cycle in higher plants: Its relationships to other xanthophyll cycles and possible functions. Functional Plant Biology 34:759–773.

Georgopoulos C, Welch WJ (1993) Role of the major heat shock proteins as molecular chaperones. Annual Review in Cell Biology 9:601-634.

Gerard VA, Driscoll T (1996) A spectrophotometric assay for Rubisco activity: application to the kelp *Laminaria saccharina* and implications for radiometric assays. Journal of Phycology 32:880-884.

Gómez I, Figueroa FL (1998) Effects of solar UV stress on chlorophyll fluorescence kinetics of intertidal macroalgae from southern Spain: a case study in *Gelidium* species. Journal of Applied Phycology 10:285–294.

Gómez I, Figueroa FL, Huovinen P, Ulloa N, Morales V (2005) Photosynthesis of the red alga *Gracilaria chilensis* under natural solar radiation in an estuary in southern Chile. Aquaculture 244:369–382.

Gómez I, Figueroa FL, Ulloa N, Morales V, Lovengreen C, Huovinen P, Hess S (2004) Patterns of photosynthesis in 18 species of intertidal macroalgae from southern Chile. Marine Ecology Progress Series 270:103–116.

Gómez I, Pérez-Rodriguez E, Viñegla B, Figueroa FL, Karsten U (1998) Effects of solar radiation on photosynthesis, UV-absorbing compounds and enzyme activities of the green alga *Dasycladus vermicularis* from southern Spain. Journal of Photochemistry and Photobiology B: Biology 47:46-57.

Goss R, Mewes H, Wilhelm C (1999) Stimulation of the diadinoxanthin cycle by UV-B radiation in the diatom *Phaeodactylum tricornutum*. Photosynthesis Research 59:73-80.

Govindjee (2002) A role for a light-harvesting antenna complex of photosystem II in photoprotection. Plant Cell 14:1663-1667.

Greenberg BM, Gaba V, Canaani O, Malkin S, Mattoo AK, Edelman M (1989) Separate photosensitizers mediate degradation of the 32-kDa photosystem II reaction centre protein in the visible and UV spectral regions. Proceedings of the National Academy of Sciences USA 86:6617-6620.

Gröniger A, Sinha RP, Klisch M, Häder D-P (2000) Photoprotective compounds in cyanobacteria, phytoplankton and macroalgae – a database. Journal of Photochemistry and Photobiology B: Biology 58:115–122.

Grossman AR, Schaefer MR, Chiang GG, Collier JL (1993) The phycobilisome, a light-harvesting-complex responsive to environmental conditions. Microbiological Reviews 57:725-749.

Häder D-P (2000) Effects of solar UV-B radiation on aquatic ecosystems. Advances in Space Research 26:2029-2040.

Häder D-P, Gröniger A, Hallier C, Lebert M, Figueroa FL, Jiménez C (1999) Photoinhibition by visible and ultraviolet radiation in the red macroalga *Porphyra umbilicalis* grown in the laboratory. Plant Ecology145:351–358.

Häder D-P, Helbling EW, Barbieri ES, Lebert M, Sinha RP (2003a) Effects of solar radiation on phycobiliproteins of marine red algae. Trends in Photochemistry and Photobiology 10:149-157.

Häder D-P, Kumar HD, Smith RC, Worrest RC (1998a) Effects on aquatic ecosystems. Journal of Photochemistry and Photobiology B: Biology 46:53-68.

Häder D-P, Lebert M, Figueroa FL, Jiménez C, Viñegla B, Perez-Rodriguez E (1998b) Photoinhibition in Mediterranean macroalgae by solar radiation measured on site by PAM fluorescence. Aquatic Botany 61:225-236.

Häder D-P, Lebert M, Flores-Moya A, Jiménez C, Mercado J, Salles S, Aguilera J, Figueroa FL (1997a) Effects of solar radiation on the photosynthetic activity of the red alga *Corallina elongata* Ellis et Soland. Journal of Photochemistry and Photobiology B: Biology 37:196-202.

Häder D-P, Lebert M, Helbling EW (2001a) Effects of solar radiation on the Patagonian macroalga *Enteromorpha linza* (L.) J. Agardh — Chlorophyceae. Journal of Photochemistry and Photobiology B: Biology 62:43–54.

Häder D-P, Lebert M, Helbling EW (2003b) Effects of solar radiation on the Patagonian rhodophyte *Corallina officinalis* (L.) Photosynthesis Research 78:119–132.

Häder D-P, Lebert M, Helbling EW (2004) Variable fluorescence parameters in the filamentous Patagonian rhodophytes, *Callithamnion gaudichaudii* and *Ceramium* sp. under solar radiation. Journal of Photochemistry and Photobiology B: Biology 73:87–99.

Häder D-P, Lebert M, Sinha RP, Barbieri ES, Helbling EW (2002) Role of protective and repair mechanisms in the inhibition of photosynthesis in marine macroalgae. Photochemical and Photobiological Sciences 1:809–814.

Häder D-P, Porst M, Herrmann H, Schäfer J, Santas R (1997b) Photosynthesis of mediterranean green alga *Caulerpa prolifera* measured in the field under solar irradiation. Journal of Photochemistry and Photobiology B: Biology 37:66-73.

Häder D-P, Porst M, Lebert M (2001b) Photosynthetic performance of the Atlantic brown macroalgae, *Cystoseira abies-marina*, *Dictyota dichotoma* and *Sargassum vulgare*, measured in Gran Canaria on site. Environmental and Experimental Botany 45:21–32.

Häder D-P, Porst M, Santas R (1998c) Photoinhibition by solar radiation in the Mediterranean alga *Peyssonnelia squamata* measured on site. Plant Ecology 139:167–175.

Häder D-P, Sinha RP (2005) Solar ultraviolet radiation-induced DNA damage in aquatic organisms: potential environmental impact. Mutation Research/Fundamental and Molecular Mechanisms of Mutagenesis 571:221-233.

Hakala M, Tuominen I, Keränen M, Tyystjärvi T, Tyystjärvi E (2005) Evidence for the role of the oxygen-evolving manganese complex in photoinhibition of photosystem II. Biochimica et Biophysica Acta 1706:68-80.

Häkkinen J, Vehniäinen E, Oikari A (2004) High sensitivity of northern pike larvae to UVB but no UV-photoinduced toxicity of retene. Aquatic Toxicology 66:393-404.

Han B-P (2002) A mechanistic model of algal photoinhibition induced by photodamage to photosystem-II. Journal of Theoretical Biology 214:519-527.

Han T, Han Y-S (2005) UV-B induction of UV-B protection in *Ulva pertusa* (Chlorophyta). Journal of Phycology 41:523-530.

Han T, Han Y-S, Kain JM, Häder D-P (2003) Thallus differentiation of photosynthesis, growth, reproduction, and UV-B sensitivity in the green alga *Ulva pertusa* (Chlorophyceae). Journal of Phycology 39:712-721.

Han T, Sinha RP, Häder D-P (2001) UV-A/blue light-induced reactivation of photosynthesis in UV-B irradiated cyanobacterium, *Anabaena* sp.. Journal of Plant Physiology 158:1403–1413.

Hancock JT, Henson D, Nyirenda M, Desikan R, Harrison J, Lewis M, Hughes J, Neill SJ (2005) Proteomic identification of glyceraldehyde-3-phosphate dehydrogenase as an inhibitory target of hydrogen peroxide in *Arabidopsis*. Plant Physiology and Biochemistry 43:828–835.

Hanelt D (1996) Photoinhibition of photosynthesis in marine macroalgae. Scientia Marina 60(Suppl 1):243-248.

Hanelt D (1998) Capability of dynamic photoinhibition in Arctic macroalgae is related to their depth distribution. Marine Biology 131:361-369.

Hanelt D, Hawes I, Rae R (2006) Reduction of UV-B radiation causes an enhancement of photoinhibition in high light stressed aquatic plants from New Zealand lakes. Journal of Photochemistry and Photobiology B: Biology 84:89-102.

Hanelt D, Nultsch W (1990) Daily changes of the phaeoplast arrangement in the brown alga *Dictyota dichotoma* as studied in field experiments. Marine Ecology Progress Series 61:273-279.

Hanelt D, Nultsch W (1991) The role of chromatophore arrangement in protecting the chromatophores of the brown alga *Dictyota dichotoma* against photodamage. Journal of Plant Physiology 138:470-475.

Hanelt D, Roleda MY (2009) UVB radiation may ameliorate photoinhibition in specific shallow-water tropical marine macrophytes. Aquatic Botany 91:6–12.

Hanelt D, Tüg H, Bischof K, Gross C, Lippert H, Sawall T, Karsten U, Wiencke C (2000) Light regime in an Arctic fjord: A study related to stratospheric ozone depletion as a basis for determination of UV effects on algal growth. Marine Biology 138:649-658.

Hanelt D, Wiencke C, Bischof K (2003) Photosynthesis in marine macroalgae. In: Larkum AWD, Douglas SE and Raven JA (eds.) Photosynthesis in Algae. Kluwer Academic Publisher, The Netherlands: pp. 413-435.

Hanelt D, Wiencke C, Nultsch W (1997) Influence of UV radiation on the photosynthesis of Arctic macroalgae in the field. Journal of Photochemistry and Photobiology B: Biology 38:40-47.

Haugan JA, Liaaen-Jensen S (1994) Algal carotenoids 54. Carotenoids of brown algae (Phaeophyceae). Biochemical Systematics and Ecology 22:31-41.

Havaux M, Niyogi KK (1999) The violaxanthin cycle protects plants from photooxidative damage by more than one mechanism. Proceedings of the National Academy of Science USA 96:8762–8767.

He Y-Y, Häder D-P (2002) Reactive oxygen species and UV-B: Effect on cyanobacteria. Photochemical and Photobiological Sciences 1:729-736.

Heckathorn SA, Downs CA, Coleman JS (1999) Small heat shock proteins protect electron transport in chloroplasts and mitochondria during stress. American Zoologist 39:865–876.

Heckathorn SA, Mueller JK, LaGuidice S, Zhu B, Barrett T, Blair B, Yan Dong (2004) Chloroplast small heat-shock proteins protect photosynthesis during heavy metal stress. American Journal of Botany 91:1312-1318.

Heelis PF, Hartman RF, Rose SD (1995) Photoenzymic repair of UV-damaged DNA: A chemist's perspective. Chemistry Society Reviews 24:289–297.

Heinz Walz GmbH (2003) Portable Chlorophyll Fluorometer PAM-2100: Handbook of Operation. Heinz Walz GmbH, Germany. 195 pp.

Helbling EW, Barbieri ES, Sinha RP, Villafañe VE, Häder D-P (2004) Dynamics of potentially protective compounds in Rhodophyta species from Patagonia (Argentina) exposed to solar radiation. Journal of Photochemistry and Photobiology B: Biology 75:63–71.

Helmig D, Oltmans SJ, Carlson D, Lamarque J-F, Jones A, Labuschagne C, Anlauf K, Hayden K (2007) A review of surface ozone in the polar regions. Atmospheric Environment 41:5138-5161.

Henkel SK, Hofmann GE (2008) Differing patterns of *hsp70* gene expression in invasive and native kelp species: Evidence for acclimation-induced variation. Journal of Applied Phycology 20:915-924.

Henley WJ (1993) Measurement and interpretation of photosynthetic light response curves in algae in the context of photoinhibition and diel changes. Journal of Phycology 29:729–739.

Heo S-J, Jeon Y-J (2009) Protective effect of fucoxanthin isolated from *Sargassum siliquastrum* on UV-B induced cell damage. Journal of Photochemistry and Photobiology B: Biology 95:101-107.

Heo S-J, Ko S-C, Kang S-M, Kang H-S, Kim J-P, Kim S-H, Lee K-W, Cho M-G, Jeon Y-J (2008) Cytoprotective effect of fucoxanthin isolated from brown algae *Sargassum siliquastrum* against H_2O_2-induced cell damage. European Food Research and Technology A 288:145-151.

Heredia P, de Las Rivas J (2003) Fluorescence induction of Photosystem II membranes shows the steps till reduction and protonation of the quinone pool. Journal of Plant Physiology 160:1499–1506.

Hernández J, Escobar C, Creissen G, Mullineaux P (2006) Antioxidant enzyme induction in pea plants under high irradiance. Biologia Plantarum 50:395-399.

Herrmann H, Häder D-P, Köfferlein M, Seidlitz HK, Ghetti F (1996) Effects of UV radiation on photosynthesis of phytoplankton exposed to solar simulator light. Journal of Photochemistry and Photobiology B: Biology 34:21-28.

Hideg E, Kálai T, Hideg K, Vass I (2000) Do oxidative stress conditions impairing photosynthesis in the light manifest as photoinhibition? Philosophical Transactions of the Royal Society B 355:1511-1516.

Hollósy F (2002) Effects of ultraviolet radiation on plant cells. Micron 33:179-197.

Holm-Hansen O, Lubin D, Helbling EW (1993) Ultraviolet radiation and its effects on organisms in aquatic environments. In: Young AR, Bjorn LO, Moan J, Nultsch W (eds.) Environmental UV Photobiology. Plenum Press, New York: pp. 379–425.

Holt NE, Fleming GR, Niyogi KK (2004) Toward an understanding of the mechanism of nonphotochemical quenching in green plants. Biochemistry 43:8281-8289.

Holzinger A, Lütz C (2006) Algae and UV irradiation: Effects on ultrastructure and related metabolic functions. Micron 37:190-207.

Holzinger A, Lütz C, Karsten U, Wiencke C (2004) The effect of ultraviolet radiation on ultrastructure and photosynthesis in the red macroalgae *Palmaria palmata* and *Odonthalia dentata* from Arctic waters. Plant Biology 6:568–577.

Horton P, Ruban AV, Walters RG (1994) Regulation of light harvesting in green plants: Indication by nonphotochemical quenching of chlorophyll fluorescence. Plant Physiology 106:415-420.

Horton P, Ruban AV, Walters RG (1996) Regulation of light harvesting in green plants. Annual Review of Plant Physiology 47:655-684.

Houtz RL, Portis Jr AR (2003) The life of ribulose 1,5-bisphosphate carboxylase/oxygenase – posttranslational facts and mysteries. Archives of Biochemistry and Biophysics 414:150-158.

Huner NPA, Maxwell DP, Gray GR, Savitch LV, Krol M, Ivanov AG, Falk S (1996) Sensing environmental temperature change through imbalances between energy supply and energy consumption: Redox state of photosystem II. Physiologia Plantarum 98:358-364.

Hynninen PH (1991) Modifications. In: Scheer H (ed.) Chlorophylls. CRC Press, Boca Raton: pp. 145-209.

Igarashi N, Onoue S, Tsuda Y (2007) Photoreactivity of amino acids: Tryptophan-induced photochemical events *via* reactive oxygen species generation. Analytical Sciences 23:943-948.

Inskeep WP, Bloom PR (1985) Extinction coefficients of chlorophyll *a* and *b* in *N,N*-dimethylformamide and 80% acetone. Plant Physiology 77:483-485.

Ireland HE, Harding SJ, Bonwick GA, Jones M, Smith CJ, Williams JHH (2004) Evaluation of heat shock protein 70 as a biomarker of environmental stress in *Fucus serratus* and *Lemna minor*. Biomarkers 9:139-155.

Ivanov AG, Miskiewicz E, Clarke AK, Greenberg BM, Huner NPA (2000) Protection of photosystem II against UVA and UVB radiation in the cyanobacterium *Plectonema boryanum:* the role of growth temperature and growth irradiance. Photochemistry and Photobiology 72:772–779.

Ivanov AG, Sane PV, Hurry V, Öquist G, Huner NPA (2008) Photosystem II reaction centre quenching: Mechanisms and physiological role. Photosynthesis Research 98:565-574.

Ivey III RA, Subramanian C, Bruce BD (2000) Identification of a Hsp70 recognition domain within the Rubisco small subunit transit peptide. Plant Physiology 122:1289–1299.

Jackson-Constan D, Akita M, Keegstra K (2001) Molecular chaperons involved in chloroplast proteins import. Biochimica et Biophysica Acta 1541:102–113.

Jassby AD, Platt T (1976) Mathematical formulation of the relationship between photosynthesis and light for phytoplankton. Limnology and Oceanography 21:540–547.

Ji BH, Jiao DM (2000) Relationships between D1 protein, xanthophyll cycle and photodamage resistant capacity in rice (*Oryza sativa L.*). Chinese Science Bulletin 45:1569-1575.

Jin ES, Yokthongwattana K, Polle JEW, Melis A (2003) Role of the reversible xanthophyll cycle in the photosystem II damage and repair cycle in *Dunaliella salina*. Plant Physiology 132:352–364.

Johansson G, Snoeijs P (2002) Macroalgal photosynthetic responses to light in relation to thallus morphology and depth zonation. Marine Ecology Progress Series 244:63-72.

Johnson GA, Day TA (2002) Enhancement of photosynthesis in *Sorghum bicolour* by ultraviolet radiation. Physiologia Plantarum 116:554–562.

Jordan BR (2002) Molecular response of plant cells to UV-B stress. Functional Plant Biology 29:909-916.

Jordan BR, He J, Chow WS, Anderson JM (1992) Changes in mRNA levels and polypeptide subunits of ribulose-1,5-bisphophate carboxylase in response to supplementary ultraviolet B radiation. Plant, Cell and Environment 15:91-98.

Joshi PN, Ramaswamy NK, Iyer RK, Nair JS, Pradhan MK, Gartia S, Biswal B, Biswal UC (2007) Partial protection of photosynthetic apparatus from UV-B-induced damage by UV-A radiation. Environmental and Experimental Botany 59:166-172.

Kakani VG, Reddy KR, Zhao D, Sailaja K (2003) Field crop responses to ultraviolet-B radiation: A review. Agricultural and Forest Meteorology 120:191-218.

Kane RP (2008) Is ozone depletion really recovering?. Journal of Atmospheric and Solar-Terrestrial Physics 70:1455-1459.

Karsten U, Franklin LA, Lüning K, Wiencke C (1998) Natural ultraviolet radiation and photosynthetically active radiation induce formation of mycosporine-like amino acids in the marine macroalga *Chondrus crispus* (Rhodophyta). Planta 205:257-262.

Keiller DR, Mackerness SA, Holmes MG (2003) The action of a range of supplementary ultraviolet wavelengths on photosynthesis in *Brassica napus* L. in the natural environment: effects on PSII, CO_2 assimilation and level of chloroplast proteins. Photosynthesis Research 75:139-150.

Keren N, Berg A, van Kan PJM, Levanon H, Ohad I (1997) Mechanism of photosystem II photoinactivation and D1 protein degradation at low light: the role of back electron flow. Proceedings of the National Academy of Sciences USA 94:1579–1584.

Kettunen R, Tyystjärvi E, Aro E-M (1996) Degradation pattern of photosystem II reaction centre protein D1 in intact leaves: The major photoinhibition-induced cleavage site in D1 polypeptide is located amino terminally of the DE loop. Plant Physiology 111:1183-1190.

Kirilovsky D (2007) Photoprotection in cyanobacteria: The orange carotenoid protein (OCP)-related non-photochemical-quenching mechanism. Photosynthesis Research 93:7-16.

Knopf JA, Shapira M (2005) Degradation of Rubisco SSU during oxidative stress triggers aggregation of Rubisco particles in *Chlamydomonas reinhardtii*. Planta 222:787-793.

Kovács E, Keresztes Á (2002) Effect of gamma and UV-B/C radiation on plant cells. Micron 33:199-210.

Kräbs G, Bischof K, Hanelt D, Karsten U, Wiencke C (2002) Wavelength-dependent induction of UV-absorbing mycosporine-like amino acids in the red alga *Chondrus crispus* under natural solar radiation. Journal of Experimental Marine Biology and Ecology 268:69-82.

Krause GH, Weis E (1991) Chlorophyll fluorescence and photosynthesis: The basics. Annual Review of Plant Physiology and Plant Molecular Biology 42:313-349.

Krieger-Liszkay A, Fufezan C, Trebst A (2008) Singlet oxygen production in photosystem II and related protection mechanism. Photosynthesis Research 98:551-564.

Kropat J, Oster U, Rüdiger W, Beck CF (1997) Chlorophyll precursors are signals of chloroplast origin involved in light induction of nuclear heat-shock genes. Proceedings of the National Academy of Sciences USA 94:14168-14172.

Laemmli UK (1970) Cleavage of structural proteins during assembly of the head of bacteriophage T4. Nature 227:680-685.

Lao K, Glazer AN (1996) Ultraviolet-B photodestruction of a light-harvesting complex. Proceedings of the National Academy of Sciences USA 93:5258-5263.

Lazár D (1999) Chlorophyll a fluorescence induction. Biochimica et Biophysica Acta 1412:1-28.

Lee T-S, Shiu C-T (2009) Implications of mycosporine-like amino acid and antioxidant defences in UVB radiation tolerance for the algae species *Ptercladiella capillacea* and *Gelidium amansii*. Marine Environmental Research 67:8–16.

Lesser MP (2006) Oxidative stress in marine environments: Biochemistry and physiological ecology. Annual Review of Physiology 68:253-278.

Lewis S, Donkin ME, Depledge MH (2001) Hsp70 expression in *Enteromorpha intestinalis* (Chlorophyta) exposed to environmental stressors. Aquatic Toxicology 51:277-291.

Li R, Brawley SH (2004) Improved survival under heat stress in intertidal embryos (*Fucus* spp.) simultaneously exposed to hypersalinity and the effect of parental thermal history. Marine Biology 144:205–213.

Little EE, Fabacher D (2003) UVR-induced injuries in freshwater vertebrates. In: Helbling EW, Zagareses H (eds.) UV Effects in Aquatic Organisms and Ecosystem. Royal Society of Chemistry Publishing, Cambridge: pp. 431-154.

Lohr M, Wilhelm C (1999) Algae displaying the diadinoxanthin cycle also possess the violaxanthin cycle. Proceedings of the National Academy of Science USA 96:8784-8789.

Long SP, Humphries S, Falkowski PG (1994) Photoinhibition of photosynthesis in nature. Annual Review of Plant Physiology and Plant Molecular Biology 45:633-662.

Lorenz M, Schubert H, Forster RM (1997) *In vitro*- and *in vivo* effects of ultraviolet B radiation on the energy transfer in phycobilisomes. Photosynthetica 33:517–527.

Lüning K (1990) Seaweeds: Their Environment, Biogeography and Ecophysiology. John Wiley and Sons, NY: pp.3-21.

Mackerness SAH, John CF, Jordan BR, Thomas B (2001) Early signalling components in ultraviolet-B responses: distinct roles for different reactive oxygen species and nitric oxide. FEBS Letters 489:237-242.

Mackerness SAH, Jordan BR, Thomas B (1999) Reactive oxygen species in the regulation of photosynthetic genes by ultraviolet B radiation (UV-B: 280–320 nm) in green and etiolated buds of pea (*Pisum sativum* L.). Journal of Photochemistry and Photobiology B: Biology 48:180-188.

Madueno F, Napier JA, Gray JC (1993) Newly imported Rieske Iron-Sulfur protein associates with both Cpn60 and Hsp70 in the chloroplast stroma. Plant Cell 5:1865-1876.

Marquardt J, Hanelt D (2004) Carotenoid composition of *Delesseria lancifolia* and other marine red algae from polar and temperate habitats. European Journal of Phycology 39:285-292.

Masojídek J, Kopecký J, Koblížek M, Torzillo G (2004) The xanthophyll cycle in green algae (Chlorophyta): Its role in the photosynthetic apparatus. Plant Biology 6:34-349.

Máté Z, Sass L, Szekeres M, Vass I, Nagy F (1998) UVB induced differential transcription of psbA genes encoding the D1 protein of photosystem II in the cyanobacterium *Synechocystis* 6803. Journal of Biological Chemistry 273:17439–17444.

Maxwell DP, Falk S, Huner N (1995) Photosystem II excitation pressure and development of resistance to photoinhibition (I. Light-Harvesting Complex II abundance and zeaxanthin content in *Chlorella vulgaris*). Plant Physiology 107:687-694.

Maxwell K, Johnson GN (2000) Chlorophyll fluorescence – a practical guide. Journal of Experimental Botany 51:659-668.

McKenzie R, Smale D, Kotkamp M (2004) Relationship between UVB and erythemally weighted radiation. Photochemical and Photobiological Sciences 3:252-256.

Melis A (1999) Photosystem-II damage and repair cycle in chloroplasts: what modulates the rate of photodamage *in vivo*? Trends in Plant Science 4:130-135.

Melis A, Nemson JA, Harrison MA (1992) Damage to functional components and partial degradation of photosystem II reaction centre proteins upon chloroplast exposure to ultraviolet B radiation. Biochimica et Biophysica Acta 1100:312–320.

Merzlyak MN, Pogosyan SI, Lekhimena L, Zhigalova TV, Khozina IF, Cohen Z, Khrushchev SS (1996) Spectral characterization of photooxidation products formed in Chl solution and upon photodamage to the cyanobacterium *Anabaena variabilis.* Russian Journal of Plant Physiology 43:160–168.

Michelet L, Zaffagnini M, Marchand C, Collin V, Decottignies P, Tsan P, Lancelin J-M, Trost P, Miginiac-Maslow M, Noctor G, Lemaire SD (2005) Glutathionylation of chloroplast thioredoxin f is a redox signalling mechanism in plants. Proceedings of the National Academy of Sciences USA 102:16748-16483.

Michler T, Aguilera J, Hanelt D, Bischof K, Wiencke C (2002) Long-term effects of ultraviolet radiation on growth and photosynthetic performance of polar and cold-temperate macroalgae. Marine Biology 140:1117-1127.

Miller-Morey JS, Van Dolah FM (2004) Differential responses of stress proteins, antioxidant enzymes, and photosynthetic efficiency to physiological stresses in the Florida red tide dinoflagellate, *Karenia brevis*. Comparative Biochemistry and Physiology C: Toxicology and Pharmacology 138:493-505.

Mimuro M, Katoh T (1991) Carotenoids in photosynthesis: Absorption, transfer and dissipation of light energy. Pure and Applied Chemistry 63:123-130.

Mishra NP, Fatma T, Singhal GS (1995) Development of antioxidative defence system of wheat seedlings in response to high light. Physiologia Plantarum 95:77-82.

Miyake C, Horiguchi S, Makino A, Shinzaki Y, Yamamoto H, Tomizawa K (2005) Effects of light intensity on cyclic electron flow around PSI and its relationship to non-photochemical quenching of Chl fluorescence in tobacco leaves. Plant and Cell Physiology 46:1819-1830.

Miyake C, Shinzaki Y, Miyata M, Tomizawa K (2004) Enhancement of cyclic electron flow around PSI at high light and its contribution to the induction of non-photochemical quenching of chl fluorescence in intact leaves of tobacco plants. Plant and Cell Physiology 45:1426-1433.

Miyake C, Yonekura K, Kobayashi Y, Yokota A (2002) Cyclic electron flow within PSII functions in intact chloroplasts from spinach leaves. Plant and Cell Physiology 43:951-957.

Montero O, Lubián LM (2003) Mycosporine-like amino acids (MAAs) production by *Heterocapsa* sp. (Dinophyceae) in indoor cultures. Biomolecular Engineering 20:183-189.

Müller P, Li X-P, Niyogi KK (2001) Non-photochemical quenching. A response to excess light energy. Plant Physiology 125:1558–1566.

Murata N, Takahashi S, Nishiyama Y, Allakhverdiev SI (2007) Photoinhibition of photosystem II under environmental stress. Biochimica et Biophysica Acta 1767:414-421.

Murthy KNC, Vanitha A, Rajesha J, Swamy MM, Sowmya PR, Ravishankar GA (2005) *In vivo* antioxidant activity of carotenoids from *Dunaliella salina* — a green microalga. Life Sciences 76:1381-1390.

Nakamoto HN, Suzuki S, Roy R (2000) Constitutive expression of a small heat-shock protein confers cellular thermotolerance and thermal protection to the photosynthetic apparatus in cyanobacteria. FEBS Letters 483:169-174.

Nakano H, Gasparro FP, Uitto J (2001) UVA-340 as energy source, mimicking natural sunlight, activates the transcription factor AP-1 in cultured fibroblasts: evidence for involvement of protein kinase-C. Photochemistry and Photobiology 74:274-281.

Naletova IN, Muronetz VI, Schmalhausen EV (2006) Unfolded, oxidized, and thermoinactivated forms of glyceraldehyde-3-phosphate dehydrogenase interact with the chaperonin GroEL in different ways. Biochimica et Biophysica Acta 1764:831-838.

Necchi Jr O (2004) Light-related photosynthetic characteristics of lotic macroalgae. Hydrobiologia 525:139-155.

Nesatyy VJ, Suter MJF (2007) Proteomics for the analysis of environmental responses in organisms. Environmental Science and Technology 41:6891-6900.

Nishiyama Y, Allakhverdiev SI, Murata N (2006) A new paradigm for the action of reactive oxygen species in the photoinhibition of photosystem II. Biochimica et Biophysica Acta 1757:742-749.

Nishiyama Y, Yamamoto H, Allakhverdiev SI, Inaba M, Yokota A, Murata N (2001) Oxidative stress inhibits the repair of photodamage to the photosynthetic machinery. EMBO Journal 20:5587-5594.

Niyogi KK (1999) Photoprotection revisited: Genetic and molecular approaches. Annual Review of Plant Physiology and Plant Molecular Biology 50:333-359.

Niyogi KK (2000) Safety valves for photosynthesis. Current Opinion in Plant Biology 3:455-460.

Niyogi KK, Björkman O, Grossman AR (1997) The roles of specific xanthophylls in photoprotection. Proceedings of the National Academy of Science USA 94:14162-14167.

Nobel PS (2005) Photochemistry of photosynthesis. In: Physichochemical and Environmental Plant Physiology, 3rd edn. Academic Press, London: pp. 219-266.

Noguchi K, Yoshida K (2008) Interaction between photosynthesis and respiration in illuminated leaves. Mitochondrion 8:87-99.

Ohnishi N, Allakhverdiev SI, Takahashi S, Higashi S, Watanabe M, Nishiyama N, Murata N (2005) Two-step mechanism of photodamage to Photosystem II: step 1 occurs at the oxygen-evolving complex and step 2 occurs at the photochemical reaction centre. Biochemistry 44:8494-8499.

Olszówka D, Maksymiec W, Krupa Z, Krawczyk S (2003) Spectral analysis of pigment photobleaching in photosynthetic antenna complex LHCIIb. Journal of Photochemistry and Photobiology B: Biology 70:21-30.

Osmond CB (1994) What is photoinhibition? Some insights from comparisons of shade and sun plants. In: Baker NR, Bowyer JR (eds.) Photoinhihition of Photosynthesis: From Molecular Mechanisms to the Field. BIOS Scientific Publishers Ltd., Oxford: pp. 1-24.

Osmond CB, Badger M, Maxwell K, Björkman O, Leegood R (1997) Too many photons: photorespiration, photoinhibition and photooxidation. Trends in Plant Sciences 2:119–121.

Osmond CB, Grace SC (1995) Perspectives on photoinhibition and photorespiration in the field: quintessential inefficiencies of the light and dark reactions of photosynthesis? Journal of Experimental Botany 46:1351–1362.

Papageorgiou GC, Tsimilli-Michael M, Stamatakis K (2007) The fast and slow kinetics of chlorophyll a fluorescence induction in plants, algae and cyanobacteria: a viewpoint. Photosynthesis Research 94:275-290.

Park Y-I, Chow WS, Anderson JM, Hurry VM (1996) Differential susceptibility of photosystem II to light stress in light-acclimated pea leaves depends on the capacity for photochemical and non-radiative dissipation of light. Plant Science 115:137-150.

Pattison DI, Davies MJ (2006) Actions of ultraviolet light on cellular structures. In: Bignold LP (ed.) Cancer: Cell Structures, Carcinogens and Genomic Instability. Birkhäuser Verlag, Switzerland: pp. 131–157.

Pavia H, Cervin G, Lindgren A, Åberg P (1997) Effects of UVB radiation and simulated herbivory on phlorotannins in the brown alga *Ascophyllum nodosum*. Marine Ecology Progress Series 157:139-146.

Peter T (1994) The stratospheric ozone layer – An overview. Environmental Pollution 83:69-79.

Poppe F, Hanelt D, Wiencke C (2002) Changes in ultrastructure, photosynthetic activity and pigments in the Antarctic red alga *Palmaria decipiens* during acclimation to UV radiation. Botanica Marina 45:253–261.

Poppe F, Schmidt RAM, Hanelt D, Wiencke C (2003) pEffects of UV radiation on the ultrastructure of several red algae. Phycological Research 51:11-19.

Portis AR Jr (1992) Regulation of ribulose 1,5-bisphosphate carboxylase/oxygenase activity. Annual Review of Plant Physiology and Plant Molecular Biology 43:415-437.

Portis AR Jr. (2003) Rubisco activase – Rubisco's catalytic chaperone. Photosynthesis Research 75:11-27.

Post A, Larkum AWD (1993) UV-absorbing pigments, photosynthesis and UV exposure in Antarctica: comparison of terrestrial and marine algae. Aquatic Botany 45:231-243.

Powles SB (1984) Photoinhibition of photosynthesis induced by visible light. Annual Review of Plant Physiology 35:15-44.

Provasoli L (1968) Media and prospects for the cultivation of marine algae. In: Watanabe A, Hattori A (eds.) Cultures and Collections of Algae. Proceedings of the U.S.-Japan Conference in Hakone, Japan, September 1966. Published by the Japanese Society of Plant Physiologists: pp. 63-75.

Quesada A, Mouget J-L, Vincent WF (1995) Growth of Antarctic cyanobacteria under ultraviolet radiation: UVA counteracts UVB inhibition. Journal of Phycology 31:242-248.

Rae R, Hanelt D, Hawes I (2001) Sensitivity of freshwater macrophytes to UV radiation: Relationship to depth zonation in an oligotrophic New Zealand lake. Marine and Freshwater Research 52:1023-1032.

Ralph PJ, Gademann R (2005) Rapid light curves: A powerful tool to assess photosynthetic activity. Aquatic Botany 82:222–237.

Rascher U, Nedbal L (2006) Dynamics of photosynthesis in fluctuating light. Current Opinion in Plant Biology 9:671-678.

Rautenberger R, Bischof K (2006) Impact of temperature on UV-susceptibility of two *Ulva* (Chlorophyta) species from Antarctic and Subantarctic regions. Polar Biology 29:988-996.

Ravanat J-L, Douki T, Cadet J (2001) Direct and indirect effects of UV radiation on DNA and its components. Journal of Photochemistry and Photobiology B: Biology 63:88-102.

Raven JA, Geider RJ (2003) Adaptation, acclimation and regulation in algal photosynthesis. In: Larkum WA, Douglas E, Raven JA (eds.) Photosynthesis in Algae. Kluwer Academic Publisher, The Netherlands: pp. 385-412.

Ricaud P, Lefévre F (2006) Chapter 1: Fluorine in the atmosphere. Advances in Fluorine Science 1:1-32.

Rinalducci S, Hideg E, Vass I, Zolla L (2006) Effect of moderate UV-B irradiation on Synechocystis PCC 6803 biliproteins. Biochemical and Biophysical Research Communications 341:1105–1112.

Rinalducci S, Pedersen JZ, Zolla L (2008) Generation of reactive oxygen species upon strong visible light irradiation of isolated phycobilisomes from *Synechocystis* PCC 6803. Biochimica et Biophysica Acta 1777:417-424.

Rmiki N-E, Brunet C, Cabioch J, Lemoine Y (1996) Xanthophyll-cycle and photosynthetic adaptation to environment in macro and microalgae. Hydrobiologia 326-327:407-413.

Rodrigues GC, Jansen MAK, van den Noort ME, van Rensen JJS (2006) Evidence for the semireduced primary quinone electron acceptor of photosystem II being a photosensitizer for UVB damage to the photosynthetic apparatus. Plant Science 170:283–290.

Roháček K, Barták M (1999) Technique of the modulated chlorophyll fluorescence: Basic concepts, useful parameters, and some applications. Photosynthetica 37:339-363.

Roleda MY, Dethleff D, Wiencke C (2008) Transient sediment load on blades of Arctic *Saccharina latissima* can mitigate UV radiation effect on photosynthesis. Polar Biology 31:765-769.

Roleda MY, Hanelt D, Kräbs G, Wiencke C (2004a) Morphology, growth, photosynthesis and pigments in *Laminaria ochroleuca* (Laminariales, Phaeophyta) under ultraviolet radiation. Phycologia 43:603-613.

Roleda MY, Hanelt D, Wiencke C (2005) Growth kinetics related to physiological parameters in young *Saccorhiza dermatodea* and *Alaria esculenta* sporophytes exposed to UV radiation. Polar Biology 28:539-549.

Roleda MY, Hanelt D, Wiencke C (2006a) Exposure to ultraviolet radiation delays photosynthetic recovery in Arctic kelp zoospores. Photosynthesis Research 88:311–322.

Roleda MY, Hanelt D, Wiencke C (2006b) Growth and DNA damage in young *Laminaria* sporophytes exposed to ultraviolet radiation: implication for depth zonation of kelps in Helgoland (North Sea). Marine Biology 148:1201-1211.

Roleda MY, van de Poll WH, Hanelt D, Wiencke C (2004b) PAR and UVBR effects on photosynthesis, viability, growth and DNA in different life stages of two coexisting Gigartinales: implications for recruitment and zonation pattern. Marine Ecology Progress Series 281:37–50.

Roleda MY, Wiencke C, Hanelt D (2006c) Thallus morphology and optical characteristics affect growth and DNA damage by UV radiation in juvenile Arctic *Laminaria* sporophytes. Planta 223:407-417.

Roleda MY, Wiencke C, Hanelt D, Bischof K (2007) Sensitivity of the early life stages of macroalgae from the Northern hemisphere to ultraviolet radiation. Photochemistry and Photobiology 83:851-862.

Roy S (2000) Strategies for the minimisation of UV-induced damage. In: de Mora S, Demers S, Vernet M (eds.) The Effects of UV Radiation in the Marine Environment. Cambridge University Press, Cambridge: pp. 177-205.

Runcie JW, Gurgel CFD, Mcdermid KJ (2008) In situ photosynthetic rates of tropical marine macroalgae at their lower depth limit. European Journal of Phycology 43:377-388.

Sachindra NM, Sato E, Maeda H, Hosokawa M, Niwano Y, Kohno M, Miyashita K (2007) Radical scavenging and singlet oxygen quenching activity of marine carotenoid fucoxanthin and its metabolites. Journal of Agricultural and Food Chemistry 55:8516-8522.

Salvucci ME (2008) Association of Rubisco activase with chaperonin-60beta: a possible mechanism for protecting photosynthesis during heat stress. Journal of Experimental Botany 59:1923-1933.

Sancar GB (2000) Enzymatic photoreactivation: 50 years and counting. Mutation Research 451:25-37.

Santabarbara S (2006) Limited sensitivity of pigment photo-oxidation in isolated thylakoids to singlet excited state quenching in photosystem II antenna. Archives of Biochemistry and Biophysics 455:77-88.

Sass L, Spetea C, Máté Z, Nagy F, Vass I (1997) Repair of UVB induced damage of photosystem II *via de novo* synthesis of the D1 and D2 reaction centre subunits in *Synechocystis* sp. PCC 6803. Photosynthesis Research 54:55–62.

Scarpeci TE, Zanor M, Valle EM (2008) Investigating the role of heat shock proteins during oxidative stress. Plant Signalling and Behavior 3:856-857.

Schansker G, Tóth SZ, Strasser RJ (2006) Dark recovery of the Chl a fluorescence transient (OJIP) after light adaptation: The qT-component of non-photochemical quenching is related to an activated photosystem I acceptor side. Biochimica Biophysica Acta 1757:787-797.

Schauffler SM, Heidt LE, Pollock WH, Gilpin TM, Vedder JF, Solomon S, Lueb RA, Atlas EL (1993) Measurements of halogenated organic compounds near the tropical tropopause. Geophysical Research Letters 20:2567–2570.

Schmitz G, Schmidt M, Feierabend J (1996) Comparison of the expression of a plastidic chaperonin 60 in different plant tissues and under photosynthetic and non photosynthetic conditions. Planta 200: 326-334.

Schneider G, Lindqvist Y, Brändén C-I (1992) RUBISCO: Structure and mechanism. Annual Review of Biophysics and Biomolecular Structure 21:119-143.

Schreiber U (2004) Pulse-amplitude (PAM) fluorometry and saturation pulse method – An overview. In: Papageorgiou G, Govindjee (eds.) Chlorophyll Fluorescence: A Signature of Photosynthesis. Kluwer Academic Publishers, The Netherlands: pp. 279-319.

Schreiber U, Schliwa U, Bilger W (1986) Continuous recording of photochemical and non-photochemical chlorophyll fluorescence quenching with a new type of modulation fluorometer. Photosynthesis Research 10:51-62.

Schroda M, Kropat J, Oster U, Rüdiger W, Vallon O, Wollman F-A, Beck CF (2001) Possible role for molecular chaperones in assembly and repair of photosystem II. Biochemical Society Transactions 29:413-418.

Schroda M, Vallon O, Wollman F-A, Beck CF (1999) Chloroplast-targeted heat shock protein 70 (HSP70) contributes to the photoprotection and repair of photosystem II during and after photoinhibition. Plant Cell 11:1165–1178.

Schubert H, Andersson M, Snoeijs P (2006) Relationship between photosynthesis and non-photochemical quenching of chlorophyll fluorescence in two red algae with different carotenoid compositions. Marine Biology 149:1003–1013.

Schubert N, García-Mendoza E (2006) Carotenoid composition of marine red algae. Journal of Phycology 42:1208–1216.

Seely GR, Duncan MJ, Vidaver WE (1972) Preparation and analytical extraction of pigments from brown algae with dimethyl sulfoxide. Marine Biology 12:184–188.

Sharkey TD (2000) Photosynthetic carbon reduction. In: Raghavendra AS (ed.) Photosynthesis: A Comprehensive Treatise. Cambridge University Press, London: pp. 111-123.

Sharkey TD, Schrader SM (2006) High temperature stress. In: Rao KVM, Raghavendra AS, Reddy KJ (eds.) Physiology and Molecular Biology of Stress Tolerance in Plants. Springer, The Netherlands: pp.101-129.

Sheath RG (2003) Red algae. In: Wehr JD, Sheath RG (eds.) Freshwater Algae of North America: Ecology and Classification,. Elsevier Science, USA: pp. 197-224.

Shelly K, Heraud P, Beardall J (2003) Interactive effects of PAR and UVB radiation on PSII electron transport in the marine alga *Dunaliella tertiolecta* (Chlorophyceae). Journal of Phycology 39:509-512.

Shen KP, Harte J (2000) Ecosystem climate manipulations. In: Sala OE, Jackson RB, Mooney HA, Howarth RW (eds.) Methods in Ecosystem Science. Springer-Verlag Inc, New York: pp. 353-372.

Shen Y-K, Chow WS, Park J-I, Anderson JM (1996) Photoinactivation of photosystem II by cumulative exposure to short light pulses during the induction period of photosynthesis. Photosynthesis Research 47:51-59.

Shiu C-T, Lee T-M (2005) Ultraviolet B-induced oxidative stress and responses of the ascorbate–glutathione cycle in a marine macroalga *Ulva fasciata*. Journal of Experimental Botany 56:2851–2865.

Sicora C, Máté Z, Vass I (2003) The interaction of visible and UV-B light during photodamage and repair of photosystem II. Photosynthesis Research 75:127–137.

Sicora C, Szilárd A, Sass L, Turcsányi E, Máté Z, Vass I (2006) UVB and UVA radiation effects on photosynthesis at the molecular level. In: Ghetti F, Checcucci G, Bornman JF (eds.) Environmental UV Radiation: Impact on Ecosystems and Human Health and Predictive Models. Springer, The Netherlands: pp. 121-135.

Sinha RP, Häder D-P (2002) UV-induced DNA damage and repair: a review. Photochemical and Photobiological Sciences 1:225-236.

Sinha RP, Häder D-P (2008) UV-protectants in cyanobacteria. Plant Science 174:278-289.

Sinha RP, Klisch M, Gröniger A, Häder D-P (1998) Ultraviolet-absorbing/screening substances in cyanobacteria, phytoplankton and macroalgae. Journal of Photochemistry and Photobiology B: Biology 47:83-94.

Sinha RP, Klisch M, Helbling EW, Häder D-P (2001) Induction of mycosporine-like amino acids (MAAs) in cyanobacteria by solar ultraviolet-B radiation. Journal of Photochemistry and Photobiology B:Biology 60:129-135.

Smith RC, Mobley CD (2007) Underwater light. In: Björn VLO (ed.) Photobiology: The Science of Life and Light, 2nd edn. Springer, New York: pp. 131-138.

Smith RC, Prézelin BB, Baker KS, Bidigare RR, Boucher NP, Coley T, Karentz D, MacIntyre S, Matlick HA, Menzies D, Ondrusek M, Wan Z, Waters KJ (1992) Ozone depletion: ultraviolet radiation and phytoplankton biology in Antarctic waters. Science 255:952–959.

Sokal PR, Rohlf FJ (1995) Biometry: The Principles and Practice of Statistics in Biological Research, 3rd edn. W.H. Freeman, San Francisco. 887 p.

Strasser RJ, Srivastava A, Govindjee (1995) Polyphasic chlorophyll a fluorescent transient in plants and cyanobacteria. Photochemistry and Photobiology 61:32-42.

Strid Å, Chow WS, Anderson JM (1990) Effects of supplementary ultraviolet B radiation on photosynthesis in *Pisum sativum*. Biochimica et Biophysica Acta 1020:260-268.

Strid Å, Chow WS, Anderson JM (1994) UVB damage and protection at the molecular level in plants. Photosynthesis Research 39:475-489.

Strid Å, Porra RJ (1992) Alterations in pigment content in leaves of *Pisum sativum* after exposure to supplementary UVB. Plant and Cell Physiology 33:1015-1023.

Sullivan J, Rozema J (1999) UV-B effects on terrestrial plant growth and photosynthesis. In: Rozema J (ed.) Stratospheric Ozone Depletion, the Effects of Enhanced UV-B Radiation on Terrestrial Ecosystems. Backhuys, Leiden: pp. 39-57.

Szilárd A, Sass L, Deák Z, Vass I (2007) The sensitivity of photosystem II to damage by UV-B radiation depends on the oxidation state of the water-splitting complex. Biochimica et Biophysica Acta 1767:876-882.

Takagi S (2003) Actin-based photo-orientation movement of chloroplasts in plant cells. Journal of Experimental Biology 206:1963-1969.

Takahashi S, Bauwe H, Badger M (2007) Impairment of the photorespiratory pathway accelerates photoinhibition of photosystem II by suppression of repair but not acceleration of damage processes in *Arabidopsis*. Plant Physiology 144:487-494.

Takahashi S, Murata N (2005) Interruption of the Calvin cycle inhibits the repair of photosystem II from photodamage. Biochimica et Biophysica Acta 1708:352 – 361.

Takahashi S, Murata N (2006) Glycerate-3-phosphate, produced by CO_2 fixation in the Calvin cycle, is critical for the synthesis of the D1 protein of photosystem II. Biochimica et Biophysica Acta 1757:198–205.

Takahashi S, Murata N (2008) How do environmental stresses accelerate photoinhibition? Trends in Plant Science 13:178-182.

Takeuchi A, Yamaguchi T, Hidema J, Strid Á, Kumagai T (2002) Changes in synthesis and degradation of Rubisco and LHCII with leaf age in rice (*Oryza sativa* L.) growing under supplementary UVB radiation. Plant, Cell and Environment 25:695-706.

Talarico L, Maranzana G (2000) Light and adaptive responses in red macroalgae: An overview. Journal of Photochemistry and Photobiology B: Biology 56:1-11.

Tartarotti B, Tores JJ (2009) Sublethal stress: Impact of solar UV radiation on protein synthesis in the copepod *Acartia tonsa*. Journal of Experimental Marine Biology and Ecology 375:106-113.

Tomek P, Lazár D, Ilik P, Naus J (2001) On the intermediate steps between the O and P steps in chlorophyll a fluorescence rise measured at different intensities of exciting light. Australian Journal of Plant Physiology 28:1151-1160.

Torres MA, Barros MP, Campos SCG, Pinto E, Rajamani S, Sayre RT, Colepicolo P (2008) Biochemical biomarkers in algae and marine pollution: A review. Ecotoxicology and Environmental Safety 71:1-15.

Torres MA, Sousa APA, Filho EATS, Melo DF, Feitosa JPA, de Paula JCM, Lima MGS (2007) Extraction and physicochemical characterization of *Sargassum vulgare* alginate from Brazil. Carbohydrate Research 342:2067-2074.

Tripp CS, Blomme EAG, Chinn KS, Hardy MM, LaCelle P, Pentland AP (2003) Epidermal COX-2 induction following ultraviolet irradiation: suggested mechanism for the role of COX-2 inhibition in photoprotection. Journal of Investigative Dermatology 121:853–861.

Tsugeki R, Nishimura M (1993) Interaction of homologues of Hsp70 and Cpn60 with ferredoxin-NADP1 reductase upon its import into chloroplasts. FEBS Letters 320:198–202.

Turco RP, Whitten RC (1975) Chlorofluoromethanes in the stratosphere and some possible consequences for ozone. Atmospheric Environment 9:1045-1061.

Turcsányi E, Vass I (2000) Inhibition of photosynthetic electron transport by UVA radiation targets the photosystem II complex. Photochemistry and Photobiology 72:513–520.

Tyystjärvi E (2008) Photoinhibition of photosystem II and photodamage of the oxygen evolving manganese cluster. Coordination Chemistry Reviews 252:361-376.

Uhrmacher S, Hanelt D, Nultsch W (1995) Zeaxanthin content and the degree of photoinhibition are linearly correlated in the brown alga *Dictyota dichotoma.* Marine Biology 123:159-165.

van de Poll WH, Eggert A, Buma AGJ, Breeman AM (2001) Effects of UV-B-induced DNA damage and photoinhibition on growth of temperate marine red macrophytes: Habitat-related differences in UV-B tolerance. Journal of Phycology 37:30–37.

van de Poll WH, Janknegt PJ, van Leeuwe MA, Visser RJW, Buma AGJ (2009) Excessive irradiance and antioxidant responses of an Antarctic marine diatom exposed to iron limitation and to dynamic irradiance. Journal of Photochemistry and Photobiology B: Biology 94:32-37.

van den Hoek C, Mann DG, Jahns HM (1995) Algae: An Introduction to Phycology. Cambridge University Press, Cambridge. 306 p.

van Kooten O, Snel JFH (1990) The use of chlorophyll fluorescence nomenclature in plant stress physiology. Photosynthesis Research 25:147-150.

van Wijk KJ, Eichacker L (1996) Light is required for efficient translation elongation and subsequent integration of the D1-protein into photosystem II. FEBS Letters 388:89-93.

Vass I, Cser K, Cheregi O (2007) Molecular mechanisms of light stress of photosynthesis. Annals New York Academy of Sciences 1113:114-122.

Vass I, Kirilovsky D, Etienne A-L (1999) UV-B radiation induced donor- and acceptor-side modifications of photosystem II in the cyanobacterium *Synechocystis* sp. PCC 6803. Biochemistry 38:12786–12794.

Vass I, Sass L, Spetea C, Bakou A, Ghanotakis DF, Petrouleas V (1996) UVB induced inhibition of photosystem II electron transport studied by EPR and chlorophyll fluorescence. Impairment of donor and acceptor side components. Biochemistry 35:8964–8973.

Vass I, Styring S, Hundal T, Koivuniemi A, Aro E-M, Andersson B (1992) Reversible and irreversible intermediates during photoinhibition of photosystem II: stable reduced Q_A species promote

chlorophyll triplet formation. Proceedings of the National Academy of Sciences USA 89:1408-1412.

Vass I, Szilárd A, Sicora C (2005) Adverse effects of UVB light on the structure and function of the photosynthetic apparatus. In: Pessarakli M (ed.) Handbook of Photosynthesis, 2nd edn. CRC Press, USA: pp. 827-844.

Vass I, Turcsányi E, Touloupakis E, Ghanotakis D, Petrouleas V (2002) The mechanism of UVA radiation-induced inhibition of photosystem II electron transport studied by EPR and chlorophyll fluorescence. Biochemistry 41:10200–10208.

Vayda ME, Yuan ML (1994) The heat shock response of an Antarctic alga is evident at 5 degrees C. Plant Molecular Biology 24:229–233.

Villafañe VE, Gao K, Helbling EW (2005) Short- and long-term effects of solar radiation on the red algae *Porphyridium cruentum* (S. F. Gray) Nägeli. Photochemical and Photobiological Sciences 4:376-382.

Villanueva RD, Hilliou L, Sousa-Pinto I (2009) Postharvest culture in the dark: An eco-friendly alternative to alkali treatment for enhancing the gel quality of κ/ι-hybrid carrageenan from *Chondrus crispus* (Gigartinales, Rhodophyta). Bioresource Technology 100:2633-2638.

Vincent WF, Neale PJ (2000) Mechanisms of UV damage to aquatic organisms. In: de Mora S, Demers S, Vernet M (eds.) The Effects of UV Radiation in the Marine Environment. Cambridge University Press, Cambridge: pp. 149-176.

Voss P, Hajimiragha H, Engels M, Ruhwiedel C, Calles C, Schroeder P, Grune T (2007) Irradiation of GAPDH: A model for environmentally induced protein damage. Biological Chemistry 388:583–592.

Wang W, Vinocur B, Shoseyov O, Altman A (2004) Role of plant heat-shock proteins and molecular chaperones in the abiotic stress response. Trends in Plant Science 9:244-252.

Weber S (2005) Light-driven enzymatic catalysis of DNA repair: A review of recent biophysical studies on photolyase. Biochimica et Biophysica Acta 1707:1-23.

Wehr JD (2003) Brown Algae. In: Wehr JD and Sheath RG (eds.) Freshwater Algae of North America: Ecology and Classification. Elsevier Science, USA: pp. 757-773.

Weykam G, Gómez I, Wiencke C, Iken K, Klöser H (1996) Photosynthetic characteristics and C:N ratios of macroalgae from King George Island (Antarctica). Journal of Experimental Marine Biology and Ecology 204:1-22.

White AJ, Critchley C (1999) Rapid light curves: A new fluorescence method to assess the state of the photosynthetic apparatus. Photosynthesis Research 59:63-72.

White AL, Jahnke LS (2002) Contrasting effects of UVA-A and UV-B on photosynthesis and photoprotection of β-carotene in two *Dunaliella* spp. Plant and Cell Physiology 43:877-884.

Wiencke C, Clayton MN, Schoenwaelder M (2004) Sensitivity and acclimation to UV radiation of zoospores from five species of Laminariales from the Arctic. Marine Biology 145:31–39S

Willekens H, Chamnogopol S, Davey M, Schraudner M, Langebartels C (1997) Catalase is a sink for H_2O_2 and is indispensable for stress defence in C_3 plants. EMBO Journal 16:4806–4816.

Wilson KE, Ivanov AG, Öquist G, Grodzinski B, Sarhan F, Huner NPA (2006) Energy balance, organellar redox status, and acclimation to environmental stress. Canadian Journal of Botany 84:1355-1370.

Wilson MI, Ghosh S, Gerhardt KE, Holland N, Babu TS, Edelman M, Dumbroff EB, Greenberg BM (1995). *In vivo* photomodification of ribulose-1,5-bisphosphate carboxylase/oxygenase holoenzyme by ultraviolet B radiation: Formation of a 66-kilodalton variant of the large subunit. Plant Physiology 109:221-229.

Wu H, Gao K, Wu H (2009) Responses of a marine red tide alga *Skeletonema costatum* (Bacillariophyceae) to long-term UV radiation exposures. Journal of Photochemistry and Photobiology B: Biology 94:82-86.

Wulff A, Roleda MY, Zacher K, Wiencke C (2008) UV radiation effects on pigments, photosynthetic efficiency and DNA of an Antarctic marine benthic diatom community. Aquatic Biology 3:167–177.

Xiong F (2001) Evidence that UVB tolerance of the photosynthetic apparatus in microalgae is related to the D1-turnover mediated repair cycle *in vivo*. Journal of Plant Physiology 158:285–294.

Xu C, Sullivan JH, Garrett WM, Caperna TJ, Natarajan S (2008) Impact of solar ultraviolet B on the proteome in soybean lines differing in flavonoid contents. Phytochemistry 69:38-48.

Xue L, Zhang Y, Zhang T, An L, Wang X (2005) Effects of enhanced ultraviolet-B radiation on algae and cyanobacteria. Critical Reviews in Microbiology 31:79-89.

Yaakoubd B, Andersen R, Desjardins Y, Samson G (2002) Contributions of the free oxidized and Q_B-bound plastoquinone molecules to the thermal phase of chlorophyll-a fluorescence. Photosynthesis Research 74:251-257.

Yan X, Chuda Y, Suzuki M, Nagata T (1999) Fucoxanthin as the major antioxidant in *Hijikia fusiformis*, a common edible seaweed. Bioscience, Biotechnology and Biochemistry 63:605–607.

Yokthongwattana K, Chrost B, Behrman S, Casper-Lindley C, Melis A (2001) Photosystem II damage and repair cycle in the green alga *Dunaliella salina*: Involvement of a chloroplast-localized HSP70. Plant and Cell Physiology 42:1389-1397.

Yong ZH, Chen GY, Shi JN, Xu DQ (2006) *In vitro* reassembly of tobacco ribulose-1,5-bisphosphate carboxylase/oxygenase from fully denatured subunits. Acta Biochimica et Biophysica Sinica 38:737-45.

Yosef I, Irihimovitch V, Knopf JA, Cohen I, Orr-Dahan I, Nahum E, Keasar C, Shapira M (2004) RNA binding activity of the ribulose-1,5-bisphosphate carboxylase/oxygenase large subunit from *Chlamydomonas reinhardtii*. Journal of Biological Chemistry 279:10148-10156.

Zhu X-G, Govindjee, Baker NR, deSturler E, Ort DR, Long SP (2005) Chlorophyll a fluorescence induction kinetics in leaves predicted from a model describing each discrete step of excitation energy and electron transfer associated with photosystem II. Planta 223:114-133.

Zsiros O, Allakhverdiev SI, Higashi S, Watanabe M, Nishiyama Y, Murata N (2006) Very strong UV-A light temporally separates the photoinhibition of photosystem II into light-induced inactivation and repair. Biochimica et Biophysica Acta 1757:123-129.

Zudaire L, Roy S (2001) Photoprotection and long-term acclimation to UV radiation in the marine diatom *Thalassiosira weissflogii*. Journal of Photochemistry and Photobiology B: Biology 62:26-34.

Zvezdanović J, Cvetić T, Veljović-Jovanović S, Marković D (2009) Chlorophyll bleaching by UV-irradiation *in vitro* and *in situ*: Absorption and fluorescence studies. Radiation Physics and Chemistry 78:25–32.

APPENDIX

APPENDIX 1

SAMPLES

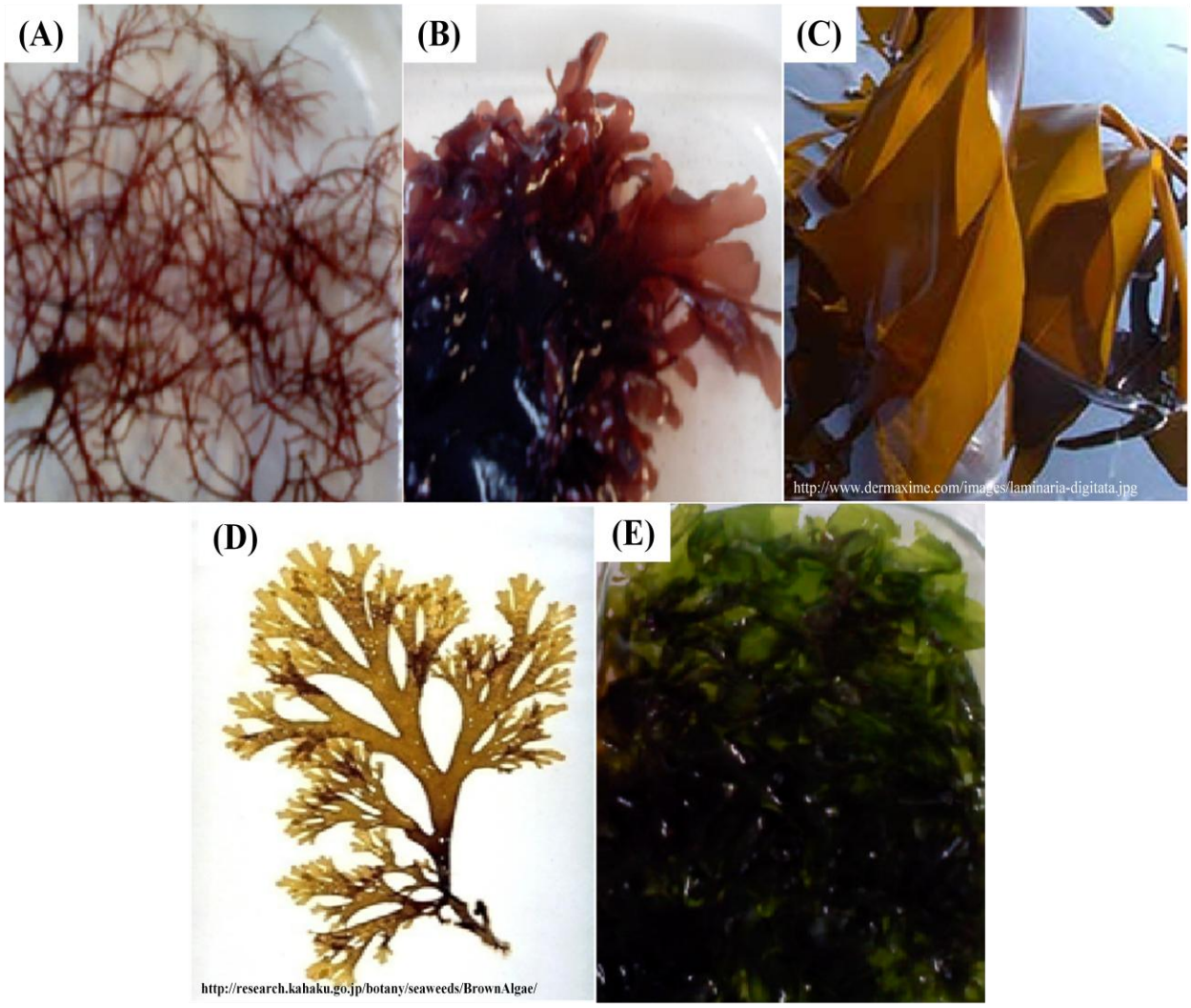

Fig. 44: The five marine macroalgae examined in this study. *A: Solieria chordalis, B: Palmaria palmata, C: Laminaria digitata, D: Dictyota dichotoma* and *E: Ulva lactuca*. Note: Photos A, B and E are taken by the author while photos C and D are taken from the web.

APPENDIX 2

EXPERIMENTAL SETUPS

Fig. 45: A simple setup of the fluorescent lamps chamber. 1 are the fluorescence and the daylight tubes side by side; 2 is the step-up ladder where the petri dish containing the samples was mounted; 3 is the black-curtain acting as a screen; and 4 is an example of the cut-off filter used.

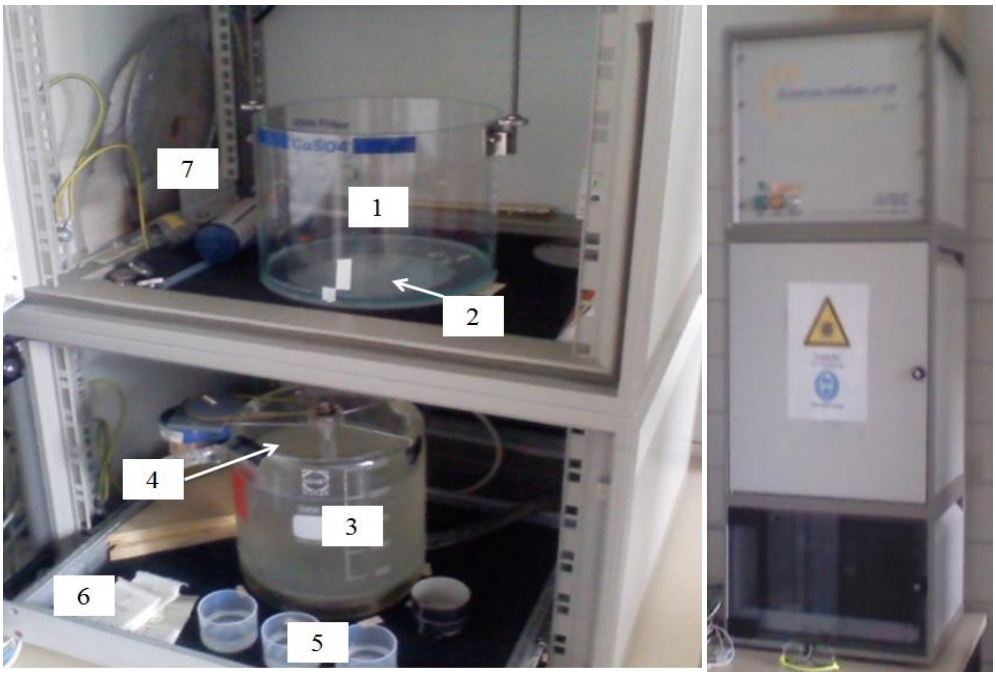

Fig. 46: (*figure on the left*) Components of the sun simulator experimental setup. 1 is the quartz jar for the liquid filter, shown here is for $CuSO_4$ solution (the bluish liquid in the jar); 2 is the thick, whitish diffuser plate beneath the liquid filter; 3 is the double-walled, water-filled glass jar, note the tube at the back of the jar, which connects the jar with a thermostat underneath the simulator; 4 is the rotating plate where the beakers containing the samples were mounted; 5 are the plastic beakers for the samples, the black beaker is for the sample receiving only UVR; 6 are the radiation cut-off filters (which are actually inside the envelopes) and 7 is the wire mesh. (*figure on the right*) The sun simulator, SonSi (iSiTEC GmbH, Germany).

APPENDIX 3

Buffers prepared for SDS-PAGE and Western blotting were as follows (Note: deionized water was used to make up solutions to the required volume):

A. SDS-PAGE

1. 1x sample/loading buffer (in 25 mL, pH 6.8):

500 µL β-Mercaptoethanol,
0.50 g SDS,
2.5 mL glycerol,
2 mL 1M Tris-HCl, and,
some bromophenol.

2. 1x running buffer (in 1L, pH not adjusted):

3.00 g Tris,
12.40 g glycine,
2.50 g SDS, and,
1 mL β-Mercaptoethanol.

B. Western Blotting

1. Transfer buffer (in 1L, pH not adjusted):

3.03 g Tris,
14.42 g glycine, and,
150 mL methanol

2. 10x TBS buffer (in 1L, pH 7.4):

24.23 g Tris, and,
87.66 g NaCl

for working buffer of 1x TBS (in 1L), 100 mL of 10x TBS was diluted in 900 mL deionized water.

3. 1x TBST buffer (in 1L):

0.05 g Tween-20, and,
100 mL 10x TBS buffer

4. 5% blocking buffer (in 100 mL):

5.00 g non-fat milk powder, and,
100 mL 1x TBST buffer

5. 2% blocking buffer (in 100 mL):

2.00 g non-fat milk powder, and,
100 mL 1x TBST buffer

6. Alkaline phosphatase (AP) buffer (in 100 mL, pH 9.5):

1.21 g Tris, and,
1.23 g $MgSO_4.7H_2O$

APPENDIX 4

FLUORESCENCE TRACES

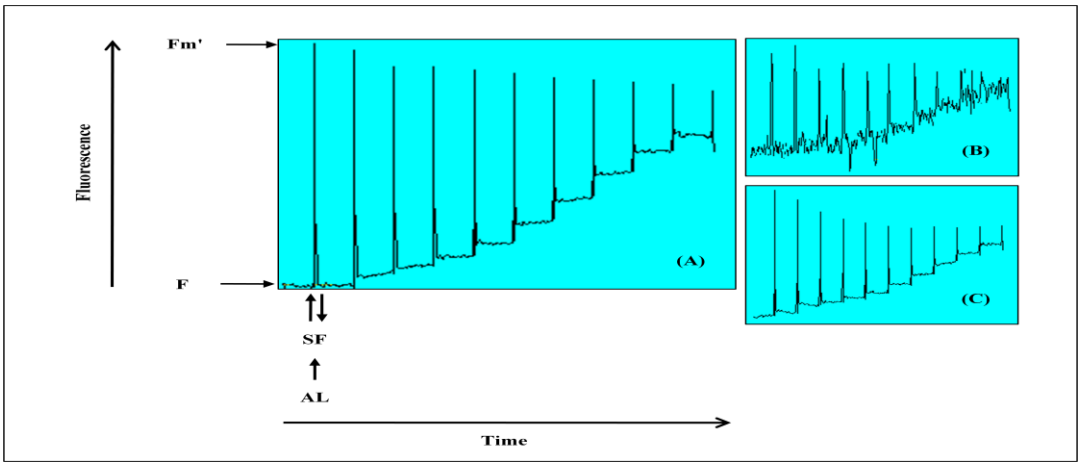

Fig. 47: Examples of fluorescence traces from the PAM-2100 Light Curve (RLC) recorded from pre-irradiaton *U. lactuca* (*A*), after 5 h irradiation to PAR+UVA+UVB (*B*, post-irradiation), and after 18 h recovery under dim light (*C*, post-recovery). Following the first saturation flash (SP), actinic light (AL) is switched on and progresses at increasing actinic irradiances. Duration of separate actinic irradiances was 20 s. Each AL was followed by a SP of 0.6-0.8 s, generating a series of 11 fluorescence maxima (F_m'). Standard total recording time was 220 s. AL steps ranged from about 9 to 665 µmol m^{-2} s^{-1} depending on the species.

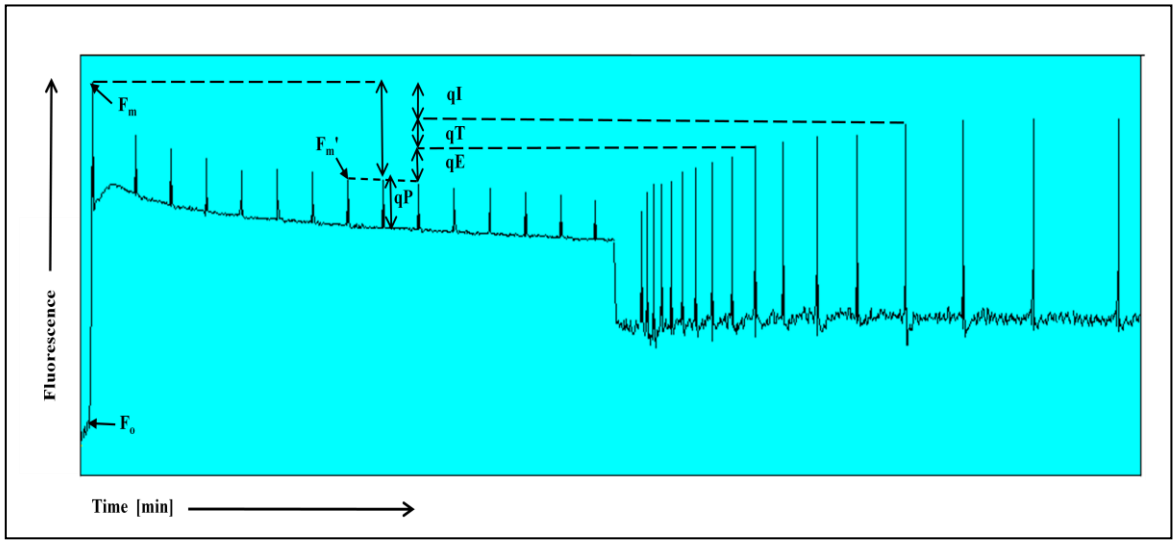

Fig. 48: Chl fluorescence measurement from *S. chordalis* showing the induction and relaxation kinetics. In the experiment, the presence of only weak ML produces the minimal fluorescence, $F_{o;}$ the first SP was recorded after 60 s of ML in which the photosynthetic light reactions are saturated and fluorescence reaches a maximum level (F_m); AL follows each subsequent SP which is switched on every 20 s; immediately after AL, far-red light (FR) was given to give F_o' values. For recording of the induction kinetics, the AL was switched on for 5 min. During this recording, a combination of qP and NPQ lowers the fluorescence yield. After switching off the AL, recovery of F_m' within a few minutes reflects relaxation of the qE component of NPQ. NPQ (qE+qT+qI) can be seen as the difference between F_m and the measured maximal fluorescence after a SP during illumination (F_m'). SP was stopped manually after 10 min of recordings. The details on the figure are based on Müller et al. (2001).

ACKNOWLEDGEMENTS

My heartfelt and warmest gratitude goes to my supervisor, Prof. Dr. Dieter Hanelt, whom had helped me a lot during my four years here in Hamburg; for all the ideas and suggestions; and, for reading and improvising this thesis. His co-operation, thoughtfulness, patience and kindness are highly appreciated.

My thanks are also to my co-supervisor, Prof. Dr. Kai Bischof for reading and improvising this thesis, for the ideas and suggestions, and for his help during my few days in Kiel.

Credit also goes to Frau Allmuth Andres whom had always been there to lend a hand and for her thoughtfulness and kindness, making me feel at home; to Herr Andreas Wagner for providing the samples from Helgoland and never give up searching even though the algae were not 'in season'; to Dr. Ralf Rautenberger for his help and co-operation in teaching me how to extract the proteins and providing me information on the antioxidative enzymes assays; to Frau Alice Schneider whom had taught me the SDS-PAGE as well as Western blotting; to Dr. Dietrich Lorch for giving me the permission to use the spectrophotometer and for his constant help, especially with the translation, and suggestions; and, to all members of the *Prüfungsausschuss* and *Promotionsausschuss* (i.e. PD Dr. Hartwig Lüthen, Prof. Dr. Reinhard Lieberei, PD Dr. Sabine Lüthje, PD Dr. Dörthe Müller-Navarra and Dr. Christoph Reisdorff).

Not to be forgotten are the people whom had always been nice to me and had helped me to adapt to the life in Hamburg: Frau Puttfarken, Marija, Frau Wagner, Kerstin, Christa, Frau Mörke, Kak Normah, Sharifah Intan Baizura, Intan Fareha, Fatin, Frau Viana, Dr. Nora and others whom I had forgotten their names but will never forget their kindness.

To the government of Malaysia through the Ministry of Higher Education and Embassy of Malaysia, Frankfurt and to Universiti Malaysia Terengganu (UMT) for giving me this golden opportunity to do my PhD in Germany. To all my friends and colleagues in the Department of Biological Sciences, Faculty of Science and Technology, for giving me support and encouragement.

Last but not least, my deepest love and appreciation goes to my wonderful parents whom had constantly supported me with their love, encouragement and prayers; also to my brothers, sisters, sisters-in-law and my cute little nephews and nieces, whom had keeping me strong all these years abroad, I missed you all so much.